STABLE ISOTOPE ECOLOGY BASELINES AND HUMAN DIET RECONSTRUCTION: AN EXAMPLE FROM BASKETMAKER II BURIALS AT CEDAR MESA, UTAH

by

Michael David Lewis

A dissertation submitted to the faculty of
The University of Utah
in partial fulfillment of the requirements for the degree of

Doctor of Philosophy

Department of Anthropology

The University of Utah

May 2018

The University of Utah Graduate School

STATEMENT OF DISSERTATION APPROVAL

The dissertation of **Michael David Lewis**
has been approved by the following supervisory committee members:

Duncan Metcalfe ,	Chair(s)	**5 Dec 2017** Date Approved
Joan B. Coltrain ,	Member	**15 Dec 2017** Date Approved
Alan Rogers ,	Member	**15 Dec 2017** Date Approved
James O'Connell ,	Member	**19 Dec 2017** Date Approved
Mitchell Power ,	Member	**19 Dec 2017** Date Approved

by **Leslie A. Knapp** , Chair/Dean of
the Department/College/School of **Anthropology**
and by **David B. Keida** , Dean of The Graduate School.

ABSTRACT

Recent interest in the Basketmaker-to-Pueblo (or Full Formative) transition on the Colorado Plateau indicates the need for better characterization of the subsistence strategies of the Basketmaker II period (500 BC–500 AD). While the human stable isotope record for this period is extensive, regional resource isotope data are less robust, inhibiting formal modeling. This dissertation presents new carbon and nitrogen isotope data for modern flora, the results of roasting experiments on banana yucca tissues, archaeofauna, and maize specimens from Cedar Mesa, Utah.

Ecological patterning is not seen at the chosen scale of analysis; δ^{13}C does not correlate with elevation gradients and δ^{15}N does not correlate with visual assessments of cryptobiotic crust development. However, relative to other regions in the Intermountain West, Cedar Mesa flora and fauna (and previously published human values) show significant depletion in Nitrogen 15, suggesting that the fixation of atmospheric nitrogen by cryptobiotic crusts sets a unique δ^{15}N baseline for local food-webs—potentially biasing formal modeling.

Mixing models calculated using the Bayesian mixSIAR framework show strong correlations between feasible source proportions. Such correlation permits extrinsic linear constraints and a posteriori aggregation of resource proportions to substantially narrow diet model outcomes, and suggest that Cedar Mesa Basketmaker II diets were comprised of between 70 and 90% maize.

For my grandparents who laid down the path. For my parents David and Ellen who have shaped and encouraged all my studies, and to my wife Kali from whom I shall continue to learn for the rest of my days

CONTENTS

LIST OF FIGURES

LIST OF TABLES

ACKNOWLEDGEMENTS

No research project such as this can be brought to completion without the assistance, contributions and support of numerous friends, family and colleagues. I would acknowledge a number of individuals without whom this work would not exist in its present form.

First, I would thank those who shaped my mind before my graduate career. To my late grandmother Eleanor Lewis, whose gift of the volume *Life in the Ancient World* first introduced an eight year old to the wonder of the Egyptians, Greeks and Babylonians. To my parents, Ellen Green and David Lewis, who have supported me, intellectually spiritually and materially through decades of study. To the tutors at Saint John's College, especially Jorge Aigla and Robert Sacks, who first opened to my understanding mathematical models.

I would also thank those whom I have studied from and with during my time at the University of Utah. To Corrine Springer, Shannon Boomgarden and the staff of Range Creek Canyon Archaeological Field School. To the faculty and graduate students at the University of Utah Department of Anthropology, especially Sam Davis and Ryan Bohlender– for the years of morning coffee and discussion). To R.E. Burrillo, for introducing me to Cedar Mesa, and for the hiking and talking out its landscapes and its history. To Bill Lipe and R.G. Matson, for generously sharing their advice and insights into Cedar Mesa archaeology and ecology. And to any whom I have forgotten to name.

I would thank those persons and agencies giving logistical and material support for this project. To my parents (again) for the use of their truck. To the Bureau of Land Management and the United States Forest Service for assistance with permitting and access. Isaac Hart for identifying our faunal specimens. The Global Change and Sustainability Center at the University of Utah gave grant support for the field component of this project. A National Science Foundation Doctoral Dissertation Improvement Grant (award number 10037620) provided funds for laboratory analysis.

I would thank my committee members. Mitch Powers for practical advice on botan-

ical collection. James O'Connell for shaping my sense of the discipline of archaeology. Alan Rogers, for encouraging my study of quantitative modeling. Duncan Metcalfe, for demanding precision in scientific argument and for years of intellectual and institutional support.

I would also like to thank Mr. Benson for generously allowing me to reproduce in Figure his climate maps from (Benson 2011) and providing me with high quality images for reproduction. Figures 2.1, 2.2 and 2.3 contain silhouette images that are the work of a number of individuals held under creative commons licenses (see references). The creators are Oscar Sanisidro (Sanisidro 2018), Tracy A. Heath (Heath 2018), Sarah Werning (Werning 2018), Andreas Trepte (Trepte and Keesey 2018), an unknown individual (unattributed 2018) and Pearson Scott Foresman (Foresman 2018). Many thanks for those permitting the use of their work by others. I also note that Figure 2.1 is free to be used and modified (with attribution) under the terms of the "share alike" license on one of the images used (Trepte and Keesey 2018).

Finally, I have two special thanks. To Joan Coltrain, for her patience, teaching and support, from our first talk in Range Creek Canyon, to this day. Through your advice and guidance, I have changed from student to colleague, and I hope that we shall ever remain friends.

To my wife Kali whose support and help has given more to this project and to my life's delight than I can ever say or you will ever know.

CHAPTER 1

ARCHAEOLOGICAL BACKGROUND

The American Southwest has one of the best preserved, detailed, temporally controlled, and documented prehistoric archaeological records in the world—spanning terminal Pleistocene big-game hunting to regional protostates (e.g., Hohokam, Chaco, Aztec) and exhibiting public architecture, long distance trade, and centrally organized labor (Ortiz 1979; Plog 2008; Lekson 2008). This archaeological record is matched by the region's high resolution paleoclimatic data (Irwin-Williams and Haynes 1970; Adams and Petersen 1999; Benson and Berry 2009; Benson 2011; Benson et al. 2013; Bellorado and Anderson 2013), making the Southwest uniquely situated to address the Grand Challenges of Archaeology: questions of universal human behavioral responses to changes in ecology, demographics, economy, technology, and ideology (Kintigh et al. 2014).

On the Colorado Plateau, recent studies have focused on the social and technological changes associated with the adoption of ceramics, village life, and recognizably Puebloan life-ways (Feinman, Lightfoot, and Upham 2000; Kohler 2013; Kohler and Varien 2012; Kohler et al. 2012b; Reed 2002; Wilshusen, Schachner, and Allison 2012; Wilshusen and Perry 2008). Such models invite worldwide comparisons and suggest the Old World Mesolithic-to-Neolithic transition through similarities in paleodemographic shifts (Kohler et al. 2014, 2008; Bellwood and Oxenham 2011; Bocquet-Appel 2002), linguistic distributions (Bellwood and Renfrew 2002; Kemp et al. 2010), patterns of violence and defensive architecture (Kohler et al. 2014; LeBlanc 1999; Glen Rice and LeBlanc 2001; Keeley 1996; Lekson 2002; Wilcox and Haas 1994), technological change (Crown and Wills 1995; Adams 2014; Hard, Mauldin, and Raymond 1996), gender dynamics (Crown 2000), and development of private ownership (Altschul and Huber 2000; Ortman et al. 2016).

Unfortunately, while the ceramic periods (Basketmaker III and Pueblo I–IV) of the Colorado Plateau are subject to detailed modeling, the prior a-ceramic agricultural period—

Basketmaker II—is less well understood. The lower population density and greater mobility of Basketmaker II populations produced fewer and less visible sites, making modeling of Basketmaker II economies less robust and detailed. The conclusions reached by current stable isotope diet models also differ in several dimensions from the results obtained from more conventional archaeological metrics. In consequence, different investigators—using different lines of archeological evidence—offer substantially differing reconstructions of Basketmaker II subsistence, resulting in conflicting starting points when modeling the Basketmaker-to-Pueblo transition.

This dissertation offers a partial solution to that problem, through improved stable isotope models of Basketmaker II diets at Cedar Mesa, Utah. While this study is limited to a single region and time period, the methodological issues raised and the resource data obtained are necessary prerequisites for accurately interpreting the human stable isotope record throughout the southern Colorado Plateau—recommending the addition of this data-type to discussions of the New World Neolithic—or Full Formative—Revolution.

Chapters are summarized as follows:

- Chapter 1 reviews Basketmaker II research and outlines the major spatial and temporal divisions recognized in the period, and then presents an ecological synthesis of Basketmaker II subsistence variation.
- Chapter 2 reviews stable isotope techniques, the method by which diet can be reconstructed, and the existing body of Basketmaker II stable isotope research. Given this regional record, the limitations of stable isotope methodology are outlined—the greatest of which is the lack of a robust database of stable isotope values from local resources.
- Chapter 3 outlines the project methodology for creating a local resource isotope database including modern botanical sampling on Cedar Mesa, archaeofaunal analysis, and laboratory experiments on roasting the stems of banana yucca (*Yucca baccata*).
- Chapter 4 presents the results from this study including statistical tests of ecological effects on δ^{13}C and δ^{15}N, and estimates for the uncertainty introduced by combining species into a single taxon.
- Chapter 5 compares Cedar Mesa resource isotope values with previous published datasets from the Intermountain West and formally calculates Cedar Mesa Basket-

maker II diet proportions. A comparison of models using varying input parameters and extrinsic constraints frames a discussion of the role of mixing model geometry on the interpretation of prehistoric diets at Cedar Mesa.

- Chapter 6 summarizes and critiques the experimental and modeling work of the previous five chapters and suggests further directions for research.

1.1 A History of Basketmaker II Archaeology

The Holocene prehistory of the Colorado Plateau can be divided into three parts. The first is the Archaic (7000–500 BC), a foraging adaptation. The second, Basketmaker II (500 BC–500 AD) is a dispersed settlement, agricultural adaptation. The third encompasses Basketmaker III (500–800 AD) to Pueblo I–IV (800–1500 AD), and entails an agricultural adaptation that includes aggregated villages or towns and the beginnings of regional political organization. Basketmaker II is thus the earliest maize-based archaeological period or culture on the Colorado Plateau, and is critical for understanding both the process of agricultural adoption at the start of the period and the transition to village life at its end.

The history of Basketmaker II research can be divided into three temporally overlapping intellectual phases. The first phase of research revolved around identifying and defining Basketmaker II. In the 1890s, Richard Wetherill first distinguished the a-ceramic Basketmakers from the Ancestral Puebloan culture. Temporal relationships were established at Cave 7, a rock shelter on Cedar Mesa, in one of the first uses of stratigraphic inference in the western United States (McNitt 1966; Atkins and McClanahan 1990; Blackburn and Williamson 1997). Cave sites with similar material culture were identified by Kidder and Guernsey in northeastern Arizona (Guernsey 1931; Guernsey and Kidder 1921; Kidder and Guernsey 1919) and Basketmaker became incorporated into the regional developmental phases of the Pecos Classification as follows: "Basketmaker II or Basket Maker—The agricultural, atlatl using, non-pottery-making stage, as described in many publications. Late Basketmaker, Basket Maker III, or Post-Basketmaker—the pit and slab-house-building, pottery-making stage" (Kidder 1927, 556).

The technological changes associated with Basketmaker III (ceramic technology, the transition from atlatl to bow and arrow, the replacement of basin by trough metates and the development of coursed masonry habitations in place of pithouses), reinforced with

the expectation of continuous development, suggested that Basketmaker II was less agriculturally dependent than later periods (Kidder 1924; Morris and Burgh 1954)—an idea rejected in the late 20th century.

The second phase of Basketmaker II research began with Morris and Burgh's excavations of rock shelters near Durango, Colorado (Morris and Burgh 1954). This study distinguished the Eastern Basketmakers of Durango from the "classic" or Western Basketmakers identified by Kidder. Material culture differences included projectile point morphology, basketry, and pit house design (Morris and Burgh 1954). Subsequent work, continuing to the present, confirmed this material culture distinction and defined its spatial extent (Charles and Cole 2006). The Eastern Basketmaker II inhabited the upper and middle reaches of the San Juan drainage, particularly the Animas and La Plata rivers (Eddy 1972; Charles, Sesler, and Hovezak 2006), the area around Moab UT (Fahrni 2011; Cole and Moe 2001), and the Chuska mountains AZ (Gilpin 1994). The Western Basketmaker II inhabited the lower reaches of the San Juan drainage and the mesa country to the west, including the area around Kanab, Glen Canyon (Geib and Spurr 2000), Cedar Mesa UT (Matson 1991), and Black Mesa AZ (Powell and Smiley 2002).

The material culture differences between Eastern and Western Basketmaker II suggested differing cultural antecedents and perhaps different biological origins. Eastern Basketmaker II basketry, flaked stone technology and pithouse form show affinity with the Colorado Plateau Archaic (Matson 1991, 2006) and Fremont (Geib 1996; Geib 2011) populations. Further supporting this connection, the recently identified Archuleta phase ((Sesler and Hovezak 2011) see also "Eastern Farming" below) may be evidence of occupational and material cultural continuity between San Juan Basin Archaic populations and Basketmaker II agriculturalists.

Western Basketmaker II basketry and flaked stone technology show affinities with Archaic populations from southern New Mexico and Arizona such as the San Pedro stage of the Cochise culture (Morris and Burgh 1954). R.G. Matson suggests (Matson 2006, 158) that Irwin-Williams (1967) was the first to propose that Western Basketmaker II represents a portion of the San Pedro Cochise population who migrated onto the Colorado Plateau. This concept quickly entered the standard understanding of Western Basketmaker II (Berry 1982; Berry and Berry 1986; Matson 1991; Lekson 2008), particularly as subsequent research

has indicated the San Pedro phase was fully agricultural—with a few direct dates on southeastern Arizona maize falling between 2100–1200 BC and widespread use of maize between 1200–800 BC (Mabry 2005).

The third phase of Basketmaker archaeology coincides with the development of salvage archaeology and cultural resource management. While many studies continued to use the cultural framework outlined by Morris and Burgh (see reviews in (Matson 1991, 2006; Charles and Cole 2006)), the spatial coverage required by compliance projects forced investigators to focus on the relationship between landscape ecology and human behavior in a way not previously emphasized.

Both the Navaho Reservoir Project (Eddy 1966) and the Glen Canyon Project (Jennings 1966; Geib 1996) linked Basketmaker II settlement patterns to specific physiographic contexts; the latter in turn launched studies of Basketmaker II settlement patterns on the Red Rock Plateau (Lipe 1970), which in turn expanded into the Cedar Mesa Project (Matson, Lipe, and Haase 1990; Matson 1991). Through an examination of land use (Matson, Lipe, and Haase 1988; Matson 1994; Pollock 2001), archaeobotanical analyses (Aasen 1984; Androy 2003) and stable isotope studies of human burials (Chisholm and Matson 1994; Matson and Chisholm 1991), the Cedar Mesa project demonstrated that Basketmaker II at Cedar Mesa (e.g., the Grand Gulch Phase: 100–300 AD) was fully agriculturally dependent.

Concurrently, the Black Mesa Archaeological Project identified a local Lolomai phase paralleling the Cedar Mesa Grand Gulch in settlement location, period (1–400 AD) and maize use. New dates on artifacts collected by Kidder and Guernsey in the 1930s identified a pre–AD 1 transitional "White Dog" phase (see discussion below). Subsequently, the Navaho Mountain Roads Archaeological Project (Geib 2011), examined sites in the Kayenta region. Geib's was the first study to identify pre–AD 1 Basketmaker II settlement patterns, demonstrating an alluvial maize farming orientation at 500 BC and calling into question the "White Dog" designation.

Meanwhile, in the Eastern Basketmaker II regions, studies including the Fruitland Project (Hovezak, Sesler, and Fuller 2002) and the Animas La Plata Archaeological Project (Potter 2008) examined Basketmaker II settlement patterning in the upper San Juan basin, extending the recognition of alluvial farming recognized at Durango and Navaho Reservoir (Hovezak and Sesler 2006; Sesler and Hovezak 2011; Bellorado 2009) and identifying

the Eastern Basketmaker II material culture throughout the area.

As the major survey projects have transitioned to the cultural resource management industry, academic research has taken a more regional and problem oriented approach. For example, research at Cedar Mesa has continued building on collections and data from the Cedar Mesa project and derivative investigations (e.g., see (Lipe 2007; Hasse 1983; Ellwood et al. 2013; Aasen 1984; Androy 2003; Matson, Lipe, and Haase 1988, 1990; Pollock 2001)). In the 1990s the provenience of Wetherill's Cedar Mesa collections was rediscovered through historical documents and inscriptions (Blackburn and Williamson 1997), leading to a number of new analyses on old collections (Atkins and McClanahan 1990; Coltrain, Janetski, and Lewis 2012; Coltrain and Janetski 2013; Geib and Hurst 2013).

As a result of this dual investigative pattern, the Basketmaker II record is quite robust with specialist studies including ancient DNA (Kemp et al. 2010; LeBlanc et al. 2007), macrobotanical (Aasen 1984; Androy 2003), experimental archaeology (Ellwood et al. 2013; Haas Jr 2001; Bellorado 2009), gender and social structure (Hays-Gilpin 2000; Crown 2000; Mowrer 2006), rock art (Cole 1994; Hays-Gilpin 1996), violence (LeBlanc 1999; Glen Rice and LeBlanc 2001), and—as will be seen in Chapter 2—stable isotope analysis. However, this level of specialization has resulted in regional syntheses of Basketmaker II that have not emphasized ecological variability. Both major recent Basketmaker II literature reviews explicitly use material-culture-based approaches (Matson 2006; Charles and Cole 2006).

One result of this theoretical orientation is that variation in Basketmaker II subsistence patterns are written off as products of culture, leading to conflicting characterizations of Basketmaker II subsistence and demographic change at the end of the period. For example, there is considerable debate about agricultural dependence and scheduling conflicts as drivers of ground stone morphology (Adams 2014, 1999; Hard, Mauldin, and Raymond 1996; Morris 1990) and similar arguments regarding the changing role of agricultural dependence in paleodemographic models (Kohler et al. 2008; Kohler and Reese 2014).

1.2 Cultural and Ecological Variation in Basketmaker II Subsistence

The remainder of this chapter describes Basketmaker II subsistence behaviors as responses to variation in local ecology. This orientation does not invalidate culture historical

approaches; rather, the ecological framework provides an explanatory basis for Basketmaker II subsistence variation that will facilitate the contrast of stable isotope dietary models in Chapter 2 with reconstructions from other lines of archeological evidence. This discussion will also provide constraints on how far the Cedar Mesa subsistence pattern can be extended to Basketmaker II in general.

1.2.1 Unresolved Questions on Basketmaker II Subsistence: Question 1, The Perennial "White Dog" Problem

Since the Pecos definition, the relationship of Basketmaker II to maize agriculture has been a major subject of research. While Basketmaker II as a whole can no longer be seen as transitional between foraging and agriculture, the spatial and temporal uniformity of the period continues to be questioned. Before summarizing the current evidence for spatial variability in Basketmaker II subsistence patterns, it is necessary to address a tenuously pervasive concept that recurs in the literature without supporting evidence.

The idea of a "mobile transitional economy" between foraging and farming predates (or is synchronic with) Wetherill's discovery of the Basketmakers at Cave 7 ((Nordenskiöld 1893, 168), compare (Kidder 1924, 326)). Kidder's original developmental concept—or at least the way it was interpreted until the 1980s—viewed Basketmaker II as intermediate between hunting and gathering and "full" agriculture accompanied by pottery and improved grinding implements. The Cedar Mesa project used settlement patterning, macrobotanical, and stable isotope data to show that the "classic" Basketmaker II occupation of Cedar Mesa was fully agriculturally dependent by 100 AD and that the Basketmaker II period as a whole could not be a transitional economy. In consequence, the theoretical "mobile transitional economy" simply moved back in time.

The "White Dog" phase was originally proposed for material collected by Kidder and Guernsey in Marsh Pass, Arizona (Colton 1939), but the concept became developmentally significant with the discovery of the Lolomai phase during the Black Mesa Archaeological Project (Powell and Smiley 2002). Re-dating existing collections of "White Dog" cultural material (Parry, Smiley, and Burgett 1994; Smiley 1998) showed that it predated 1 AD, while the "classic" Lolomai mesa-top farming phase postdated 1 AD. An influential description of this new "White Dog" concept was based on Paiute ethnography and described a mobile seasonal foraging round, utilizing rock shelter habitations rather than

pithouses, and supplementing foraged resources with maize (Powell and Smiley 2002, 47-48).

However, isotopic analysis of "White Dog" (e.g., pre–1 AD) burials from Marsh Pass indicates full maize dependency from the start of the occupation (Coltrain, Janetski, and Carlyle 2007). Further, recent findings from the Navaho Mountain Road Project (Geib and Hurst 2013) show high maize ubiquities from 500 BC, and alluvium-oriented habitations dating to the same period (Geib and Hurst 2013). A similar settlement pattern is found on the Red Rock Plateau (Matson 2006, 154), Glen Canyon (Geib 1996) and Comb Wash near Cedar Mesa (Hurst, Smiley, and Robins 2011). The early dates for this habitation pattern remove the behavioral distinctions between the "White Dog" and classic (e.g., Lolomai and Grand Gulch) Basketmaker II phases.

Consequently, Matson (2006) proposed that the "White Dog" concept should be abandoned and earlier maize adaptions be described in a new behaviorally based phase (e.g., prepottery preformative, or Basketmaker I (Matson 2006, 159))—a phase that is quite ephemeral: "These BMI manifestations may be (or may include) episodes of maize use during particularly good times on the Colorado Plateau, and may be followed by other times where maize was not grown" (Matson 2006, 160).

It is not clear—aside from theoretical aesthetics—why a "mobile transitional economy" needs to be posited. While absence of evidence is not necessarily evidence of absence, it certainly may be. If maize arrives with migrating farmers—as the current orthodox model suggests—there is no reason why a transitional phase between foraging and farming should have existed in that location—let alone be archaeologically visible.

1.2.2 Unresolved Questions on Basketmaker II Subsistence: Question 2, Regional Differences in Basketmaker II Culture, Behavior and Ecology

Eastern and Western Basketmaker II subsistence variation is the second pervasive concept in Basketmaker II research. Most investigators recognize subsistence differences based on regional variation in material culture and the conventional interpretation of such variation. However, as shall be seen in Chapter 2, such differences have limited support from the human stable isotope record. Setting aside the isotopic problem for the moment, the remainder of this chapter presents an ecologically-based synthesis of the Basketmaker II

subsistence literature. It suggests that the regional differences in subsistence metrics are best understood not as signifying large differences in agricultural dependence—or the proportion of maize in the diet—but rather as the result of differences in wild resource productivity and the corresponding ability of different ecologies to mitigate against crop losses.

Since their discovery, the Eastern Basketmaker II have been conceived of as less agriculturally oriented. Often, whether tacitly or explicitly, this difference is attributed to differences in values, ethnicity and culture:

> *Basketmaker II is characterized by similarities and diversity through time and across space. . . .this complexity resembles that of the subsequent Pueblo stages when clans and societies presumably determined the patterns of settlement, subsistence and ideology. (Charles and Cole 2006, 203-204)*

However, broad-scale ecological differences between Western and Eastern Basketmaker II regions exist and suggest differences in subsistence, irrespective of the nature of Basketmaker II material culture distinctions. The Western Basketmaker II populations are largely confined to the lower San Juan drainage and the heart of the Colorado Plateau canyon country (Charles and Cole 2006). Here, a tableland topography results in expansive areas of nearly identical elevation covered with the same biological communities: saltbush and sagebrush dominated scrubland and pinyon-juniper woodland.

The Eastern Baskemaker II areas with the longest and best-developed subsistence records are the drainages of the middle and upper San Juan, along the southern slopes of the La Plata and San Juan Mountains (Charles and Cole 2006). Here, changes in elevation result in a more spatially compact set of local environments, traveling up or downhill one encounters in relatively short distances desert scrub, pinyon-juniper, ponderosa pine, and mixed conifer forests (see Figure 1.1, Benson et al. (2013) Figure S1, and Morris and Burgh (1954)).

These botanical differences reflect underlying ecological trends. As a prerequisite to paleoecological modeling, Benson reports modern annual and seasonal precipitation and temperature values across the Four Corners area (Benson 2011) (see also Figure 1.1), and assumes that relative changes in temperature and precipitation with elevation were characteristic of prehistory (Benson et al. 2013).

The Lower San Juan areas inhabited by Western Basketmaker II are—and almost as-

suredly were—substantially drier and hotter than the middle and upper San Juan inhabited by the Eastern Basketmaker II—the moisture in the latter area being due to orthographic precipitation in the San Juan and La Plata Mountains. These ecological patterns correlate with differences in maize ubiquity, faunal indices, and settlement patterning for both Archaic foragers and Basketmaker II farmers, providing a unified explanation for subsistence variability during the Basketmaker II period, whether or not ethnic distinctions are postulated. Issues relating to maize ubiquity and settlement patterning are explored further below.

1.2.2.1 Maize Ubiquities: Interpretive Issues

The major subsistence distinction in the present Basketmaker II literature between Eastern and Western regions is the timing of agricultural dependence, traditionally estimated by the amount of maize in the diet. This transition is archaeologically instantaneous in the Western Basketmaker II and appears slower in Eastern Basketmaker II. While this argument is supported by settlement pattern data, it relies most heavily on temporal differences in maize ubiquity—a problematic proxy for the amount of maize in the diet.

Maize ubiquity can reflect people's reliance on maize, but determining this requires simplifying the interpretative framework. Without any interpretation, maize ubiquity is defined as the number of analytic units (usually flotation samples) containing maize divided by the total number of samples analyzed. The first level of interpretation requires the assumption that each analytic unit corresponds to some discrete human activity. If the units analyzed are an adequate sample of the human activities undertaken, maize ubiquity becomes a measure of the proportion of archaeologically detected human activities involving maize.

The assumption that analytic units are an adequate metric of human activity may be violated if there is autocorrelation of site type and maize (see discussion in Geib 2011 Chapter 5). For example, let two regional surveys analyze flotation samples associated with primary habitations, logistical camps, and lithic procurement sites for several periods. If maize is present only in primary habitations, and primary habitations are over-represented in one survey, the difference in ubiquity may not reflect a difference in maize use.

The lower San Juan shows a sharp, step-like change in maize ubiquity from the Archaic

to Basketmaker II and little change between Basketmaker II and later periods (Table 1.1). The upper San Juan shows a more gradual change. Assuming that this pattern is not due to systematic taphonomic bias across the basin, or biases in site type, the above interpretive framework suggests that the Western Basketmaker II had few activities in which maize was not present, a pattern similar to later Puebloan occupations. Phil Geib makes the same case; when maize arrives in the northern Kayenta region, it is everywhere at once (Geib 2011, 223). For the Western Basketmaker II, maize is life.

For the Eastern Basketmaker II, in contrast, half or more of daily activities did not include maize, with a greater percentage of activities associated with maize in latter periods. The relative decline in maize ubiquity could be systematic (no maize on hunting trips), or it could reflect periods where maize was not used in any activity (crop failure), or it could indicate the partial adoption of agriculture, or some combination thereof. When only maize ubiquity is considered, in the absence of site type designations, the interpretation is unclear.

1.2.2.2 Archaic Settlement as a Foraging Baseline Proxy

However, Archaic and Basketmaker II settlement patterns and continuity also suggest that the wild resource base was richer in the east than the west and that the sharp, step-like transition in maize ubiquity associated with the Western Basketmaker II reflects a wild resource base incapable of supporting a farming population during periods of agricultural failure.

One proxy for wild resource abundance is the density of the permanent foraging population. For much of the area occupied by the Western Basketmaker II, the Archaic occupational pattern is less dense than in surrounding regions. The upland areas of the lower San Juan drainage—Cedar Mesa and Black Mesa—are marked by a paucity of Archaic sites (note that this area straddles and extends beyond the western boundaries of Benson's environmental maps–e.g., Figure 1.1): "In the greater Cedar Mesa area no definitive patterns [for archaic occupation] have emerged" (Spangler, Yentsch, and Green 2010, 74), "the small size of the sample of such [Black Mesa Archaic] sites. . .precludes any sort of definitive study of site locational criteria. . ." (Powell and Smiley 2002, 32). Summarizing the results from Glen Canyon (Geib 1996, 34) and the Kayenta region, Geib attributes the

lack of Archaic sites in both as due to the tendency of such sites to lie on alluvial surfaces. "Archaic archaeological record of the N15 ROW and elsewhere across much of the Kayenta region is largely a buried phenomenon" (Geib 2011, 142,180). This argument is repeated by Spangler et al. to explain the lack of Archaic sites in the canyons surrounding Cedar Mesa: "A similar [to Glen Canyon] distribution of Archaic sites in sheltered riverine settings and upland base camps had not yet been documented in the Cedar Mesa area, although such sites likely existed." (Spangler, Yentsch, and Green 2010, 73). Again, while absence of evidence is not necessarily evidence of absence, it certainly may be.

In all cases, full time Archaic occupation is rejected throughout the Western Basketmaker II region on ecological grounds: "it is doubtful that a strictly collecting strategy was a realistic possibility in the Glen Canyon region until the Formative. Without farming, subsistence resources were probably never sufficiently abundant, predictable and concentrated to allow establishment of long term residential base camps" (Geib 1996, 155). At Black Mesa, "the evidence indicates a sporadic, generally non-intensive occupation constrained by the relatively low resource supply of the mesa top" (Powell and Smiley 2002, 34). In the Navaho Mountain Road Project ". . .the subsistence resources available to archaic foragers. . .were probably never sufficiently abundant, predictable and concentrated to allow the establishment of long term residential base camps or what might be termed permanent residences" (Geib and Hurst 2013, 165).

While Lipe and Pitblado (1999) describe the central and upper San Juan Archaic record as "not greatly different" from Geib's reconstructions of Archaic lifeways in Glen Canyon, I disagree. The central San Juan Basin has a substantial Archaic record "literally hundreds of sites" (see review (Sesler and Hovezak 2011, 12))—a record sufficiently robust and varied to result in arguments about where on the forager-collector spectrum Archaic populations should be classed. Almost all authors working in the Eastern Basketmaker II region recognize seasonal mobility in local Archaic populations, but also the importance of stored seeds in permanent winter camps (Vierra and Doleman 1994; Elyea and Hogan 1983). Simmons (1989) and Vogler (1993) suggest that Archaic populations targeted ecologically diverse localities to be able to utilize a variety of seasonally available resources. Lipe and Pitblado (1999) suggest seasonal mobility as an explanation for the distribution of Archaic sites in southeastern Colorado while Reed and Metcalf (1999) suggest larger seasonal rounds

with populations moving across elevation gradients between the southern and northern Colorado Plateau.

While the distinction is subtle, the existence in the Eastern Basketmaker II region of an Archaic record that can be debated in this way suggests a denser Archaic population than that detected in the Western Basketmaker II region. Further, the ecological variation and seasonal movement inferred for the Eastern San Juan Archaic are central to current models of agricultural adoption and Basketmaker II settlement strategies:

> *Populations in the central San Juan Basin's low elevation grassland appear to have declined after 400 BC, during the latter part of the En Medio phase. Rather than representing an occupational hiatus, Elyea and Hogan (1983) suggest a shift in occupation away from summer seed-gathering locales and towards the mid-elevation areas around the periphery of the basin for the purpose of maize cultivation. (Sesler and Hovezak 2011, 12)*

Looking at Benson climate maps (Benson 2011) in Figure 1.1 above, a movement from the San Juan Basin to the upland margins would entail a decrease in Growing Degree Days (GDD) to below 1000, making maize cultivation difficult due to to lack of heat for ripening the crop. However, if the advantage of maize lies in bringing a storable seed resource to basin edge locations that gave access to a variety of elevations, ecologies and resources, then this development can be seen as a modification and optimization of the Archaic seasonal round. The high cost of moving stored seed resources tethers a population to the central basin giving little access to resources in other elevations and ecologies. In contrast a cultigen such as maize can be grown and stored in sites at the edge of the basin, permitting access to resources from a variety of elevations and access to a storable dietary staple.

1.2.2.3 Western Basketmaker II Farming Settlements

Differences in Western and Eastern Basketmaker II ecology also suggest differing responses to variation in maize yields and wild resource abundance. In the Lower San Juan, pre–1 AD occupations are concentrated on watered alluvium and show few discontinuities. After AD 1, occupation moves to the mesa-tops, and periods of occupation closely correlate with periods of adequate rainfall, leading to local occupational hiatuses.

On Black Mesa, "the Lolomai phase appears to correlate with a 300 year period of low-frequency dendroclimatic variability measured by tree ring data [Dean et al. 1985:841, Curve C]. At approximately 1700 BP a precipitous and apparently cyclical crash occurs"

(Powell and Smiley 2002, 52). The same discontinuity is found in uplands throughout the Western Basketmaker II region

> *Northern Black Mesa was one of the several areas abandoned (at least in terms of habitation settlements) after a Basketmaker II occupation. . .The Red Rock Plateau was occupied in Late Basketmaker II times then abandoned [Lipe 1970]. . .Cedar Mesa also was abandoned following a Basketmaker II occupation. (Powell and Smiley 2002, 70)*

On Cedar Mesa, the same climatic shifts bound the Grand Gulch Phase: 200 AD—400 AD (Matson, Lipe, and Haase 1988; Matson 1994), (Spangler, Yentsch, and Green 2010, 24), Table 1.6, and a return of climatic stability from 542-725 AD corresponds with the Basketmaker III Mossbacks Phase on Cedar Mesa and a shift in occupation upslope onto Elk Ridge (Wilshusen, Schachner, and Allison 2012, Chapter 2).

Neither Glen Canyon nor the Navaho Mountain Road project show this occupational discontinuity around Basketmaker II, though in both cases alluvial rather than upland farming is emphasized. Glen Canyon lacks Basketmaker III, though Fremont sites are occupied in the same period (Geib 1996, 96). Geib identified the Kayenta occupational pattern with studies from the upper San Juan as a locale where a smooth Basketmaker II-III transition is detectable (Geib 2011, 288). In this sense, the northern Kayenta region is perhaps more similar to the middle and upper San Juan in having a sufficiently rich set of riparian resources to enable continuous occupation.

In addition to occupational continuity, one technological development among the upland Western Basketmaker II also suggests unusually high maize diets, consistent with low wild resource inputs. High maize diets are deficient in a number of micronutrients (Matson 2016); the use of basket boiling (Burrillo 2015) with limestone may have overcome this nutritional deficiency in Basketmaker II (Ellwood et al. 2013; Holstad 2010; Kemp, Lipe, and Matson 2011). Nutritional deficiencies from chronically low faunal inputs (Reynolds 2012; Badenhorst and Driver 2009) have been suggested as a common factor behind Basketmaker II weedy plant consumption (Battillo 2017), the use of beans in Basketmaker III, and turkey raising in the Pueblo III period (Bocinsky 2011; Lipe et al. 2017; Matson 2016; McCaffery et al. 2014), which may suggest economic or dietary/ nutritional similarities between Western Basketmaker II and later periods.

1.2.2.4 Eastern Basketmaker II Farming Settlements

In contrast to the high maize inputs in the Western Basketmaker II, The Archuleta phase 500 BC —1 AD is thought to be characterized by a mixed agricultural and foraging strategy: "The early maize producing sites are predominantly located in canyon floor and lower bench settings. . .capable of supporting floodwater or sub-irrigated farming" (Sesler and Hovezak 2011, 14). Similarly, most of the later "classic" Eastern Basketmaker II phases are oriented towards alluvial farming. Navaho Reservoir settlement patterns track alluvium (Eddy 1966), a pattern that holds for the Animas and La Plata drainages (Sesler and Hovezak 2011).

The primary constraint on agriculture in this area is temperature, as verified by experimental work (Bellorado 2009). Eastern Basketmaker II settlement patterns are not affected by periods of lowered precipitation, or by colder summer temperatures (Bellorado 2011, 41), both correlated with lower agricultural returns. Only in the fourth century AD do lower summer temperatures correlate with a movement of population to lower elevations and the first adoption of dry farming (Charles and Cole 2006), (Hovezak and Sesler 2006, 253), (Bellorado 2011, 42). However, the higher elevations are not abandoned at this time (Potter 2011). Rather, agricultural fields are positioned in the warmest locations at these elevations. Unlike the Western Basketmaker II areas, climatic shifts do not force abandonment of some portion of the eastern region.

This relative robustness in the face of climatic change is attributed to higher wild resource consumption. Eastern Basketmaker II site choice may have been as dependent on wild resource access as agricultural potential (Bellorado 2011, 36), (Potter 2011). Furthermore, archaeological assemblages from the eastern region contain higher proportions of large game than in the west, suggesting greater hunting success (Reynolds 2012; Potter 2008), while the variation in the macrobotanical record is often interpreted—correctly or not—as suggesting widespread use of wild resources.

1.2.3 A Synthetic View of Spatial Variation in Basketmaker II Subsistence

Ecological contrasts in the San Juan Basin and the resulting contrast in agricultural responses parallel recent developments in the southeastern Arizona, where east-west gradients in seasonality, species diversity and resource patchiness are understood in terms

of "collector" and "forager" (sensu Binford (1980)) gathering strategies and correlate with agricultural niche variation (Mabry 2005). In his study of environmental variability and foraging strategies, Doleman identifies two factors needed for floodwater farming in southeastern Arizona: suitable landforms and reliable water sources, and "compact high diversity environments that allowed access to a wide variety of resources with minimal travel" (Doleman 2005, 123). In contrast, upland environments in southwestern New Mexico were too stochastic to permit residual sedentism, requiring greater mobility for success. For the Basketmaker II, the western region shows greater stochastic variation in resource abundance while the eastern region shows the compact high-diversity environments associated with floodwater farming.

The lack of a permanent Archaic population across most of the Western Basketmaker II region suggests that the wild resource base was insufficient to support a sedentary foraging population. According to Benson's environmental data (Figure 1.1 above), the constraining factor for maize agriculture in the Western Basketmaker II region was precipitation (e.g., failure when summer rainfall $<$15 cm or annual rainfall $<$30 cm (Benson et al. 2013), rather than temperature, where 1500–2000 Growing Degree Days (GDD) are needed for native maize types (Bellorado 2009)). Since wild resource abundance and maize harvests both correlate with sufficient summer moisture, agricultural failure would suggest diminished foraging returns, limiting the capacity of Western Basketmaker II farmers—in particular mesa top dry farmers—to mitigate against crop losses. The observed high maize ubiquities in the western region are a reflection of the necessity of maize for survival in this landscape.

In contrast, the middle and upper San Juan show a substantial permanent Archaic population. Movement towards the edge of the basin places the Eastern Basketmaker II in areas with sufficient rainfall for farming, but constrained by the length of the growing season. Figure 1.1 shows the minimal maize farming requirements noted above. Much of the modern central San Juan Basin is better in terms of summer precipitation than the Lower San Juan. Why, then, would the first Eastern Basketmaker II farmers move into regions where they must—to borrow a phrase—"push the limits and torment corn seeds" (Bellorado 2011)? The answer may be that maize was being used as a way to transport a storable seed resource to a central place that permitted access to ecological niches whose

sheer variety offered mitigation against crop failure in a way not possible in the west.

Agricultural failure for the Eastern Basketmaker II is correlated with cold and wet summer conditions. Most edible wild grasses on the Colorado Plateau are cool season grasses with shallow root systems dependent on summer rains (Schwinning et al. 2008), whose germination (Bernstein et al. 2014) and growth rates (Smeal, O'Neill, and Arnold 2005; Comstock and Ehleringer 1992) are correlated with increased moisture and inversely correlated with temperature (Munson et al. 2011), suggesting that the same conditions that cause maize harvests to fail would increase yields of cool season grasses and the fauna they support. The continuity of occupation in the eastern region at elevations where maize returns would be marginal further suggests this complementary strategy. In this case, the lower maize ubiquities of Eastern Basketmaker II groups may be a function of periods where wild resources contributed proportionally more to the diet—at least over short timescales.

1.3 Chapter 1: Review and Conclusions

Over a century of Basketmaker II research has both expanded the range of inquiry and specified the questions being asked of the archaeological record. Having moved from questions of definition and tracing culture histories across time and space, Basketmaker II studies have begun to seek economic and ecological explanations for human behavioral variability. However, the recurring ideas of a "White Dog" transitional economy, and the continuation of culture historical frameworks for "explaining" spatial variation in subsistence patterns hinder meaningful regional synthesis.

The preliminary synthesis of Basketmaker II subsistence studies presented above provides a potential ecological explanation for broad east-west patterning in maize ubiquity, settlement patterning and continuity, faunal indices and technological adoption. This explanation is independent of the reality or nonreality of Eastern and Western Basketmaker II as ethnic identities, and suggests three well-defined and testable hypotheses about Basketmaker II subsistence—the third of which is the only one capable of being assessed in this study.

1. Western Basketmaker II consumed more maize than Eastern Basketmaker II
2. Western Basketmaker II consumed less animal protein than Eastern Basketmaker II

3. Western Basketmaker II diets were dominated by maize.

Chapter 2 will examine stable isotope models of Basketmaker II diet. As will be shown, this methodology should provide an ideal test for these hypotheses. Unfortunately, the Basketmaker II isotope data and models published to date do not always coincide with the reconstructions suggested by other aspects of the archaeological record. Resolving this conflict will require a careful reassessment of the assumptions underlying stable isotope models of Basketmaker II diets.

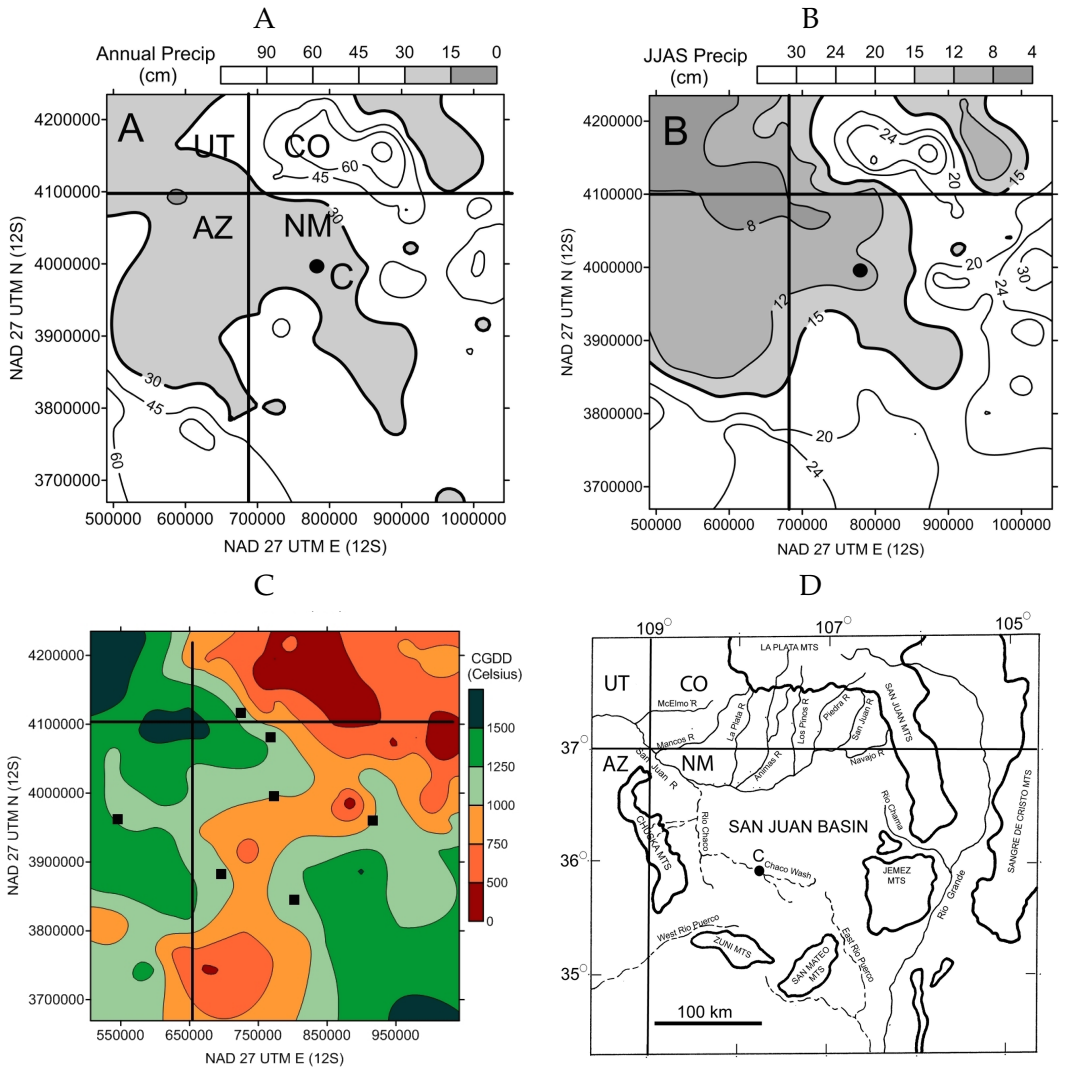

Figure 1.1: Four Corners Area climatic models. A: annual precipitation. B: summer (June, July, August, September) precipitation. C: Growing Degree Days (GDD). D: regional geographic features. All figures reproduced from (Benson 2011) (or color versions of plates) with permission. Note that scale is not consistent. Chaco Canyon appears at point C as reference point in maps A,B and D. Eastern BMII farming models are based on sites between the La Plata and Navajo rivers, south of the La Plata Mountains. Cedar Mesa lies in extreme upper left corner (e.g., approximately A and B). Note differences in precipitation and GDD and precipitation between these areas.

Table 1.1: Maize ubiquities from Eastern and Western Basketmaker II regions. Note that Basketmaker III is classed with Puebloan (e.g., ceramic) when data are available (compare (Huckell 1996) and (Matson 2006) for definitional difficulties).

Study	Archaic	Basketmaker II	Puebloan
Eastern Baskermaker II Region			
Fruitland (Brandt 2002)	11%	16%	84%
Animas La-Plata (Adams and Murray 2008)		41%	81%
(Hovezak, Sesler, and Fuller 2002)		20%	
Central San Juan (Vierra 2008)	2%	15%	
Upper Puerco (McBride 1994)		40%	90%
Western Baskermaker II Region			
Kayenta (Geib and Spurr 2000; Geib 2011)		75-90%	78%
Kayenta (Brand 1994)		84%	80-100%
Western Anasazi (BMII from Cedar Mesa)			
(Brand 1994, Table 4) (Aasen 1984)		89%	68-100%
Chuska BMIII (Kearns, McVickar, and Reed 2000)			79-94%
Chuska BMII (Vierra 2008, Figure 5)		70%	85%
Black Mesa (note data quality issues)			
(Hard, Mauldin, and Raymond 1996, Table III)		35%	59-70%

CHAPTER 2

STABLE ISOTOPE ANALYSIS BACKGROUND AND METHODOLOGIES

The initial stable isotope analyses of Cedar Mesa burials (Matson and Chisholm 1991; Chisholm and Matson 1994; Matson 1991) were instrumental in changing the concept of Basketmaker II from a "mobile transitional economy" to a fully agricultural adaptation. More recently, studies of Eastern and "White Dog" Basketmakers have expanded on this work (Coltrain, Janetski, and Carlyle 2006; 2007). Further, analysis of "classic" Western Basketmaker II burials from Wetherill's Cave 7 have shown age- and sex-based patterning in isotopic ratios (Coltrain and Janetski 2013), while longitudinal studies of human hair from Cedar Mesa have suggested seasonal variation in diet (Cooper et al. 2016).

Concurrent with this regional research, the capacity for modeling diets through stable isotopes has increased dramatically, so much so that authors have begun to express concern that available human datasets and modeling capacity are often reaching beyond the applicability of the resource databases upon which current models are founded (Phillips et al. 2014).

> *Over the last thirty years, light stable isotope analysis has become a standard tool of archaeological inquiry, and it has expanded our understanding of shifting global subsistence strategies and dietary practices over time. During subsistence reconstruction, idealized plant types and isotopic values are typically used as input parameters in paleodietary models; however, as archaeologists increasingly employ isotopic evidence in high-resolution paleodietary studies, a more detailed understanding of the underlying food-web is required. (Warinner, Garcia, and Tuross 2013, 868)*

2.1 Chapter 2: Overview

To understand how this issue manifests in the Basketmaker II isotopic record, this chapter reviews isotope diet models from the ground up. It first presents a simple terrestrial stable isotope diet model based on broad patterning in carbon and nitrogen isotope ratios.

Second, it reviews sources of ecological variation in isotopic baselines (e.g., the range of isotopic values associated with different levels of a food-web in a given locality) and trophic level enrichment uncertainties. Such variation limits the applicability of the simple model at finer scales. The third part of this chapter examines the Basketmaker II stable isotope record and the scale of isotopic difference exhibited.

Resolving diets at this finer scale requires formal modeling. The fourth part of this chapter reviews three recent isotope mixing model programs and shows that the estimates of diet proportions output by the models are a function of both input parameter uncertainties and the isotopic geometry of the food-web. The latter permits the legitimate use of source aggregation and linear constraints in limiting source proportion estimates–the discussion in the fifth part of this chapter.

From this reveiw, the principles that structure the sampling and experimental design of Chapters 3 and 4, and the concepts behind the revised formal calculations of Cedar Mesa Basketmaker II diets presented in Chapter 5 are derived.

2.2 Stable Isotopes: Basic Terminology and a Simple Diet Model

Isotopes are species of the same element, whose difference in mass results in different reaction rates. Consequently, the ratio of heavier to lighter isotopes changes during physical transformations and chemical reactions, allowing the movement of matter through a system to be traced. By convention, the ratio of heavy to light isotopes is measured relative to a global standard and expressed as a 'delta value' (δ) in parts per mil (‰) defined as:

$$\delta_{smp} = \left(\frac{R_{smp} - R_{std}}{R_{std}} \right) 10^3‰ \tag{2.1}$$

where R_{smp} is the ratio of isotopic species in the sample and R_{std} the ratio in the standard (Criss 1999). By convention, a sample may be *enriched* (e.g., more positive delta value) or *depleted* (e.g., more negative delta value) in the heavier isotope relative to another sample.

For diet models, the basic logic is that the delta value of any consumer tissue is a function of the average of the delta values of all consumed resources, weighted by their proportions in the diet. In the simplest model, this function is additive and may be represented by:

$$\delta_{con} = \Sigma \delta_i p_i e_i + \delta_{TLE} \tag{2.2}$$

where δ_{con} is the delta value of the consumer tissue, δ_i is the delta value of the ith resource, p_i is the proportion of that resource in the diet, e_i is the elemental concentration for that isotope and resource and δ_{TLE} is the trophic level enrichment (e.g., a constant offset) between the δ value of the tissue of interest and the whole diet δ value.

2.2.1 Trophic Level Enrichment

Figure 2.1 plots a hypothetical food-web in carbon and nitrogen isotope space, which, while ideal, illustrates real world principles of inference using stable isotopes. The isotope value of each consumer δ^{13}C and δ^{15}N follows Equation 2.2 (note that e_i is held constant in this initial discussion) and is visualized as a weighed whole diet average plus a fractionation factor or trophic level enrichment (δ_{TLE}). For simplicity, each diet is comprised of two resources, but the same general principles will hold for diets with a larger number of consumed resources.

Since bone preserves better than soft tissue, this study's model is calibrated with reference to bone collagen for which the fractionation factors of both carbon and nitrogen are well established though experimental and naturalistic studies (Lee-Thorp 2008). The offset between plant and bone collagen $\delta^{13}C_i$ is +5‰, with an approximate +1‰ offset for diets composed of animal protein (Schoeninger and DeNiro 1984). Muscle tissue δ^{13}C is depleted relative to collagen (e.g., $\delta^{13}C_{mus} + 2‰ = \delta^{13}C_{col}$)—a correction that must be made prior to using fauna as resource inputs (such as for the carnivore in Figure 2.1).

Nitrogen fractionation is relatively constant across trophic levels at +2-4‰ with +3 the most commonly used estimate (Schoeninger and DeNiro 1984; Schwarcz and Schoeninger 1991)) though values as high as +6‰ have been observed (Lee-Thorp 2008). The +3 δ^{15}N trophic level fractionation means that, within terrestrial food-webs, more positive δ^{15}N values are often an indication of a higher proportion of animal protein in the diet. Most natural plant tissues show δ^{15}N values of between +2 and +6 (but see section 'Environmental Variability' below), resulting in herbivore tissue δ^{15}N values of +5 to +9 and carnivore values between +8 to +13 (Schwarcz and Schoeninger 2012, 732). Omnivores take intermediate δ^{15}N values depending on the proportion of plant and animal tissue consumed.

These trophic level offsets can be used to group and compare consumers in isotope space (see Figure 9.21 in (White 2013, 396) for example), providing the most basic model of dietary composition: the comparative method.

2.2.2 Photosynthetic Pathway Variation

Trophic level patterning in $\delta^{13}C$ is less regular due to the wide variation in plant $\delta^{13}C$ based on differences in photosynthetic pathways. Plants have evolved to use the C3, C4, or CAM pathway; each has different isotopic effects on plant tissue.

In plants using C3 photosynthesis (most dicots and temperate grasses), CO_2 is exchanged between the atmosphere and photosynthesizing cells near the surface of the plant. This exchange allows both photosynthesis (the conversion of CO_2 to simple sugars through the Krebs cycle) and dark respiration (the "accidental" burning of sugar through the Krebs cycle releasing CO_2) to discriminate against carbon-13 resulting in negative values relative to atmosphere. C3 plants show $\delta^{13}C$ values of -35 to -20 to (Dawson et al. 2002),

In contrast, the C4 pathway mitigates against dark respiration. C4 plants (tropical grasses and a small suite of forbs) convert CO_2 into an organic acid and transport converted carbon to "bundle sheath cells" in the interior of the plant (Ehleringer and Cerling 2002). This process inhibits the loss of carbon to the atmosphere, resulting in less discrimination against carbon-13 in C4 plant tissues. C4 plants have $\delta^{13}C$ values around -12 to -10 (Schwarcz and Schoeninger 2012; Gannes, Del Rio, and Koch 1998)

The Crassulacean Acid Metabolism (CAM) photosynthetic pathway evolved in response to highly xeric conditions where retaining moisture is a priority. CAM plants (mostly succulents) open stomata at night to take in CO_2, but close stomata diurnally to prevent water loss, also mitigating against respired CO_2 loss. Thus, unlike C3 plants, whose stomata are always open to the atmosphere, CAM plants fix nearly all the CO_2 available, resulting in a relatively enriched $\delta^{13}C$ values between those of C3 and C4 plants (Gannes, Del Rio, and Koch 1998).

This differences in $\delta^{13}C$ between C3, C4 and CAM species make the proportion of plant types in the diet the primary determining factor in herbivore (and by extension carnivore) $\delta^{13}C$ values (see Figure 2.1). Since maize uses the C4 photosynthetic pathway, but the majority of the natural resources available on the Colorado Plateau use the C3 pathway,

human $\delta^{13}C$ values have served as a proxy for agriculture in the region.

2.3 Complications to the Simple Diet Model

This simple model has a number of parameters, most of which are subject to either uncertainty in estimation or systematic bias from physiological variation or environmental effects. Propagating such uncertainties through the model and checking for stability ensures that interpretations encompass all possibilities implied by model inputs and are not a function of a specific parameterization. While such uncertainty is rarely large enough to change C3 vs C4 or trophic level characterizations, it can affect finer grained applications of the diet model, and limit the ability to interpret population level differences in consumer isotope values.

2.3.1 Model Parameter Certainties

Consider again Equation 2.

$$\delta_{con} = \Sigma \delta_i p_i e_i + \delta_{TLE} \tag{2.3}$$

For comparisons of δ_{con} to be a valid foundation for inference, the difference between consumer delta values must be predominantly a function of differences in source proportions (p_i)—thus, variation in other parameters must be small and not systematically biased.

Several parameters are well established, and do not vary between models or regions. Elemental concentrations e_i for carbon and nitrogen may be measured directly from plant samples during isotopic analysis while animal tissue elemental concentrations may be estimated from bovid muscle tissue C_{conc} = 54.3 %, N_{conc} = 14.2 % ((Blaxter and Rook 1953; Maclean et al. 2003)). While technically nondirect estimates, these values are well established by experimental work and the uncertainties in the parameters are considered trivial.

Similarly, certain adjustments within the model are sufficiently established to treat as certain. The $\delta^{13}C$ value of modern specimens must be corrected for the Seuss effect, a -1.5‰ change in atmospheric $\delta^{13}C$ arising from industrial burning of fossil fuels (Marino and McElroy 1991). Muscle tissue with lipids removed are approximately 1–2‰ enriched in $\delta^{13}C$ over diet in studies of mice (Arneson and MacAvoy 2005), fox (Roth and Hobson

2000) and seal (Hobson et al. 1996), whereas muscle tissues including lipids exhibit values depleted by 1–2‰ relative to diet in mice (DeNiro and Epstein 1978), gerbils (Tieszen et al. 1983), rats (Yoneyama, Ohta, and Ohtani 1983), and pigs (Nardoto et al. 2006). By assuming that lean muscle is the dominant faunal tissue consumed in terrestrial settings, uncertainties in estimating the isotopic composition of the edible portion of fauna from collagen may be reduced to minimal levels.

In contrast, trophic level enrichments δ_{TLE} vary by tissue sampled and dietary composition, and different tissues integrate dietary signals over different temporal periods. Source delta values δ_i vary with environmental trends. Strictly speaking, in these cases interpretation of isotope ratios cannot be directly compared but must be translated through formal mixing models.

2.3.2 Trophic Level Enrichment Uncertainties

The bonds of lighter carbon isotopes are preferentially broken during respiration, resulting in an enrichment in δ^{13}C in the body—which drives the Trophic Level Enrichment (TLE) of carbon. Early models based on laboratory controlled diets (Schoeninger and DeNiro 1984) suggest that this enrichment was different for herbivores ($\delta^{13}C_{TLE}$= +5) than for carnivores ($\delta^{13}C_{TLE}$= +1).

Subsequent work has shown that in addition to diet composition, TLE is a function both of the species examined and the tissue sampled (Caut, Angulo, and Courchamp 2009). The complexity is introduced because of differences in tissue composition and tissue turnover rates (Wolf, Carleton, and Rio 2009). Both are significant to model interpretation.

Different amino acids fractionate isotopes at different rates and are constructed from different dietary sources. Since different proteins are composed of different proportions of amino acids, differences in tissue and organ δ^{13}C and δ^{15}N become apparent (Caut, Angulo, and Courchamp 2009; Schoeller 1999)—also lipids are depleted in δ^{13}C relative to protein (Logan et al. 2008), which can potentially bias measurements of tissue. Tracing such differences is the basis for several more complex isotopic diet models based on protein (Kellner and Schoeninger 2007) and individual amino acid routing (Hoen et al. 2014; Germain et al. 2013).

This level of analysis is not required for modeling Basketmaker II diets. While con-

trolled feeding studies have suggested that bone appatite is a better index of whole diet values (Ambrose and Norr 1993), this difference disappears among terrestrial herbivores (Warinner and Tuross 2009; Froehle, Kellner, and Schoeninger 2010). Given the high maize inputs suggested by Basketmaker II δ^{13}C values, collagen provides a suitable proxy for diet, without recourse to routing models.

Consequently, this study assumes that the collagen δ^{13}C TLE identified for herbivores (+5) and carnivores (+1) accurately represents the enrichment during consumption and assimilation of plant and animal protein by human beings—an assumption supported by experimental feeding studies of pigs (Warinner and Tuross 2009)—a species whose digestive physiology is similar to humans'. Similarly the TLE for nitrogen is relatively constant at (+2 to +4) per trophic level regardless of tissue or species sampled. However, all estimates are subject to some uncertainty; mammalian uncertainty in collagen TLE is approximately SE= 0.5‰ (Caut, Angulo, and Courchamp 2009).

Such uncertainty can affect outcomes, particularly when trying to distinguish dietary differences from small variations in consumer isotope values. To see the problem, consider the model for two hypothetical rabbits in Figure 2.2. Each rabbit has the same diet, but differences in the estimate of TLE values imply different rabbit tissue δ^{13}C values (the example is merely illustrative; the principle also applies to δ^{15}N). As the TLE is never perfectly known, being able to formally incorporate TLE uncertainties prevents model bias arising from the modeler's selection of a specific TLE value.

The differences in tissue turnover time also affect the interpretation of isotope diet models by giving measures of diet over differing temporal periods (Wolf, Carleton, and Rio 2009; Olive et al. 2003)). Teeth and hair form sequentially, permitting the detection of dietary changes with weaning and seasonality, respectively (Dalerum and Angerbjörn 2005). Bone collagen and apatite give dietary signals at a multidecadal timescale (Lee-Thorp 2008). Consequently, comparison of dietary models using different tissues must account for such differences in time integration (e.g., hair and collagen may not represent the same dietary average), and studies of tissues with long integration time must adjust for changes in diet over that period (e.g., juveniles whose δ^{15}N is enriched due to enrichment in infancy from nursing should be excluded from formal mixing models).

2.3.3 Uncertainties from Source Variability

In addition to the uncertainties of tissue-level differences in trophic level enrichment and the temporal scale of the dietary signal, there are potential biases arising from variation in the isotope ratios of sources. Figure 2.3 plots whole diet delta values ($\delta_{con} - \delta_{TLE}$ see Equation 2.2) for two hypothetical rabbits. The first rabbit diet delta value results from resources A and B in a 50/50 proportion. The second rabbit delta value may results either from consuming resources A and B in a 30/70 proportion, or from consuming resources A' and B' in a 50/50 proportion. The magnitude of this shift in model outputs is a function of how much each resource shifts (e.g., A-A',B-B') relative to the difference between resources (e.g., A-B). When analyzing bone collagen stable isotope values, these shifts are averaged over the adult life span of a short lived taxon such as a rabbit, or over approximately 30 years, the turnover rate of adult human bone collagen.

The difference between the rabbit delta values may be behavioral or a result of differences in resource delta values. The latter may arise both because of sampling bias or because resource delta values systematically vary on a variety of spatial scales.

2.3.4 Environmental Variability

C3 and CAM plant δ^{13}C values (and thus potentially the entire food-web) vary systematically with water stress. In both cases, water loss is regulated by the opening and closing of stomata, small apertures in the surface of the leaf, across which both atmospheric H_2O and CO_2 diffuse prior to uptake by the plant. The size of the stomata openings alter the CO_2 diffusion rate and the associated δ^{13}C values (Ehleringer and Cerling 2002); (Farquhar, Ehleringer, and Hubick 1989). More negative δ^{13}C values result from lower water stress, due either to wetter soils, cooler temperatures and/or higher humidity (Dawson et al. 2002). At coarse resolution, average δ^{13}C correlate with latitude and annual rainfall (Ehleringer 1995; Ehleringer and Monson 1993). Locally, elevation and water availability may contribute to δ^{13}C variability in C3 and CAM species (Ehleringer and Cooper 1988; Eickmeier and Bender 1976; Szarek and Troughton 1976; Szpak et al. 2013). These changes will primarily affect C3 plants, and result in δ^{13}C differences on the order of 5‰ across elevation gradients in the American Southwest (van de Water, Leavitt, and Betancourt 2002).

Most natural terrestrial plant δ^{15}N values fall between +2 to +6, a product of obtaining nitrogen from decayed organic matter (Schwarcz and Schoeninger 2012). In contrast, plants with an atmospheric nitrogen fixing bacterial association generally have δ^{15}N values in the range of -4 to +2‰ (White 2013). However, soil nitrogen concentrations and isotope ratios are determined by a dynamic balance of soil inputs, bacterial and chemical action and offgassing, making predictive modeling difficult (Amundson et al. 2003). General trends have been noted. High aridity is correlated with more positive δ^{15}N in herbivores (Heaton 1986; Schwarcz, Dupras, and Fairgrieve 1999) and high salinity correlates with more positive δ^{15}N as well, (Ugan and Coltrain 2011; Karamanos and Rennie 1981; van Groenigen and van Kessel 2002).

On the Colorado Plateau, many soils have quite low organic proportions (Benson et al. 2013). The presence of cryptobiotic crusts (associations of cyanobacteria, fungi, lichens and moss) convert atmospheric nitrogen into a biologically usable form (Belnap, Williams, and Kaltenecker 1999; Belnap 2002; Evans and Belnap 1999). Such crusts can provide greater than 70% of total soil nitrogen (Belnap, Prasse, and Harper 2001) and result in entire biological communities exhibiting negative δ^{15}N values usually associated with species in symbiosis with nitrogen fixing bacteria (Flanagan, Cook, and Ehleringer 1997). In San Juan County, Utah, several isotopic studies show whole plant communities for which crustal inputs are the primary nitrogen source (Evans and Belnap 1999; Flanagan, Cook, and Ehleringer 1997; Lewis and Coltrain 2014; Lewis, Coltrain, and Burrillo 2017).

When modeling human diets on the Colorado Plateau, the difference in δ^{13}C between C3 and C4+CAM species ($\approx$ 10‰) is greater than most environmental effects (maximum 5‰, smaller locally), and will have minimal effects on model outputs. On the other hand, shifts in δ^{15}N due to crustal inputs and salinity are on the order of 3–4‰: equal to one trophic level, the approximate range of available resources for humans and fauna in terrestrial ecosystems. Such shifts may be transmitted up the food-web and affect both consumer and resources (both floral and faunal) δ^{15}N, resulting in potential change in model outputs.

Thus, while $\delta^{13}C_i$, $\delta^{15}N_i$ and e_i values for wild plant resources can be calculated from ancient or modern flora, attention must be paid to the potential for environmental variability on different spatial scales. The amount of variably within a human foraging catchment will vary by local ecology and will need to be determined experimentally through ap-

propriately designed sampling regimes. In addition to environmental variables, different plant tissue components (e.g., starch, lignin, cellulose, etc.), whole tissues, and entire organs can exhibit a range of δ^{13}C and δ^{15}N values (Bowling, Pataki, and Randerson 2008; Carlson and Kingston 2014; Hobbie and Werner 2004). Chapter 3 describes the approach to these issues at Cedar Mesa.

2.4 The Basketmaker II Stable Isotope Record

The simple model outlined above with its ability both to distinguish C3 and C4 based diets and to make trophic level comparisons has driven the majority of Basketmaker II isotopic studies—often coming into conflict with the conventional wisdom or interpretation of the Basketmaker II archaeological record. While more recent analyses have begun to address some of the uncertainties arising from tissue differences and source variability, interpretation is hindered by a lack of robust, local resource sampling.

The first isotope studies of Basketmaker II human burials were part of the Cedar Mesa Project (Matson and Chisholm 1991; Chisholm and Matson 1994). The δ^{13}C values obtained mapped into the C4 herbivore space, and a one-dimensional C3/C4 mixing model suggested a diet high in maize (80-90%, (Matson 1991), in contrast to the single archaic burial from Sand Dune Cave (Matson and Chisholm 1991). Studies from Black Mesa (Martin 1991) and the Virgin River Anasazi (Martin 1999) confirmed this regional pattern. These analyses provided an independent line of evidence for high maize diets and were instrumental in changing the view of Basketmaker II from a "mobile transitional economy" to full-time agriculturalists.

The "White Dog" phase was similarly challenged by isotopic studies. Examining Basketmaker II burials from the American Museum of Natural History, Coltrain and colleagues (Coltrain, Janetski, and Carlyle 2007) radiocarbon dated "White Dog" phase individuals from Marsh Pass Arizona, obtaining dates prior to 1 AD. However, the δ^{13}C values suggested maize dependence (see Table 2.1), providing independent confirmation of a fully agricultural population from 500 BC.

Studies of Eastern Basketmaker II have been more limited. Collections of southwestern Colorado burials identified as Basketmaker II by material culture in fact dated to Basketmaker III and/or Puebloan periods (see discussion in (Coltrain, Janetski, and Carlyle

2006)). Only six adult burials from Durango, Colorado, dated to the Basketmaker II period, of which only the two earliest burials may indicate moderate C3 inputs. The sample size makes inference hazardous, but suggests that some Eastern Basketmakers were fully agriculturally dependent and that the subsistence differences between Western and Eastern Basketmakers II—identified by other archaeological metrics—may have varied in time and space.

Dating issues have also arisen in a reanalysis of specimens obtained from Wetherill's excavations at Cave 7 and sites on Cedar Mesa which suggested that despite evidence for interpersonal violence, the original interpretation of the site as a "massacre" may not be accurate (Coltrain, Janetski, and Lewis 2012) (but see also (Geib and Hurst 2013)). The stable isotope values are similar to other Basketmaker populations (Figure 2.4, Table 2.1), but the sample size was large enough to identify age and sex based differences in δ^{15}N suggesting that men consumed more animal protein than women and children.

Most recently, Cooper and colleagues (Cooper et al. 2016) identified cyclical (seasonal) variation in isotope ratios in 1 cm lengths of human hair from Basketmaker II contexts in Turkey Pen Ruin on Cedar Mesa. Within hair strands, average shifts are 2.9‰ $\delta^{13}C$ and 1.1 ‰ $\delta^{15}N$, suggesting seasonal changes in maize and animal protein consumption. Interpretation was not taken beyond identification of the variation and comparison with herbivore values.

It should be noted that, with one exception (Coltrain and Janetski 2013), these studies have relied on the comparative method of isotope analysis—that is, population averages are compared with one another and to herbivore and carnivore isotope ratios, and inferences drawn from those relationships. This comparison has been aided by the development of comparative burial assemblages, both from formative populations on the Northern Colorado Plateau (Coltrain and Stafford Jr 1999; Coltrain 1996) and hunter-gatherers in the Great Basin (Schoeninger 1999), and also from later puebloan occupations on the Colorado Plateau and in the Rio Grande Valley (see Summary in Matson and Chisholm (2007): for Pecos see (Spielmann, Schoeninger, and Moore 1990), and for the Central Mesa Verde region see (Decker and Tieszen 1989; Varien 1999)).

However, while simple comparison of consumer isotope ratios is suitable for identifying broad differences, such as C3 or C4 dominated diets (differences of 10‰), and for

distinguishing between trophic levels (3‰), it is less useful for interpreting the smaller (0.2-1.0‰) differences associated with spatial, temporal and sex-based isotopic differences in the Basketmaker II isotopic record (Figures 2.4, 2.5; Table 2.1).

Translating these smaller differences in δ^{13}C or δ^{15}N into behavioral analogues requires accurately parameterizing isotope mixing models, and propagating uncertainties into model outputs. To do so requires using formal mixing models and examining the uncertainties inherent in model underdetermination.

Even if input parameter uncertainties (e.g., resource and consumer δ^{13}C and δ^{15}N) were reduced to zero, there is still the problem of underdetermination in most mixing models. Recall that an analytic solution for n unknowns is possible for a system of $n + 1$ linear equations. A separate version of Equation 2.2 may be given for each isotopic pair measured (e.g., δ^{13}C, δ^{15}N etc) and by definition the sum of the source proportions must equal unity $\Sigma p_i = 1$. This means that intake of m sources can be analytically determined by $m - 1$ isotopic pairs. That is, if only δ^{13}C and δ^{15}N are measured, then an analytic solution is possible for no more than three sources.

As sources usually exceed isotopic pairs measured, alternative methods are needed—several have been developed. The interpretation of the output of these methods is subject to considerable debate. That debate and the implications for modeling Basketmaker II diets is the subject of the remainder of this chapter.

2.5 Stable Isotope Mixing Model Calculators

It is the common view among the users (and creators) of stable isotope mixing models that model outputs represent a distribution of source proportion estimates that can be interpreted as simple probabilistic estimates—for example, if estimates of source proportions are approximately normally distributed, the central values are more likely. Fry (2013a, 2013b) objected to this interpretation on theoretical grounds, but did not formulate his objection within a Bayesian probability framework. This difference in framework resulted in a cursory rejection of his argument by Semmens et al. (2013) who asserted that uncertainties in model inputs (e.g., source [or resource] and mixture [or consumer "whole diet" values] isotope values), combined with the Bayesian prior requires that outputs be interpreted as simple probability distributions.

Both Fry and Semmens are fundamentally correct, but they have misidentified the source of their disagreement. Mixing model outputs are probability distributions of source proportion estimates; however, the dependence of any one estimate on all other parameter estimates means that some portion of the output distribution is solely a function of mixing model geometry. Parameter estimates determined by this portion of the distribution cannot be considered jointly on account of the estimates' interdependences.

This is a complex concept and the two extreme cases may provide clarity. In the first case, input uncertainties are the sole cause of the indeterminateness of the system (that is, parameter best-estimates result in a perfectly determined system). In this case, the model output distributions reflect only propagated uncertainties and the relative probabilities of specific combinations of sources. Model outputs are largely independent of one another and may be considered jointly.

In the second case, mixture and source uncertainty is lacking and model output distributions are solely a function of system underdetermination (too many sources to permit analytic solution) and isotope geometry. In this case, source estimates are entirely interdependent and reflect the relative counts of specific estimate values in the set of equally probable combinations of sources. Such interdependent estimates cannot be considered jointly.

Most modeled systems fall between these extremes. Semmens and Fry differ in interpretation both due to the difference between their modeling approaches and because they favor examples, respectively, from the first and second extreme cases. To provide a clearer foundation for modeling Cedar Mesa Basketmaker II diets, three mixing model approaches are reviewed which together illustrate (but do not quantify) how both model underdetermination and input uncertainties affect mixing model outcomes. The argument may be summarized as follows:

1. The mixing programs ISOSOURCE and SISUS both explicitly uniformly sample from source combinations (e.g., "feasible solutions") within an N dimensional "feasible region" defined by source values.

2. The Bayesian Markov Chain Monte Carlo (MCMC) process of MixSIAR ends with a "stable" sample of solutions. If no source or mixture uncertainties are included,

this process results in a uniform sampling of the same "feasible region" of SISUS and ISOSOURCE. In all three systems, all solutions are equally likely from a computational perspective.

3. In mixSIAR, if source and mixture uncertainties are incorporated into the model, these effects extend the "feasible region" to include combinations of sources that fit the data less well. Thus, any mixSIAR model contains a "core" of feasible solutions with approximately equal likelihoods (these would be uniformly sampled if uncertainty were ignored), and a periphery of feasible solutions with varying but lower likelihoods.

4. For a uniform sampling of the "feasible region," distributions of source proportions in "feasible solutions" are a function of the geometric shape of the "feasible region," which is determined by the number of sources and their values.

5. The principle of indifference (any solution is equally likely) permits uniform sampling of solutions within the "feasible region" to identify the most frequent values for the proportional contribution of any source. However, these frequencies cannot be used concurrently to identify more likely "feasible solutions" (since by definition all uniformly sampled solutions in the "feasible region" are equally likely).

6. The same principles and objections extend to distributions of source proportions that are weighted by the likelihoods of individual sources.

In consequence, both Semmens (2013) and Fry (2013b) are correct, albeit only for the extreme cases of mixing models (e.g., otherwise determined systems with input uncertainties, and undetermined systems with no input uncertainties). Until such time as methods are developed to quantify the relative contributions of input uncertainties and model geometry to mixing model outputs, the range rather than summary statistics of parameter estimates should be used for inference—though the shape of the distribution and "feasible region" considered together can give the most complete picture of the model.

This is the reason behind the common warning

> *Just as it is important to incorporate sources of variability and uncertainty and not just rely on point estimates in mixing model inputs, researchers should report the distributions of source proportion estimates and not just summary values (e.g.,*

means or medians) in mixing model outputs. As Phillips and Gregg (2003) (Phillips and Gregg 2003) stated in their concluding sentence, "To avoid misrepresenting the uniqueness of the results, users should report the distribution of feasible solutions rather than focusing on a single value such as the mean." (Phillips et al. 2014, 831)

2.5.1 ISOSOURCE: a Brute Force Calculator

ISOSOURCE is an early mixing calculator that uses brute force calculation to map the feasible region(Phillips and Gregg 2003; Phillips, Newsome, and Gregg 2005; Fry 2013a). Since there are an infinite number of possible source proportions between 0 and 100%, ISOSOURCE constrains these proportions to a level determined by the user (e.g., θ_i is calculated at a 1% or 0.5% step) and then calculates the resulting finite number of mixtures. Each set of θ_i (e.g., $[\theta_1, \theta_2 ... \theta_n]$), resulting in a δ_{mix} within a certain user-defined proximity to the observed mixture value (δ_{obs}) is defined as a "feasible solution" and recorded. The set of "feasible solutions" defines the "feasible region" from which the output distributions of each source proportion can be obtained.

This process can be understood through the analogy of the topographic map as follows (refer to Figure 2.6): for every x, y pair at a user-defined resolution, ISOSOURCE calculates the elevation (z) and then subsets those x, y pairs where $z > Z$ (where Z is a user defined "close enough" threshold). The subset of x, y, pairs defines the "feasible region." Note that this process results in a nearly uniform sampling of the "feasible region" (excepting approximation errors), and that, while a distribution of mapped points can be formed, the entire range of feasible values results in valid solutions.

Technically ISOSOURCE can incorporate uncertainties in source and mixture isotope values into the model—by combining multiple model runs of varying input parameters. However, the procedure is "clunky" and computationally intensive. For example, one could run the ISOSOURE model three separate times using the mixture isotope values for the mean, mean+1 SD, and mean-1 SD. This could be done for every isotopic pair and the results combined to define a "feasible region" incorporating mixture uncertainty. Theoretically the same procedure could be repeated at $\pm$2SD and extended to source uncertainties—but the number of model runs (and computational time) increases exponentially. A different approach is needed based on more efficient sampling.

2.5.2 SISUS: a "Feasible Region" Sampler

SISUS uses a two-step procedure to approximate the range and distribution of the feasible region (Erhardt et al. 2014). The first step defines the boundaries of the feasible region by calculating the most extreme solutions; the second step samples solutions uniformly within this boundary (Figure 2.7).

Both SISUS and ISOSOURCE uniformly sample the "feasible region." The latter does so through sequential sampling across each dimension at a defined resolution, the former through a series of random jumps through the "feasible region." While it may take a long sequence of random jumps to adequately sample the "feasible region," SISUS is considerably faster than ISOSOURE and has the advantage of sampling at an effectively infinite resolution

Because SISUS is computationally less intensive than ISOSORUCE, it would be possible to incorporate mixture, source, and even trophic level enrichment uncertainties into the model without prohibitive computational times. However, uncertainties of model inputs such as mixture, source and trophic level enrichment values have not been implemented in SISUS calculations according to the current version of the SISUS manual (3.1.16-3.1.17 of 2014 SISUS manual (Erhardt et al. 2014)). Consequently, the edge of the feasible region is approximately identical with ISOSOURCE. The speed of computation permits users to make calculations for multiple input values (e.g., δ^{15}N trophic level offsets for +2, +3 and +4), but model uncertainties have not been propagated into model outputs. To do so requires using a full Bayesian modeling system.

2.5.3 MixSIAR: a Bayesian Markov Chain Monte Carlo (MCMC) Estimator

MixSIAR takes a different approach to mapping the feasible region. Both ISOSOURCE and SISUS defined, albeit in different ways, the edges of the "feasible region." MixSIAR does not formally define the edge of the feasible region. Rather it creates a sampling system such that the eventual distribution of sampled points coincides with a "feasible region." This idea is complex and a full mathematical treatment can be found elsewhere (Stock and Semmens 2013; Moore and Semmens 2008; Holmes 2017).

The basic concept is that it is possible to construct an algorithm that generates a chain of source proportion estimates that will eventually converge on and map the extent of

the "feasible region." The basic algorithm used to update source estimates in mixSIAR is the Gibbs Sampler which sequentially calculates a conditional probability distribution for the proportion values of a single source, given the current estimates of all other source proportion values, and the observed source and mixture data and uncertainties. It has been shown that sequentially updating all parameter estimates by the Gibbs Sampler method results in distributions of parameter estimates that converge on the posterior joint probability distribution of all parameters, given current knowledge. The Gibbs Sampler will converge on this posterior probability distribution regardless of initial source proportion estimates (usually chosen as "uninformative" with all values equally likely).

The process generates a sample of sets of parameter estimates (e.g., a sample or chain of the continually updating set $[\theta_1, \theta_2 ... \theta_n]$) that converges on a sample whose sampling density is proportional to the joint probability distribution for all parameters in the set. Inverting the mathematical process clarifies how the method functions. Although not strictly accurate, since the joint probability distribution is calculated after the sampling process—the Gibbs Sampler can be thought of as "climbing" likelihood hills—albeit hills that do not exist until after they are mapped. The sampler movement has a random component due to the shape of the conditional probability function which allows limited downward movement, preventing the algorithm from getting stuck at a local (but not global) high point. The size of the jump is arbitrarily limited to force the algorithm to "explore" locally as it moves (Figure 2.8).

If the chain is sufficiently long, it will generate a representative sample of points in the "high likelihood" region. Further sampling will not change the relative densities of sampled points and the sample density will be equivalent to the joint probability for all parameters. Such stability is measurable by standard statistical tests, and the computational speed of calculation is increased by "burn in" (ignoring the early values) and "thinning" (see Figure 2.8). Once a chain achieves stability, the "feasible region" may then be defined by a Bayesian credible interval.

2.5.4 Interpreting Mixing Model Outputs

These three models all define the "feasible region" in different ways. In ISOSOURCE, the region is approximated by mapping weighted averages that yield a delta value suffi-

ciently close to the consumer's isotopic composition. SISUS formally calculates this same boundary, and then uses sampling to speed up the process of generating stable distributions of source proportion values. MixSIAR uses a hill climbing algorithm to define likelihood plateaus and derives the boundaries of the feasible region around them.

Interestingly, when MixSIAR is run with high parameter certainties its solutions converge on those of ISOSOURCE and SISUS. While the convergence of model outputs does not demonstrate that the same mathematical entity is being described, the convergence does clarify how the geometry of the "feasible region" influences model outputs under all three systems.

2.5.4.1 MixSIAR with Perfectly Defined Parameters

Note that if mixture and source uncertainties are very small, almost all source combinations will either fit the data very well, or very poorly. The likelihood component in the conditional probability distribution will take values of 0 or 1 and will form a step-like or plateau-shape sampling distribution. Consequently, once a high likelihood region is found, the chain will tend to sample only the "top" of the likelihood hill and all sampled combinations of sources will have approximately the same likelihood. The distribution obtained will become approximately uniform.

This uniform sampling is illustrated by a comparison of models. Erhardt and colleagues (Erhardt et al. 2014) compared SISUS outputs for a mink diet model to a full Bayesian model (e.g., mixSIAR). While SISUS exhibited biases in source proportion estimation relative to an equivalent model in mixSIAR, it returned the same estimates as a mixSIAR model run with a tripled sample size.

> *Considering the analysis based on the original data, the posterior means based on SISUS tends to identify the major and minor sources of mink diet, but the estimates of the dominant sources are somewhat inaccurate [relative to the regular mixSIAR model]. The SISUS summaries also tend to underestimate uncertainty in the marginal posterior distributions, which is expected. The SISUS means and standard deviations for analyses based on a single isotope are much more accurate, as are the summaries for analyses in which the sample size was tripled. (Erhardt et al. 2014, 296)*

Tripled sample size greatly reduces mixture uncertainty and reduced mixture uncertainty makes the mixSIAR model tend toward uniform sampling the "feasible region," the process used explicitly in SISUS. As illustrated below, this uniform sampling is also present

within mixSIAR models that incorporate uncertainty.

2.5.4.2 Incorporating Uncertainties into MixSIAR Models

MixSIAR permits users to incorporate source, mixture and trophic level enrichment uncertainties into the model. Increasing these uncertainties changes the shape of the likelihood component of the conditional probability distribution. Combinations of source proportions may now take values intermediate to 0 and 1, which reflect source combinations that are possible but less likely given source and mixture isotope values. This increases the likelihoods of previously excluded combinations of sources and thus expands the "feasible region." However, since these solutions have a lower likelihood than the core of solutions (e.g., they are "downhill"), the algorithm will sample these lower probability solutions at a lower rate.

The "feasible region" thus has an approximately uniformly sampled "core" and a periphery of feasible solutions whose sample density is weighted according to the likelihoods of individual solutions (again, this explanation inverts the logic of the model–in reality the sampling density converges on posterior joint probability distribution of all parameters). Stability and confidence intervals (e.g., 95% of samples) still define the feasible region, but the edges of the region will now show decreasing sample density reflective of the probability of solutions in that local region.

The ability to assign probabilities to individual solutions does not mean that source proportions may be simply probabilistically described. Rather, the distributions of source proportions output by the model are a function of both solution likelihoods (derived from input uncertainties) and model geometry.

2.5.4.3 Misapplication of the "Principle of Indifference"

The above sections have described how three models calculate the set of "feasible solutions" to underdetermined isotope mixing models. All three models return outputs of the distribution of source proportions in the "feasible solutions"—distributions that are often tacitly interpreted as independent probabilistic estimates of the source proportions in the actual diet.

This view is only correct in the extreme case outlined above in which input uncertainties alone cause multiple solutions. In all real world applications, a portion of the

output distribution is determined by mixing model geometry. To see this, consider again the second extreme case in which system underdetermination is the sole cause of multiple solutions. In this case, all feasible solutions are equally likely. ISOSOURCE, SISUS and the "core" solutions in mixSIAR models generate are approximately uniform samples of the "feasible region" and thus illustrate this second extreme case. Since sampling in ISOSOURCE is easy to visualize graphically, this argument will refer to Figure 2.9 and the sampling method specific to ISOSOURCE. However, the logic applies equally to SISUS and mixSIAR.

In both models, the distributions of x and y values in the uniformly sampled pairs represent the source proportion distributions output from the model. In this example, the step = 0.5 and the frequency distribution of feasible x and y solution values is given in Table 2.2 and histograms superimposed on a plot of the feasible region sample in Figure 2.9.

The most likely x and y values are 0, 0.5 and 1, each sampled 7 times. If these distributions are taken as independent probabilities, then by joining them, the most likely feasible solutions (the central nine points in Figure 2.9) could be found. This is erroneous reasoning and contrary to the initial assumption of uniform sampling. However, it is also the natural interpretation of treating source proportion distributions as probabilistic estimates of independent parameters.

This error arises because x and y are not independent. The pair of values (x, y) represents a single feasible solution uniformly sampled from the "feasible region," a finite area. Any x value limits the possible y values sampled and vice versa. The central values in the x and y distributions do not reflect more probable solutions, but instead reflect the shape of the "feasible region"—given a uniform sampling.

For example, in Figure 2.9, the frequency of either x or y simply reflects the width of the "feasible region" in the other dimension. If the "feasible region" were a three-dimensional volume, the frequency distribution in any one dimension would reflect the cross-sectional area in the other two dimensions. The same is true in a uniform sampling in N dimensions—frequency of source proportions is a measure of the shape of the feasible region.

This can have unusual consequences. In the case of a multimodal or asymmetric "fea-

sible region," the most frequent x and y values could refer to almost entirely different sets of points—or even to pairs of x and y values that lie outside the "feasible region" entirely. In all cases, errors in reasoning arise if estimates of x and y are treated as independent and used to infer anything about the probabilities of pairs (x, y). As Fry noted *(Fry 2013b): when isotope geometry dominates the model, all feasible solutions are equally probable.

Most real world applications of mixing models incorporate both system underdetermination and input uncertainties. Both factors must be considered in interpreting model outputs.

2.5.4.4 Model Output Ranges

If all solutions in a uniformly sampled "feasible region" are equally probable, the total range of modeled source proportions is the only metric which fully captures the range of model outcomes. However, as noted above, source and mixture uncertainties can be propagated through mixSIAR, resulting in an addition of solutions to the "feasible region" whose sampling density reflects the likelihood of individual solutions, given resource and mixture uncertainties. In such a model, the distribution of source proportions (x or y) will be a combination of the shape of this expanded feasible region and is weighted according to the likelihood of each individual solution.

In consequence of this fact, reporting and inferring from the Bayesian credible interval (e.g., the range of model solution values) from mixSIAR permits both elements to be correctly interpreted. The outermost edges of the feasible region will be probabilistically defined (making the credible region usable), while the shape of the central part of the output proportion distributions will be understood to reflect the shape of the "feasible region." This shape, however, can also be approached through multidimensional plotting and analysis, allowing the identification of source correlations (Semmens et al. 2013).

At present, there is no quantitative method for partitioning the portions of parameter estimate distributions derived from propagated input uncertainties from those derived from mixing geometry. In consequence, this study reports mixing model outputs in terms of credible interval ranges for each source, but also examines the "feasible region" through the use of bivariate source plots (see Chapter 5), permitting a second diminutional description of the shape of the feasible region and better defining the combinations of sources in

"feasible solutions."

2.5.5 Isotope Mixing Models Summary

Where the feasible region is uniformly sampled, the distribution of source proportion estimates is largely a function of the shape of the "feasible region" as Fry suggests. For better determined systems with input uncertainties, the probabilistic interpretation of Semmens is valid. Consequently, source proportion ranges, supplemented by an examination of correlation between sources in feasible solutions are the best basis for behavioral interpretation. To review again the two extreme cases:

1. If the system is determined and there is a single solution based on source and mixture values, but input uncertainties expand the "feasible region," the output distribution of mixSIAR will be completely and independently probabilistic. In this case, measures of central tendency and dispersion in the posterior distribution are statistically and interpretively meaningful.

2. If there are no parameter uncertainties, the source proportions distributions of either mixSIAR, or SISUS or ISOSOURCE reflect only the shape of the "feasible region" and source interdependence. In this case, only the range of solutions and shape of feasible region are interpretively meaningful.

3. In most real applications, the output distribution will be composed of elements deriving from the mixing geometry and elements deriving from input uncertainties. In these cases, solution ranges should be reported while central tendencies—and other measures of the shape of the "feasible region"—should be used to appoximate the effects of model geometry.

Thus, under almost all real world applications, mixing model estimates should be reported as ranges, with central tendencies and dispersions used only to describe which combinations of sources are feasible. Since ranges rather than central estimates define the set of "feasible solutions," the expansion of the "feasible region" by incorporating mixing uncertainties is critical when attempting to model the diets associated with different mixture values. Without incorporating these uncertainties, models may return falsely separated source proportion ranges.

2.6 Narrowing Output Distributions via Resource Aggregation

Since the primary cause of wide source contribution estimates is an underdetermined system (more sources than isotopes), resource aggregation may be useful (Phillips, Newsome, and Gregg 2005; Phillips et al. 2014). This aggregation may be done prior to modeling (e.g., a priori) or after the model has been run (e.g., a posteriori), but each method is only appropriate in particular settings.

2.6.1 A Priori Aggregation

In a priori aggregation, resources are combined into higher taxonomic units prior to running the mixing model. The most obvious case occurs when resources are statistically indistinguishable from one another across all input parameters. In this case, one not only may choose to aggregate, but should aggregate, as the separation of identical resources will introduce additional uncertainty into the model outputs.

A priori aggregation into larger taxa may also be made for resources that are significantly different, if the within-taxa difference is small relative to the between-taxa difference. In Chapter 4, this principle is used to combine individual species into larger categories of both C3 and C4+CAM plant resources. One complication of aggregation of statistically distinct resources is that the dispersion around the estimate of the mean is no longer normal. Geometry can be used to specify the parameter space that a mixture must fall within and an estimate of dispersion obtained, but the dispersion estimate for such an aggregation must be explicitly specified.

2.6.2 A Posteriori Aggregation

In a posteriori aggregation each valid solution is calculated and resource proportions are combined within each calculated solution (preserving the covariance of the aggregated resource contribution estimates) and the resulting distribution described.

Such aggregation may be made independent of the isotopic similarity of the resources, but will only aid interpretation if the resulting taxonomic category is interpretively useful. Thus, shellfish and shore fish may be combined, if littoral resources are of interest (Newsome et al. 2004). However, this aggregation will narrow resource proportion estimates only if the estimates of individual resource proportions are negatively correlated. Such

negative correlation in resource proportions implies that the resources substitute for one another within the model and that no amount of increased precision in measuring source isotope values will improve model power. In Chapter 5, this technique is utilized and the interpretive problems that arise from such aggregation are discussed.

2.6.3 A Posteriori Linear Constraints

Linear constraints on model outputs can also be used to narrow the range of solutions. If the investigator can posit that resource A could not have contributed more than 20% to the diet, the feasible mixtures can be subset to exclude those where $A < 20\%$. Linear constraints will be most effective at reducing the ranges of source proportions when model outputs are correlated—since constraining one resource will also constrain the second. While the logic of the constraint is easy to understand, linear constraints, like source aggregation, do require additional assumptions extrinsic to the mixing model.

2.7 Chapter 2: Review and Conclusions

At the level of approximate trophic level and C3 vs C4+CAM inputs, simple isotope models mapping human whole diet values into herbivore, carnivore, or C3 and C4 isotopic spaces are adequate, and have contributed substantially to the interpretation of the Basketmaker II isotopic record. As that record increases in size, intergroup variation (e.g., sex-based, Eastern vs. Western, temporal) on the order of 0.5-1‰ has been observed. Interpreting this level of variation requires the use of formal mixing models, which have now become sufficiently sophisticated to incorporate source uncertainties.

There is a widespread misconception that mixing model output distributions can be interpreted and simple and independent probabilistic estimates of source proportion. Consideration of three mixing model programs and their underlying assumptions shows that both brute force calculators and Bayesian estimators will return output distributions for under-determined systems that are structured by a combination of source uncertainty and isotope geometry.

1. To date, only the Bayesian estimators have implemented an effective means for incorporating and propagating input uncertainties (uncertainties in mixture and source delta values and trophic level enrichment factors) through the model.

2. The output distribution in any model is a combination of solutions arising from system underdetermination (too many sources), and those arising from the incorporation of model uncertainty.
   (a) The solutions arising purely from geometric underdetermination cannot be treated probabilistically. All solutions are equally probable and central tendencies in source proportion distributions are artifacts of the shape of the "feasible region."
   (b) The expanded range of source proportions in the "feasible region" arising from the incorporation of input uncertainties can be treated probabilistically, but current methods cannot distinguish between these two causes of model underdetermination.
   (c) Real world models contain both elements, requiring inference from both the credible interval range for source estimates, and an understanding of the shape of the feasible region derived from source estimate distribution shapes and correlations.
3. Methods for reducing output distribution ranges have been developed, including resource aggregation—both a priori and a posteriori—and linear constraints on modeled outputs. Successful application of these techniques requires examination of the correlations in model outputs and the relationship of source and mixture values in isotope ratio space. However, such constraints cannot be based solely on model outputs, but require justification through theoretical considerations and independent data.

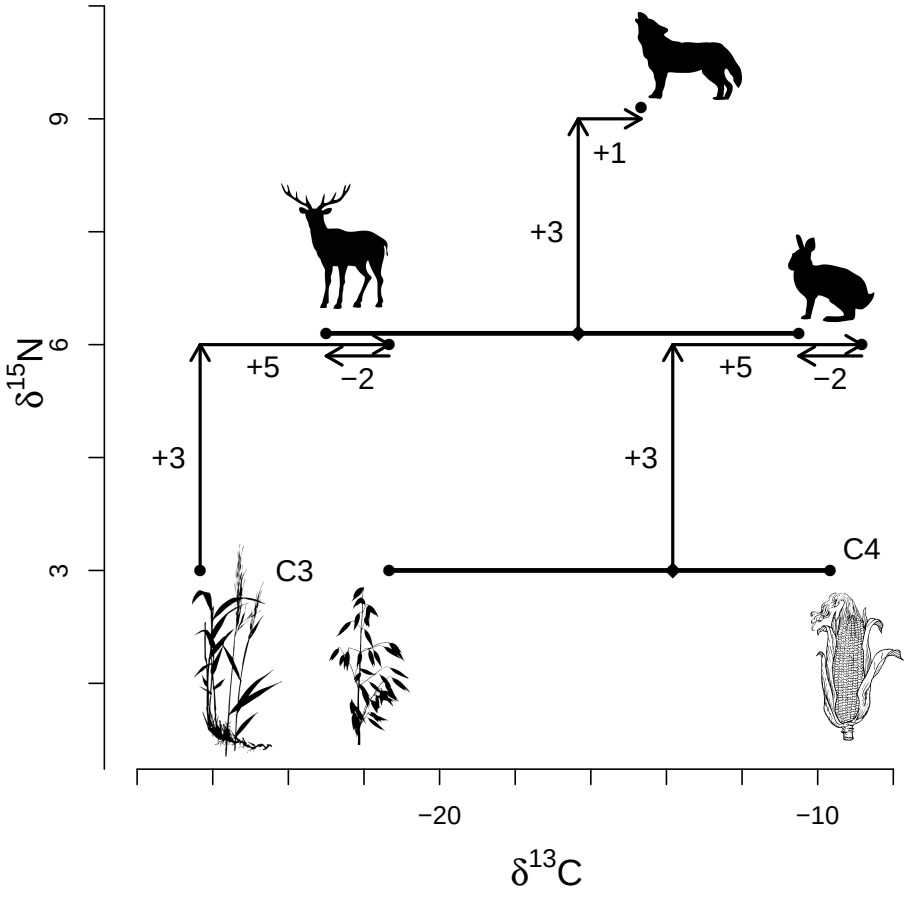

Figure 2.1: Isotopic ratios of plant tissue bone collagen and lean muscle in an ideal food-web. Consumer collagen values are determined by a weighted average of the resources consumed and a Trophic Level Enrichment (TLE): δ^{13}C (+5 for plant diets,+1 for animal protein) and δ^{15}N (+3). Lean muscle (the faunal tissue consumed) is 2‰ depleted in δ^{13}C relative to faunal bone collagen.

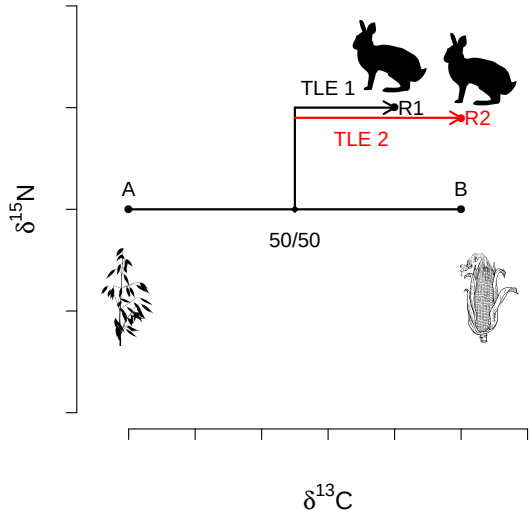

Figure 2.2: Effects of Trophic Level Enrichment (TLE) uncertainty. The same diet (50% A, 50% B) yields different δ^{13}C tissue values depending on the TLE estimate chosen. Since TLE estimates vary, a range of dietary solutions is implied by any single tissue isotope value.

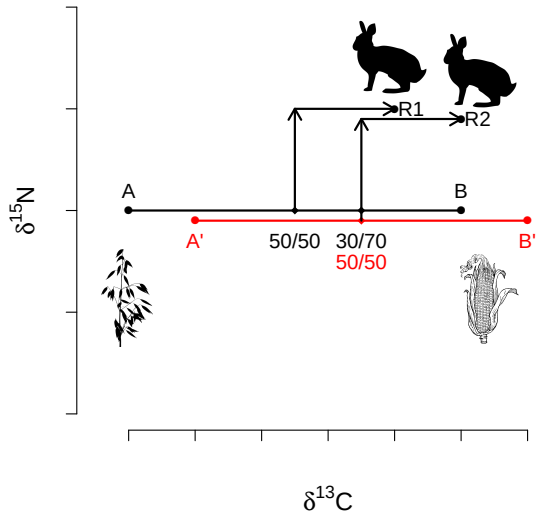

Figure 2.3: Effects of source uncertainty on diet models. Two rabbits with different isotope ratios R1,R2 imply diets with differing proportions of A and B. Systematic changes in source values (A′,B′) change the implied diet. Consequently models must control for environmental variation in resource isotope values, ideally at the spatial scale of the consumer's foraging catchment.

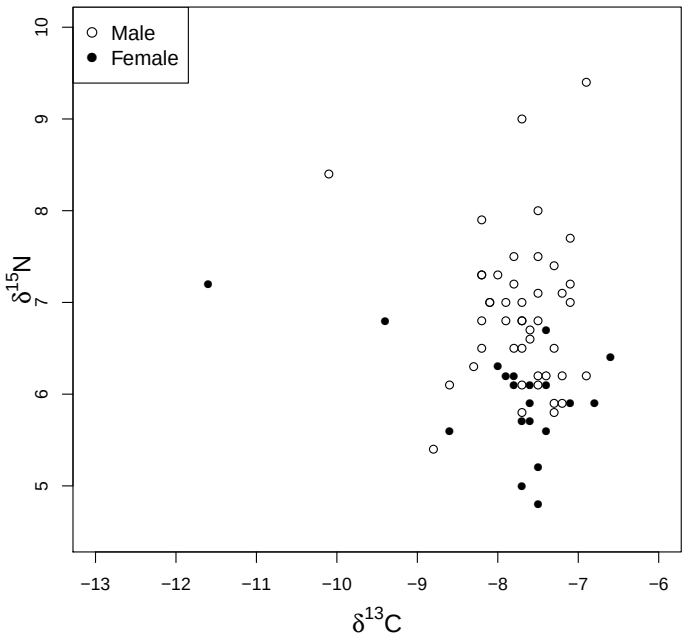

Figure 2.4: Stable isotope carbon and nitrogen delta values for Cedar Mesa Basketmaker II adults by sex.

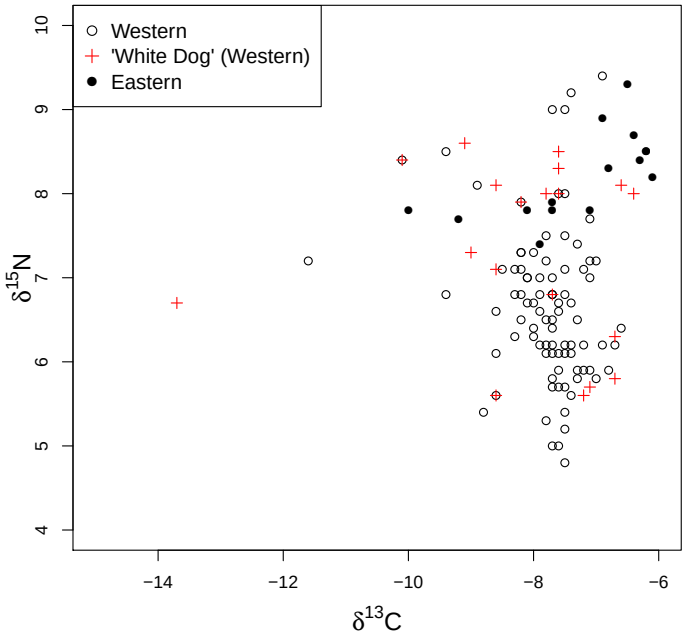

Figure 2.5: Stable Isotope values for Western and Eastern Basketmaker II and III burials. Pre- AD 1 Western "White Dog" Basketmaker II burials plotted as red crosses.

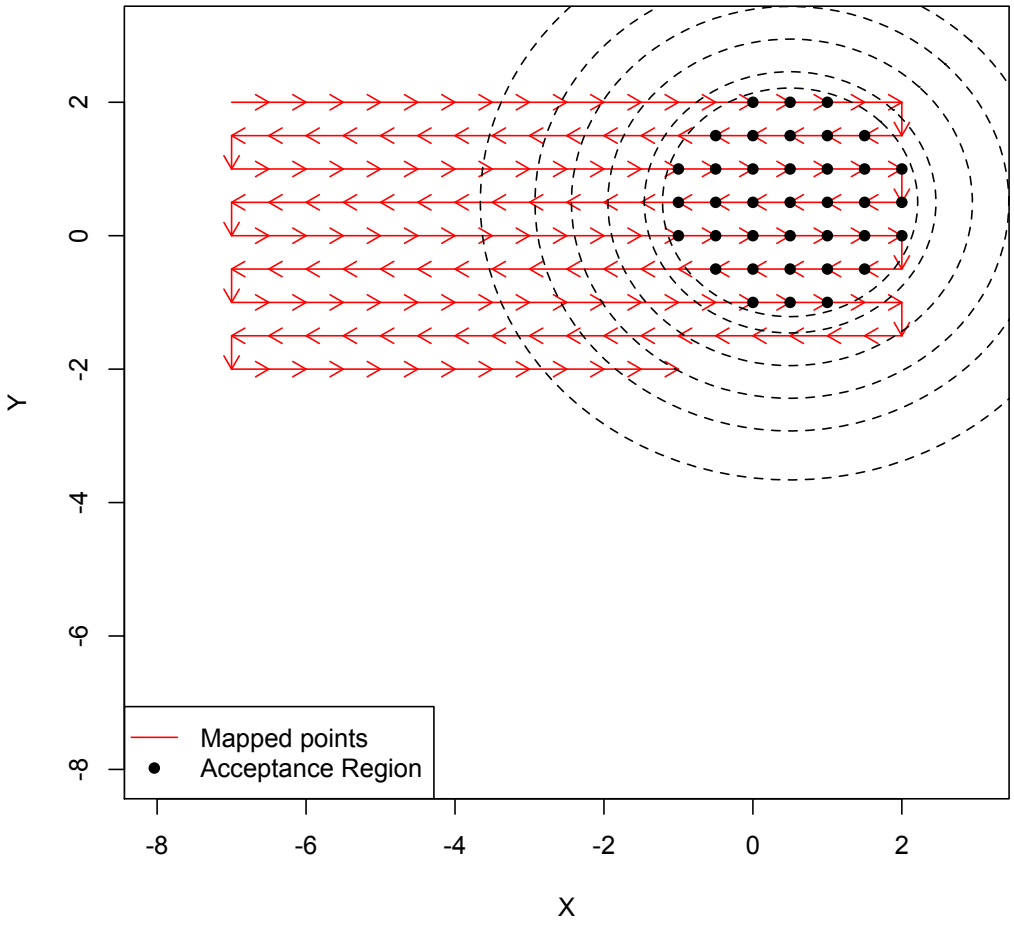

Figure 2.6: Schematic of brute force (ISOSOURCE) calculation of peak of hill/butte on topographic map (concentric circles). In the function $z = f(x, y)$, z is a measure of how closely $f(x, y)$ approaches some observed mixture value. Then, by sequential calculation a complete map of z may be obtained. By subsetting only those z (or x, y pairs) with elevation (or goodness of fit) higher than a user specified threshold Z, the set of x, y defining the "acceptance" or "feasible region" can be identified. Note that computation becomes costly as uncertainties in mixture and source values are incorporated into the model.

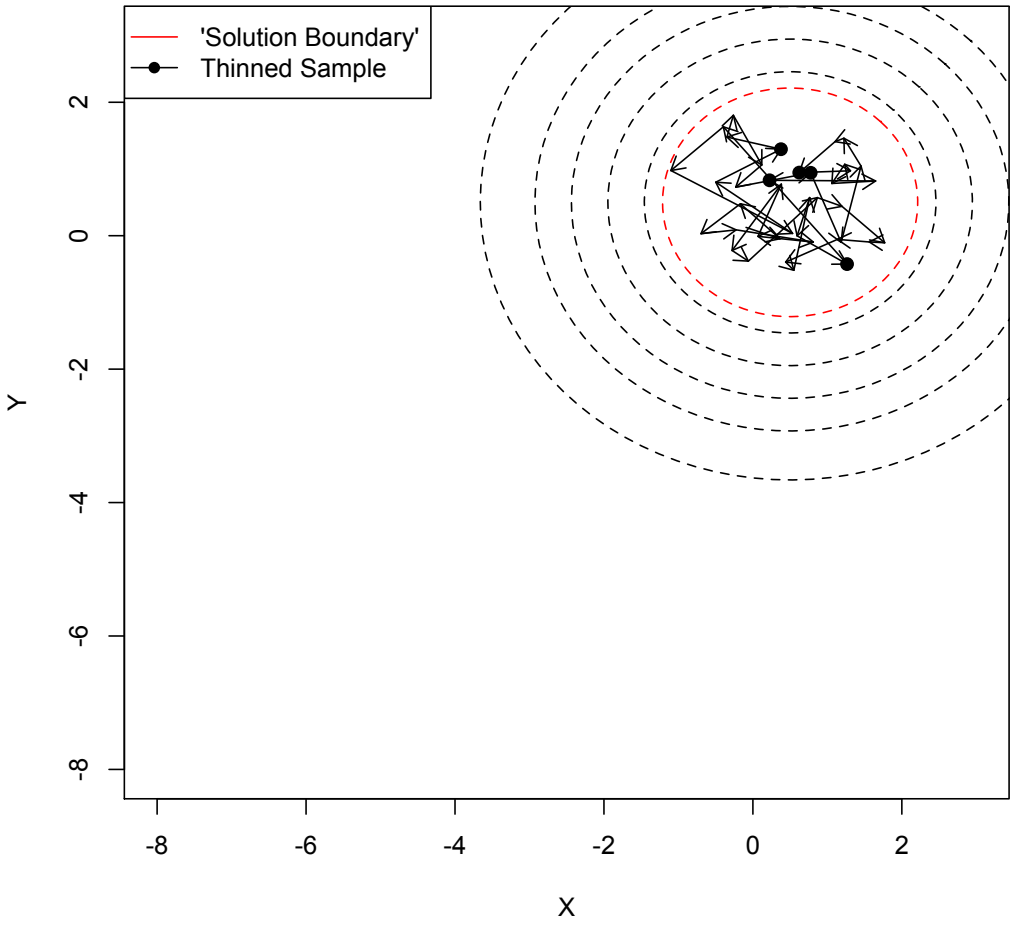

Figure 2.7: Schematic for SISUS uniform sampling model. SISUS first computes the outer boundaries of the solution space then samples within that space using an algorithm based on sequential uniformly sized and directed movements. Unlike ISOSOURCE there is no user defined "resolution" to the values tested, and the computation only needs to be carried out to the point where an appropriate sample of the "feasible region" has been obtained. This process results in significantly faster computation without loss of information.

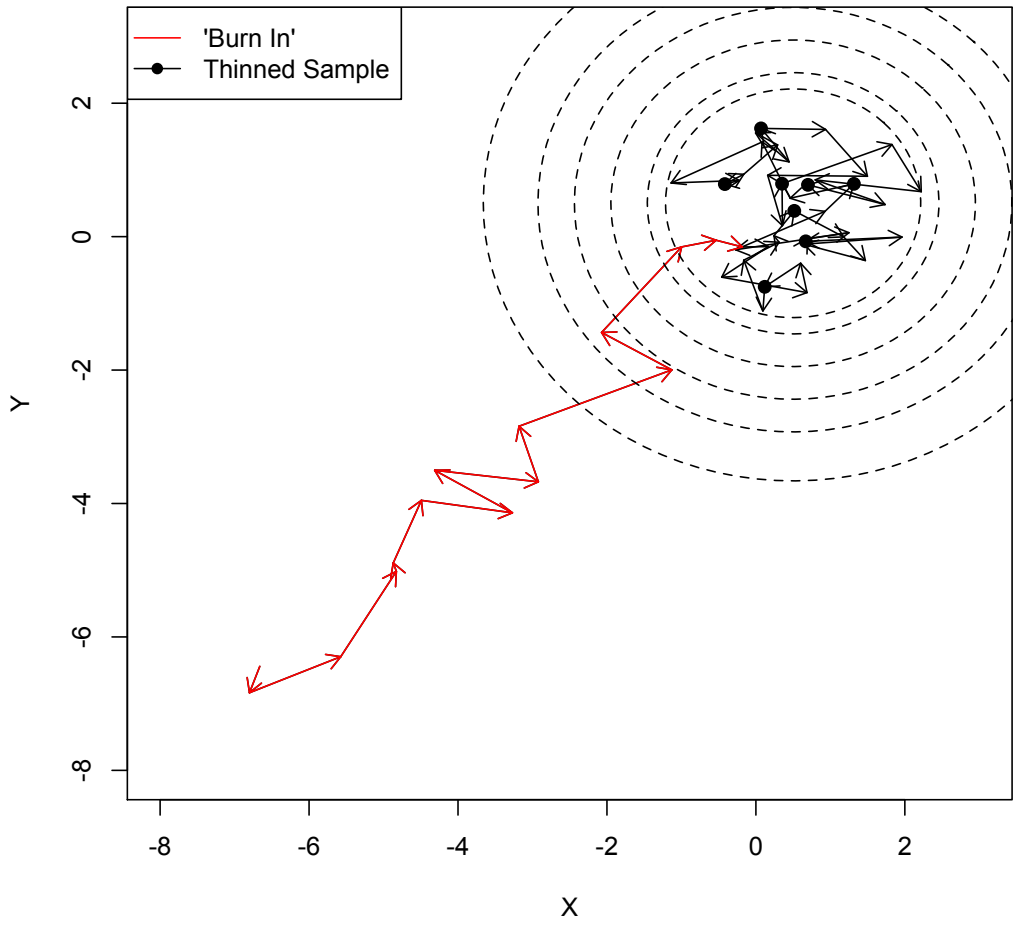

Figure 2.8: MCMC simulation schematic. Mapping path is stochastic but with greater chance of moving "up hill." The "burn in" period will place mapping algorithm near top of hill, where it freely moves around peak but rarely moves downhill. Thinning (e.g., taking every nth sample) removes any patterning derived from the recursive pathing calculation. With a sufficiently long run (not plotted for clarity), the distribution of x and y values in the thinned sample will stabilize at the peak and will approximate the distribution of x and y values associated with the acceptable region in Figure 2.6. In contrast to Figure 2.7 however the sampling within the solution space will reflect the underlying surface.

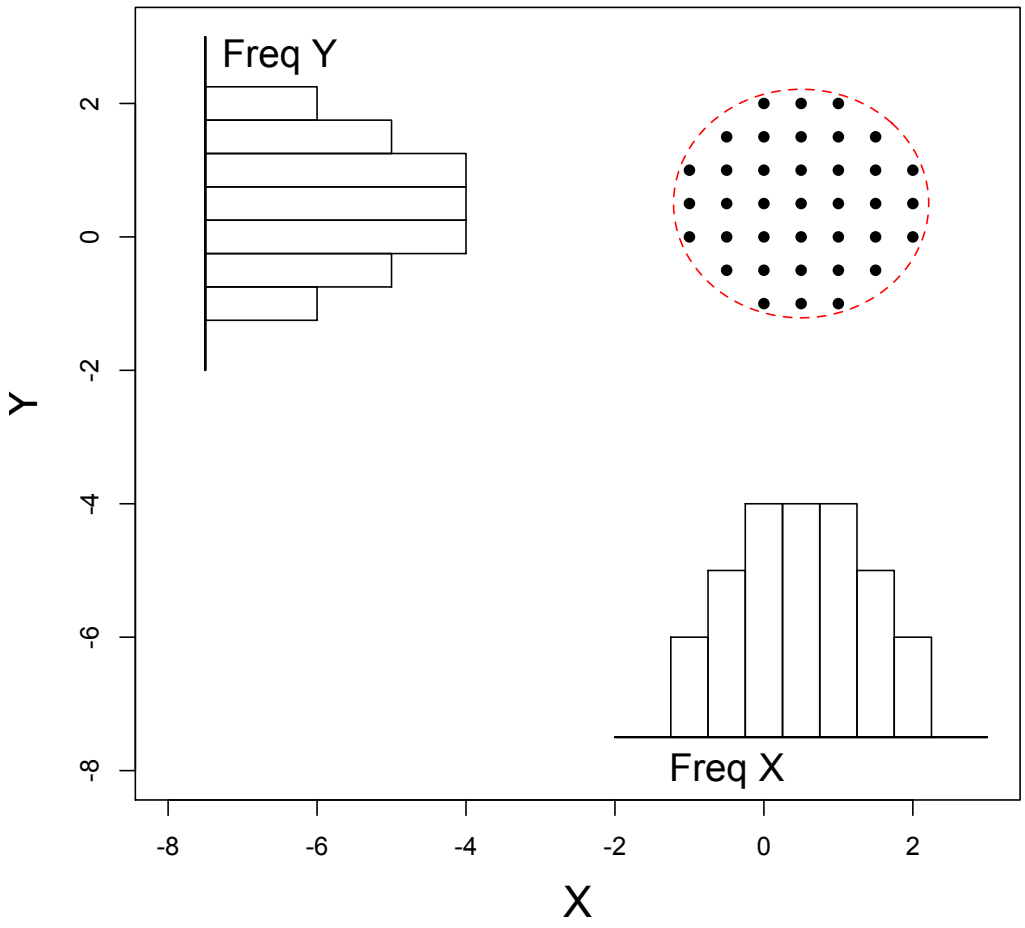

Figure 2.9: Uniform sampling of hypothetical feasible region and resulting x and y distributions (Table 2.2). Frequency distributions of sampled x and y values (equivalent to the source proportion distributions output by mixing models) plotted as indicated. Central tendencies in both x and y are a function of the shape of the "feasible region."

Table 2.1: Summary statistic for Basketmaker II and III adult stable isotope data. Data from (Coltrain, Janetski, and Carlyle 2006, 2007; Coltrain and Janetski 2013). Note that some Cedar Mesa adults could not be sexed.

Area		δ^{13}C	SD	δ^{15}N	SD	N
La Plata (BMIII)	600AD–800AD	-6.5	0.4	8.5	0.4	9
Durango	400 BC–400 AD	-8.4	1	7.7	0.2	6
Marsh Pass	500 BC–50AD	-8.2	1.7	7.3	1.1	19
Cedar Mesa	200 BC–200AD	-7.8	0.7	6.6	0.9	86
Cedar Mesa (male)		-7.8	0.6	6.8	0.7	45
Cedar Mesa (female)		-7.8	1	6.0	0.6	22

Table 2.2: Frequency values for uniform sampling of hypothetical feasible region in Figure 2.9

X value	-1	-0.5	0	0.5	1	1.5	2
Frequency	3	5	7	7	7	5	3
Y value	-1	-0.5	0	0.5	1	1.5	2
Frequency	3	5	7	7	7	5	3

CHAPTER 3

SAMPLING DESIGN AND EXPERIMENTAL METHODS

Chapter 1 noted the ecological differences in Western and Eastern Basketmaker II regions and posited that dietary modeling using stable isotope analysis could provide insight into both spatial and temporal patterning in Basketmaker II material culture. To date, the most comprehensive isotope mixing model of Basketmaker II diets is a study by Coltrain and Janetski (2013), in which $\delta^{13}C$ and $\delta^{15}N$ of bone collagen from 149 Basketmaker II burials from Wetherill's Cave 7 were combined with a regional resource database through the linear mixing program SISUS; results indicated differences in both maize and large game consumption between men and women.

However, as noted in Chapter 2, stable isotope chemistry diet models require accurate estimates of resource isotope values. Unfortunately, the large sample of Basketmaker II burials analyzed in Coltrain and Janetski is not matched by a similarly robust set of local resource isotope data. If recent analyses of turkeys are ignored (Bocinsky 2011; Rawlings and Driver 2010), then, at Cedar Mesa, the only previous study (Chisholm and Matson 1994) generating a local isotope database sampled six mountain sheep (*Ovis*) and four seeds of Indian ricegrass (*Oryzopsis hymenoides*: note that our nomenclature follows that of the first edition of *A Utah Flora* (Welsh et al. 1987)). Coltrain and Janetski overcame this problem by compiling regional floral and faunal data from across Utah and beyond, regional data that may or may not correspond to the isotope values of local Cedar Mesa resources.

3.1 Overview: Chapters 3 and 4

This study was designed to remedy this deficit through isotopic sampling of local floral and faunal resources at Cedar Mesa. Chapter 3 begins with a review of Cedar Mesa ecology and its potential isotopic effects on local resources, and proceeds through study design,

field sampling, and laboratory methods. Chapter 4 describes isotopic results and statistical analysis—culminating in a table of local resource input values for formal diet modeling in Chapter 5.

3.2 Background: Cedar Mesa Ecology

Cedar Mesa is situated on the Colorado Plateau, northwest of the towns of Bluff and Mexican Hat at 6000 ft elevation, in San Juan County, southeast Utah. Local topography consists of flat benches and sheer-sided sandstone cliffs, resulting in step-like tablelands covered with a mix of residual and aeolian deposited soils (Matson, Lipe, and Haase 1988; Spangler, Yentsch, and Green 2010)—the areas favored for dry farming by the Basketmaker II (Matson 1991; Geib 1996). Water erosion has carved these benches into deep canyons and deposited the resulting alluvium along the canyon bottoms (Hansen and Fish 1993).

Along its southern edge, local relief attains 1500 ft over close-set cliff faces. To the west, Cedar Mesa is drained by Grand Gulch, an extensive system of sinuous canyons. To the east lie two broad north-south running valleys: Comb Wash and Butler Wash, separated by Comb Ridge. Cave 7, the site from which the majority of the Cedar Mesa Basketmaker II burials were excavated, is situated just north of Butler Wash in a tributary of Cottonwood Wash (the two drainages were conflated for over a century).

To the north, Cedar Mesa rises to Elk Ridge and the Bears Ears. This high local relief results in temperature and precipitation differences largely constrained by elevation (Table 3.2). These gradients are reflected in elevation banding of biological communities (Geib 1996), an ecological distribution which packrat midden studies suggest has been stable since the middle Holocene (Betancourt 1984).

Previous studies on Cedar Mesa have described a number of botanical communities using varying definitions: Matson Lipe and Haase (1988); Betancourt (1984); Haase (1983); Aasen (1984); Spangler Yentsch and Green (2010). Table 3.1 describes the communities utilized in the present study.

These communities are generally bounded at a 0.1-10km spatial scale, and are correlated with soil depth, geologic substrate, distance to water, prevailing winds (Hasse 1983; Matson, Lipe, and Haase 1988) and/or temperature/precipitation gradients. All of these dimensions may affect C3 and CAM plant $\delta^{13}C$ values (see Chapter 2). Further, since

nitrogen-fixing cryptobiotic soil crusts are widespread on Cedar Mesa and fixation is a function of soil moisture (see Chapter 2), $\delta^{15}N$ may also vary with community.

Despite the diversity of factors shaping the variation in microenvironmental ecology, all investigators recognize elevation as the primary determinant of botanical community distributions. For the Cedar Mesa Basketmaker II, this elevation pattern is thought to have provided different but complementary wild resources in the sage/salt scrubland ('midlands' in (Geib 1996)) and the pinyon-juniper woodland, canyon rim and sage flat communities (Matson 1991). Since a number of wild food species exist in communities at both high and low elevations (see Tables 3.1, 3.2), any estimate of Cedar Mesa $\delta^{13}C$ and $\delta^{15}N$ resource values must incorporate samples from multiple elevations and encompass food species unique to both settings.

3.3 Methods: Study Design, Sampling Strategy, Laboratory Protocols

The ecological variation on Cedar Mesa provided a variety of foraging niches for Basketmaker II populations, niches whose isotope ecology may systematically vary with species, location and part of resource consumed. This study design identified three dimensions of potential sampling bias:

1. Selection bias: What plant taxa were consumed by Basketmaker II on Cedar Mesa, based on archaeological data and inference from ethnographic accounts?
2. Sampling bias: Does the isotope chemistry of commonly exploited plant taxa vary significantly with differences in elevation, soil moisture, cryptobiotic crust presence, physiographic feature, etc.?
3. Processing bias: Are all components of commonly exploited plant taxa consumed, and, if not, do the edible and inedible portions of the plant differ isotopically from one another?

By testing for these effects and comparing the effect sizes with the uncertainty introduced by combining resources into larger taxa (e.g., C3 plants, C4 plants, artiodactyls etc.), potential biases in the diet model can be identified.

3.3.1 Study Design: Selection Bias

To address the potential for selection bias, sampled plant species were chosen based on their presence in the Cedar Mesa archaeological record (Aasen 1984; Androy 2003; Matson and Chisholm 2007)), or Pueblo/Navajo ethnographies (Castetter 1935; Bell and Castetter 1941).

The sampling regime is necessarily representative rather than comprehensive, and encompasses variation in photosynthetic pathway used and organ consumed (e.g., seed, nut, fruit, root), both potential sources of isotopic variation. This study errs on the side of wider sampling—e.g., including *Opuntia* as a major component in Archaic macrobotanicals at Dust Devil cave whose use with one exception is inferred on Cedar Mesa (Matson and Chisholm 1991), but see summary of data from (Reinhard 1988) in (Matson and Chisholm 2007). It is always possible to exclude a sampled tissue from analysis post-hoc—but a taxon never sampled can only generate speculation about how it might change model outcomes.

- Two C4 seed resources were sampled. Pigweed (*Amaranthus spp*) and four-wing saltbush (*Atriplex canescens*).
- Four C3 seed resources were sampled. Seeds of sunflower (*Helianthus annuus*), desert blazingstar (*Mentzelia multiflora*), bee-weed (*Cleome lutea*) and indian ricegrass (*Oryzopsis hymenoides*).
- Two C3 tree and shrub resources were sampled: pinyon (*Pinus edulis*) and lemonade berry (*Rhus trilobata*).
- Cattail root (*Typha angustafolia*), a C3 resource, was sampled for its potential difference due to organ consumed.
- Two edible CAM plants are widespread on Cedar Mesa: banana yucca *Yucca baccata* and prickly pear cactus (*Opuntia sp*). Both fruiting bodies and pads of Opuntia can be consumed, and fruit, seeds and roasted stems of yucca can be consumed (see below for experimental roasting).

Faunal data were likewise representative, with selection made based on those most widely represented in Basketmaker II faunal assemblages (Reynolds 2012). Since archaeological faunal material recovered from Cedar Mesa sites is limited, only specimens that date to the Puebloan period were available in sufficient quantity for this study. Permission

was granted from the Natural History Museum of Utah for destructive analysis of 40 faunal specimens recovered from salvage excavation during the construction of Utah State Highway 95 (Dalley 1973; Wilson 1974). Turkey (*Meleagris gallopavo*) specimens were also analyzed and are reported, due to recent interest in the timing of turkey domestication (Bocinsky, Chisholm, and Kemp 2011; Rawlings and Driver 2010), and one *Canis* specimen is reported but neither is included in the Basketmaker II formal diet model.

In conjunction with an oxygen isotope study of Cedar Mesa (Burrillo, Coltrain, and Lewis. 2015) agricultural techniques, 12 maize cobs from two sites on Cedar Mesa were sampled; temporal control to the Basketmaker II period is not assumed. 42SA4409 is a mid- elevation (5700 ft) storage structure from Hardscrabble Mesa on the southwestern edge of Cedar Mesa. Cobs were collected as part of the canyon inventory of the Cedar Mesa Project. Three Fingers is a high elevation site (7200 ft) from Elk Ridge, with cobs collected by R.E. Burrillo (Burrillo personal communication 2017). Although the location of the fields in which these cobs were grown prior to storage cannot be known, these two sites encompass the geographic and elevation range of farmable environments on Cedar Mesa.

3.3.2 Study Design: Ecological Bias

Ecological bias can occur in two dimensions, space and time. Based on a small pilot study of banana yucca (Lewis and Coltrain 2014), this study anticipated ecological variation in $\delta^{13}C$ based on elevation, and variation in $\delta^{15}N$ based on the level of development in cryptobiotic crusts. Both factors vary with botanical community. Since Basketmaker II foragers used both upland pinyon-juniper and canyons for wild resource acquisition, sampling across elevations and botanical communities allows us to estimate the total isotopic variation within a typical foraging catchment on Cedar Mesa. Crustal development levels—which on a large (1–2km) spatial scale vary with elevation–were assumed to show enough spatial variation to be captured opportunistically.

To encompass spatial variation in stable isotope values, each wild plant species sampled was collected both from low elevation sites in the canyons and valleys (largely salt-scrub communities), and from the higher elevation mesa top or ridge slopes (largely pinyon-juniper communities). Riparian communities containing largely similar species were sam-

pled at both high and low elevations. Since the majority of the Basketmaker II burials came from Cottonwood Wash northeast of Cedar Mesa, the primary focus of this collection was the eastern margin of Cedar Mesa, and Comb and Butler washes (Figure 3.1). For yucca and bee-weed, suitable specimens could be located only in a single biological community, representing a smaller elevation gradient.

A representative sample size for each taxon was determined based on the range of variability present in a pilot study of banana yucca from Cedar Mesa (Lewis and Coltrain 2014). The range of intrasite variability in yucca leaf $\delta^{13}C$ and $\delta^{15}N$ is typically no more than 2‰. Using an iterative sample size calculation (Brown 2013), this design estimated that a sample size of 12 specimens per elevation would give an estimate of the mean to within 0.1‰ the equivalent of the analytical uncertainty for a single assay of carbon.

The sampling strategy had to be modified in the field due to modern disturbances. Grazing is presently permitted over much of Cedar Mesa and coincided with the collection period. Much of the high elevation central mesa—which has the highest concentration of Basketmaker II habitation sites—was effectively stripped of vegetation by cattle during the collection period. Elsewhere, tamarisk and cheatgrass are displacing native riparian communities in several drainages including Grand Gulch, where they form miles long thickets in the canyon bottom. Both species can alter local soil chemistry (Pataki et al. 2005; Sperry, Belnap, and Evans 2006). Since both factors when present hinder the collection of local flora, sampling locations were largely chosen from nonaffected areas.

Temporal bias is more challenging and is only indirectly addressed by this study. Measuring temporal bias directly would require comparing modern floral and faunal isotope distributions with archaeological specimens controlled for elevation—a nearly impossible condition to meet at a sufficient sample size for most species. However, since trophic level offset estimates are known, the comparison of modern plant values with the values of archaeofaunal herbivores provides a rough check on temporal variation.

3.3.2.1 Field Collection and Sample Preparation

Sample site locations were recorded with handheld GPS. Site access information and descriptions of site physical and biological characteristics, including an estimate of color and thickness of soil crusts, were recorded and digital photographs of each sample site

were taken and were digitally archived for future reference. All sample sites were within six miles of nearest vehicle access to facilitate future studies; a number of sample sites were within sight of the road when suitably large patches of a resource were observed. As whole yucca stems/plants proved cumbersome to transport by hand, four survey transects were made along county and BLM access roads (see Figure 3.1) to 50 m on each side of the road.

Summary of sample sites, species collected, physiographic context and botanical community present are given in Table 3.3. Floral specimens were identified in the field. Herbaceous plant samples were dried in a plant press. Yucca fruits and hearts were cut and sun/air dried using botanical drying sheets on a vehicle dashboard.

Sample loss was limited to one yucca stem accidentally rehydrated in the field during a thunderstorm, and partial loss (e.g., less than 1/4 of fruit) of several yucca fruits collected before the dashboard drying method was instituted. All samples were transported to the Archaeological Center Research Facility for Stable Isotope Chemistry in the Department of Anthropology at the University of Utah and dried at 60° C in a drying oven. Approximately one gram of edible plant tissue was homogenized with mortar and pestle. For research continuity, one herbarium-quality specimen of each taxon was archived at the Garrett Herbarium in the Natural History Museum of Utah.

For archaeofaunal specimens, collagen extraction follows procedures previously evaluated (Cleland, Voegele, and Schweitzer 2012; Sealy et al. 2014). Cortical bone fragments were cleaned and demineralized in 0.6 N HCl at 4° C. Type II water was used throughout in glassware baked out at 550° C. Fresh HCl was added and the sample visually evaluated every 24 hours. Demineralization proceeded as long as calcium phosphate (visible as a density gradient in the supernatant) was observed. The collagen pseudomorph was then rinsed to neutrality and soil contaminants removed by soaking in 5% KOH, and the base solution replaced daily until the supernatant was clear. The sample was then rinsed to neutrality and gelatinized in 5 ml Type 2 H_2O (pH 3) at 90° C for 24 hours. Water-soluble and insoluble phases were separated with a PVDF membrane 0.45 mum syringe filter and the water-soluble phase was lyophilized and weighed for a final collagen yield.

Both plant material and faunal bone collagen were analyzed on a MAT Delta Plus XL mass spectrometer with Carlo Erba EA1110 CHN interface. Stable carbon and nitrogen isotope measurements and elemental concentrations were obtained from a single sample

combustion. Analytic uncertainty is $\pm 0.1‰$ for $\delta^{13}C$ and $\pm 0.2‰$ for $\delta^{15}N$.

3.3.3 Study Design: Processing Bias

The isotopic similarity of $\delta^{13}C$ values for CAM plants and C4 plants (including maize) potentially confounds the use of $\delta^{13}C$ as a measure of maize use (Matson and Chisholm 1991). In this study, two CAM species were sampled: prickly pear and banana yucca. The latter is well attested ethnographically, with fruit, seeds and roasted stems (see Figure 3.2) being consumed (Bell and Castetter 1941; Castetter 1935). The roasted stems are particularly noted as a starvation food among Pueblo groups (Castetter 1935, 14,56). Ethnographically recorded starvation foods are thought to have made up a larger proportion of diets in prehistory and are often well represented in the archaeological record (Minnis 2000).

At Cedar Mesa, roasting has been proposed as a function for certain types of slab-lined pits (Matson 1994), and yucca quids—chewed fibers—have been recovered from caves in the Cedar Mesa area (LeBlanc et al. 2007), some with morphologies indicating processing for consumption (Haas Jr 2001). Yucca macrofossils have not been identified in Basketmaker II coprolites (Matson and Chisholm 2007), due in part to the total consumption of the resource (Louderback, Pavlik, and Spurling 2013). However phytoliths—morphologically distinct silicate crystals formed between cell walls—occur in Cedar Mesa BMII (Battillo 2017) and PIII coprolite samples (Reinhard and Danielson 2005), and occur extensively in regional Archaic populations (Danielson and Reinhard 1998; Reinhard et al. 2012). Yucca DNA was found in over half of the Basketmaker II coprolites sampled from Cedar Mesa (Battillo 2017), further supporting the consumption of this resource.

Since stem consumption involves separation of the edible tissue from fiber, and since intertissue $\delta^{13}C$ and $\delta^{15}N$ differences are known to exist in a variety of species, this study developed a laboratory procedure designed to test whether a difference exists between the fiber portion of yucca stems and the edible nonfiber portion.

3.3.3.1 Experimental Processing of *Yucca baccata*

Ethnographic accounts of yucca and agave processing follow a similar pattern (Zigmond 1981, 69-70)—including social prohibitions during cooking (Fowler 1986). In both cases, the long roasting period—and wet roasting environment—serves to break down

toxins, and convert complex starches into more easily digestible sugars (Wandsnider 1997). After roasting the basal portion of the leaves and stem, this "heart" may be chewed, the sugars consumed and the fibers spit out as "quids," the primary archaeological evidence of yucca consumption. This experimental setup simulated both the long moist cooking of an earth oven, and the separation of edible tissue from yucca fiber. By analyzing seed, fruit, and stem tissue both before and after roasting as well as analyzing the fiber and nonfiber portions of the stem, isotopic differences between the consumed resource and the raw whole stem tissue could be assessed

For yucca stems, preparation was adapted from ethnographic accounts of yucca or agave preparation. First, the lower portions of the leaves were removed (Figure 3.3), exposing the stem on the lower portion of the heart. At the apex of the stem, leaves were trimmed so that only the white base of the young leaf was exposed. Tissue embedded with soil was removed from the bottom 1-5cm of the stem. The resulting "heart" or stem was weighed dry and then soaked for 12 hours in Type 2 water, weighed "wet," and quartered, lengthwise (Figure 3.4).

Each quarter was weighed and one quarter (A) was reserved as the "raw stem sample." One quarter (B) was wrapped in foil and 10-15 ml of Type II water added to the sample. Two quarters (C, D) were wrapped in foil together with 20-30 ml of water. Samples were baked in a household oven at 220° F (105° C), the average temperature of "food packets" in an experimental earth-oven (Leach and Sobolik 2010). A tray of water was placed at bottom of the oven, monitored and refreshed as needed to maintain a moist roasting environment critical for the success of earth oven cooking. The B quarters were removed after 12 hours and refrigerated. Quarters C and D were removed after 24 hours and refrigerated.

Physical changes were noted during roasting.. The color of the stem was transformed from white to light to dark brown, the sample becoming easier to crush and the taste noticeably sweeter. Sample weights at 12 hours were 92% of initial weight on average, while by 24 hours the samples are reduced to about 84% of initial weight, likely largely due to water loss.

For quarters B and C, mastication was simulated by placing the sample in a pestle, adding 15-20 ml of water and grinding to make a "paste" (Figure 3.5). A 10 ml subsample

of this paste was set aside as a "whole tissue" sample. A second 10 ml subsample of "paste" was placed in scintillation vial and 10 ml of Type II water added. The vial was agitated for 1 minute and the sample removed to a crucible where the liquid was pressed from the sample and retained in a scintillation vial. This fluid, containing both dissolved sugars and a colloidal suspension of largely nonfiber plant tissues freed during grinding and agitation, represents the consumed "nonfiber" portion of the yucca stem.

A subsample of the fibers from which the fluid was pressed was removed to a third vial and 15 ml of water added. This sample was agitated for 30 seconds, poured off and rinsed with 20 ml of water. This process was repeated three times, resulting in a "clean" network of yucca fibers (Figure 3.6). All samples were removed to a drying oven at 60 C until thoroughly dry. Remaining yucca tissue was frozen for the duration of the project. The fluid "nonfiber" samples dehydrated into a syrup consistency within 12-18 hours and crystalized into a solid within 48 hours. No macroscopic signs of biological activity (e.g., "yeasty" scent or bubbles indicating fermentation) were observed during dehydration.

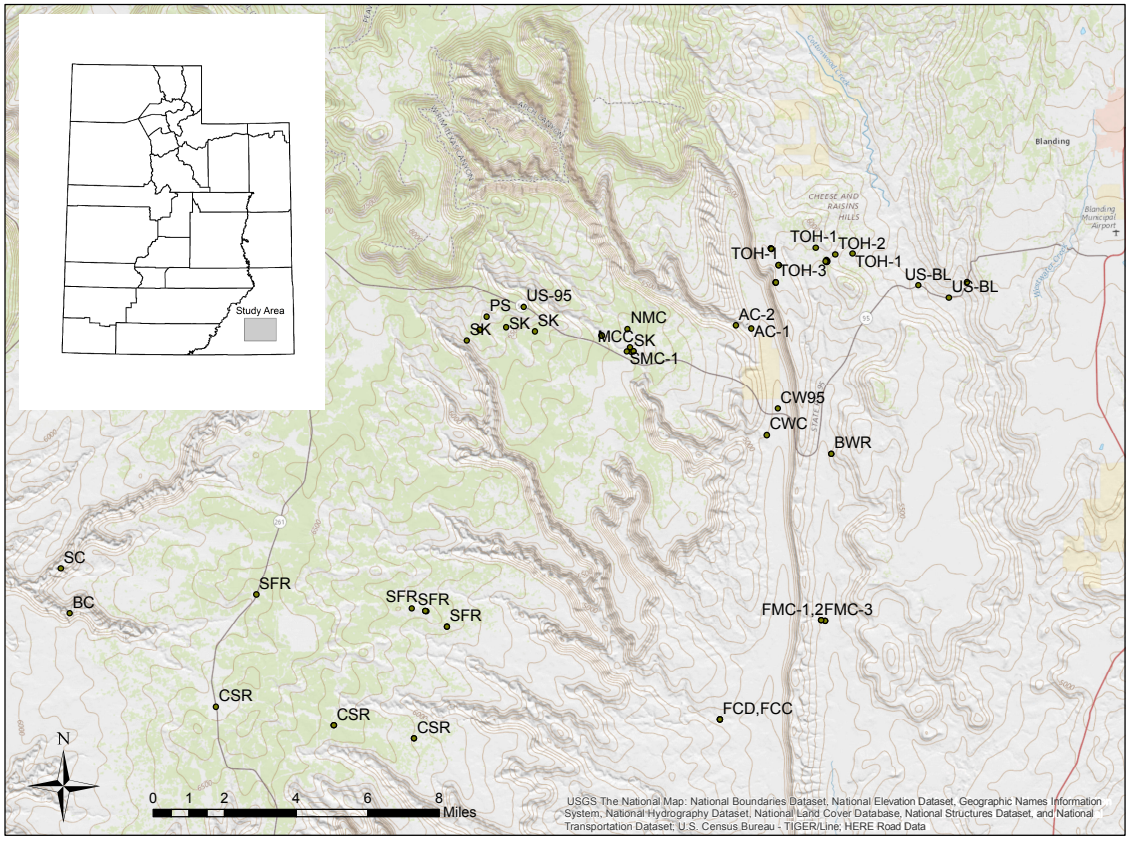

Figure 3.1: Cedar Mesa study area and sampling site locations: see Table 3.3 for sampling site descriptions. See Appendix for UTM data

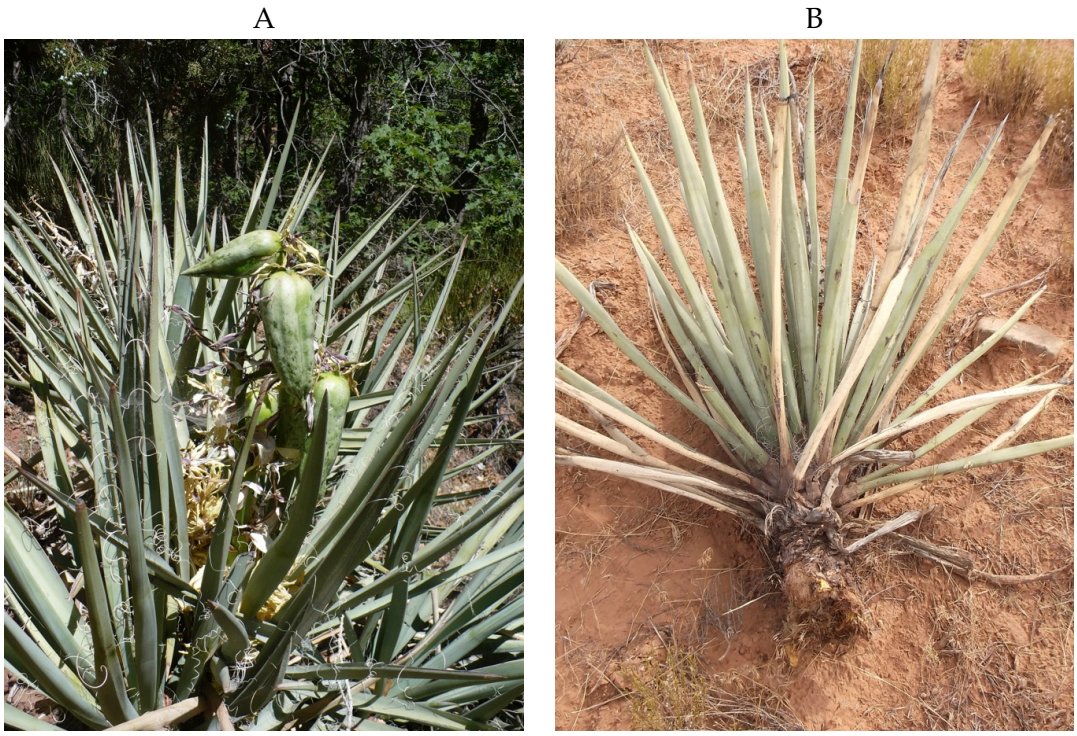

Figure 3.2: Edible parts of banana yucca plant. A: fruits contain seeds which may be eaten. B: a whorl of spike-like leaves surrounds the central stem or "heart" which may be roasted.

Figure 3.3: Stages of removing leaves to expose the "heart." Note: different specimens used to illustrate each stage.

Figure 3.4: Yucca "heart" before and after roasting. From left to right: quarter A raw, quarter B 12 hours roasting, Quarters C,D 24 hours roasting.

Figure 3.5: Artificial mastication: the roasted stem is crushed or ground into a paste.

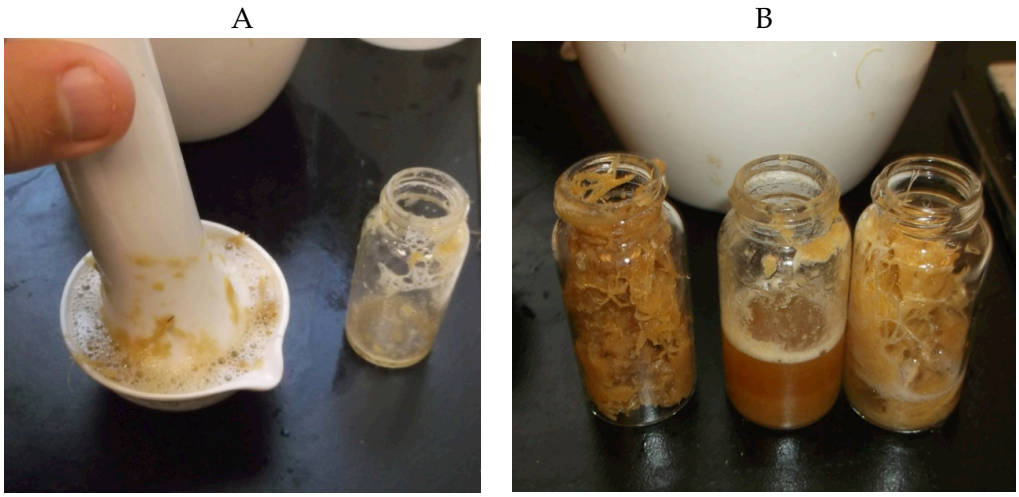

Figure 3.6: Yucca tissue separation. A: agitating the "paste" in water results in a starchy colloidal suspension that can be separated from the fibers (pseudo-quids) and poured off. B: (left to right) sampled paste, nonfiber colloidal suspension, and "clean" fibers.

Table 3.1: Botanical communities of Cedar Mesa utilized in this study.

Elevation	Community (species)	Photo
High above 5800-6100 ft (Hasse 1983)	Pinyon-Juniper Woodland: Varies in density on mesa tops ridges and slopes. At lower elevations juniper dominates. Pinon is primary foodsoure, scattered yucca. Major Species: Pinyon (*Pinus edulis*), Juniper (*Juniperus sp.*), Roundleaf Buffaloberry (*Shepherdia rotundifolia*), Mormon Tea (*Ephedra viridis*), Banana Yucca (*Yucca baccata*).	
High above 5800-6100 ft (Hasse 1983)	Open Pinyon-Juniper or Canyon Rim: on shallow soils at edge of mesa top or near bedrock outcropping. Tree density is low but understory becomes more varied. Pinon, Seed, succulent and fruit bearing food-sources. Major Species: Pinyon (*Pinus edulis*), Juniper (*Juniperus sp.*) Sagebrush (*Artemisia tridentata*). Minor Species: Roundleaf Buffaloberry (*Shepherdia rotundifolia*), Mormon Tea (*Ephedra viridis*), Utah Serviceberry (*Amelanchier utahensis*), Prickly Pear cactus (*Opuntia spp.*), Claret Cup cactus (*Echinocereus triglochidiatus*), Goosefoot (*Chenopodium spp.*), Banana Yucca (*Yucca baccata*), Rabbitbrush (*Chrysothamus nauseosus*), Indian ricegrass (*Oryzopsis hymenoides*), Needle-and-Thread Grass (*Stipa comata*).	
High above 5800-6100 ft (Hasse 1983)	Sage Parkland: occurs on thick mesa-top soils in cold air drainages inhibiting PJ growth. Some seed foods present. Major Species: Major Species: Sagebrush (*Artemisia tridentata*), Rabbitbrush (*Chrysothamus nauseosus*), Goosefoot (*Chenopodium spp.*), Indian ricegrass (*Oryzopsis hymenoides*), Needle-and-Thread Grass (*Stipa comata*).	
High: mostly above 6100 ft (Betancourt 1984).	Ponderosa Forest: community is present in a few sampled high elevation canyons mixed with dry and wet riparian species. Fruiting species present. Major Species: Ponderosa (*Pinus ponderosa*), Douglas Fir (*Pseudotsuga menziesii*), Aspen (*Populus tremuloides*) Utah Serviceberry (*Amelanchier utahensis*), Rose (*Rosa viginianis*), Lemonade Berry (*Rhus trilobata*) Western Chokecherry (*Prunus virginiana*).	

Table 3.1: continued

Elevation	Community (species)	Photo
High and Low	Dry Riparian: occurs at all elevations where subsurface moisture or periodic flood can support riparian species, mostly in canyon settings. Weedy seeds and fruit species present. Major Species: Cottonwood (*Populus fremontii*), Willow (*Salix spp.*), Boxelder (*Acer negundo*) Minor Species: Lemonade Berry (*Rhus trilobata*), Reeds (*Phragmites spp.*), Cattails (*Typha a*).	
High and Low	Wet Riparian: occurs at all elevations wherever water-table is present at surface. Often surrounded by dry riparian zone. Fruit. Root and seed foods present. Major Species: Cottonwood (*Populus fremontii*), Willow (*Salix spp.*), Boxelder (*Acer negundo*) Minor Species: Lemonade berry (*Rhus trilobata*), Reeds (*Phragmites spp.*), Cattails (*Typha a*).	
Low: below 5800 ft (Haase 1983)	Sage/Salt Scrub: Lower elevation analogue to Sage Flats. Seed and succulent foods present. Major Species: Sagebrush (*Artemisia tridentata*), Four-wing Saltbush (*Atriplex canescens*), Shadscale (*Atriplex concertifolia*), Greasewood (*Sarcobatus spp.*)	
Low: Comb Wash	Open scrub/Grass: only observed on old alluvial bench in western Comb Wash. Sandy soils support very sparse salt-brush with abundant patches of bunch-grasses and weedy forbs. Four-wing Saltbush (*Atriplex canescens*), Indian ricegrass (*Oryzopsis hymenoides*), Needle-and-Thread Grass (*Stipa comata*), Prickly Pear cactus (*Opuntia spp.*)	

Table 3.2: Physical parameters for selected communities on Cedar Mesa: temperature decreases and precipitation increases with increasing elevation. References are to soil types in Hanson and Fish (1993).

Sample Site	Community	Elevation (ft)	Precipitation (in)	Mean Annual Temp.	Frost-Free Days
Comb Wash (Fish Cyn)	Salt-Scrub	4000	6-8	50-52	160-200
Comb Wash (Arch Cyn)	Sage-scrub	5000	8-12	49-54	140-180
Upper Mule Canyons	Pinyon-Juniper Woodland	6000	12-16	46-50	100-140
Bears Ears (not in study area)	Ponderosa Forest	8000	12-16	45-50	80-140

Table 3.3: Descriptions of Cedar Mesa modern flora sampling sites. []

ID	Sample Site	Species	Elev. (ft)	Crust Level	Physical Context	Botanical community (major species)
AC-1	Arch Canyon 1	*Typha a*	4864	0, periodically disturbed soils	Stony dry streambed arroyo on alluvial fan in front of mouth of Arch Canyon in Comb Wash.	Dry Riparian: *Populus sp, Tamarix sp, Rhus trilobata, sedges, Chrysothamnus sp*.
AC-2	Arch Canyon 2	*Typha a*	4981	0, in standing water in streambed	In streambed within in a wet riparian environment spanning width of canyon bottom.	Wet Riparian: *Salix Populus sp, Tamarix sp, Rhus trilobata, sedges, Chrysothamnus sp, Phragmites*.
BC	Bullet Canyon	*Cleome l*	5466	1, light soil colored	First bench (alluvial floodplain/fill) in Bullet Canyon approx. 0.5 m above arroyo level.	Medium density sage/scrub community *Artemisia tridentata, Chrysothamnus sp* between nearby ($<$ 30m) colluvial slopes supporting pinyon-juniper woodland and dry riparian communities.
BWR	Butler Wash Road	*Mentzelia m, Oryzopsis a*	5232	1, moderate soil colored crust	Colluvial slopes 200m east of bedrock cliffs.	Very open pinyon juniper woodland: *Pinus edulis, Juniperus Osteosperma, Yucca augustissima, Oryzopsis hymenoides, Hesperostipa comata*.
CWC	Comb Wash Camp	*Mentzelia m*	4833	0, disturbed soils	Sandy alluvial floodplain/first bench 1-3 inches above primary drainage of Comb Wash. *Mentzelia* concentrated on margins of soil disturbance	margin of Sage-scrub and dry riparian *Artemisia tridentata Atriplex canescens, Chrysothamnus sp, Populus sp, Tamarix sp*.
CW-95	Comb Wash 95	*Rhus t*	4542	2, moderate soil colored to thick black crusts	First bench (alluvial plain) of Comb Wash, 50 m from current arroyo.	Dense sage-scrub but with dry riparian species closer to arroyo. *Artemisia tridentata Pinus edulis, Aster ascendens, Cleome Lutea, (dry riparian: Populus sp, Salix sp, Chrysothamnus sp*.
FCC	Fish Canyon Canyon	*Cleome l*	4611	1, light soil colored crust	First Bench (alluvial plain/fill) 1m above arroyo level in lower Fish Canyon.	Medium density sage/salt scrub: *Atriplex canescens, Atriplex confertifolia, Aster ascendens, Artemisia tridentata, Chrysothamnus sp, Chenopodium sp*.
FCD	Fish Canyon Dunes	*Mentzeila m, Oryzopsis a, Cleome l*	4542	1, light soil colored crust	Remnant older second bench of sandy alluvium on west side of Comb Wash above current alluvial plain.	Unusual open/sparse salt/sage-scrub cover with more extensive bunchgrass coverage than elsewhere in study area *Oryzopsis hymenoides, Atriplex canescens, Aster ascendens, Artemisia tridentata, Hesperostipa comata, Kali tragus*.
FMC-1	Fish Mouth Canyon 1	*Amaranthus r, Atriplex c*	4742	0, disturbed sandy soils in creek-bed	Seasonal arroyo at intersection of Butler Wash and mouth of drainage below Fish Mouth Cave. One sample of *Atriplex c* was taken from alluvial plain 2-3 m above current arroyo.	Dry riparian, *Chrysothamnus sp, Populus sp, Tamarix sp, Kali tragus, Atriplex canescens, Atriplex confertifolia*
FMC-2	Fish Mouth Canyon 2	*Rhus t*	4750	1, light soil colored crust	In dry streambed/arroyo (approx. 2m deep) growing on slopes/wall.	Dry riparian: *Chrysothamnus sp, Populus sp, Rhus t, Toxicodendron radicans*, assorted forbs.

Table 3.3: continued

ID	Sample Site	Species	Elev. (ft)	Crust Level	Physical Context	Botanical community (major species)
FMC-3	Fish Mouth Canyon 3	*Opuntia*	4932	3, black soil crust some very well developed	East slope of Comb Ridge, shallow soils over exposed bedrock and aeolian/alluvial sediments trapped in drainages.	Open pinyon juniper community with diverse understory (canyon rim) *Pinus edulis, Juniperus Osteosperma, Artemisia tridentata, Hesperostipa comata, Oryzopsis hymenoides, Opuntia sp, Echinocereus triglochidiatus, Shepherdia sp.*
MCC	Mule Canyon Corral	*Orozopsis h, Opuntia sp*	6045	2, moderate to heavy black crust	Shallow aeolian soils covering bedrock on mesa-top "ridge" between North and South Mule Canyon.	Open pinyon juniper community with diverse understory (canyon rim) *Pinus edulis, Juniperus Osteosperma, Artemisia tridentata, Hesperostipa comata, Oryzopsis hymenoides, Opuntia sp, Echinocereus triglochidiatus, Shepherdia sp.*
NMC	North Mule Canyon	*Rhus t*	5940-6047	1, light soil colored crust	Foot of colluvial slopes flanking alluvium in North Mule Canyon minimal arroyo downcutting noted.	Dry riparian/ponderosa forest *Populus sp, Pinus ponderosa, Pinus edulis, Juniperus Osteosperma, Chrysothamnus sp, Toxicodendron radicans.*
PS	Pine Springs	*Typha a*	6611	0, disturbed alluvium in wash and standing water near spring.	Intermittent streambed in arroyo at Pine Springs. Sandy sediments with evidence of recent flash flooding.	Riparian/Ponderosa forest flanking arroyo for 20-30 m surrounded by open pinyon-juniper woodland surrounding. *Salix sp, Pinus ponderosa, Quercus gambellii, Pinus edulis, Juniperus Osteosperma, Arctostaphylos sp, Rosa sp, Amalanchier utahensis, Shepherdia sp.*
SC	Sheiks Canyon	*Cleome l*	5505	1, light soil colored	Second alluvial bench 10 m + above current arroyo.	Dense sage/salt scrub *Artemisia tridentata, Atriplex canescens, Hesperostipa comata.*
SFR/CSR	Snow Flat Road / Cigarette Springs Rd	*Atriplex c*	6512, 6526	1, light to moderate soil colored	Deep Mesa Top aeolian soils near center of mesa.	Sage flats, flanked by pinyon-juniper within 50-100m *Artemisia tridentata, Atriplex canescens, Aster ascendens, Chrysothamnus sp, Chenopodium sp, (Pinus edulis, Juniperus Osteosperma).*
SFR/CSR-2	Snow Flat Road/Cigarette Springs Rd 2	*Yucca b*	6076-6463	1-2, light soil colored to well developed black	Mesa Top with mix of deeper aeolian soils and shallower soils at rocky outcropings and near canyons.	Pinyon juniper woodland and Canyon Rim communities present, often grading into one another. *Pinus edulis, Juniperus Osteosperma, Artemisia tridentata, Ephedra, Hesperostipa comata, Oryzopsis hymenoides, opuntia sp, Echinocereus triglochidiatus, Shepherdia sp.*
SK	Salvation Knoll	*Yucca b*	5959-7014	1-2, light soil colored to well developed black	Mesa top with mix of deeper aeolian soils and shallower soils at rocky outcroppings and near canyons.	Mostly Pinyon juniper woodland with some and canyon rim communities present, *Pinus edulis, Juniperus Osteosperma, Artemisia tridentata, Ephedra.*
SMC-1	South Mule Canyon 1	*Amaranthus r*	5877	0, vegetation too thick to support crusts	On first bench /alluvial fill, Approximately 1 m higher than creek-bed, in South Mule Canyon. Flash flooding evident.	Grassy, dry riparian supporting *Chrysothamnus sp, Populus sp, alix sp, Oryzopsis hymenoides, Chenopodium sp.* assorted grasses.

Table 3.3: continued

ID	Sample Site	Species	Elev. (ft)	Crust Level	Physical Context	Botanical community (major species)
SMC-2	South Mule Canyon 2	*Oryzopsis hymenoides, Rhus t*	5940	1, light soil colored	Alluvial fill/first bench 0.5 m above arroyo and margin of alluvium and colluvial slopes.	Dry riparian *Pinus edulis, Juniperus Osteosperma, Salix sp, Amelanchier utahensis, Rhus trilobata, Hesperostipa comata, Quercus gambellii, Rosa sp, Aster ascendens, Populus sp, Chrysothamnus sp.*
TOH-1	The Old Highway 1	*Mentzelia m*	5766	1, light soil colored	Colluvial slope from actively eroding bedrock outcropping, patch is largely extensive with slope.	Open pinyon juniper woodland *Pinus edulis, Juniperus Osteosperma, Artemisia tridentata, Oryzopsis hymenoides.*
TOH-2	The Old Highway 2	*Oryzopsis h*	5638	2 moderate black crust	Patch localized on sandy alluvium surrounded by colluvium slopes in seasonal drainage below bedrock cliffs.	Open pinyon juniper woodland with diverse understory *Pinus edulis, Juniperus Osteosperma, Artemisia tridentata Chrysothamnus sp Oryzopsis hymenoides Hesperostipa comata, Aster sp.*
TOH-3	The Old Highway 3	*Yucca b, (Opuntia)*	5324-5961 (5831)	1-2, light soil colored to black	Transect from upslope of Cottonwood Wash to top of Comb Ridge. Colluvial slopes and aeolian deposited sediments of varying depths. Opuntia collected at top of transect.	Pinyon juniper woodland: lower elevations are juniper dominated with scrub oak present at summit of Comb Ridge. *Pinus edulis, Juniperus Osteosperma, Artemisia tridentata Chrysothamnus sp Oryzopsis hymenoides Hesperostipa comata, Quercus gambelii, Opuntia sp.*
US-95	US-95	*Helinathus a*	6777	0, gravelly matrix spreading from roadbed.	Mesa-top Aeolian soils overlain by exotic gravel matrix from roadbed.	Dense Pinyon Juniper woodland: *Pinus edulis, Juniperus Osteosperma, Aster sp, Chrysothamnus sp., Oryzopsis hymenoides.*
US-B	US-95 Blanding	*Helinathus a*	5235-5456	0, mixed soil gravel matrix	Colluvial/alluvial slopes and alluvial fill in Cottonwood wash mixed with roadbed gravels.	Open Pinyon Juniper Woodland and sage-scrub supporting *Pinus edulis, Juniperus Osteosperma, Oryzopsis hymenoides, Chrysothamnus sp.*

CHAPTER 4

STATISTICAL ANALYSIS AND LOCAL RESOURCE ISOTOPE AVERAGES

Chapter 3 reviewed the considerations of local ecology, plant physiology, and archaeo- and ethnobotany that determined sampling and experimental design. This design was structured to address three potential biases in estimating stable isotope ratios for local resources—the input values for stable isotope diet models. Three such biases were identified:

1. Selection bias: species selection may introduce bias into averaged resource values.
2. Sampling bias: differences in local ecology and soil may result in a biased estimate of individual resource values.
3. Processing bias: tissue differences may bias individual resource values if the tissue sampled is different than the tissue consumed.

This chapter presents the statistical analyses used to examine how this study's experimental design addressed each of the above biases. It first examines interspecies and intersite variability in stable isotope ratios and explores intertissue differences in banana yucca. Having defined these differences, the chapter concludes by using the logic of mixing models to estimate the uncertainties introduced by these three variabilities relative to the uncertainty about which combination of species were consumed.

4.1 Controlling for Sampling Bias

Complete data-tables for Cedar Mesa flora and fauna can be found in the Appendix. Concentration dependent effects on δ^{15}N are present in the data where the nitrogen concentration was less than 0.5‰ (e.g., the analytic limit of each element). To avoid biasing results, all specimens with nitrogen concentration less than 0.5 were removed prior to analysis.

Further, two extreme plant tissue outliers were removed from the data-set prior to analysis. *Sylvilagus* and *Lepus* bone morphology is similar save in size, but the two genera have distinct δ^{15}N values (Ugan and Coltrain 2011). One faunal specimen, originally classed as *Sylvilagus*, exhibited δ^{13}C and δ^{15}N values more than 2 SD from *Sylvilagus* means, but consistent with *Lepus* values. One sample originally designated *Lepus* also returned values consistent with *Sylvilagus*. These specimens were reassigned prior to analysis.

4.1.1 Controlling Selection Bias: Interspecies Variability

Sampled flora and fauna are summarized in Tables 4.1 and 4.2. Distributions of δ^{13}C and δ^{15}N for plant and animal species are plotted in Figures 4.1, 4.2 and 4.3. δ^{13}C values follow expectations from the photosynthetic pathway: C4 species averages between -12 and -14‰, CAM species -12 to -15‰ and C3 species between -23 and -29‰. *Amaranthus* and *Cleome* seeds are 1-2‰ more positive in δ^{13}C than leaves, which is unexpected given that lipids are generally significantly depleted relative to bulk leaf values (Bowling, Pataki, and Randerson 2008).

δ^{15}N values are suggestive. As noted in Chapter 2, plant tissue δ^{15}N differs depending on the source of nitrogen available, with δ^{15}N =2 defining the boundary between legumes and nonlegumes. Legumes derive nitrogen from bacterial fixation from the atmosphere and have δ^{15}N values of -4 to +2. Nonlegumes derive nitrogen primarily from decayed organic matter and have δ^{15}N values of +2 to +6‰. Arid regions generally show higher δ^{15}N values in plants (Schwarcz and Schoeninger 2012), making the +2‰ boundary a conservative estimate. Eight of 15 tissues sampled have mean δ^{15}N values below 2‰, firmly in the region of nitrogen fixation. Three have "borderline" values of +2.2, +2.5 and +2.6‰, and four tissues have values greater than +3‰, suggesting mostly nonatmospherically fixed nitrogen sources.

Archaeological maize cobs were sampled from two sites. However, several samples (from both sites) had borderline low nitrogen concentrations and will require a second analyses to confirm the findings reported here. All maize samples will be reanalyzed, but to avoid confusion in reporting data only summary statistics from the first analysis are described in the present study. The six samples from the lower elevation Hardscrabble

(5700 ft) site had a mean δ^{13}C of -11.8‰ and a range of -11.0 to -12.9‰. Mean δ^{15}N is 5.3‰ with a minimum of 3.7‰ and a maximum of 8.1 ‰ (note that the next highest δ^{15}N value is 5.9). The higher elevation Three Fingers site (7200 ft) has a mean δ^{13}C of -11.2 ‰ with a range of -10.1 to -12.8‰. Mean δ^{15}N is 1.6‰ with a minimum of 0.5‰ and a maximum of 2.2‰. The full separation of the distributions of δ^{15}N values between sites was unexpected, but is consistent with microenviromental effects observed in native flora (see below).

Sampled fauna are given in Table 4.2 and Figure 4.3 (note that *Canis* is for comparative purposes rather than dietary reconstruction). Using herbivore trophic level offsets between whole diet and collagen of δ^{15}N +3 and δ^{13}C +5 (carnivore offsets of +3 and +1 ‰ respectively), the consistency of modern flora and archeofauna isotope values may be examined.

Sylvilagus value of 3.6‰ suggests a plant δ^{15}N value of 0.6‰ and *Ovis* at 4.7‰ suggests a plant δ^{15}N value of 1.7‰, consistent with modern flora averages of $\delta^{15}\text{N} < 2$ per mil, due to crypto-biotic crust nitrogen inputs.

Herbivore diets suggest plant δ^{13}C values of between -21 and -25‰ consistent with a C3-dominated diet. *Ovis* from this study closely approximates the values given for six Cedar Mesa *Ovis* in Chisholm and Matson 1994. *Canis*, a carnivore, suggests diet δ^{15}N values of 4.6‰ and δ^{13}C of -16.5‰, approximating *Ovis* and *Sylviagus* and *Cynomys* averages. This consistency between flora, herbivore and carnivore data suggests that modern flora broadly reflect the flora encountered by ancient foragers (both faunal and human).

While likely dating later than Basketmaker II as a faunal resource, turkey (e.g., *Meleagris*) δ^{15}N is high relative to local plant δ^{15}N, which might suggest some insect protein inputs. However, turkey values (δ^{15}N = 6.1) are consistent with a high maize diet given that average maize δ^{15}N is 2.9‰ and a trophic level enrichment of +3‰. Turkey δ^{13}C values suggest a whole diet δ^{13}C of -12 to -13‰ suggesting a C4 (maize) based diet with supplemental C3 (wild forage or insect) inputs.

4.1.2 Controlling Ecological Bias: Intersite Variability

This sampling strategy was designed to test two hypotheses about Cedar Mesa isotope ecology:

1. That δ^{13}C is inversely correlated with elevation (e.g., lower δ^{13}C at higher elevation with lower temperatures and higher moisture)
2. That δ^{15}N is inversely correlated with a visual scale of crustal development (e.g., more developed crust fixes more nitrogen lowering δ^{15}N values)

Since δ^{13}C varies with photosynthetic pathway and organ sampled, each type of resource may be assessed separately for elevation effect.

Figure 4.4 gives data and least squares regression lines for each resource sampled. Table 4.3 gives parameter estimates and p-values for the Kendall rank order correlation test (preferred to Spearman due to multiple ties in elevation). Only *Typha* and *Helianthus* are significantly negatively correlated with elevation, while yucca seed is significantly positively correlated. No overall direction in nonsignificant trends is observed.

To test whether the level of crustal development affects δ^{15}N values, a three-point scale was applied to systematic descriptions of crust from each sampling site (see Figure 4.5). The levels are *1* no crust present, *2* soil colored crust: smooth to bumpy with $<$ 3 cm local relief, and *3* black crust: smooth to very bumpy with $>$ 3 cm local relief and significant lichen coverage (see Figure 4.5). Table 4.4 uses Kendall's tau rank order coefficient to test for significant effects of increasing crustal development. Most species were sampled from sites with no variation in crust levels. Only *Rhus* and *Cleome* shows significant correlations (in opposite directions).

While crustal development level does not correlate with δ^{15}N, a post-hoc analysis shows that δ^{15}N correlates negatively with elevation for *Amaranthus*, *Mentzelia*, *Oryzopsis* and *Rhus* , while *Cleome* and *Opuntia* show nonsignificant negative trends, while Yucca, *Atriplex* and *Typha* show nonsignificant positive trends and *Helianthus* is positively correlated with elevation (see Table 4.5 and Figure 4.6).

Fixation in soil crusts increases with soil moisture (Belnap 2002), which could generate a negative correlation of δ^{15}N and elevation, but the species-level variation in trend direction and significance suggests another dynamic.

4.1.2.1 Discussion of Ecological Trends: Four Species and the Case for Microenvironmental Effects

The lack of trend in δ^{13}C was surprising, given that a number of species were sampled across 1000-2000 ft of elevation difference, with an observed change in botanical community suggesting increased moisture/lower temperature. Similarly, the lack of correlation between crust levels (for many species, this is effectively crust presence vs. absence) is also puzzling—especially since plant δ^{15}N values indicate nitrogen fixation.

While it is possible that the study area—with an elevation change of 2000 ft—was too limited to detect an elevation effect, it is also possible that these results are confounded by ecological variation on a smaller spatial scale. Soil and moisture differences within elevation bands also structure biological communities. Figure 4.7 shows a south-facing view of Comb Wash and illustrates the spatial distribution of ecological communities at a single elevation. The colluvial slopes on either side of Comb Wash support pinyon juniper woodland (vegetation brown-green), while the alluvial plain is largely sage-scrub (grey), with a narrow dry riparian community following the arroyo (green).

A similar ecological mosaic can be seen in the distribution of sage-flat, pinyon juniper woodland and canyon rim biological communities. Figure 4.8 shows satellite imagery for the area around the head of Sheik's canyon, and shows the common pattern of sage flats along shallow drainages, flanked by pinyon juniper woodland. While hard to see in the satellite imagery, canyon rim communities are coincident with shallow soils over bedrock.

Unfortunately, given the wide variety of ecological contexts sampled from (see Table 3.3) and a sample size of six per sampling site, the data are not structured to formally assess this possibility. However, the potential for isotopic effects on a fine spatial scale is suggested post-hoc by anecdotal evidence from two taxa: *Rhus* and *Atriplex*.

Rhus was sampled from a sage-scrub context at Comb Wash U-95 (U-95) and from a dry riparian context at Fish Mouth Cave (FMC-2); the depleted δ^{13}C values in the latter is consistent with increased soil moisture (Figure 4.9). South Mule Canyon (SMC-2) is a dry riparian setting 1000 ft higher than FMC, and shows more positive δ^{13}C values, suggesting greater water stress at higher elevation. North Mule Canyon (NMC) is also a dry riparian setting with ponderosa forest species present, suggesting a cooler microenvironment and showing a depleted δ^{13}C. Both Mule Canyon sites are within 1 km of each other and

differ by less than 10m elevation, suggesting that ecological differences within a single elevation may have as large or larger effect than elevation effect across the same botanical community.

δ^{15}N values are also be affected by local soil moisture conditions. Drier sampling sites as measured by botanical community may show significant differences in δ^{15}N. For *Atriplex c*, the association with soil moisture is quite obvious (Figure 4.10). All but one of the *Atriplex c* samples from Fish Mouth Canyon were taken from the arroyo in Butler Wash and exhibit a significant depletion in δ^{15}N relative to other sites sampled on alluvial plains or mesa-top contexts (Mann-Whitney U test, U = 16, p-value = 0.01231). One specimen from Fish Mouth Cave was taken from the alluvial plain 2 m above the arroyo but within 30 m horizontally of other samples (see Figure 4.11). This sample does not show the same depletion, suggesting that soil moisture is determining δ^{15}N values at a fine spatial scale. This δ^{15}N variation parallels fine-grained (10-50 m) variation in δ^{13}C from studies of wash/arroyo communities in southern Utah (Ehleringer and Cooper 1988).

There are two species for which the issue of fine-grained ecological variability does not apply. *Typha* and *Helianthus* were both sampled from nearly identical ecological milieu at both high and low elevations. Both show the expected correlation of δ^{13}C and elevation.

Typha only exists in either standing water or periodically flooded soils. This study sampled from each context at two sites and found that samples within permanent standing water have more negative δ^{13}C than periodically watered sites, but that elevation has a larger effect (Figure 4.12).

Helianthus was only present along the highway margins in a matrix of local soils and roadway gravels (see Figure 4.13). While the δ^{13}C value observed may be an elevation effect, the low δ^{13}C values relative to other seeds suggest that the gravels may be producing a mulching effect (Benson 2011) that decreases soil water-loss. If this is the case, the difference in the degree of gravel and local soil mixing (see Table 3.3) could drive the lower δ^{13}C effect and explain why the lower elevation site (with less gravel and more crust-covered soil) shows higher nitrogen fixation (more negative δ^{15}N).

This study was not designed to analyze isotopic variation on this finer grained scale, but to capture the isotopic variation at Cedar Mesa on the scale of human foraging. Table 3.3 in Chapter 3 indicates that sampled species were taken from a variety of contexts

including streambeds/arroyos, canyon alluvial fill, higher benches or colluvium slopes and aeolian mesa top soils. While not every species occupies each context, both C3 and C4+CAM taxa contain specimens from each category. If the supposition is correct, that microenvironmental conditions are the primary driver of Cedar Mesa δ^{13}C and δ^{15}N, and since human bone collagen averages diet over long windows of time, then wide sampling of species and ecological contexts is perhaps the only economical way to achieve an average of the types of resources encountered and consumed by the Cedar Mesa Basketmaker II.

4.1.2.2 Cedar Mesa Maize Variability

The archaeological maize cob δ^{15}N values from Cedar Mesa sites cited above have nonoverlapping ranges. Three Fingers shows δ^{15}N values consistent with modern plant specimens growing on crypto-biotic soils, while the Hardscrabble Mesa site shows δ^{15}N values consistent with decayed organic nitrogen inputs.

Two alternative explanations of the Hardscrabble δ^{15}N are consistent with the ecological milieu. The Hardscrabble site seems an unlikely venue for mesa-top farming. Satellite imagery shows extensive exposed bedrock around the canyon for about 1-2 km. Further, the original survey team thought that part of the canyon bottom could have been farmed (the canyon wall is less than 100 ft high at this point) using rain-capture (Matson and Lipe personal communication). This suggests two possible explanations.

1. The positive δ^{15}N could be the result of seep or spring based subirrigation. Springs and seeps support higher biomass and in consequence often have more plant litter and likely higher soil organics than surrounding areas.
2. The positive δ^{15}N could be the result of collected organic material washed into the canyon. Zuni ethnography records a similar use of organic matter in fertilizing maize fields (Sandor et al. 2007; Homburg, Sandor, and Norton 2005).

Recent oxygen isotope models of irrigation may provide some traction on this question (Burrillo, Coltrain, and Lewis. 2015), but further field sampling for δ^{15}N at the scale of transects across farmable drainages is needed to definitively resolve this issue. Such research lies beyond the scope of the present project. In consequence, the models in the next chapter will use mean maize values but incorporate the wide SD—in spite of the bimodality of the

distribution—in order to reflect the present lack of knowledge. Maize cob δ^{13}C values are depleted relative to kernel values by about 0.5 per mil and δ^{15}N by about 1 (Brenner, Boomgarden, and Lewis 2014).

4.1.3 Controlling Processing Bias: Intertissue Variability

Estimating the isotopic ratios of *Yucca baccata* fruit and seed may be done by directly measuring the organ. Yucca stem is more complicated. Both the process of roasting the stem and the separation of the edible portion from the nonedible fiber may change isotope ratios. Knowing both: 1) the isotopic relationship between raw stem and edible portion and 2) the relationship between fiber and edible portion will facilitate future studies using modern botanical specimens and archeological quids.

Isotopic changes were evidenced during the roasting process resulting in significant differences between raw and roasted stem δ^{15}N values (see Table 4.7). During roasting, many specimens exuded a starchy fluid, which was not retained in subsequent processing but could be associated with this change.

Alternatively, this difference may be the result of a flaw in the experimental protocol. Roasted whole stem tissue was sampled after crushing the roasted sample, while raw stem was sampled from an uncrushed cross-section of the stem. If during sampling of roasted stem, fibers were preferentially sampled, then a similar offset would result, since fiber and nonfiber portions of the stem also show distinct δ^{15}N values.

Roasted whole fiber and nonfiber δ^{13}C values are statistically indistinguishable (Table 4.6). Roasted stem δ^{15}N values fall between fiber, and nonfiber values, consistent with roasted stem being a mixture of these two tissues (Table 4.6, Figure 4.15). Assuming that this procedure adequately isolated the nonfiber portion of the stem, then, while raw stem is a suitable proxy for δ^{15}N values of the nonfiber portion of the stem, it is a biased estimator of nonfiber portion (δ^{13}C being 0.5 too negative relative to the nonfiber portion). This difference is unlikely to be significant at the scale of whole diet.

4.2 Combining Taxa: Comparing Variability in Source Isotope Values

Isotopic diet models are highly sensitive to the resources included in the model. Failure to include a resource can yield dramatically different reconstructions (Phillips et al. 2014).

However, due to mixing geometry, the number of input sources is often inversely related to the specificity of model outputs. More sources yield more feasible combinations and wider resource mixture proportion estimates. Because of this, it is often useful to aggregate resources into larger taxa prior to diet modeling. There are two conditions when aggregation is warranted (Phillips and Gregg 2003).

First, when resources are statistically indistinguishable in isotope space, aggregation is both intuitive and necessary. When sources have statistically indistinguishable delta values, they may be combined without implying any specific mixture of sources. That is, for isotopically indistinguishable resources a 20/80, 50/50 or 70/30 mixture will yield the same average delta values. Arbitrary separation of the sources can still be made, but no further information will be obtained (e.g., if resource A and B are statistically identical and together make up 30% of the mixture, the possible contributions of both A and B will vary between 0 and 30%).

Alternatively, large sample sets may express statistically different means, whose small separation will not be distinguishable in the diet mixing model. This case is often implicitly assumed when combing species level data into higher taxa (e.g., CAM/C4 plants, C3, artiodactyls etc.), but the data are sufficiently robust to make the assumption explicit.

Wild plant resources were selected to capture the range of isotopic variation in dietary elements; therefore, an unweighted average may over-represent minor sources. Conversely, any investigator's arbitrary weighting (including flat or unweight averages) of resources invites the critique that the weightings selected are inappropriate.

One way around this problem is to compare the isotopic spaces inhabited by different mixtures. Figure 4.15 plots means and 4x Standard Error of the Mean (SEM) ranges (e.g., -2 SEM to +2 SEM) for wild C3 resources. The dashed polygon defined by the outermost resource averages approximates the total range of weighted averages (e.g., 0-100% contribution from each resource) obtainable from this set of resources assuming the average for each resource is accurate. The thin solid polygon gives the same range using only seed resources (also mixes with a trivial amount of nonseed inputs). The thicker solid polygon defines the space taken up all mixtures of seed resources where no resource contributes more than 50% of the total (see (Fry 2013a) for proof of concept). The unweighted average for all plant resources and for all seeds is also plotted; the difference in means is 0.64 for

δ^{13}C and -0.52 for δ^{15}N.

Seed resources dominate the wild species found in Cedar Mesa flotation and coprolites samples (Matson and Chisholm 2007). In Figure 4.16, averages of seed resources will fall within the solid black line, while averages constrained so that no resource contributes more than 50% to the C3 class must fall within the green line. From this it may be inferred that if seed resources dominate the wild C3 taxa, the total range of variation in the C3 taxa mean is about 2-3 ‰ the equivalent of a SE of 0.5–0.75. Further, both unweighted and weighted average will return results within these polygons, suggesting that alternative weightings are unlikely to substantially alter the C3 stable isotope average.

If *Helianthus* is more negative than other seed resource in δ^{13}C due to gravel mulching, these averages may be slightly (up to approximately 1 per mil) too negative in δ^{13}C.

Figure 4.17 plots mean and 4 SEM ranges for wild C4 and CAM resources. *Atriplex* provides the majority of the δ^{15}N variability in this resource set, but is rather poorly attested archaeologically. The remaining resources show an approximate 3‰ range in δ^{13}C and δ^{15}N (solid line).

As a representative of the "cheno-am" taxon, *Amaranthus* is widely attested in the Basketmaker II record, while *Yucca* and *Opuntia* are less common. The thick solid line returns the space associated with more than 50% of wild C4 kcals coming from *Amaranthus* seed. The result is a polygon with 2-3‰ variance, suggesting an SE of 0.5-0.75‰. Here the unweighted average falls outside this boundary. Instead, this study posits that 50% *Amaranthus* seed and 50% everything else would make a more accurate estimate and in consequence adopt this weighed average in this study's model. However, the difference between the unweighted and 50% Amaranth Seed weighting is 0.50 for δ^{13}C and -0.35 for δ^{15}N.

For fauna, medium artiodactyls could not be identified to species but are statistically indistinguishable from *Ovis* c in δ^{13}C and δ^{15}N (assuming normality) and may be combined for the purposes of analysis. Figure 4.18 plots mean and 4 SEM ranges for sampled fauna. Note that *Canis*, *Cynomys*, and *Meleagris* are only comparative and not included among Basketmaker II resources.

Sylvilagus, *Ovis* and *Lepus* differ significantly from one another in at least 1 dimension. *Medium artiodactyl* is statistically indistinguishable from *Ovis*. As explained at the begin-

ning of this section, the arbitrary separation of taxa only serves to expand the range of feasible proportions in the separated taxa; no new information is provided by the separation. However, for consistency with previous studies, this study recognizes the three faunal categories used in Coltrain and Janetski (2013).

4.3 Chapters 3 and 4: Review and Conclusions

The reconstruction of diets using stable isotopes requires accurate estimates of the isotopic ratios of the resources consumed. This chapter has described a sampling and experimental regime that tests for several dimensions of isotopic variation in the Cedar Mesa area.

1. Modern flora have δ^{15}N values consistent with atmospherically fixed nitrogen from local cryptobiotic soil crusts, but visual metrics of soil crust development do not correlate with δ^{15}N values.
2. Cedar Mesa exhibits elevation effects on precipitation, temperature and botanical communities, but shows minimal correlation of elevation and δ^{13}C;
3. Elevation correlates with δ^{15}N for half of sampled species, but the effect size is less than 0.5‰ across the sampled elevation of Cedar Mesa
4. Local (e.g., 50-500m) microenvironmental effects on soil moisture may provide an explanation for the lack of observed trends in δ^{13}C and partial trends in δ^{15}N
5. Archaeofauna return isotopic results consistent with modern flora, suggesting that modern sampling is isotopically consistent with prehistoric foodwebs.
6. Simulated roasting and mastication of *Yucca baccata* suggest that raw stem is approximately 0.7 ‰ more negative in δ^{13}C than the edible nonfiber portion of the stem.
7. A comparison of behaviorally sensible weightings indicates that the isotopic averages of C3 and C4+CAM plant taxa are stable to within 1 to 1.5‰, suggesting that taxon composition has a larger impact on δ^{13}C and δ^{15}N than environmental or processing effects.

Taken together, these results suggest that the sampling of Cedar Mesa resources in this study is isotopically representative of the variation encountered by Basketmaker II forager-farmers, and appropriate for use in formal diet modes. As will be seen in the next

chapter, the local resource data form an excellent fit with human isotope data from Cedar Mesa.

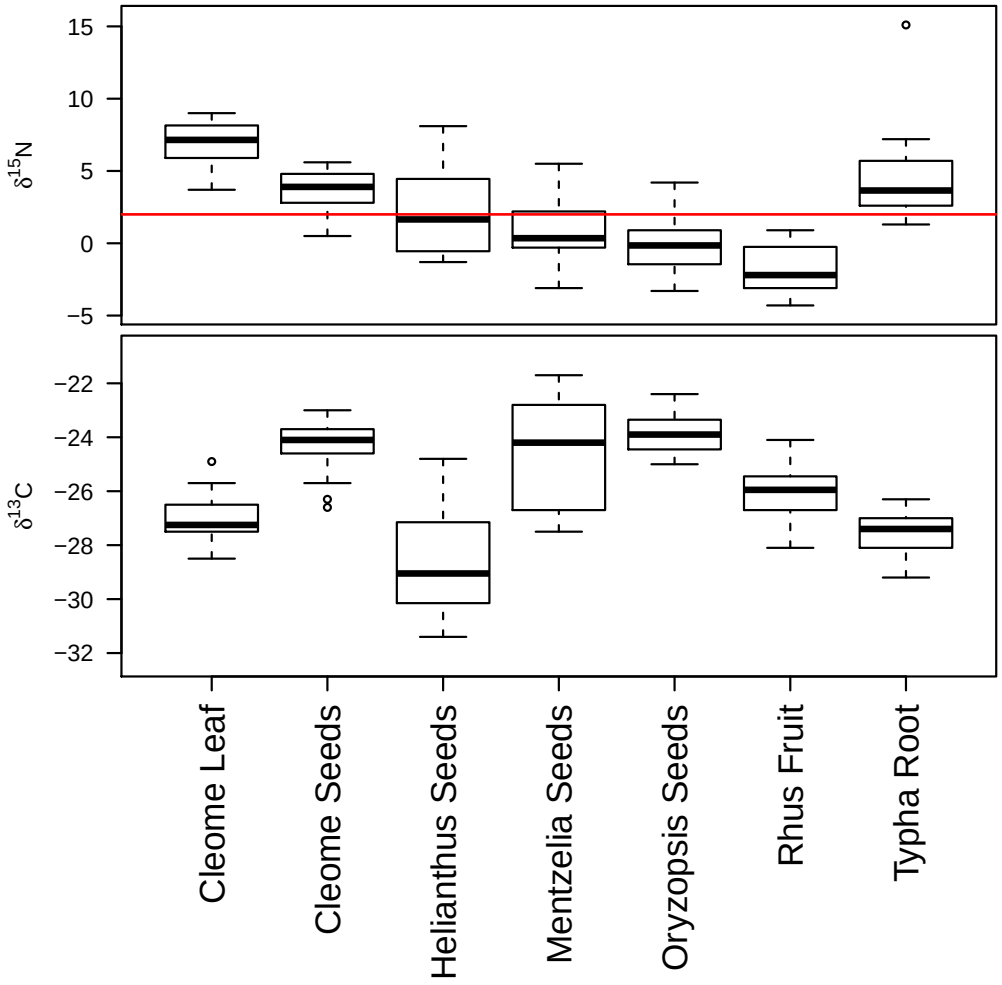

Figure 4.1: Stable isotope values for C3 plants. Median values shown by thick line. Boxes indicate interquartile range, whiskers indicate 5th and 95th quantiles. Horizontal line at $\delta^{15}N = 2$ the boundary between plants tissues with atmospherically fixed nitrogen and plants using decayed organic matter.

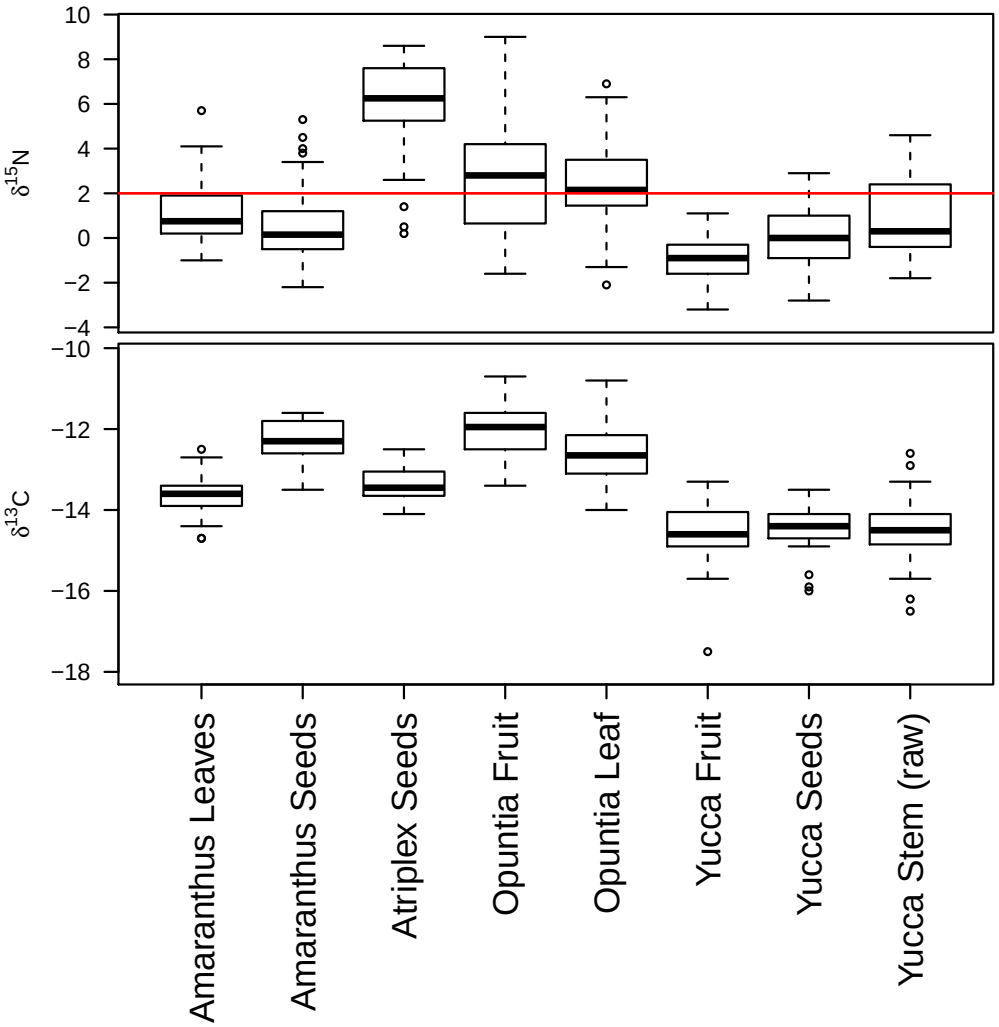

Figure 4.2: Stable isotope values for C4+CAM plants. Median values shown by thick line. Boxes indicate interquartile range, whiskers indicate 5th and 95th quantiles. Horizontal line at $\delta^{15}N = 2$ the boundary between plants with tissues atmospherically fixed nitrogen and plants using decayed organic matter.

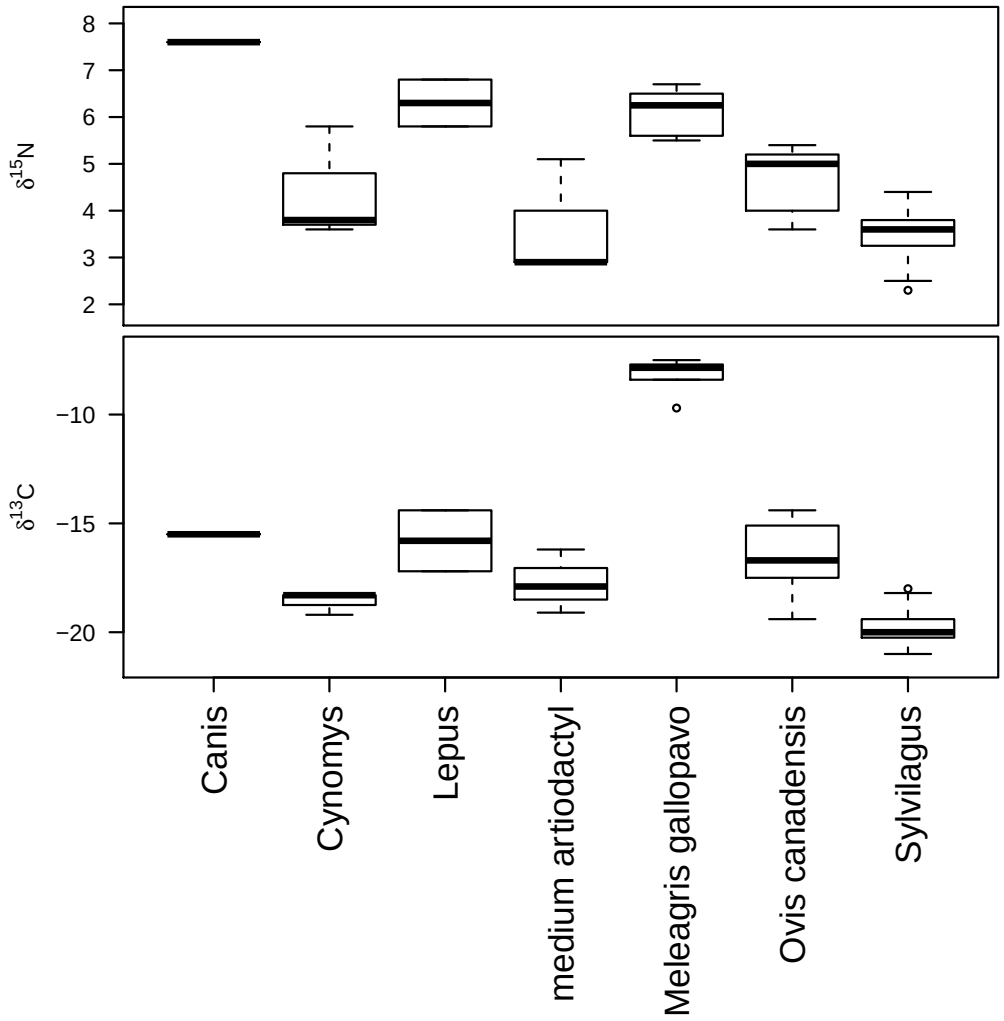

Figure 4.3: Stable carbon (δ^{13}C) and nitrogen (δ^{15}N) values for archaeological fauna from Cedar Mesa. Median values shown by thick line. Boxes indicate interquartile range, whiskers indicate 5th and 95th quantiles.

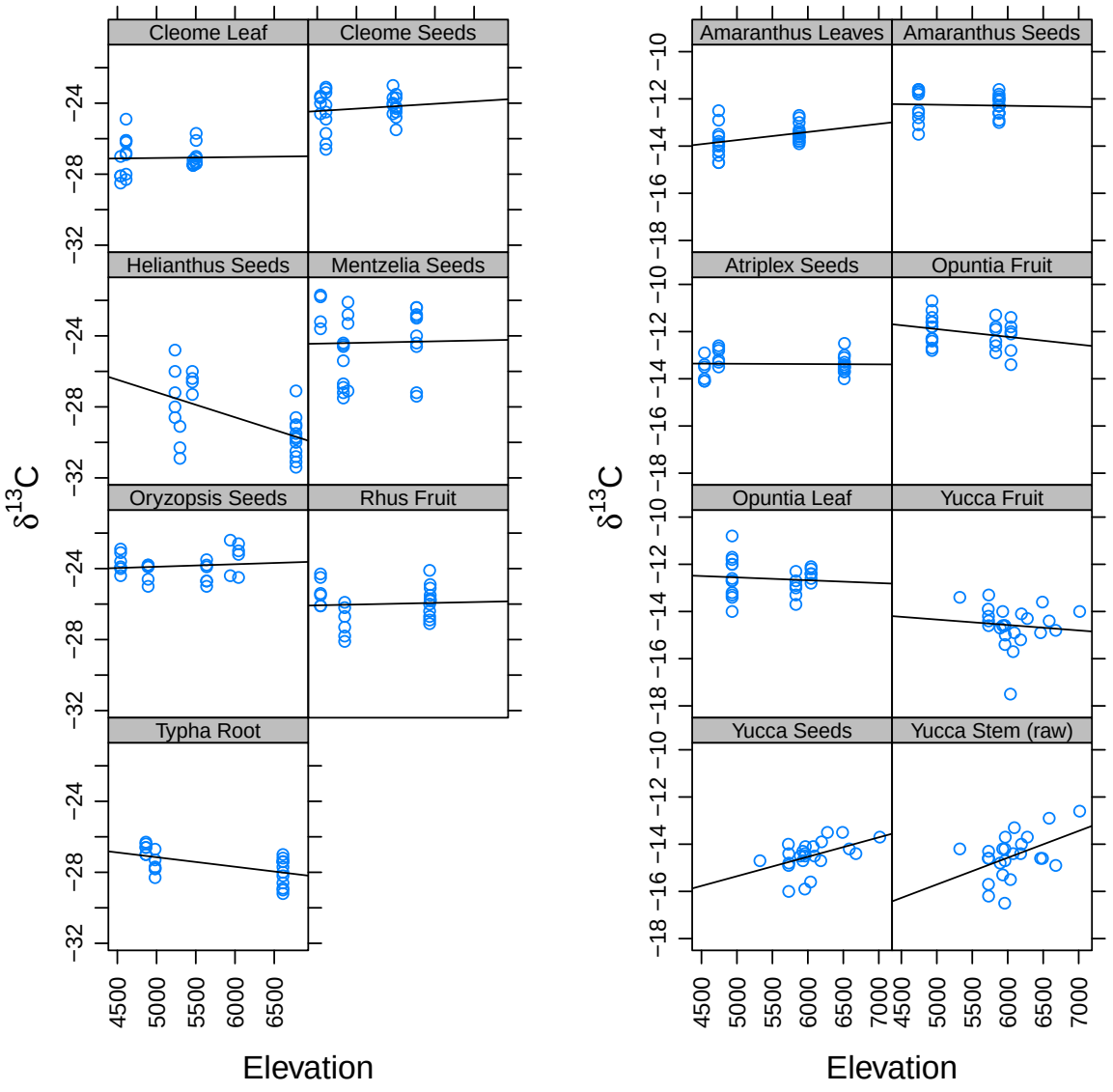

Figure 4.4: Least squares regression of $\delta^{13}C$ and elevation for C3 and C4+CAM species. Only *Typha*, *Helianthus* and *Yucca* show significant correlations at the 0.05 level. See Table 4.3.

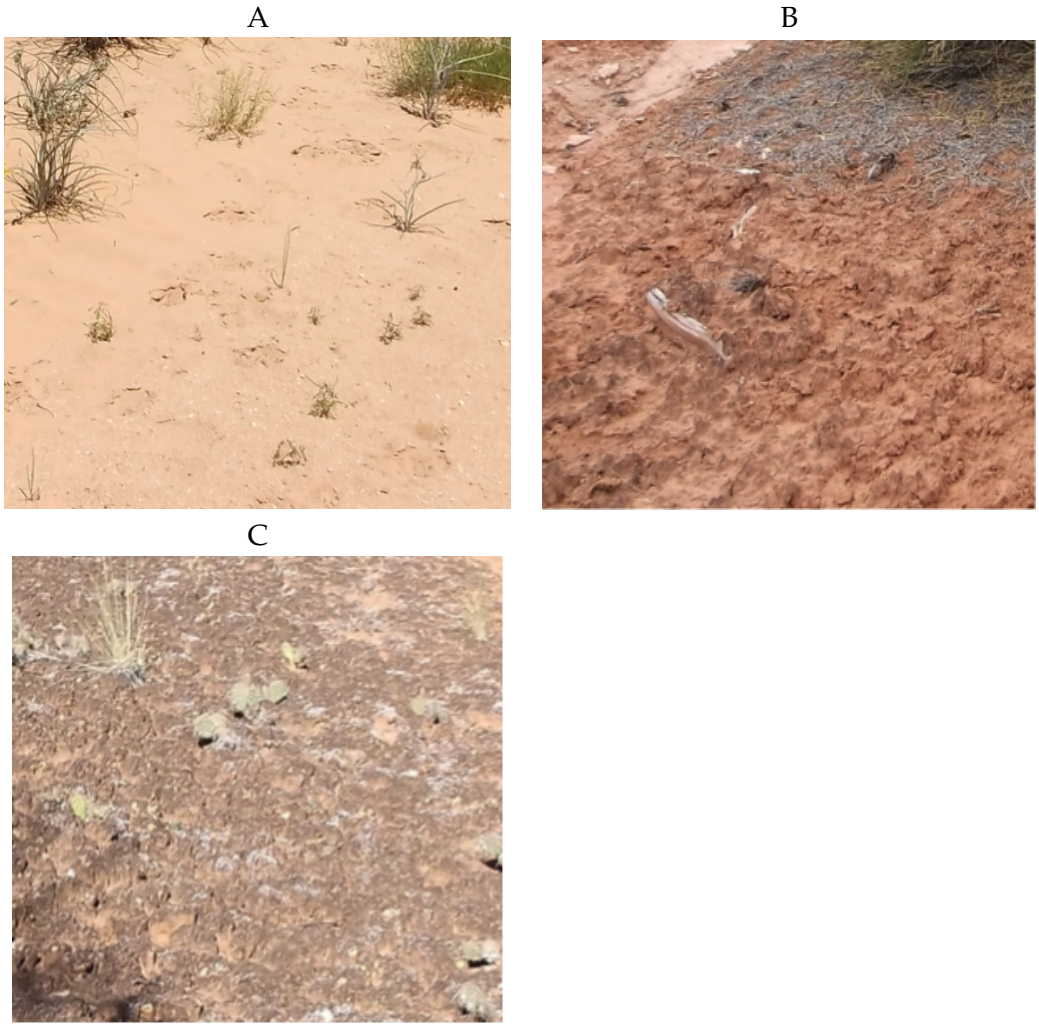

Figure 4.5: Crustal development levels. A: 0, no crust. B: 1, soil colored crust generally with local relief up to 3cm. C: 2, black colored crust, often with lichen.

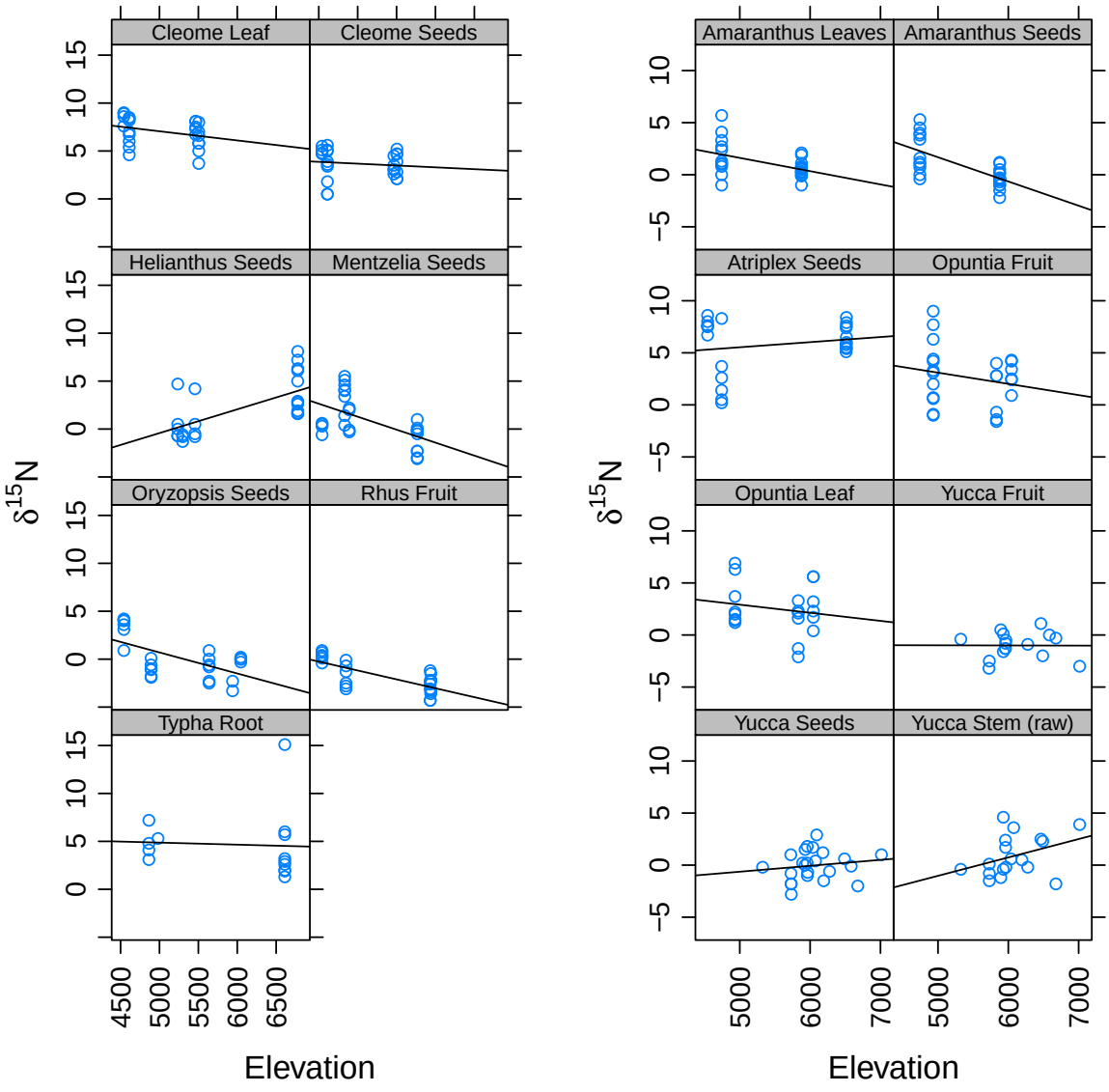

Figure 4.6: Least squares regression of $\delta^{15}N$ and elevation for C3 and C4+CAM species. *Amaranthus*, *Cleome*, *Helianthus*, *Mentzelia*, *Oryzopsis* and *Rhus* show significant trends. See Table 4.5.

Figure 4.7: Spatial distribution of low elevation botanical communities. Comb Ridge (left) and Comb Wash (center) facing south. Cedar Mesa at right. Note U-95 highway cut in Comb Ridge. Cedar Mesa and colluvium below Comb Ridge support pinyon-juniper woodland, the alluvial plain of Comb Wash is predominantly Sage-scrubland with a narrow dry riparian corridor following the main arroyo.

Figure 4.8: High elevation plant community spatial distribution. Google Earth satellite imagery of area around head of Sheik's Canyon showing defined boundaries between pinyon juniper woodland and sage flats. The Canyon Rim community is harder to see in satellite imagery but the exposed white bedrock in the upper middle indicates the associated thinly deposited soils.

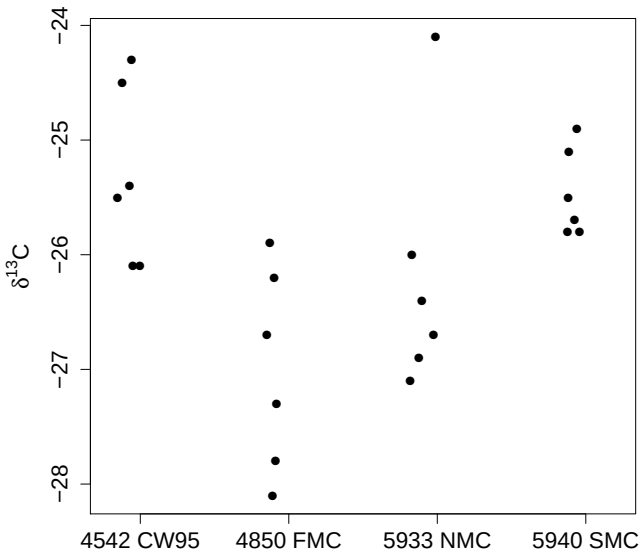

Figure 4.9: *Rhus* δ^{13}C. Fish Mouth Canyon (FMC-2) a dry riparian site shows more depleted δ^{13}C values than CW-95 site a sage-scrub site suggesting greater water stress in the latter. However, sites in North and South Mule Canyon (NMC, SMC-2) are both dry riparian—North Mule Canyon is a dry riparian site with ponderosa forest species—and show similar differences in δ^{13}C despite being separated by 1 km and < 10 m elevation. Differences associated with these shifts in botanical community are larger than any elevation effect.

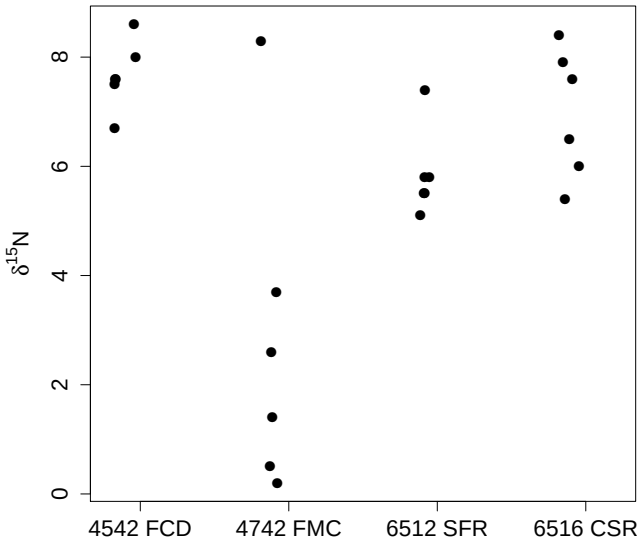

Figure 4.10: *Atriplex* δ^{15}N values by sample site. Fish Mouth Canyon (FMC-1) alone is taken from an arroyo context, but the outlying data-point was sampled from the alluvial plain above the arroyo, illustrating the effect of microenvironment on δ^{15}N.

Figure 4.11: Fish Mouth Canyon (FMC-1) sampling site. Note elevation difference between bottom of arroyo and level of alluvial plain (rise in left background). Most *Atriplex* were taken from the arroyo but the one outlier was taken from the alluvial plain.

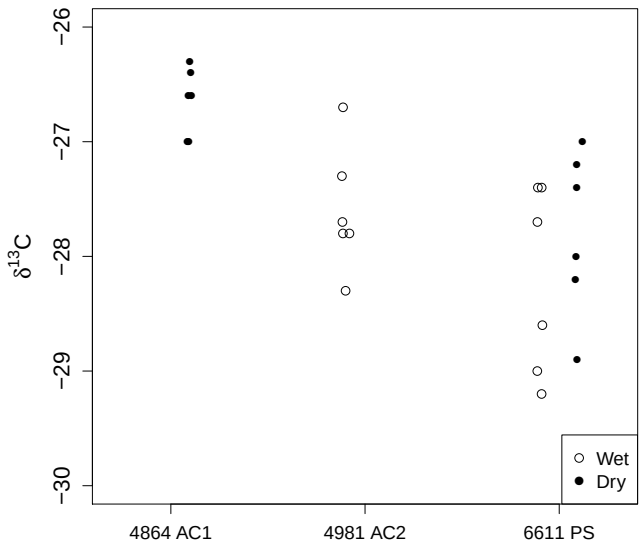

Figure 4.12: *Typha* from two elevations and two contexts. Arch Canyon (AC-1, AC-2) is a low elevation riparian site (4900 ft) while Pine Springs (PS) is a high elevation riparian site. Both sites contained areas of standing water (wet) and seasonally inundated sediments (dry). Note that increasing access to water results in more negative δ^{13}C values and the predicted elevation effects also are seen when ecological context is held constant.

A

B

Figure 4.13: Helianthus sampling sites. A: US-B Blanding sampling sites facing south: *Helianthus* scattered along highway margin west for 1 km but distribution extended into rocky soils in arroyos. B: U-95 sample site facing east, *Helianthus* confined to gravel matrix of roadbed

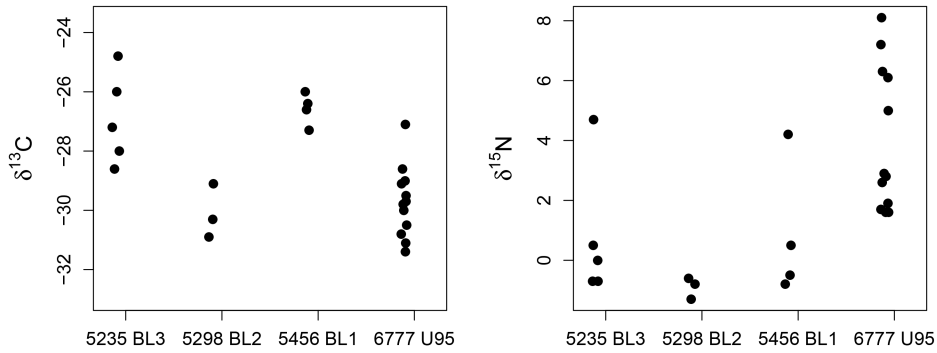

Figure 4.14: *Helianthus* δ^{13}C and δ^{15}N. BL1-3 (collectively the US-B sample site) are three areas sampled along a 1 km section of highway US-95 in Cottonwood Wash. U-95 is a highway sample site on the top of Cedar Mesa. The U-95 site showed generally greater roadbed gravel coverage, the mulch effect of which could explain the more negative δ^{13}C, and the associated lack of crusts could explain the more positive δ^{15}N.

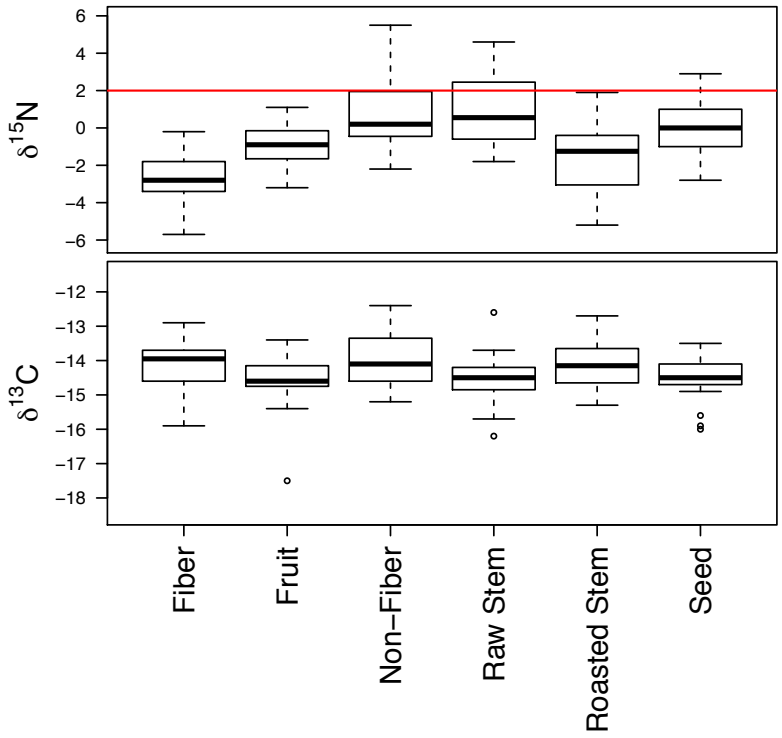

Figure 4.15: δ^{13}C and δ^{15}N variation in *Yucca b* tissues. Median values shown by thick line. Boxes indicate interquartile range, whiskers indicate 5th and 95th quantiles. Horizontal line at $\delta^{15}N = 2$ the boundary between plants with tissues atmospherically fixed nitrogen and plants using decayed organic matter.

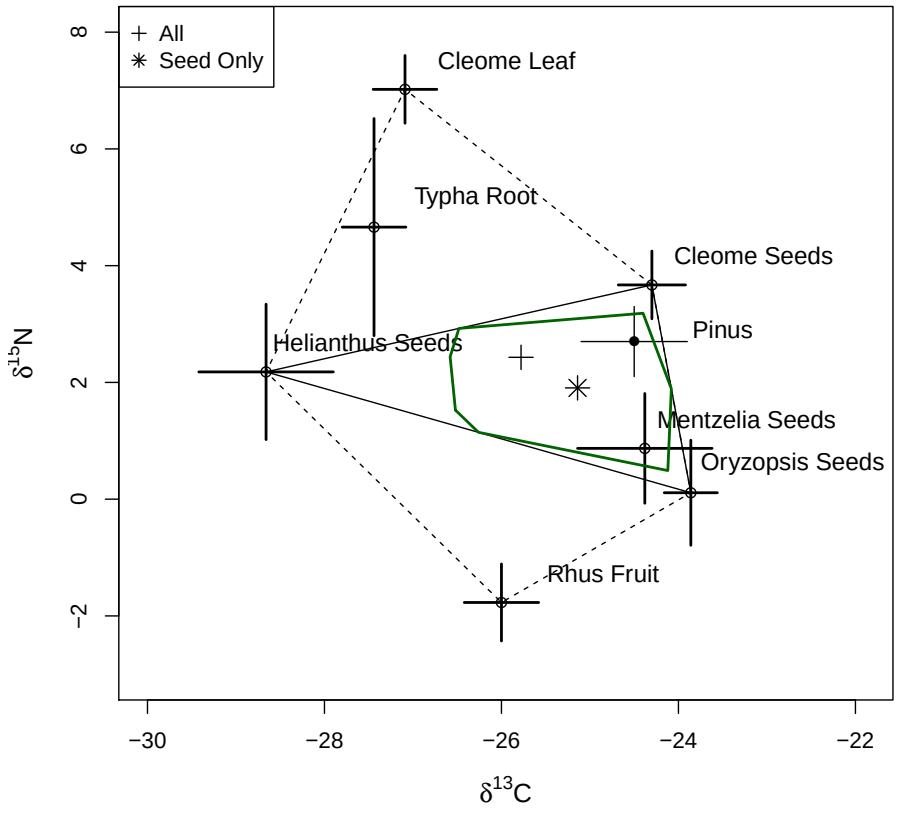

Figure 4.16: Mean and 4 SEM δ^{13}C and δ^{15}N ranges for wild C3 resources. The dashed polygon defined by the outermost resource averages approximates the total range of weighted averages (e.g., 0-100% contribution from each resource) obtainable from this set of resources. The solid polygon gives the same range using only seed resources (or using mixes with a trivial amount of nonseed inputs). The green polygon gives the range of results when only seed resources are used and when no resource contributes more than 50% to the C3 class. Note that *Pinus* is taken from Comb Village (reported in Coltrain and Janetski (2013)) and is not a local value and that δ^{13}C has been adjusted -1.5 per mil for comparison with modern flora.

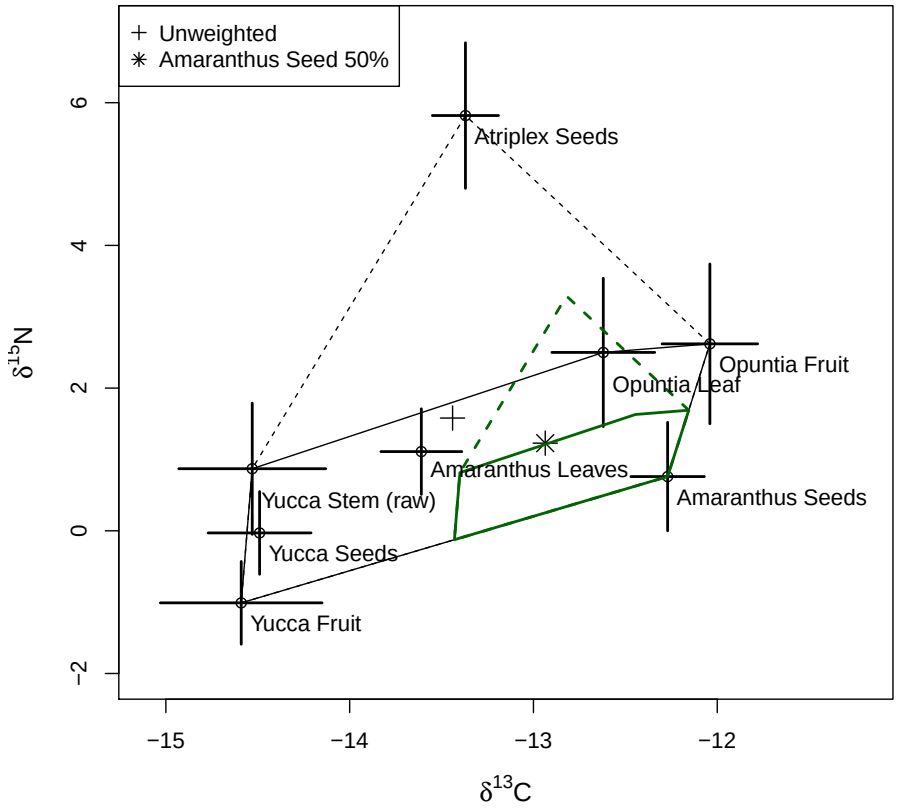

Figure 4.17: Mean and 4 SEM δ^{13}C and δ^{15}N ranges for wild C4 and CAM resources. The dashed polygon defined by the outermost resource averages approximates the total range of weighted averages (e.g., 0-100% contribution from each resource) obtainable from this set of resources. The solid polygon gives the same range for only succulents and "weedy" *Amaranthus*. The green polygons are scaled to reflect all mixes with a 50% *Amaranthus* seed contribution.

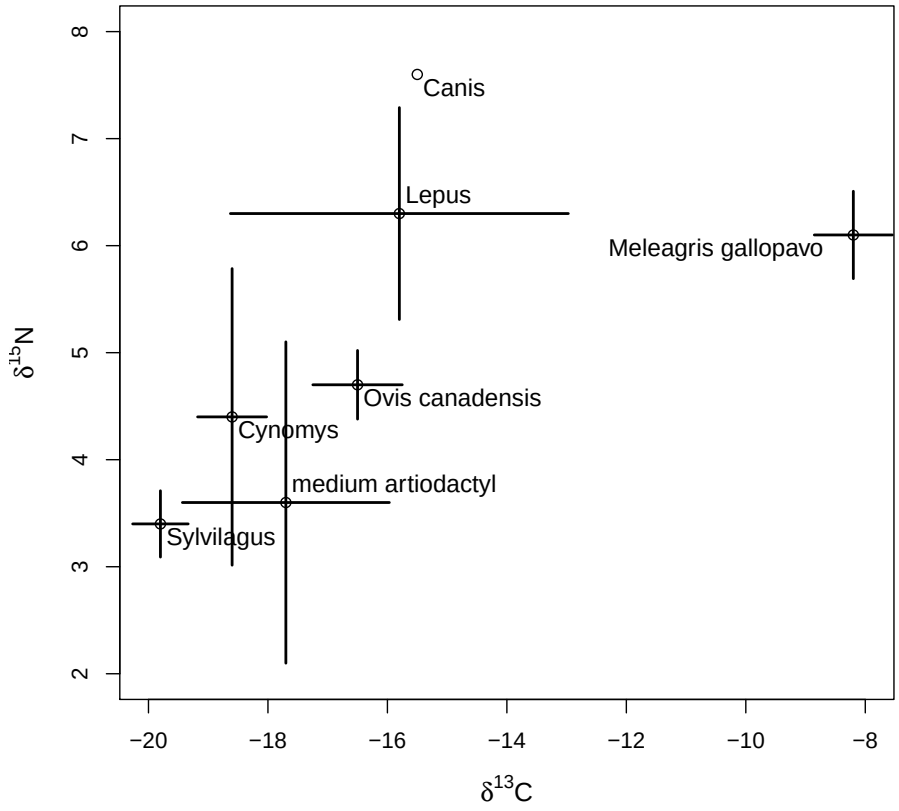

Figure 4.18: Mean and 4 SEM δ^{13}C and δ^{15}N ranges for archaeological fauna from Cedar Mesa.

Table 4.1: Summary statistics for modern Cedar Mesa flora by organ sampled. Parentheses give number of samples for $\delta^{15}N$ when excluding Wt % $N < 0.5$. Abbreviations are defined as follows: Amar. = *Amaranthus r*, Atri. = *Atriplex c*, Cleo. = *Cleome l*, Heli. = *Helinanthus a*, Ment. = *Mentzelia m*, Opun. = *Opuntia spp.*, Oryz. = *Oryzopsis h*, Rhus = *Rhus t*, Typha = *Typha a*, Yucca = *Yucca b*.

Species	Organ	Photo	$\delta^{13}C$	C SD	$\delta^{15}N$	N SD	Wt%C	Wt%N	N
Amar.	Leaves	C4	-13.6	0.6	1.1	1.5	34.2	4	26(26)
Amar.	Seed	C4	-12.3	0.5	0.8	1.9	44.3	3.3	26(26)
Atri.	Seed	C4	-13.4	0.5	5.8	2.5	42.2	1.4	24(24)
Cleo.	Leaves	C3	-27.1	0.9	7	1.4	41.6	5.1	24(24)
Cleo.	Seed	C3	-24.3	0.9	3.7	1.5	50.6	3.8	25(25)
Heli.	Seed	C3	-28.7	1.9	2.2	2.8	50.5	2.6	24(24)
Ment.	Seed	C3	-24.4	1.9	0.9	2.4	52.9	3.5	26(26)
Opun.	Fruit	CAM	-12	0.6	2.6	2.8	35.1	1.2	24(24)
Opun.	Leaves	CAM	-12.6	0.7	2.5	2.3	35	0.8	24(20)
Oryz.	Seed	C3	-23.9	0.7	0.1	2.2	43.3	1.7	24(24)
Rhus	Fruit	C3	-26	1	-1.8	1.6	49.9	1.8	24(24)
Typha	Root	C3	-27.6	0.8	4.7	3.5	39.1	1	24(14)
Yucca	Fruit	CAM	-14.6	0.9	-1	1.2	44.8	1	24(17)
Yucca	Seed	CAM	-14.5	0.7	0	1.4	54.6	2.6	23(23)
Yucca	Heart	CAM	-14.5	0.9	0.9	1.9	42.2	1	24(18)

Table 4.2: Summary statistics for Cedar Mesa fauna

Species	$\delta^{13}C$	C SD	$\delta^{15}N$	N SD	Wt%C	Wt%N	N
Canis	-15.5	NA	7.6	NA	43.2	15.6	1
Cynomys	-18.6	0.5	4.4	1.2	40.9	14.9	3
Lepus	-15.8	2	6.3	0.7	42.5	15.4	2
medium artiodactyl	-17.7	1.5	3.6	1.3	42.8	15.5	3
Meleagris gallopavo	-8.2	0.8	6.1	0.5	41.2	14.9	6
Ovis canadensis	-16.5	1.4	4.7	0.6	42.2	15.2	14
Sylvilagus	-19.8	0.9	3.4	0.6	39.6	14.2	15

Table 4.3: Correlation statistic calculations for δ^{13}C and elevation using Kendall's tau. Significant values at $p < 0.05$ given in bold. See also Figure 4.4. Abbreviations are defined as follows: Amar. = *Amaranthus r*, Atri. = *Atriplex c*, Cleo. = *Cleome l*, Heli. = *Helinanthus a*, Ment. = *Mentzelia m*, Opun. = *Opuntia spp.*, Oryz. = Oryzopsis h, Rhus = *Rhus t*, Typha = *Typha a*, Yucca = *Yucca b*.

Species	Organ	*Tau*	*z*	*p*
Amar.	Leaves	0.3327	1.9556	0.0505
Amar.	Seed	-0.1114	-0.6521	0.5143
Atri.	Seed	0.1053	0.6468	0.5177
Cleo.	Leaves	0.2114	1.2997	0.1937
Cleo.	Seed	-0.0465	-0.294	0.7687
Heli.	Seed	-0.4029	-2.4751	**0.0133**
Ment.	Seed	0	0	1
Opun.	Fruit	-0.2015	-1.1991	0.2305
Opun.	Leaves	0.0273	0.1632	0.8703
Oryz.	Seed	0.0617	0.385	0.7002
Rhus.	Fruit	0.0743	0.4634	0.6431
Typha	Root	-0.5428	-3.24	**0.0012**
Yucca	Fruit	-0.1959	-1.3202	0.1868
Yucca	Seed	0.3814	2.4956	**0.0126**
Yucca	Heart	0.2783	1.8697	0.0615

Table 4.4: Correlation statistic calculations for δ^{15}N and crust development level using Kendall's tau. Significant values at $p < 0.05$ given in bold. Note that several species could not be located on sites with more than one crustal development level. Abbreviations are defined as follows: Cleo. = *Cleome l*, Oryz. = Oryzopsis h, Rhus = *Rhus t*, Yucca = *Yucca b*.

Species	Organ	*Tau*	*z*	*p*
Cleo.	Leaves	-0.4113	-2.3519	**0.0187**
Cleo.	Seed	-0.0468	-0.2728	0.7850
Oryz.	Seed	-0.1080	-0.6158	0.5381
Rhus.	Fruit	0.6173	3.5356	**4.00E-04**
Yucc.	Fruit	-0.2711	-1.3164	0.1880
Yucc.	Seed	-0.0109	-0.0622	0.9504
Yucc.	Heart	0.1340	0.6691	0.5034

Table 4.5: Correlation statistic calculations for δ^{15}N and elevation using Kendall's tau. Significant values at $p < 0.05$ given in bold. See Figure 4.6. Abbreviations are defined as follows: Amar. = *Amaranthus r*, Atri. = *Atriplex c*, Cleo. = *Cleome l*, Heli. = *Helinanthus a*, Ment. = *Mentzelia m*, Opun. = *Opuntia spp.*, Oryz. = Oryzopsis h, Rhus = *Rhus t*, Typha = *Typha a*, Yucca = *Yucca b*.

Species	Organ	Tau	z	p.
Amar.	Leaves	-0.3973	-2.3643	**0.0181**
Amar.	Seed	-0.5754	-3.4295	**6e-04**
Atri.	Seed	0	0	1
Cleo.	Leaves	-0.455	-2.8264	**0.0047**
Cleo.	Seed	-0.2133	-1.3476	0.1778
Heli.	Seed	0.4958	3.0409	**0.0024**
Ment.	Seed	-0.4209	-2.7213	**0.0065**
Opun.	Fruit	-0.0765	-0.4619	0.6442
Opun.	Leaves	0.0585	0.3532	0.7239
Oryz.	Seed	-0.3538	-2.2277	**0.0259**
Rhus.	Fruit	-0.5559	-3.4745	**5e-04**
Typha	Root	0.0494	0.2988	0.7651
Yucca	Fruit	0.1352	0.8989	0.3687
Yucca	Seed	0.1238	0.8201	0.4121
Yucca	Heart	0.1938	1.3167	0.188

Table 4.6: Summary statistics for *Yucca baccata* tissues

Tissue	δ^{15}N	N SD	δ^{13}C	C SD
Fiber	-2.6	1.2	-14.1	0.7
Fruit	-1	1.3	-14.6	0.9
Non-Fiber	0.7	1.9	-14	0.8
Raw Stem	1	2	-14.5	0.9
Roasted Stem	-1.6	2	-14.2	0.7
Seed	-0.1	1.4	-14.5	0.7

Table 4.7: Mann-Whitney U-test p-values for pairwise comparisons of yucca stem.

Tissue	Isotope	Fiber	Non Fiber	Raw Stem	Roasted Stem
Fiber	δ^{13}C	1	0.7831	0.0737	0.5488
Non-Fiber		NA	1	0.0725	0.4395
Raw Stem		NA	NA	1	0.2216
Roasted Stem		NA	NA	NA	1
Fiber	δ^{15}N	1	<**0.0001**	<**0.0001**	0.0723
Non-Fiber		NA	1	0.082	**9.00E-04**
Raw Stem		NA	NA	1	<**0.0001**
Roasted Stem		NA	NA	NA	1

CHAPTER 5

FORMAL MIXING MODELS OF CEDAR MESA BASKETMAKER II DIETS

Having obtained estimates for Cedar Mesa resource isotope values, there are two technical modeling questions that must be resolved prior to using the Cedar Mesa human stable isotope δ^{15}N record for inference about Basketmaker II diets and economy:

1. **How does the accuracy of resource isotope values affect model results? Prior models of Cedar Mesa Basketmaker II diets used regional averages. Given the expense involved in assembling the local resource database, it is useful to know whether the result substantially changes the model reconstruction.**
2. **Given the isotopic variability seen in resource values and in trophic level enrichment estimates, are present models able to distinguish sex, age, and temporally based differences in human stable isotope values?**

The first half of this chapter addresses Question 1 through comparisons of three isotopic studies in the greater southwest and discussion of the regional average used to model Basketmaker II diet by Coltrain and Janetski (2013). The second half of the chapter examines Question 2 by comparing diet model outputs among Cedar Mesa human burials using mixSIAR.

5.1 Question 1: Regional Variation and Isotopic Baselines

To answer the question of how the accuracy of resource values changes model results, two things must be established. First, it must be shown that local Cedar Mesa resource data differ substantially from other area datasets and from the regional average employed by Coltrain and Janetski (2013). Second, diets must be formally modeled using both regional and local resource data and model outputs compared. As noted in Chapter 2, current implementations of SISUS do not utilize resource uncertainties, requiring the use of the

mixSIAR modeling system.

From Chapter 4, Cedar Mesa plant δ^{15}N values are generally below +2‰, in the range of values usually associated with legumes growing in association with nitrogen fixing bacteria. This pattern was attributed to nitrogen fixation in cryptobiotic plant crusts, though δ^{15}N does not correlate with crustal development levels.

At Cedar Mesa, more negative δ^{15}N values are not limited to modern flora. Figure 5.1 compares isotope food-webs constructed from modern plant data, adjusted for Seuss effect (e.g., plant values are adjusted to be "premodern") to three trophic levels of sampled archaeo-fuana. Data from Cedar Mesa (this study) are plotted in black, the Great Salt Lake (Coltrain and Leavitt 2002) plotted in green, and Chihuahua (Webster 2001) are plotted in gold.

Plant, herbivore, carnivore and human δ^{15}N values show relative enrichment within all three locations (note that modern Chihuahua flora δ^{15}N are not comparable to archaeo-fauna due to enrichment from modern fertilizer inputs (Webster 2001, 94). These data are omitted from Figure 5.1). However, Cedar Mesa taxa are 2-3‰ more negative than both Great Salt Lake and Chihuahua, an offset nearly as large as the usual estimate of trophic level enrichment of 3‰.

At the species level, both the Great Salt Lake and the Chihuahua datasets are small ($n<6$). However, in the Great Salt Lake study, the same δ^{15}N enrichment is seen if individual species (including those not plotted here) are combined into "small" and "large" herbivores, indicating that the offset is driven by ecology, rather than sampling or species differences. Further, the probability that sampling error can explain the differences between taxa from Cedar Mesa (which are more negative in δ^{15}N) and taxa from the Great Salt Lake (7 taxa) or Chihuahua (5 taxa) is vanishingly small.

5.1.1 Regional Variation and Consumer Values

This shift in isotopic baselines has a parallel in human isotopic data. Figure 5.2 plots data compiled from several studies of Basketmaker Fremont and hunter-gatherer populations in Utah (Stillwater Foragers (Schoeninger 1999), Fremont (Coltrain and Leavitt 2002), Basketmaker (Coltrain, Janetski, and Carlyle 2007; Coltrain and Janetski 2013)). Population variation in δ^{13}C shows a clear difference in maize (or C4+CAM) consumption, since the

interpopulation difference (≈10‰ in Figure 5.2) is larger than the ecological variability in δ^{13}C (≈1-3‰ in Figure 5.1).

A similar comparison would suggest that the higher δ^{15}N values correlate with greater animal protein inputs. This would be consistent with the idea that the Fremont economy varied from a Basketmaker II agricultural adaptation on the Colorado Plateau to more mixed economies near mountain and wetland resources (Simms 2008). In this case, however, ecological variation in δ^{15}N values makes inferences about animal protein consumption less certain. Figure 5.1 suggests that Cedar Mesa food-webs are depleted relative to Great Salt Lake food-webs by about 3‰, while the maximum interpopulation difference in δ^{15}N is about 5-6‰. This suggests that up to half of the interregional variation in human isotope values may be ecologically driven rather than being a product of dietary differences.

To put it another way, similarly plant-dominated diets on the Colorado Plateau and Great Basin wetlands would be expected to show a trophic level difference in δ^{15}N purely on the basis of local ecology—regardless of whether the plants consumed are C3 or C4+CAM. While this difference is smaller than the difference between Great Salt Lake Fremont and Basketmaker average δ^{15}N, ignoring the ecological variation would cause modelers to overestimate the dietary differences between these groups.

5.1.2 Regional Variation and Resource Polygons

Thus far δ^{13}C and δ^{15}N have been considered separately. In formal mixing models, their joint effects are analyzed. However, some the same dynamics apply: accurate dietary modeling requires using local resource data. While this principle is well known to isotopic modelers, the data obtained in our study allow for a particularly illustrative example of how different local ecologies result in isotopically distinct food-webs within the intermountain west.

Consider the simplest isotope mixing model, one that ignores resource and trophic level uncertainties, and concentration corrections. Under these assumptions, consumer whole diet values must plot within the polygon circumscribing the resources consumed (see review in Phillips et al. (2014)). Figure 5.3 plots Cedar Mesa and Great Salt Lake food-webs and the resource polygons associated with each area. Adult human agriculturalist

"whole diet" values (for Great Salt Lake only "high C4" diets are plotted) are calculated according the offsets $\delta^{13}C_{diet} + 5 = \delta^{13}C_{col}$ and $\delta^{15}N_{diet} + 3 = \delta^{15}N_{col}$.

Resource polygons are largely nonoverlapping. Great Salt Lake whole diet values fall outside the Cedar Mesa Polygon and Cedar Mesa whole diet values fall outside the Great Salt Lake polygon (maize values for Great Salt Lake are from unburned cobs in southeastern Utah reported in Coltrain and Leavitt (2002); however, these values are suggestive of organic nitrogen sources rather than atmospherically fixed nitrogen). While this example is perhaps more extreme than most regional studies are likely to encounter, it illustrates why local isotopic baselines are a prerequisite to formal diet modeling.

5.1.2.1 Resource Polygons and Assessing Human Isotope Datasets

A similar dynamic can be used to resolve differences among studies of Cedar Mesa burials. Figure 5.4 plots the Cedar Mesa resource polygon as well as Basketmaker and Puebloan whole diet averages from Coltrain and Janetski (2013) (in black) and from Matson and Chisholm (1994; 1991) (in red) . This model assumes the standard δ^{15}N trophic offset of +3. In this case, the 1991 human data fall outside the resource polygon, as does the Pueblo II/III data from Coltrain and Janetski (2013). The problem here is likely not ecological variation, but differences in analytic procedure. The Matson and Chisholm study was done before inline ignition permitted simultaneous analysis of the same sample. The investigators were unable to obtain nitrogen results for several specimens from the study, further suggesting instrumentation difficulties. Note though that *Ovis* samples from the Matson and Chisholm study closely match our results (*Ovis* collagen δ^{13}C = -17.0 in (Matson and Chisholm 1991), δ^{15}N = 4.5, our study *Ovis* Collagen δ^{13}C = -17.2, δ^{15}N = 4.7). Regardless of the instrumental reason for the more positive δ^{15}N values, the resource polygon indicates that the human isotope values from Matson and Chisholm are inconsistent with local food-webs. Caution is needed when using this older dataset.

5.1.3 Regional Variation and Regional Averages

Thus far we have looked only at local isotopic baselines. Previous models of Cedar Mesa diets used regional averages, a common occurrence in archaeological studies when local resource datasets may be unavailable or difficult and expensive to procure. However,

depending on the sampling methods used, the relationship of regional averages to local baselines is not always clear.

Figure 5.5 plots—in grey—the adult human whole diet isotope values from Coltrain and Janetski (2013). As in Figure 5.1, Great Salt Lake resource data are plotted in green, Cedar Mesa data in black, and the "All Utah" average used by Coltrain and Janetski (2013), is plotted in red. For C3, C4 (e.g C4+CAM) and *Lepus*, resources in the "All Utah" average take δ^{15}N values between Great Salt Lake and Cedar Mesa values. This is intuitive, since sites from both the Colorado Plateau (though not Cedar Mesa) and the eastern Great Basin contribute to the "All Utah" dataset. However, *Ovis* and *Silvilagus* δ^{15}N values from from "All Utah" dataset are more negative than either subregion–suggesting additional isotopic variation in the sites contributing to the "All Utah" dataset. Note that pinyon data from Cedar Mesa were not available (the year prior to sampling had a heavy mast), but previously published pinyon data from within 100 miles are in good agreement with Cedar Mesa C3 flora.

The crustal fixation effect causes the Cedar Mesa resource polygon to shift downward, better encompassing many human whole diet values, specifically many of the more negative δ^{15}N female values excluded by the "All Utah" polygon. While the circumscription of all isotope diet values by the resource polygon is not mathematically required for a model based on average female values, best practices suggest that if a substantial number of individuals fall outside a resource polygon, then sources have been inadequately sampled (Phillips et al. 2014). For Cedar Mesa female diet values, local resources provide a better set of model inputs.

On the other hand, the local Cedar Mesa dataset excludes about a dozen male individuals from the resource polygon (individuals from Pueblo II and III are also excluded). This may be due to a poor estimate of *Lepus* (n=2) collagen or to an improperly weighted average of maize from dry and spring farmed contexts (see Chapter 4). The upper edge of the polygon is sensitive to both measures, and variation of 1–2‰ will encompass several more human values. Further sampling of these resources may resolve this issue

A similar dynamic can be seen in a study of Cedar Mesa Basketmaker II hair (Cooper et al. 2016). The blue numbers plot the δ^{15}N diet values derived from hair using trophic level enrichments of +3,+4 and +5 (the hair to diet δ^{13}C conversion is complicated, but the

diets are "high C4" and have been plotted according to the range of estimates provided in Cooper et al. (2016)). An offset of +3 returns results consistent with the Coltrain and Janetski (2013) male and female δ^{15}N averages, but +4 and +5 offsets lie outside the "All Utah" dataset and can only be encompassed by local Cedar Mesa plant values.

One reason for this shift in resource values in the "All Utah" dataset is that different sources use data from different parts of the state, and thus different ecologies. This variation is manifested in several "All Utah" averages (C3, C4, *Lepus* taking δ^{15}N values intermediate to Cedar Mesa and Great Salt lake values (note that "All Utah" *Ovis* values are from the southern part of the state in an environment similar to Cedar Mesa).

The differences in weighting also may explain why the Trophic Level Enrichment (TLE) between plants and herbivores (except *Lepus*, but see Ugan and Coltrain (2011)) is relatively compressed at 0 and 2‰ for *Sylvilagus* and *Ovis*, respectively. While a 3‰ TLE is not required for model coherence—indeed, some sites like Parowan may have fauna drawn from multiple distinct ecologies (Ugan and Coltrain 2012)—its absence suggests a sampling of multiple isotopic baselines, an environmental diversity that may not be available at all locations within the region.

5.1.4 Regional Variation and Model Outputs

It is clear that changes in the local isotopic baseline can result in including or excluding some feasible diets for certain populations near the edge of the resource polygon. But how does changing the resource polygon's location change modeled outputs for feasible diets? To answer this question, several comparisons must be made.

Previous studies of Cedar Mesa isotope ecology used the SISUS mixing program and reported output results as mean and SD of the output distribution. Mean and $\pm$ SD ranges for the model of Coltrain and Janetski (2013) will first be compared with the median and output range values given by a SISUS model using the same resource inputs. This SISUS result will then be compared with two mixSIAR models, one using the resource data from Coltrain and Janetski (2013) and the other using local resource data reported in this study. Finally, noting that both mixSIAR models show highly negatively correlated maize and C4+CAM output proportions, linear constraints, and a posteriori aggregation alter model outputs. This process illustrates:

1. SISUS and mixSIAR models provide similar reconstructions of Cedar Mesa diets when mixSIAR model resource uncertainty is small.
2. MixSIAR models using local and regional data provide similar reconstructions.
3. Informative modeling requires the use of linear constrains or resource aggregation due to the negative correlation of maize and C4+CAM outputs.

These three principles will be discussed in greater detail in this section and then referenced without extended discussion for interpopulation comparisons in the second half of this chapter.

5.1.4.1 Cedar Mesa Diet Models: SISUS and MixSIAR

Figure 5.6 (see also Table 5.1) plots mean $\pm$ 1 SD for SISUS model estimates reported in Coltrain and Janetski (2013) (dashed lines) alongside median and range values of a SISUS model conducted by the author using identical inputs (solid black lines). Additionally, median and 99% credible interval values for a mixSIAR model using the Coltrain and Janetski (2013) data (green lines) and a mixSIAR model using the local resource data (blue lines) obtained from the present study are plotted (see Table 5.2 for stability statistics).

Source data SD in both mixSIAR models is set to 0.1 to simulate the fact that SISUS does not propagate source uncertainties. Attempts at smaller SD values required prohibitively long model runs, as low SD makes the likelihood surface rougher, causing the sampling algorithm to get "stuck" at "local high points" in the feasible region, precluding stability. Even with SD set to 0.1, a simulation with a chain length of 5 million was required to achieve suitable stability statistics (Table 5.2).

All three models show similar central tendencies and ranges (Figure 5.6), suggesting that the change from region to local resource inputs has a small effect on model outputs. However, note that the 99% credible range for the mixSIAR model is smaller than SISUS model. This may be due to the fact that mixSIAR determines credible intervals for each resource separately, rather than defining the edge of the n-dimensional feasible region, as does SISUS. This results in truncated tails in C4+CAM and maize proportion distributions. Solving this problem lies beyond the scope of this dissertation.

While the central tendency and range are similar in both mixSIAR models, the shape of the distribution of maize and C4+CAM proportions differs (Figure 5.7), with local resource

model giving larger tails to both. Basketmaker II whole diet values are more central to the local resource polygon than the Coltrain and Janetski (2013) model (see Figure 5.5), a geometry than generally leads to wider distributions of proportion estimates. To understand why this difference exists, we must consider the shape of the feasible region.

5.1.4.2 Cedar Mesa Diet Models: Mapping the Feasible Region

Recall from Chapter 2 that, in the mixSIAR simulation, the plotted outputs are a "cloud" of solution values, including some random "walking downhill" from the n-dimensional feasible region. Further, note that while the feasible region as a whole is approximately uniformly sampled (as when input uncertainties are small), any one or more dimensional cross-sections will show a density dependent on the shape of the feasible region in the other nonplotted dimensions. For example, if one uniformly sampled a cube but used a projection nonorthogonal to the axes of the cube (e.g., looking down on the point of one vertex), the depth of the cube would vary across the projection.

Thus the differences in the output distribution shapes are a reflection of differences in the shape of the feasible region defined by each model. This same difference is also seen in two dimensions in Figure 5.8, which plots maize and C4+CAM proportions for the solutions identified by both mixSIAR models (e.g., one using Coltrain and Janetski (2013) resource data and one using local data from this study). In both cases there is a strong negative correlation, but the Coltrain and Janetski (2013) model has a lower upper limit on C4+CAM values—and thus a higher lower limit on maize values—than the local resource model. By changing the shape of the resource polygon relative to the whole diet value, a different feasible region is defined, albeit one with a similar shape and orientation in these dimensions.

While this effect is most strongly seen with maize and C4+CAM, similar subtle changes occur in the minor resources in the model, as can be seen in bivariate resource output plots (Figures 5.9 and 5.10) and in Table 5.1.

The strong negative correlation between maize and C4+CAM allows extrinsic linear constraints and a posteriori resource aggregation to change modeled outcomes. That is, the initial stable isotope model does not contain all of our assumptions about human diet. Instead, it returns values for all mathematically possible solutions given the resources and

human input values used.

5.1.4.3 Cedar Mesa Diet Models: Model Constraints

Extrinsic constraints may be behaviorally justifiable, given the low outputs of wild resources on Cedar Mesa identified in Chapter 1. Both midden and coprolite deposits indicate that while Cheno Ams (a category which contains both C3 and C4 species) and succulents are common, the bulk of the recovered macrobotanical mass is maize—often by orders of magnitude (see Chapter 6). While the degree of constraint of C4+CAM inputs cannot be precisely known, a constraint on C4+CAM inputs to 30-20% of total diet seems conservatively broad. Rather than choose a single constraint, Table 5.3 presents model outputs for linear constraints of the maximum C4+CAM contribution of 30, 20, 10 and 5%. Figure 5.11 graphically presents the constrained models for <30% and <10% C4+CAM, respectively. In both models, lowering C4+CAM inputs narrows the maize distribution by raising its floor value (and by extension the value of the median and mean solution).

Constraints of <30% C4+CAM, result in maize distributions of 56-80% (using "All Utah" data from Coltrain and Janetski (2013)) and 54-79% (using local Cedar Mesa data)—a far more limited range of 25%. A <10% constraint yields 71-80% and 70-80%, respectively, a 10% range. Given the shape of the feasible region, even a simple conservative assumption about C4+CAM contributions to diet can restrict model outputs to a more informative range of values.

Alternatively, C4+CAM and maize categories may be aggregated a posteriori. In this case, a larger C4+CAM+maize resource category is created, and the ability to use the model outputs to answer research questions based on maize consumption is lost—unless C4+CAM inputs are posited to be trivial. In some cases, this may be justifiable. Table 5.4 displays aggregation results where fauna, C3 and C4 plant resources are the three categories used. This results in a stable and narrow estimate of C4+CAM+maize of between 78-90% ("All Utah"), and 78-90% (Cedar Mesa). In both cases, the differences in model outputs are trivial and suggest a plant-resource-dominated diet.

5.1.5 Section Summary

The results of this project indicate that substantial differences in food-web isotope values exist in the Intermountain West. Cedar Mesa flora, cultigens and fauna exhibit

δ^{15}N values several ‰ more negative than similar species sampled in northern Utah and Mexico, resulting in regionally-specific resource baselines which may not be applicable to models reconstructions of human diets from other regions.

The resource database used in Coltrain and Janetski (2013) is similar to that of Cedar Mesa in some respects, and similar to values from northern Utah in others. As a result, when models using this "All Utah" average are compared to models using local resources from Cedar Mesa broadly similar results are obtained.

Under both models, CAM and maize distribution ranges are uninformative. However, maize and CAM values are highly correlated, suggesting that information on diets can be obtained using conservative extrinsic assumptions. Moderate (10-30%) linear constraints on maximum C4+CAM inputs narrow maize estimate ranges to less than 25%. Resource aggregation provides a similar reduction in model output ranges.

In the next section, it will be shown that C4+CAM and maize output distributions for diet models using Cedar Mesa data are largely uninformative but highly negatively correlated. The ability to translate differences in bone chemistry between Cedar Mesa populations into dietary differences will consequently turn on the shape of the "feasible region" and the ability of linear constraints and resource aggregation to limit model output ranges.

5.2 Question 2: The Resolving Power of Isotope Mixing Models at Cedar Mesa

Having found that resource variation has little effect on Cedar Mesa Basketmaker II adult diets, the second question with which this chapter opened will now be examined. Do isotope mixing models have the power to translate observed differences in consumer isotope ratios into distinct subsistence behaviors?

The reminder of this chapter is largely a tabular comparison of mixSIAR model outputs, using the same set of tables described above and looking at several potential sources of variation in the Cedar Mesa and Basketmaker II human isotope records.

All models are run using a combination of data derived from local resource sampling and estimates from the existing literature. Table 5.5 gives resource model inputs for all models. Chapter 2 noted the conditions under which resource aggregation—both a priori

and a posteriori—is productive. Since pinyon falls within the range of wild C3 resources (see Chapter 4), a priori aggregation is advisable and followed. Similarly, since C4+CAM and maize output values appear highly correlated in this parameter space linear constraints and a posteriori aggregation are used. Finally since animal protein as a whole is of archaeological interest, we report both separate and aggregated faunal values for all models.

Human isotope values were compiled for early (pre-1 A.D) Basketmaker II from Marsh Pass, Arizona ((Coltrain, Janetski, and Carlyle 2007) Table 1), Grand Gulch phase Basketmaker II from Cedar Mesa ((Coltrain and Janetski 2013), Table 2), and Pueblo II and III individuals from Cedar Mesa ((Coltrain and Janetski 2013), Table 4). From this population, we include only adult ($>$ 15 yr) human isotope data, to avoid the trophic level enrichment in children's collagen.

It should be noted that no resource data exist for Marsh Pass, Arizona. However, the locality is only 50 miles southwest from Cedar Mesa and environmental/biological descriptions of Marsh Pass (Kidder and Guernsey 1919, 15), Black Mesa (to the immediate southeast of Marsh Pass (Powell and Smiley 2002, 33), and Shonto Plateau (to the immediate northwest of Marsh Pass (Geib 2011, 52), all describe the same basic biological communities. No attempt is made to model the Eastern Basketmaker II population from Durango, Colorado as the botanical communities there are more montane (Morris and Burgh 1954, 7).

Diets for each population were estimated in separate mixSIAR models, with chain lengths being increased until stability was achieved according to three metrics: the Gelman-Rubin Diagnostic, Geweke Diagnostic, and Heidelberger and Welch Diagnostic. For most models, three chains of 3 million with a burn-in of 1.5 million and thinning to every 500th solution were sufficient to achieve stability. However, both the Basketmaker II female and the Cedar Mesa Pueblo II-III populations required three chains of 5 million with a 2.5 million burn-in length and a thinning to every 1000th solution to achieve stability.

The longer required chain length may be a result of two processes. For Basketmaker II females, the centrality of the whole diet isotope value relative to the resource polygon may result in a "wider" feasible region that takes longer to fully sample. For the Cedar Mesa Pueblo II-III, the longer chain may be a function of the extreme marginality of the whole

diet value to the resource polygon, which results in the likelihood surface of the feasible region being less uniform.

The five basic models presented are:

1. Arizona (Marsh Pass) pre 1 AD Basketmaker II (but see caveat below).
2. Cedar Mesa post AD 1 Basketmaker II.
3. Cedar Mesa Basketmaker II males.
4. Cedar Mesa Basketmaker II females.
5. Cedar Mesa Pueblo II-III.

A sixth model further described below recalculates the Pueblo II-III population for a diet that includes domestic turkeys.

Figure 5.12 plots output distributions for Cedar Mesa Pueblo II-III, Marsh Pass, AZ (Early Basketmaker II), Cedar Mesa Basketmaker II (Late Basketmaker II) males, adults and females (for nonreduced plots of Cedar Mesa male and female diets see Figure 5.13. The resource polygon and whole diet values used in the model are plotted in the upper left. Several patterns are apparent. Cedar Mesa Pueblo II-III plots outside the average resource polygon—making feasible solutions dependent on resource uncertainties—and in consequence shows a narrow central distribution for maize and C4+CAM with small overlap. Marsh Pass Basketmaker II plots slightly inside the polygon and shows wider and overlapping central distributions. Cedar Mesa Basketmaker II diets plot more centrally to the polygon, and maize and C4+CAM output proportions overlap extensively; female Cedar Mesa Basketmaker II is most central, and C4+CAM and maize almost entirely overlap.

Above, when comparing mixSIAR models using the "All Utah" resource data and local Cedar Mesa data, the polygon was shifted relative to the whole diet value, resulting in a shift in the distribution peak between models—but modeled ranges were largely similar. When considering different populations, the whole diet average shifts relative to the local resource polygon, but the effects on the model are the same—distribution peaks shift, but the range of feasible proportions remains similar across all models.

Thus for maize and C4+CAM, while the central value of the distribution changes as diets plot more centrally, the total range of both C4+CAM and maize proportions does not

vary much between modeled populations (Table 5.6, Figure 5.14), and remains relatively low and uninformative (e.g., 5%-80% or 10%-70%) in all five models.

However, all five models also exhibit a similar feasible region shape, indicated by the high correlation of C4+CAM and maize proportions in feasible solutions. Figure 5.15 plots this correlation for all five models. R^2 values are, respectively, -0.95 for Arizona, -0.99 for Cedar Mesa Basketmaker II adults, and females and -0.98 for Cedar Mesa Basketmaker II males. Cedar Mesa Pueblo II show a correlation of -0.94. Such high correlation is only found between C4+CAM and Maize categories (Figure 5.16 plots the bivariate output plot for Cedar Mesa Basketmaker II adults. Other populations show similar results).

This high correlation permits the application both of linear constraints (Table 5.7, Figures 5.17 and 5.18) and of resource aggregation (Table 5.8, Figure 5.19). These techniques result in broadly similar model results. A constraint of C4+CAM$<$30% results in 50-80% maize proportions. Aggregation indicates that the combined C4+CAM/maize contributions to these diets varied from about 70-90%. Such aggregation results can be thought of as equivalent to the limit of maize input as maxCAM approaches 0%.

5.2.1 Discussion: Population Differences

The high correlation between output C4+CAM and maize proportions causes the differences in distribution shape to disappear when linear constraints or source aggregation are applied. Constraints of 30 and 10% max C4+CAM yield ranges of similar shape (for 30% and 10% constraints, respectively: Marsh Pass Basketmaker II 46-78%, and 61-78% Cedar Mesa Basketmaker II 51-80%, 66-80%, Cedar Mesa Pueblo II-III 50-82%,65-82%). Aggregation likewise limits ranges for C4+CAM+maize (Marsh Pass Basketmaker II 67-84%, Cedar Mesa Basketmaker II 75-88%, Cedar Mesa Pueblo II-III 70-88%) and for faunal inputs (Marsh Pass 9-26%, Cedar Mesa Basketmaker II 6-20%, Cedar Mesa Pueblo II-III 7-24%)

Though difficult to interpret, it is worth noting that the aggregation models suggest that the pre 1 AD Marsh Pass Arizona Basketmaker II population would have consumed 5% more large game and 5% less maize than the Cedar Mesa Basketmaker II or Pueblo II-III period. The total width of maize proportion distribution is 15%, so that the shift in values is about 33% of the total distribution width.

The posterior distribution plots in Figure 5.12, also contrast male and female source proportions. The largest difference is the inversion of median C4+CAM and maize inputs if the density of the distribution is considered. However, ranges are largely uninformative and substantially overlap. Both linear constraints and resource aggregation reflect the correlation of C4+CAM and maize. Even wide (CAM<30%) linear constraints remove the median value difference and result in ranges with small (<3%) sex-based differences in maize and individual faunal distributions. An a posteriori aggregation of C4+CAM and maize results in a narrower range of output C4+CAM+maize values (Female 77-90, Male 73-88) and show similarly small differences in aggregate faunal values (Female 4-18, Male 7-22). Thus the shift in the C4+CAM+maize distribution is about 23% of total distribution width, the shift for fauna is 21%.

Strictly speaking, if the the overlapping ranges of feasible solution values between Marsh Pass and Cedar Mesa, and between Cedar Mesa Basketmaker II males and females, are predominantly the result of model geometry, this change in distribution cannot be used to infer dietary differences between populations, as all solutions are equally probable. However, if these smaller shifts in distribution are predominantly the result of input parameter uncertainty, the shift would be a valid source of inference. In this case, the model would suggest that subtle shifts in diet occurred across the Basketmaker II period, and that men had marginally higher access to animal protein than women.

5.2.2 Pueblo II-III Turkey Consumption

The final comparison was not originally part of the study design, but was precipitated by a conversation at the 2017 Society for American Archaeology meetings in Vancouver B.C. on the evidence for turkey consumption in the terminal Pueblo III. Consistent with the results of turkey in this study, recent carbon isotope analyses of turkey bones suggest diets high in maize (Lipe et al. 2016, 109), (McCaffery et al. 2014; Rawlings and Driver 2010). Lipe and colleagues (Lipe et al. 2017) recently formalized patterns in turkey consumption (Kohler et al. 2012a; Bocinsky 2011), and declining large game indices (Badenhorst and Driver 2009) and presented a model arguing that consumption of domesticated turkey arose in response to decreasing wild faunal resources in the terminal III period.

Given the sensitivity of isotope models to the resources sampled (Phillips et al. 2014),

there is an open question of how adding turkey to the resource polygon would affect stable isotope diet models. Examining this question using Cedar Mesa resources, turkey and Pueblo II-III burial data resulted in a surprising illustration of the need for greater attention to the shape of the "feasible region."

Two models of Cedar Mesa Pueblo II-III diets were run. The first, reported above, excluded turkey as a resource. The second included turkey. Model output summary statistics (Table 5.9), output distribution plots (Figures 5.20, 5.21 and 5.22), linear constraint statistics (Table 5.10) and aggregation statistics (Table 5.11, 5.23) are given. This comparison illustrates the real-world effects on model outputs of an investigator choosing to include or exclude a single resource.

The inclusion of turkey as a dietary resource changes the shape of the resource polygon (see Figure 4.5). The adult Pueblo II-III whole diet value is on the edge of the polygon that excludes turkey but is central in the polygon that includes turkey. This change in geometry shifts the peak of the distribution of maize proportions downward and raises the peak of the C4+CAM distribution upwards for the turkey-inclusive model. However, these changes shift the aggregated category C4+CAM+maize downward by only a small amount (e.g., For the Pueblo II-III diet model without turkey the percentile range (2.5% to 97.5%) for C4+CAM+maize is 0.70-0.88, with turkey the range is 0.63 to 0.85). Without closer examination, one might conclude that including turkey in the diet marginally reduced the amount of maize consumed.

This is not the case. Instead, the shape of the feasible space must be considered. Since turkey diets are predominantly C4, turkey is isotopically substitutable with C4+CAM and maize and the source proportions for the categories C4+CAM+maize and turkey are moderately correlated, with an R^2 of 0.39 (Figure 5.24). The lower range of C4+CAM+maize when turkey is included is a function of the additional solutions made possible when turkey is 5-20% of total diet. If Lipe's estimates of the maize needed for turkey husbandry are accurate (Lipe et al. 2017), proportions of turkey greater than 5 or 10% appear unlikely.

Regardless of extrinsic assumptions, if the model is used to understand the diet at the point where turkey first is introduced as a resource, the higher CAM/Maize proportion 95% credible interval associated with a model without turkey (0.70-0.88) is more appropriate than the model with turkey (0.63-0.85). If only solutions with $<$5% turkey are

considered, the 95% credible interval (0.69 to 0.87) is practically identical to that of the turkey exclusive model. Further, note that when the proportion of turkey in the diet is near zero, the boundary of the cloud occurs at C4+CAM+maize=0.75—this is the 5th percentile under both turkey inclusive and exclusive models.

Similar inferences can be made if the source proportions of feasible diets are plotted with turkey versas aggregated wild fauna. Figure 5.25 shows this relationship for the model when turkey is included, and gives the range of outputs in the model where turkey is excluded. In both cases, if wild faunal inputs fall below 5-7% of total diet, the only way to achieve an isotopically feasible mixture is to include some proportion of turkey in the diet.

The formal logic of this type of inference is identical to that of linear constraints, but without applying an extrinsic assumption. To put it another way, strong negative correlations in resources or sets of aggregated resources can be used to establish mutually exclusive possibilities within the set of diets permitted by isotope chemistry. While the fauna versus turkey correlation is weak, the two conditions could be established: if fauna is $< 5\%$, turkey must be $> 0\%$. C4+CAM+maize and turkey show a stronger correlation and suggest that if maize inputs $< 72\%$, turkey must be $> 5\%$.

5.3 Chapter 5: Review and Conclusions

Stable isotope baselines for Cedar Mesa are depleted in δ^{15}N by the equivalent of one trophic level relative to other regions in the Intermountain West. This difference is sufficiently large to exclude the possibility of modeling diets from burials in one region with resource values from another. As such, inference from interregional comparisons of human isotope values cannot be made accurately without first referencing local isotopic baselines

Cedar Mesa Basketmaker II and Ancestral Puebloan diets show differences in δ^{15}N of 0.5 to 1‰. This difference is insufficient to detect differences in subsistence strategy through collagen stable isotope analysis alone, because the diets are dominated (70 to 90%) by a combination on C4+CAM plants and/or maize. Thus, while intergroup differences in δ^{15}N result in differing modeled proportions, this shift is largely a product of mixing geometry in which these two resources substitute for one another.

The shape of the feasible region also strongly affects model outputs. The ranges of contributions of either resource alone are wide, but when values are negatively correlated, moderate linear constraints on C4+CAM limit the range of feasible maize values. When resources are combined a posteriori, the result is a narrow estimate of C4+CAM+maize contributions to diet—an estimate that is surprisingly high and narrow at 70-90%. Similar considerations of feasible region shape suggest that the initial addition of turkey to Pueblo II-III diets took place in a context of 70-88% C4+CAM+Maize and that if wild faunal inputs were below 5-7% turkey consumption must have occurred to achieve the observed isotope chemistry.

Both the use of linear constraints and aggregation in the dietary models of this chapter, and the preliminary modeling of Cedar Mesa Pueblo II-III diets including and excluding turkey, illustrate the inferential danger of a simple comparison of model outputs. The shape of the feasible region may strongly affect the range and distribution of solutions for an individual resource. Further, the changes to the shape of the feasible region affected by the addition or subtraction of a resource must be considered also when interpreting the output values of all other resources in the model.

Correlations between resources or sets of resources can be addressed through the logic of linear constraint, either to limit model outputs or to establish possible but mutually exclusive sets of feasible solutions. This attention to the shape of the feasible region changes the use of mixing models from the endpoint of an enquiry (e.g., mixing models answer the question: "how much maize was in the diet?"), to a first-pass constraint on the set permitted dietary combinations (e.g., mixing models show which dietary combinations are chemically feasible) which can be further constrained by extrinsic assumption. As local resource databases are better compiled, this perspective on the use of mixing models will be of significant value in narrowing mixing model outputs and integrating model results with other lines of evidence.

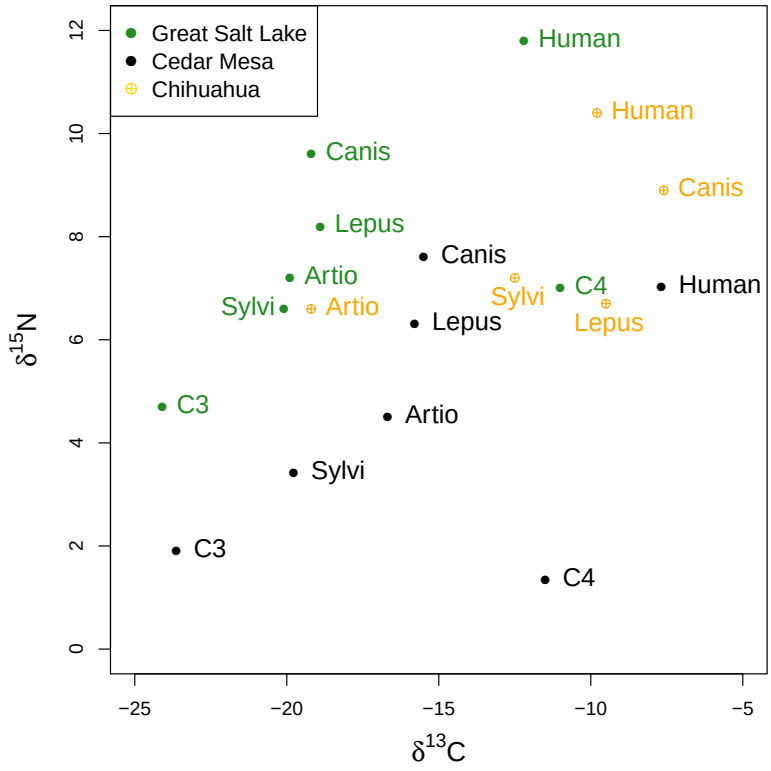

Figure 5.1: Comparative taxa from three intermountain stable isotope studies Cedar Mesa, Great Salt Lake Utah and Chihuahua Mexico. Modern flora from Chihuahua are not plotted due to δ^{15}N values reflective of modern fertilizers. While Great Salt Lake and Chihuahua show similar archaeofaunal δ^{15}N values, Cedar Mesa taxa, both modern and ancient, show more negative δ^{15}N values than both regions, illustrating the well-established fact that isotopic effects—such as that of nitrogen fixing soil crusts—are passed up the food-chain.

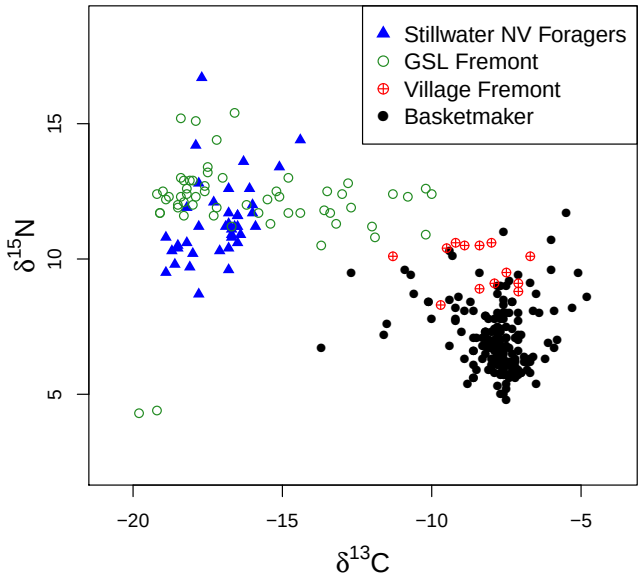

Figure 5.2: Comparison of four archaeological populations from the Great Basin (Stillwater foragers and Great Salt Lake Fremont) and Colorado Plateau (Village Fremont and Basketmaker). Given the potential differences in isotopic baselines the intergroup difference in δ^{15}N cannot be attributed to subsistence differences alone (e.g., more or less animal protein)

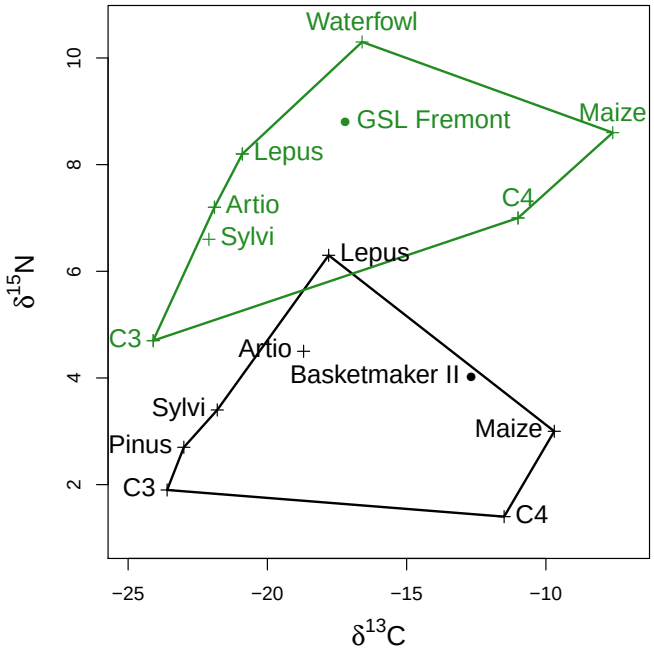

Figure 5.3: Resource polygons for Cedar Mesa and Great Salt Lake regions plotted with human whole diet values. Note that whole diet values from either region fall outside the resource polygon of the alternate region making formal diet modeling possible only when local resources are sampled.

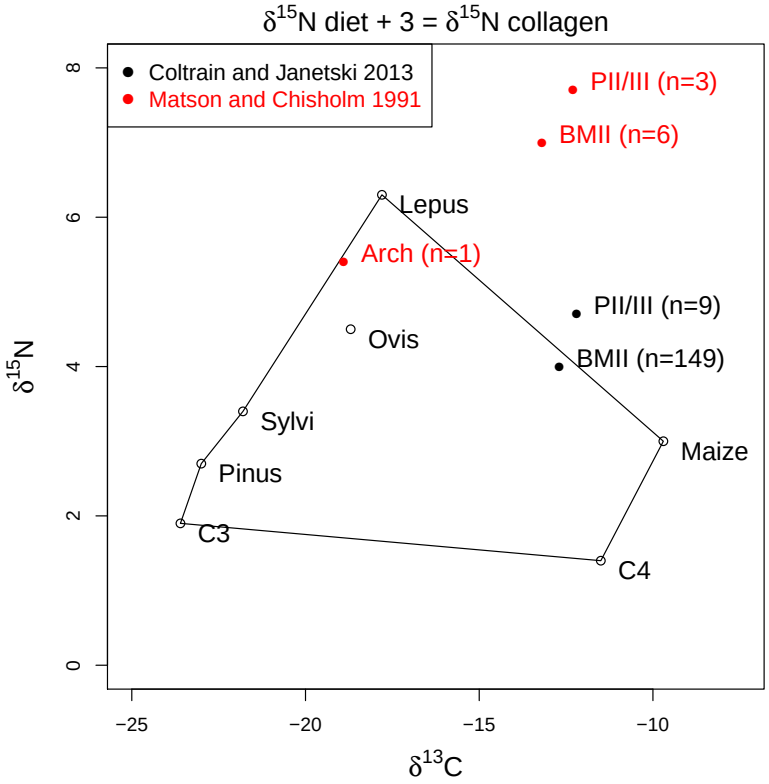

Figure 5.4: Comparison of whole diet isotope values estimated from Basketmaker II and Pueblo II-III burials analyzed by Coltrain and Janetski (2013) and Matson and Chisholm (1991). The δ^{15}N trophic level offset is +3 in this model.

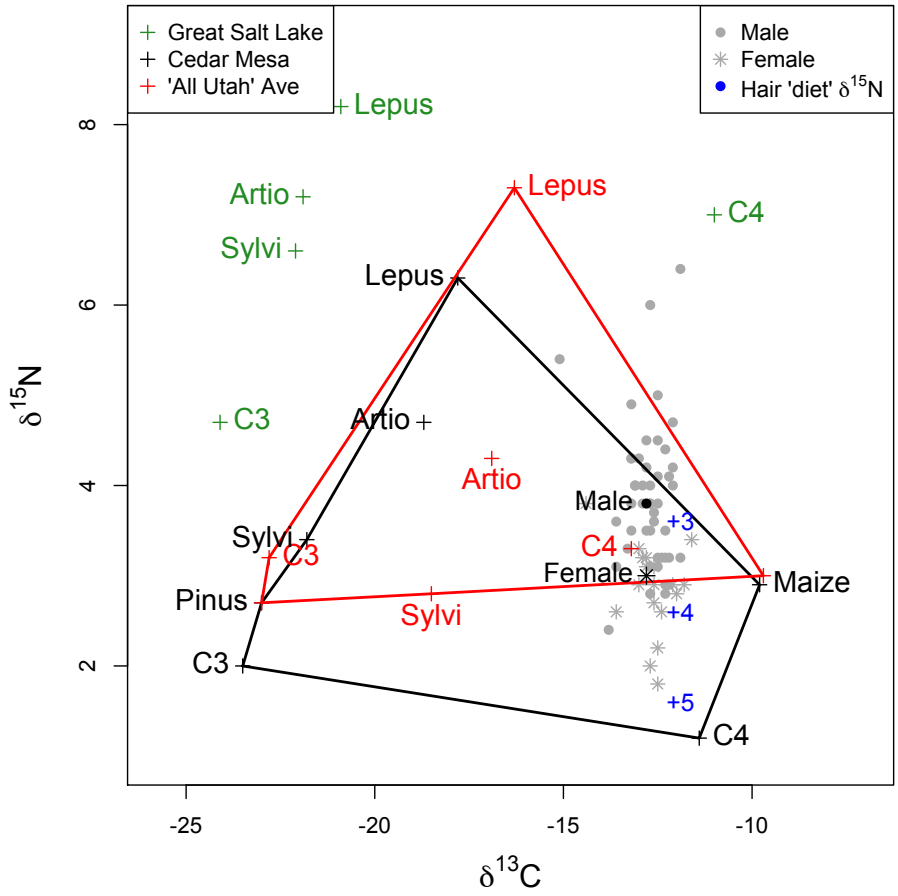

Figure 5.5: Resource polygons from Coltrain and Janetski (2013) and the present study. Grey points indicate human whole diet values for adult Cedar Mesa Basketmaker II. Male and female averages are plotted in black.. Blue numbers indicate whole diet nitrogen values from (Cooper et al. 2016).

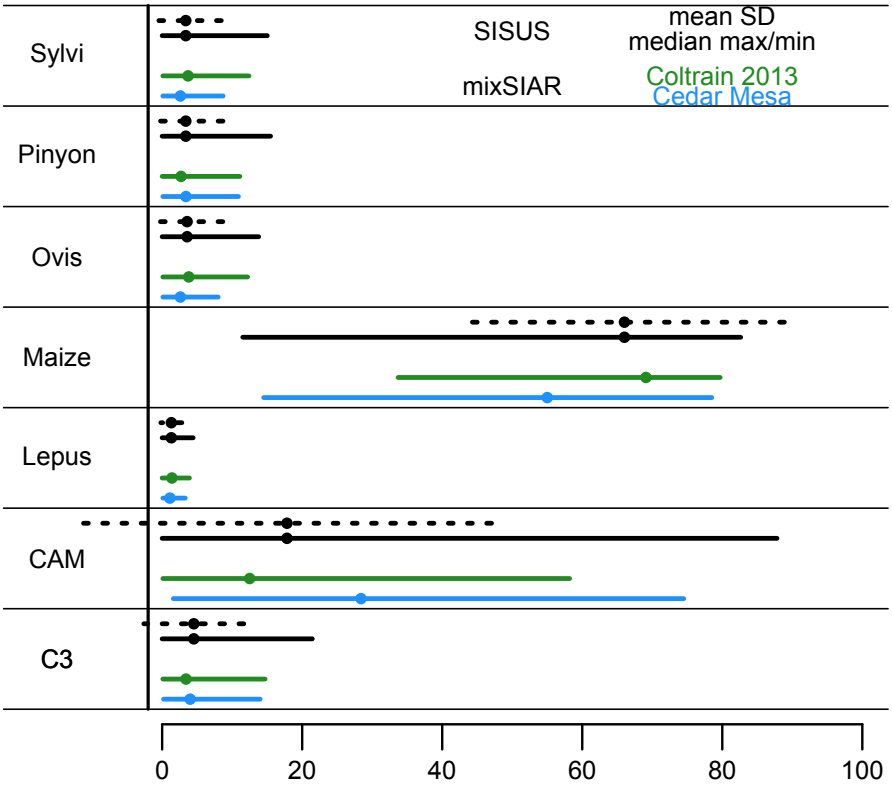

Figure 5.6: Model outputs (percentage of total diet) for seven resources (note that CAM+C4 plants are abbreviated CAM). Two SISUS models are compared (mean and 1 SD [dashed lines], median and range [solid black lines]) using resource data from Coltrain and Janetksi (2013), as are two mixSIAR models (0.95 credible region) one using resource data from Coltrain and Janetski (2013) [green lines], and one using local Cedar Mesa resource data [blue lines].

A

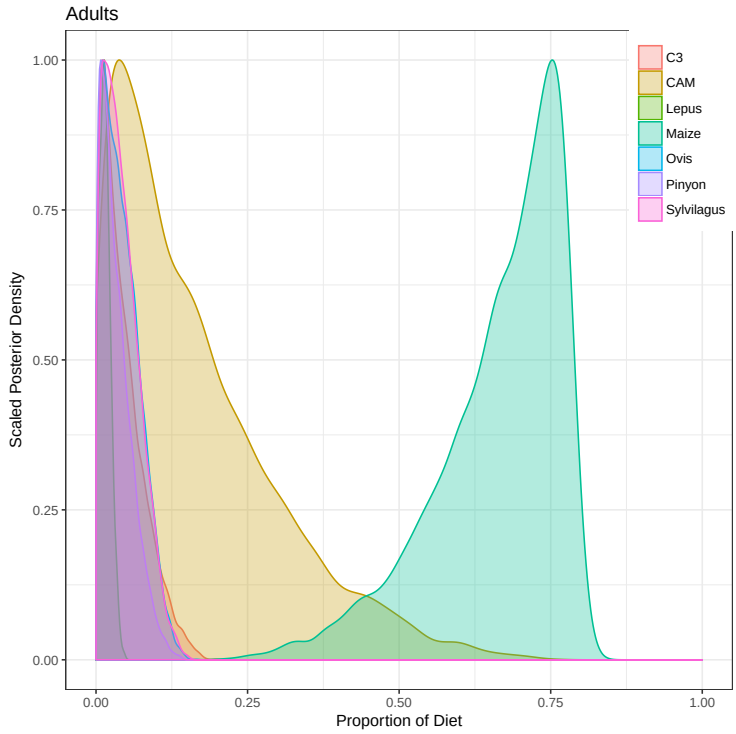

B

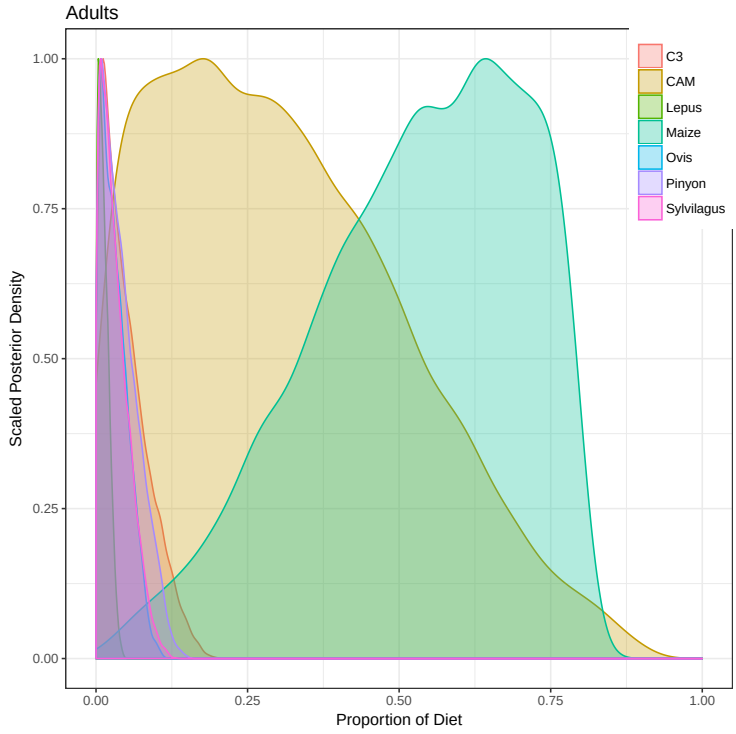

Figure 5.7: Output distributions for mixSIAR models using data from Cotrain and Janetski (Coltrain and Janetski 2013) (A) and local Cedar Mesa data (B). While peak locations are similar, peak shape is not. In both models, total distribution width makes CAM (e.g., C4+CAM) and maize estimates uninformative under both models. Note that the use of local resource values expands the width of the central portion of both C4+CAM and maize.

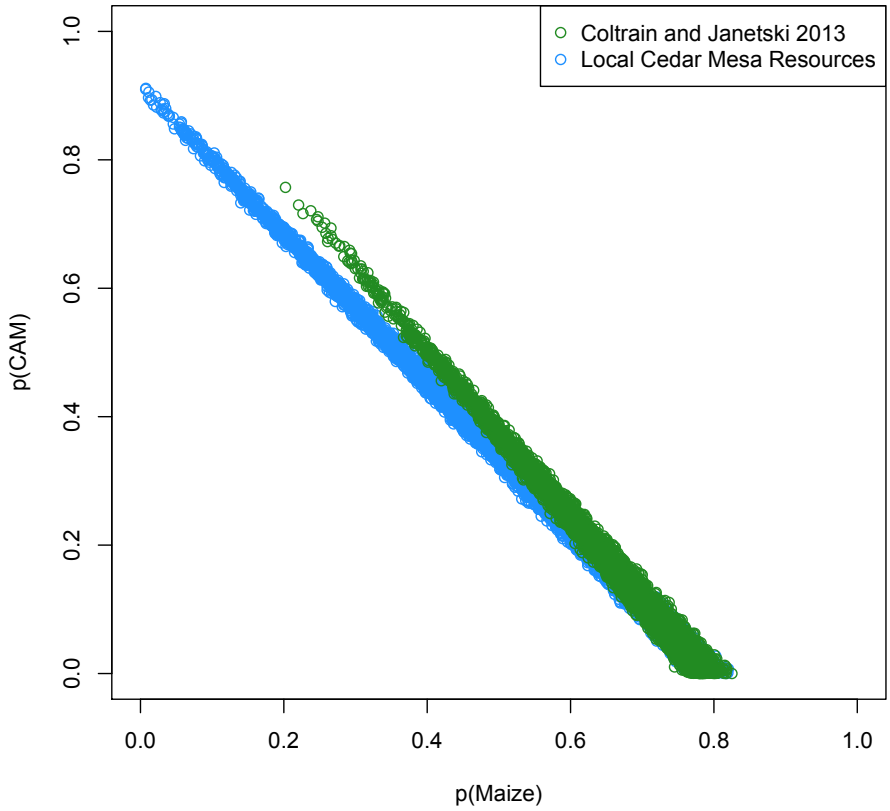

Figure 5.8: Correlation plot of the output proportions of C4+CAM and maize in the raw output solutions of mixSIAR models using the original Coltrain and Janetski (2013) data and the Cedar Mesa resource data of the present study. The x-axis plots the proportion of maize (abbreviated p(Maize)) in individual feasible solutions; the y-axis plots the proportion of C4+CAM (abbreviated p(CAM)) in each feasible solution. Note that the local data result in CAM and maize solutions better distributed across the range of solution values.

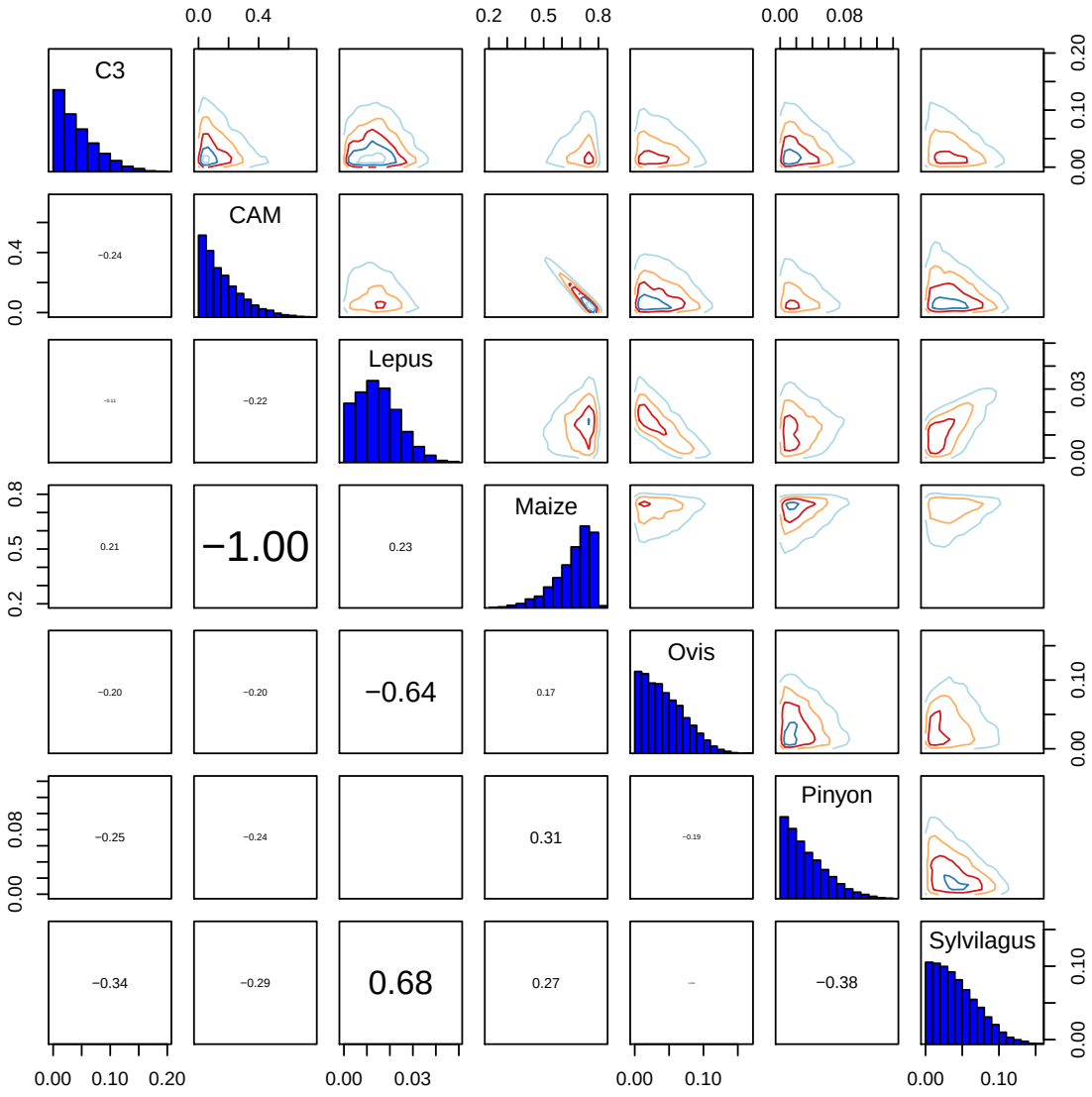

Figure 5.9: Bivariate plot of Coltrain and Janetski (2013) data model outputs. Central diagonal plots the distributions of feasible source proportions for each resource in diet. Upper right bivariate plots of source proportions for each resource in column and row, with axes scaled to the range of feasible proportions for each resource. Lower left plots correlation coefficients for corresponding bivariate plot in upper right. Coefficients are plotted proportional to magnitude. Only coefficients with absolute value larger than 0.30 are visibly plotted. Negative correlations of C4+CAM (abbreviated CAM) and maize suggest that these resources substitute for another in the feasible diet space due to their proximity in $\delta^{15}N/\delta^{13}C$ space and their similar position relative to the whole diet value.

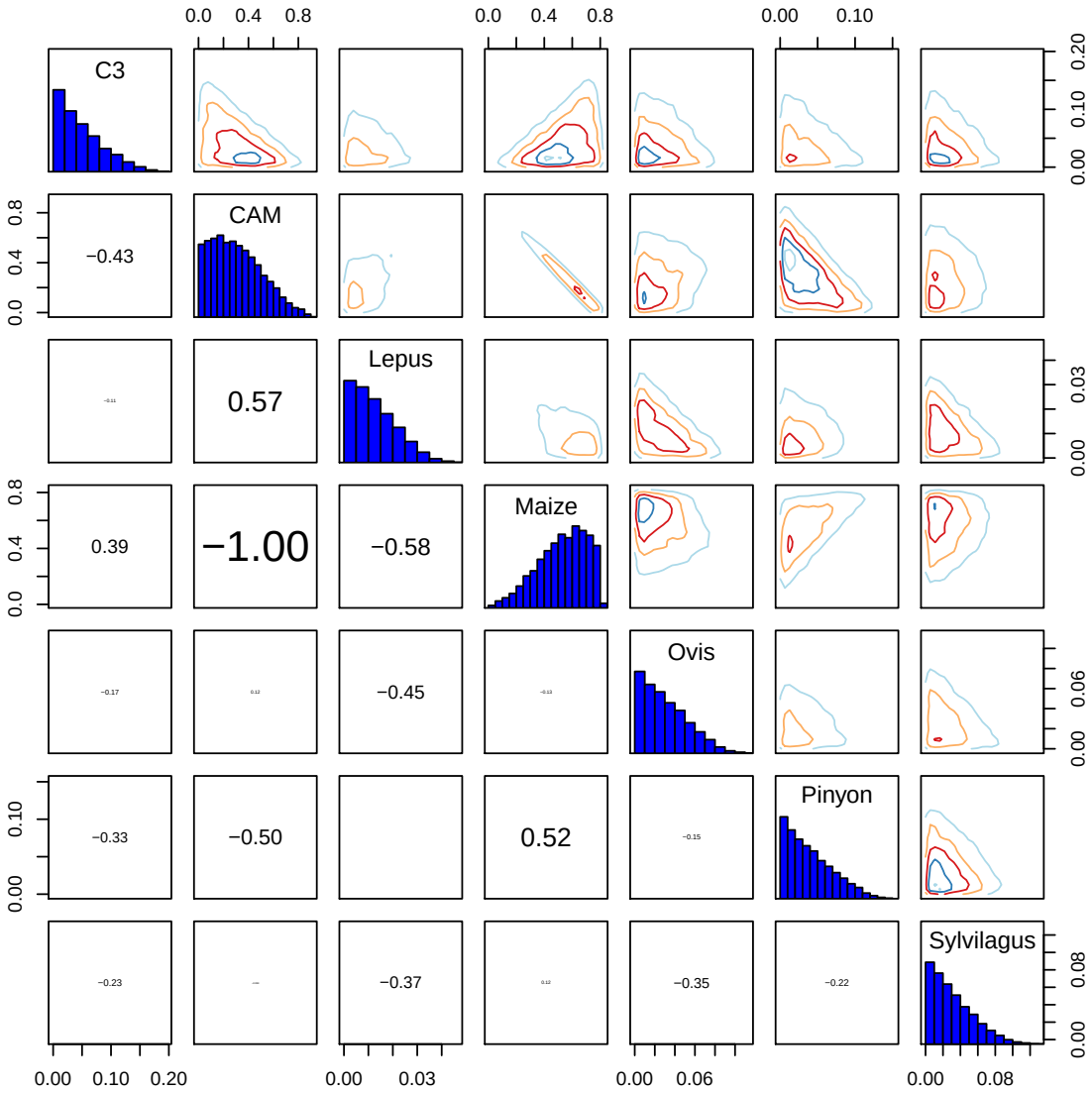

Figure 5.10: Bivariate plot of model outputs for model using source data from Cedar Mesa. Central diagonal plots the distributions of feasible source proportions for each resource in diet. Upper right bivariate plots of source proportions for each resource in column and row, with axes scaled to the range of feasible proportions for each resource. Lower left plots correlation coefficients for corresponding bivariate plot in upper right. Coefficients are plotted proportional to magnitude. Only coefficients with absolute value larger than 0.30 are visibly plotted. Note that Cedar Mesa data result in flattened distributions of maize and C4+CAM (abbreviated CAM) as greater distance in isotope space from whole diet mixture permits a wider range of combinations.

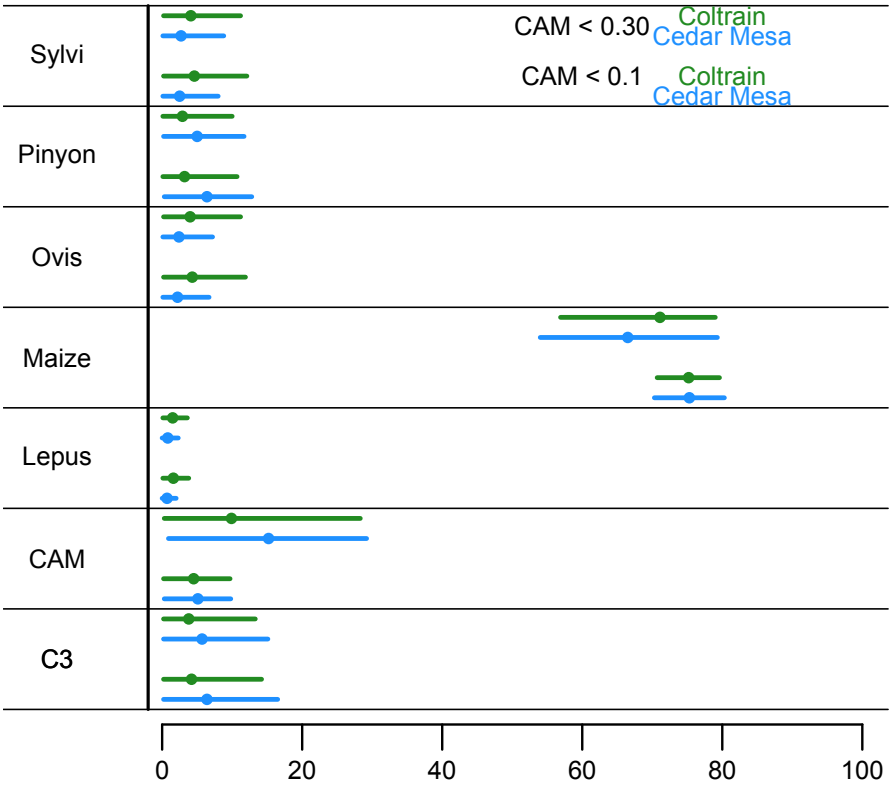

Figure 5.11: Comparison of model output distributions under linear constraints of C4+CAM < 0.30 (upper) and C4+CAM < 0.10 (lower), for resource data from Coltrain and Janetski (2013) and local Cedar Mesa resource data.

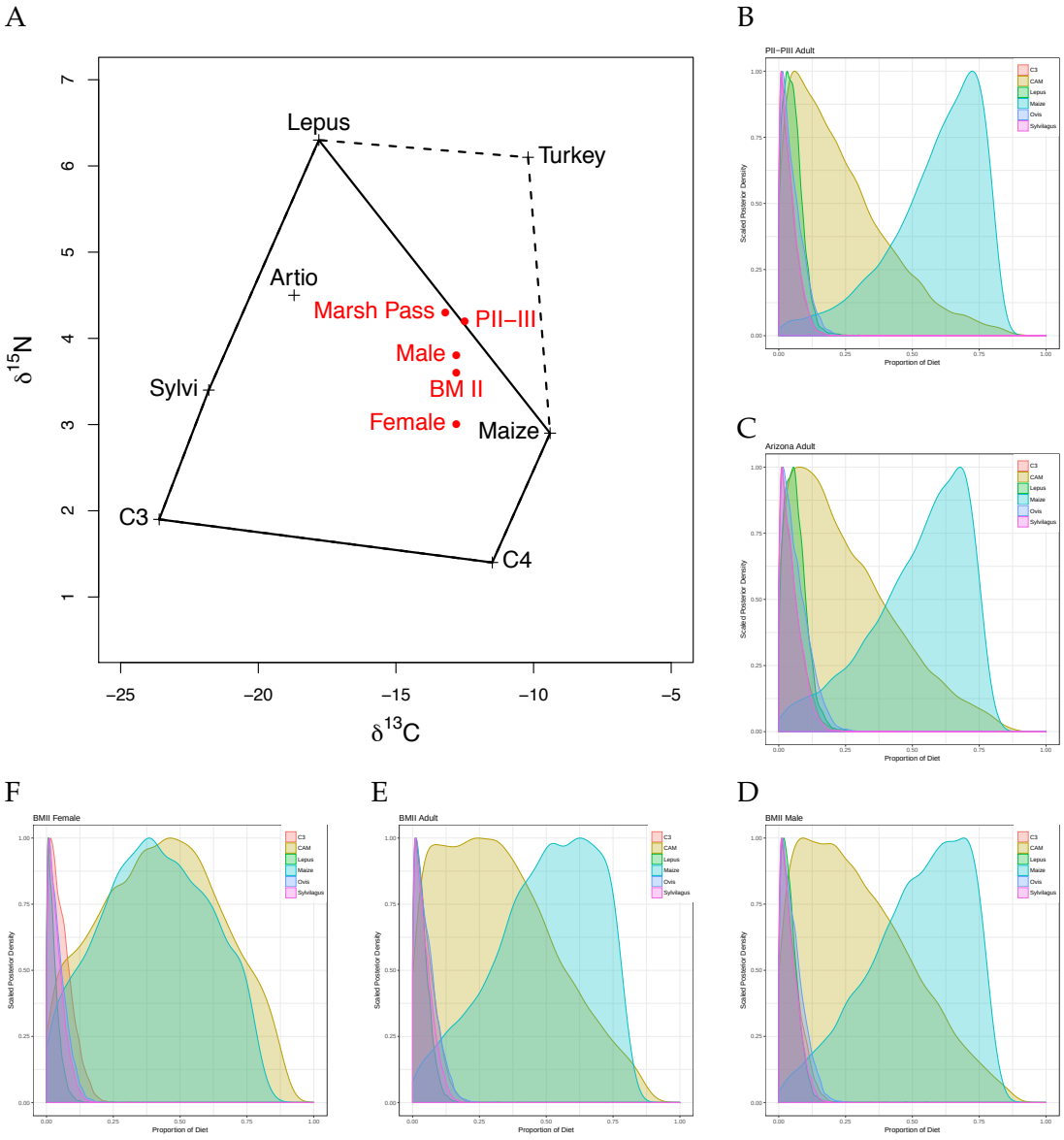

Figure 5.12: Resource polygon and whole diet values (A) and output distributions (right and below) for five modeled populations: Cedar Mesa Pueblo II-III (B), Marsh Pass (Arizona) Basketmaker II (C), Cedar Mesa, Basketmaker II males (D), adults (E) and females (F). See Figure 5.13 for full sized plots of Cedar Mesa, Basketmaker II males and females.

D

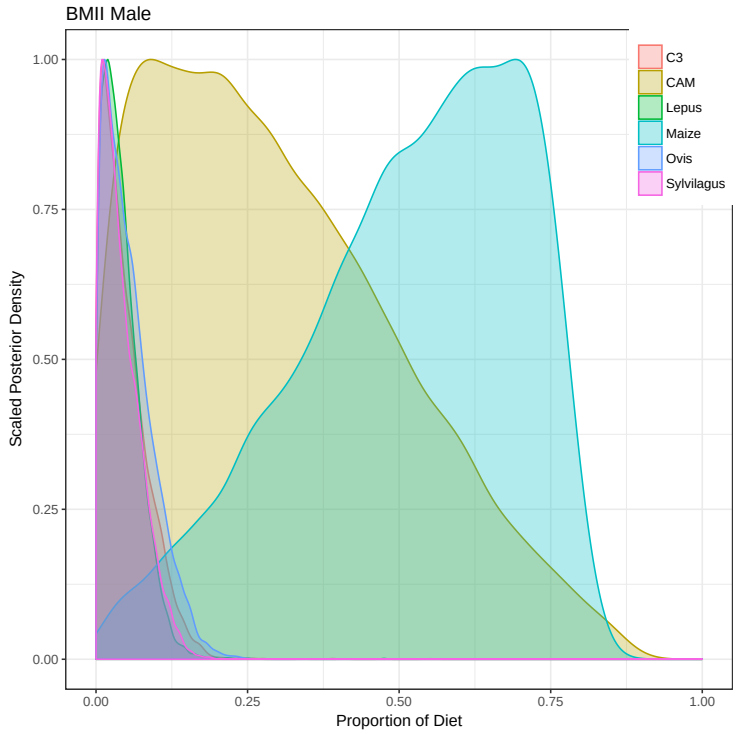

F

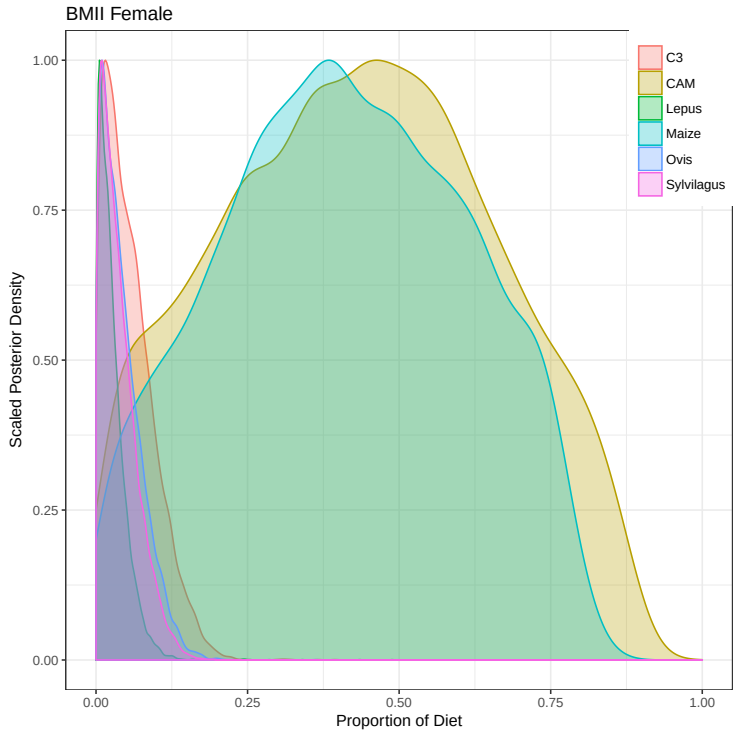

Figure 5.13: Output distributions for mixSIAR models for Cedar Mesa, Basketmaker II males (D) and females (F). Note that resource labels and axes are identical for all distributions plotted in reduced form in Figure 5.12.

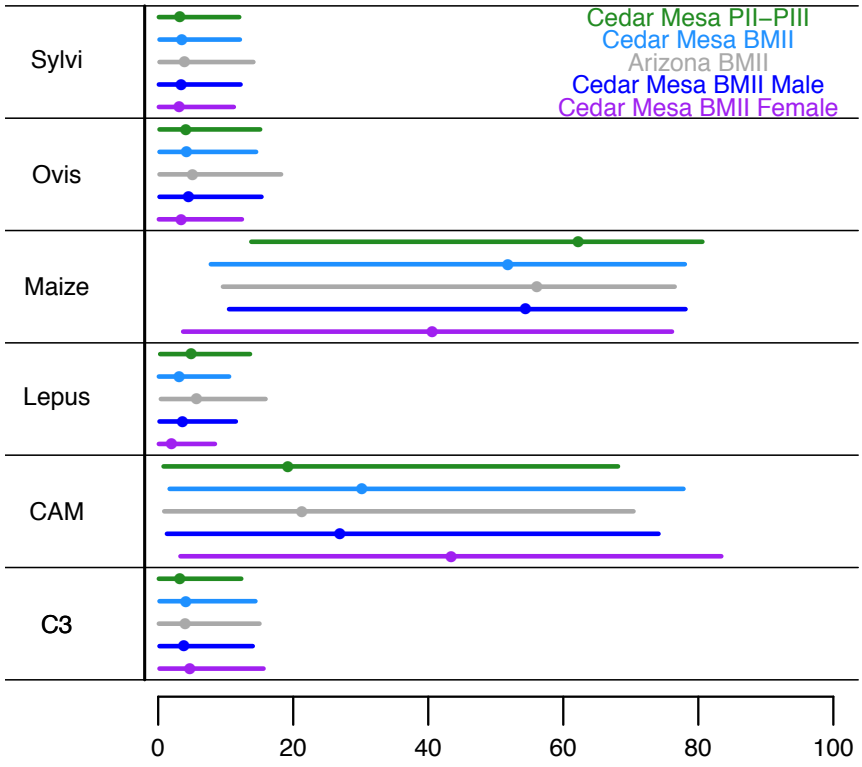

Figure 5.14: Output medians and 95% credible intervals for six resources across five modeled populations: Cedar Mesa Pueblo II-III, Marsh Pass (Arizona) Basketmaker II, Cedar Mesa, Basketmaker II adults, males and females. X axis gives the 0.95 credible interval estimate of the proportion of each resource in diet. Note the similarity in results and the low and uninformative estimates for maize and C4+CAM.

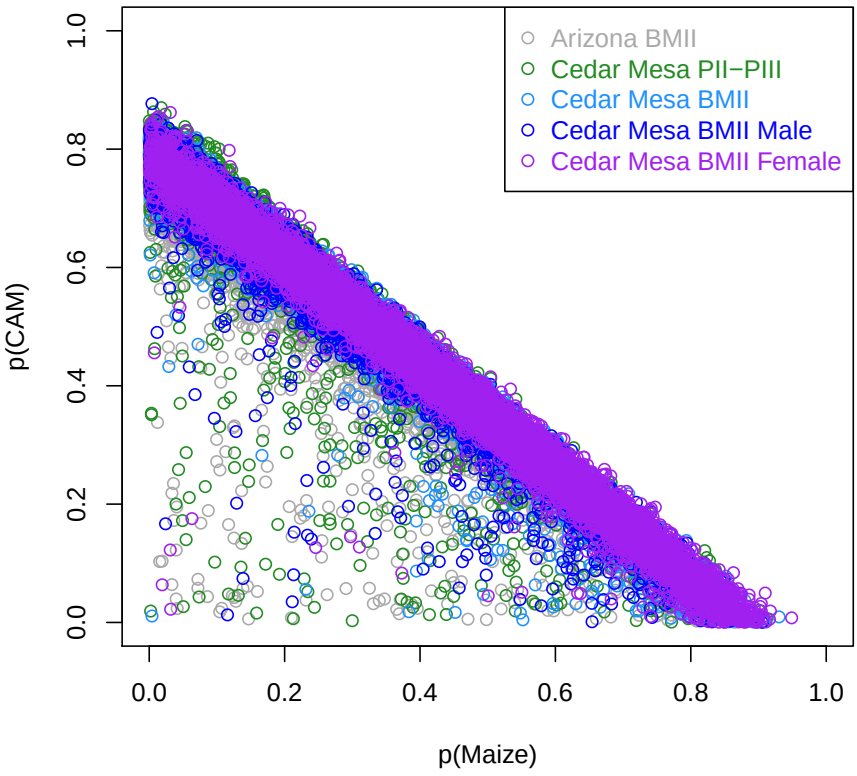

Figure 5.15: Correlation plot for proportions of Maize and C4+CAM in five populations: Marsh Pass (Arizona) Basketmaker II, Cedar Mesa Pueblo II-III, Cedar Mesa, Basketmaker II adults, males and females. Note the overlap in modeled values and the high negative correlation. Contrast with correlation Figure 5.8 above—the inclusion of parameter uncertainty has caused a moderate number of "outlier" points to be sampled.

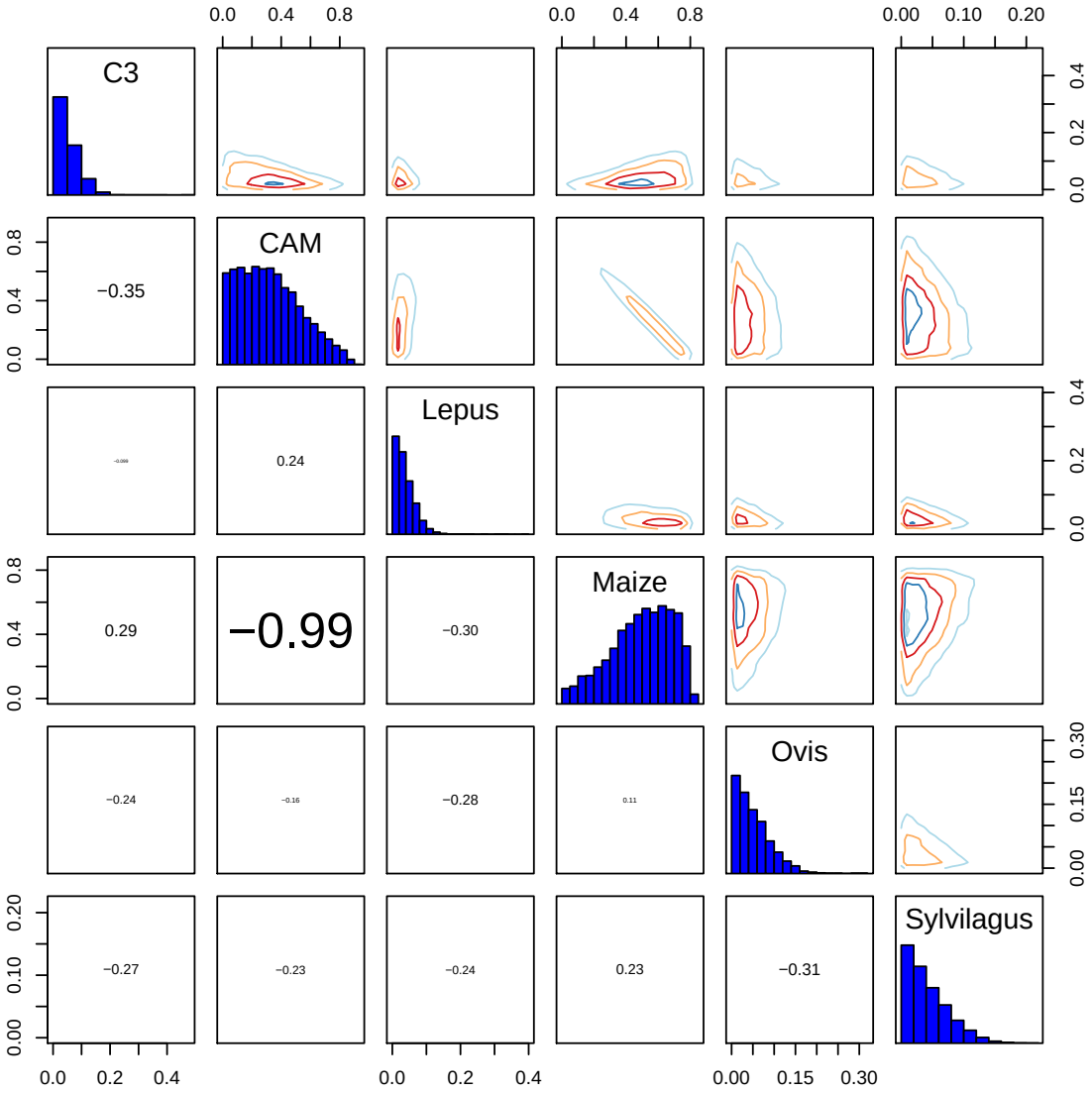

Figure 5.16: Bivariate plot for Cedar Mesa Basketmaker II adults, showing the high correlation of Maize and C4+CAM and the smaller correlations of other pairs. Central diagonal plots the distributions of feasible source proportions for each resource in diet. Upper right bivariate plots of source proportions for each resource in column and row, with axes scaled to the range of feasible proportions for each resource. Lower left plots correlation coefficients for corresponding bivariate plot in upper right. Coefficients are plotted proportional to magnitude. Only coefficients with absolute value larger than 0.30 are visibly plotted. Other populations show broadly similar results.

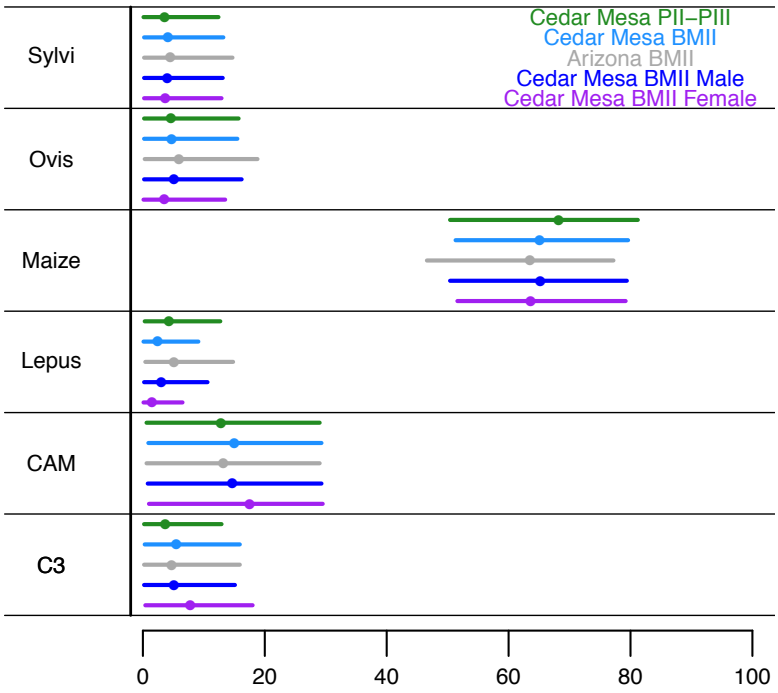

Figure 5.17: Median and range values for a linear constraint of 30% or less C4+CAM in five populations: Marsh Pass (Arizona) Basketmaker II, Cedar Mesa Pueblo II-III, Cedar Mesa, Basketmaker II adults, males and females. Note that maize medians are higher and credible interval is narrower than in unconstrained model.

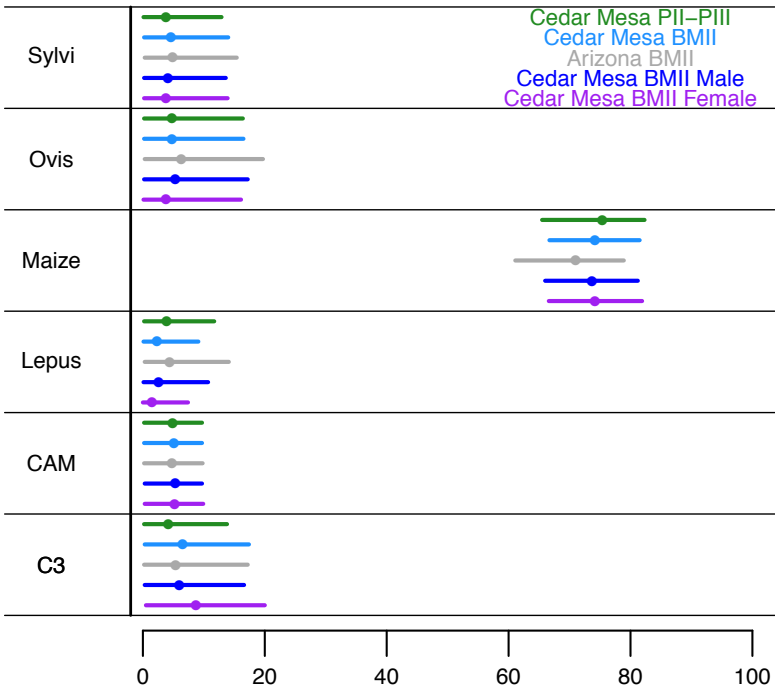

Figure 5.18: Outputs of models under linear constraint of 10% or less C4+CAM in five populations: Marsh Pass (Arizona) Basketmaker II, Cedar Mesa Pueblo II-III, Cedar Mesa, Basketmaker II adults, males and females. Note that the ranges of maize are substantially shortened and medians higher relative to the less constrained models.

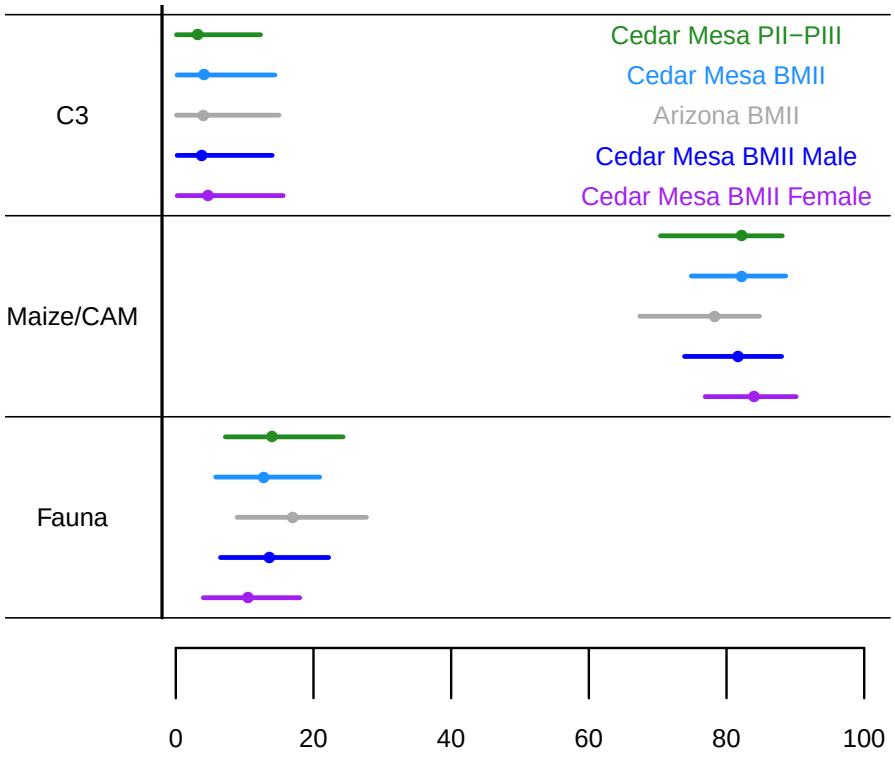

Figure 5.19: A posteriori aggregation medians and ranges for five populations: Marsh Pass (Arizona) Basketmaker II, Cedar Mesa Pueblo II-III, Cedar Mesa, Basketmaker II adults, males and females. Aggregated categories are C3 plants, C4+CAM+Maize (abbreviated Maize/CAM), and fauna (*Ovis* + *Sylvilagus* + *Lepus*).

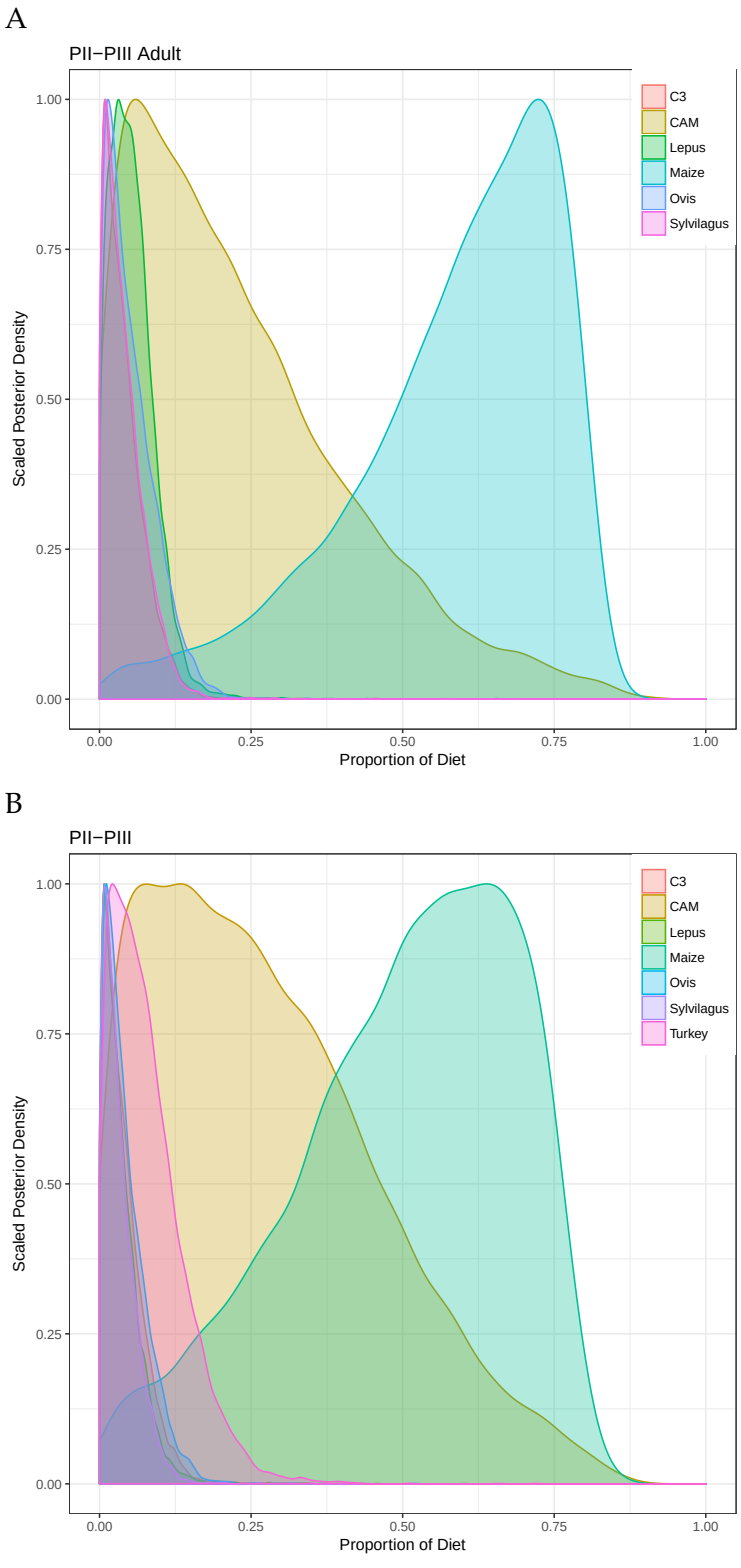

Figure 5.20: Summary statistics comparing models for Pueblo II-III diets without A and with B turkeys. Note that C4+CAM is abbreviated CAM.

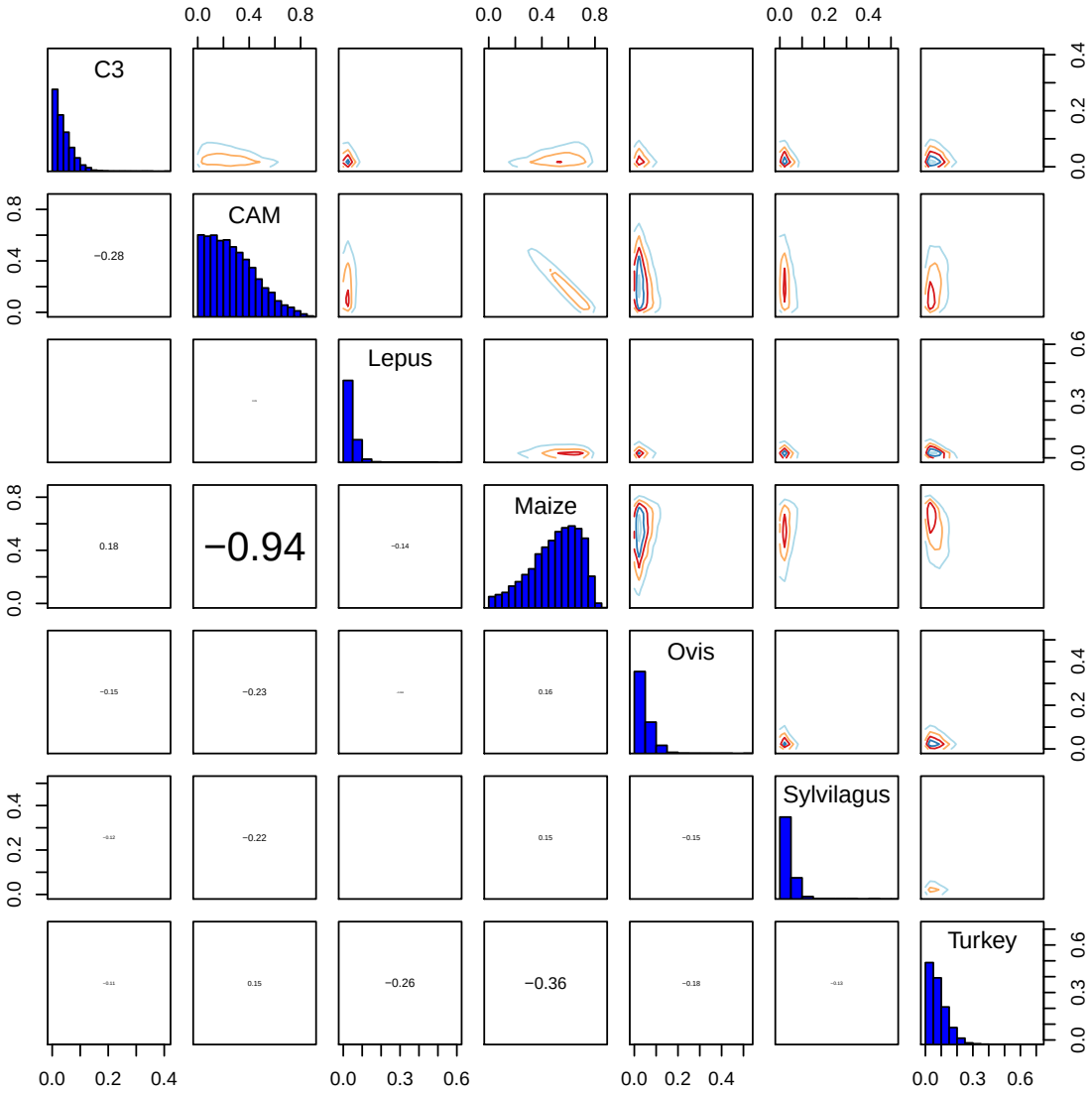

Figure 5.21: Bivariate plot for models for Pueblo II-III diets with turkeys. Note that C4+CAM is abbreviated CAM.

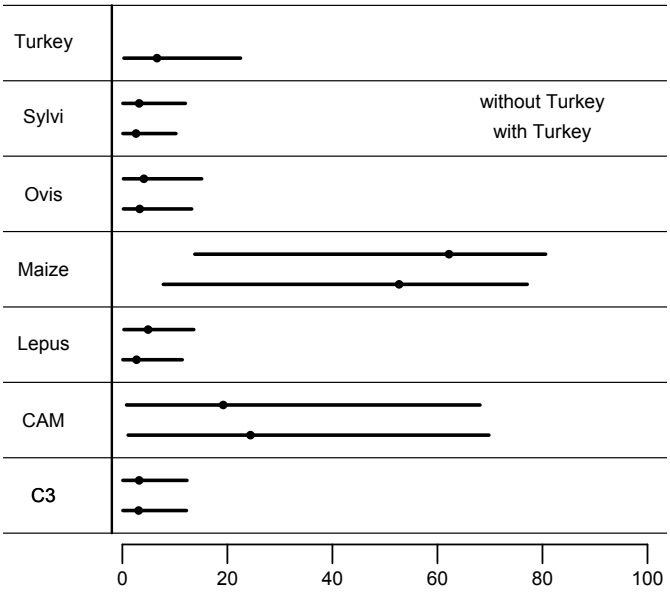

Figure 5.22: Model output plot for Cedar Mesa Pueblo II-III turkey inclusive and exclusive diet models. Note that C4+CAM is abbreviated CAM.

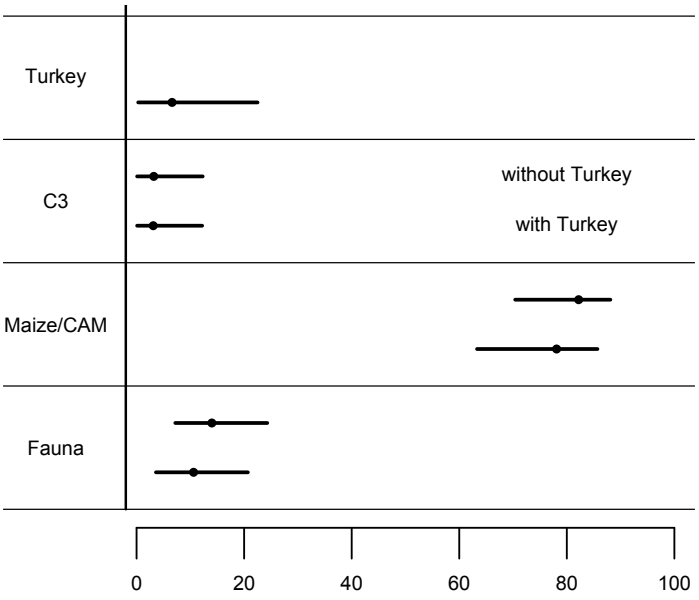

Figure 5.23: Aggregation plot for Cedar Mesa Pueblo II-III turkey inclusive and exclusive diet models. Aggregated categories are Turkey, C3 plants, C4+CAM+Maize (abbreviated Maize/CAM), and wild fauna (*Ovis* + *Sylvilagus* + *Lepus*).

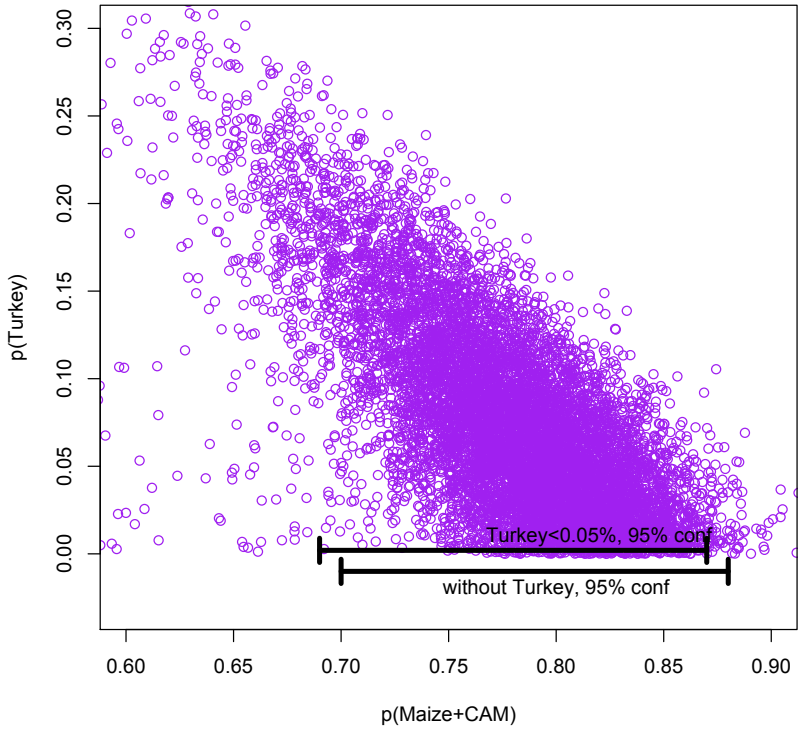

Figure 5.24: Plot of sampled solutions from model of Pueblo II-III diets with turkey included. Note that the central mass of the cloud is approximately circumscribed by the 90% confidence interval. For consistency with the tables above we report the 95% intervals for the diets with and without turkey.

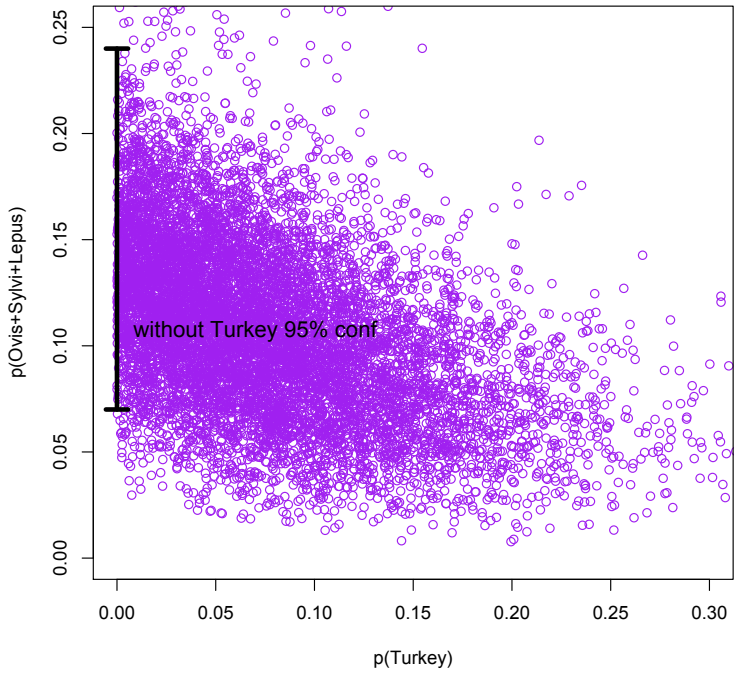

Figure 5.25: Solutions for model of Pueblo II-III diets with turkey included. Y axis plots aggregate proportion of wild resources (e.g., *Ovis* + *Sylvilagus* + *Lepus*), X axis plots proportion of turkey. 95% confidence interval for wild resources from the diet model excluding turkey is given by black line. Note that diets with less than 5-7% faunal inputs are only possible if turkey is included in the diet, as the triangular area near the origin of the plot (e.g., the area bounded by line y=0.05, x=0.0 to y=0.0, x=0.10) is empty of feasible solution values.

Table 5.1: Output table for mixSIAR model using All Utah (Coltrain and Janetski 2013) resource data and local Cedar Mesa resource data. Mean, standard deviation, 95% credible interval boundary, interquartile ranges and medians given.

	C3	CAM	*Lepus*	Maize	*Ovis*	Pinyon	*Sylvilagus*	Resource Data
Mean	0.043	0.16	0.015	0.664	0.043	0.033	0.042	All Utah
SD	0.035	0.135	0.009	0.104	0.03	0.026	0.03	All Utah
2.50%	0.001	0.001	0	0.337	0.001	0	0.001	All Utah
25%	0.015	0.053	0.008	0.608	0.018	0.012	0.018	All Utah
50%	0.034	0.125	0.014	0.691	0.038	0.027	0.037	All Utah
75%	0.063	0.233	0.021	0.746	0.063	0.048	0.062	All Utah
97.50%	0.147	0.582	0.039	0.797	0.122	0.111	0.124	All Utah
Mean	0.048	0.308	0.013	0.53	0.03	0.04	0.031	Cedar Mesa
SD	0.038	0.201	0.009	0.175	0.022	0.03	0.024	Cedar Mesa
2.50%	0.002	0.016	0.001	0.145	0.001	0.001	0.001	Cedar Mesa
25%	0.017	0.143	0.005	0.41	0.012	0.015	0.012	Cedar Mesa
50%	0.04	0.284	0.011	0.55	0.026	0.034	0.026	Cedar Mesa
75%	0.072	0.446	0.018	0.673	0.045	0.06	0.046	Cedar Mesa
97.50%	0.14	0.745	0.033	0.785	0.08	0.109	0.087	Cedar Mesa

Table 5.2: Output stability statistics (from R) for mixSIAR models using Coltrain and Janetski data (Coltrain and Janetski 2013) and local data from Cedar Mesa. Statistics for both mixSIAR models were identical.

```
Chain 5000000, burn=2500000 thin=1000

Both models showed identical stability statistics at this simulation length
Generally the Gelman diagnostic should be < 1.05
Out of 15 variables: 0 > 1.01
                     0 > 1.05
                     0 > 1.1
Heidelberger and Welch Diagnostic
             Chain 1 Chain 2 Chain 3
Stationarity       0       0       0
Half-width         0       0       0


The Geweke diagnostic is a standard z-score, so we'd expect 5\% to be outside +/-1.96
Number of variables outside +/-1.96 in each chain (out of 15):

       Chain 1 Chain 2 Chain 3
Geweke       0       0       0
```

Table 5.3: Linear constraint table for All Utah (Coltrain and Janetski 2013) resource data and local Cedar Mesa resource data showing medians and 2.5-97.5% credible intervals under constraints of maximum C4+CAM input values. Constraints of maximum of 30% C4+CAM reduce the maize input range to 52-79%, further constraining C4+CAM inputs results in an approximate 60-80% range for maize. Note that ranges for faunal inputs are largely unaffected.

	C3	C4 +CAM	*Lepus*	Maize	*Ovis*	Pinyon	*Sylvilagus*	max C4+ CAM	Resource Data
50%	0.038	0.099	0.015	0.711	0.04	0.029	0.041	0.3	All Utah
2.5%	0.002	0.003	0.001	0.569	0.002	0.001	0.002	0.3	All Utah
97.5%	0.133	0.283	0.036	0.79	0.112	0.1	0.112	0.3	All Utah
50%	0.039	0.077	0.015	0.727	0.041	0.03	0.043	0.2	All Utah
2.5%	0.002	0.003	0.001	0.636	0.002	0.001	0.002	0.2	All Utah
97.5%	0.138	0.191	0.037	0.792	0.115	0.102	0.116	0.2	All Utah
50%	0.042	0.045	0.016	0.752	0.043	0.032	0.046	0.1	All Utah
2.5%	0.002	0.002	0.001	0.707	0.002	0.001	0.002	0.1	All Utah
97.5%	0.142	0.097	0.038	0.796	0.119	0.107	0.121	0.1	All Utah
50%	0.042	0.024	0.016	0.768	0.045	0.033	0.049	0.05	All Utah
2.5%	0.002	0.001	0.001	0.739	0.003	0.001	0.002	0.05	All Utah
97.5%	0.145	0.049	0.038	0.801	0.123	0.113	0.126	0.05	All Utah
50%	0.057	0.152	0.008	0.665	0.024	0.05	0.027	0.3	Cedar Mesa
2.5%	0.002	0.009	0	0.54	0.001	0.002	0.001	0.3	Cedar Mesa
97.5%	0.151	0.292	0.023	0.793	0.072	0.117	0.088	0.3	Cedar Mesa
50%	0.062	0.103	0.008	0.707	0.023	0.056	0.026	0.2	Cedar Mesa
2.5%	0.003	0.007	0	0.624	0.001	0.003	0.001	0.2	Cedar Mesa
97.5%	0.156	0.195	0.022	0.798	0.069	0.122	0.085	0.2	Cedar Mesa
50%	0.064	0.051	0.007	0.753	0.022	0.064	0.025	0.1	Cedar Mesa
2.5%	0.002	0.003	0	0.703	0.001	0.003	0.001	0.1	Cedar Mesa
97.5%	0.165	0.098	0.02	0.803	0.067	0.128	0.08	0.1	Cedar Mesa
50%	0.064	0.025	0.007	0.776	0.022	0.072	0.023	0.05	Cedar Mesa
2.5%	0.002	0.002	0	0.741	0.001	0.005	0.001	0.05	Cedar Mesa
97.5%	0.168	0.049	0.019	0.807	0.069	0.132	0.076	0.05	Cedar Mesa

Table 5.4: A posteriori aggregation table for All Utah (Coltrain and Janetski 2013) resource data and local Cedar Mesa resource data. Fauna are *Ovis+Lepus+Sylvilagus*, C3 are C3 + pinyon. Note that the range of values is about 5% higher for cultigens than for maize under a 5% C4+CAM constraint, showing that both methods of constraining model output variance result in similar estimates.

	Fauna	C4+CAM+maize	C3	Resource Data
50%	0.089	0.817	0.084	All Utah
2.5%	0.035	0.778	0.018	All Utah
97.5%	0.155	0.903	0.159	All Utah
50%	0.074	0.836	0.088	Cedar Mesa
2.5%	0.031	0.783	0.01	Cedar Mesa
97.5%	0.121	0.903	0.174	Cedar Mesa

Table 5.5: Resource inputs: Delta values, SD, N (note that C3 and C4+CAM SD and N are approximate since weighted averages were used), concentrations, and trophic level enrichments TLE.

	δ^{13}C	SD	δ^{15}N	SD	N	Conc. C	Conc. N	TLE C	SD	TLE N	SD
Maize	-9.4	0.5	2.9	0.5	12	0.445	0.014	5	0.2	3	0.2
C3	-23.5	0.5	2.0	0.75	100	0.468	0.013	5	0.2	3	0.2
C4+CAM	-11.4	0.5	1.2	0.75	50	0.363	0.011	5	0.2	3	0.2
Sylvilagus	-21.8	0.9	3.4	0.6	15	0.543	0.142	1	0.2	3	0.2
Ovis	-18.7	1.4	4.7	0.6	14	0.543	0.142	1	0.2	3	0.2
Lepus	-17.8	2	6.3	0.7	2	0.543	0.142	1	0.2	3	0.2

Table 5.6: Model resource proportion output summary statistics for six resources in five modeled populations. Marsh Pass (Arizona) Basketmaker II, Cedar Mesa Pueblo II-III, Cedar Mesa, Basketmaker II adults, males and females.

	C3	C4+CAM	*Lepus*	Maize	*Ovis*	*Sylvilagus*	Population
Mean	0.05	0.254	0.063	0.522	0.063	0.048	Arizona Adult
SD	0.043	0.19	0.043	0.179	0.05	0.039	Arizona Adult
2.5 %	0.001	0.009	0.004	0.096	0.002	0.002	Arizona Adult
25 %	0.017	0.1	0.032	0.414	0.023	0.017	Arizona Adult
50 %	0.04	0.213	0.057	0.561	0.051	0.039	Arizona Adult
75 %	0.071	0.373	0.086	0.666	0.092	0.069	Arizona Adult
97.5 %	0.15	0.704	0.159	0.765	0.182	0.141	Arizona Adult
Mean	0.04	0.231	0.054	0.584	0.051	0.04	P II-III Adult
SD	0.038	0.179	0.038	0.173	0.042	0.034	P II-III Adult
2.5 %	0.001	0.008	0.003	0.138	0.002	0.001	P II-III Adult
25 %	0.013	0.088	0.026	0.489	0.019	0.014	P II-III Adult
50 %	0.032	0.192	0.049	0.622	0.041	0.032	P II-III Adult
75 %	0.057	0.333	0.074	0.718	0.074	0.057	P II-III Adult
97.5 %	0.123	0.681	0.136	0.806	0.151	0.12	P II-III Adult
Mean	0.05	0.325	0.036	0.496	0.051	0.042	BMII Adult
SD	0.04	0.209	0.029	0.191	0.04	0.033	BMII Adult
2.5 %	0.002	0.017	0.001	0.078	0.002	0.002	BM II Adult
25 %	0.018	0.153	0.014	0.369	0.019	0.015	BMII II Adult
50 %	0.041	0.302	0.031	0.518	0.042	0.035	BMII Adult
75 %	0.072	0.467	0.052	0.65	0.074	0.062	BMII Adult
97.5 %	0.144	0.778	0.105	0.78	0.145	0.121	BMII Adult
Mean	0.048	0.299	0.042	0.516	0.054	0.042	BMII Male
SD	0.039	0.201	0.033	0.184	0.042	0.034	BMII Male
2.5 %	0.002	0.013	0.002	0.105	0.002	0.001	BMII Male
25 %	0.017	0.134	0.018	0.394	0.02	0.016	BMII Male
50 %	0.038	0.269	0.036	0.544	0.045	0.034	BMII Male
75 %	0.069	0.436	0.059	0.665	0.078	0.062	BMII Male
97.5 %	0.14	0.741	0.115	0.781	0.153	0.122	BMII Male
Mean	0.056	0.43	0.026	0.408	0.042	0.038	BMII Female
SD	0.042	0.222	0.024	0.2	0.034	0.03	BMII Female
2.5 %	0.002	0.033	0.001	0.037	0.001	0.001	BMII Female
25 %	0.022	0.257	0.009	0.257	0.015	0.014	BMII Female
50 %	0.047	0.434	0.02	0.406	0.034	0.031	BMII Female
75 %	0.08	0.596	0.037	0.565	0.062	0.055	BMII Female
97.5 %	0.156	0.834	0.084	0.761	0.124	0.112	BMII Female

Table 5.7: Linear constraint table giving median and range values for linear constraints of 30%, 20% 10% and 5% C4+CAM, for Marsh Pass (Arizona) Basketmaker II, Cedar Mesa Pueblo II-III, Cedar Mesa, Basketmaker II adults, males and females.

	C3	C4+CAM	*Lepus*	Maize	*Ovis*	*Sylvilagus*	max C4+CAM	Population
50%	0.047	0.132	0.051	0.635	0.059	0.045	0.3	Arizona Adult
2.5%	0.002	0.006	0.004	0.466	0.003	0.002	0.3	Arizona Adult
97.5%	0.159	0.29	0.148	0.772	0.188	0.147	0.3	Arizona Adult
50%	0.05	0.096	0.047	0.67	0.06	0.046	0.2	Arizona Adult
2.5%	0.002	0.004	0.004	0.54	0.003	0.002	0.2	Arizona Adult
97.5%	0.166	0.194	0.143	0.779	0.193	0.151	0.2	Arizona Adult
50%	0.054	0.048	0.044	0.71	0.063	0.049	0.1	Arizona Adult
2.5%	0.002	0.002	0.003	0.611	0.003	0.003	0.1	Arizona Adult
97.5%	0.172	0.098	0.141	0.789	0.197	0.154	0.1	Arizona Adult
50%	0.057	0.024	0.041	0.732	0.065	0.051	0.05	Arizona Adult
2.5%	0.003	0.001	0.003	0.644	0.003	0.002	0.05	Arizona Adult
97.5%	0.174	0.048	0.141	0.799	0.211	0.156	0.05	Arizona Adult
50%	0.037	0.128	0.043	0.682	0.046	0.036	0.3	P II-III Adult
2.5%	0.002	0.006	0.003	0.504	0.002	0.001	0.3	P II-III Adult
97.5%	0.129	0.29	0.127	0.812	0.157	0.124	0.3	P II-III Adult
50%	0.039	0.091	0.04	0.716	0.048	0.037	0.2	P II-III Adult
2.5%	0.002	0.004	0.002	0.592	0.002	0.001	0.2	P II-III Adult
97.5%	0.133	0.193	0.122	0.817	0.158	0.125	0.2	P II-III Adult
50%	0.042	0.049	0.039	0.754	0.048	0.038	0.1	P II-III Adult
2.5%	0.002	0.002	0.002	0.655	0.002	0.001	0.1	P II-III Adult
97.5%	0.138	0.097	0.117	0.823	0.164	0.129	0.1	P II-III Adult
50%	0.043	0.026	0.038	0.776	0.049	0.039	0.05	P II-III Adult
2.5%	0.002	0.001	0.002	0.69	0.003	0.002	0.05	P II-III Adult
97.5%	0.141	0.049	0.119	0.83	0.162	0.134	0.05	P II-III Adult
50%	0.055	0.15	0.024	0.651	0.047	0.041	0.3	BMII Adult
2.5%	0.003	0.009	0.001	0.513	0.002	0.002	0.3	BMII Adult
97.5%	0.159	0.293	0.091	0.796	0.155	0.132	0.3	BMII Adult
50%	0.06	0.1	0.024	0.698	0.048	0.042	0.2	BMII Adult
2.5%	0.003	0.005	0.001	0.595	0.002	0.002	0.2	BMII Adult
97.5%	0.165	0.195	0.091	0.805	0.158	0.135	0.2	BMII Adult
50%	0.065	0.051	0.023	0.742	0.048	0.046	0.1	BMII Adult
2.5%	0.003	0.002	0.001	0.667	0.002	0.002	0.1	BMII Adult
97.5%	0.174	0.097	0.091	0.815	0.165	0.14	0.1	BMII Adult
50%	0.066	0.025	0.022	0.764	0.051	0.048	0.05	BMII Adult
2.5%	0.003	0.001	0.001	0.693	0.002	0.002	0.05	BMII Adult
97.5%	0.181	0.049	0.094	0.821	0.175	0.143	0.05	BMII Adult
50%	0.051	0.147	0.03	0.652	0.051	0.04	0.3	BMII Male
2.5%	0.002	0.008	0.002	0.504	0.002	0.002	0.3	BMII Male
97.5%	0.151	0.293	0.106	0.794	0.162	0.131	0.3	BMII Male
50%	0.056	0.099	0.028	0.695	0.051	0.042	0.2	BMII Male
2.5%	0.002	0.005	0.001	0.584	0.002	0.002	0.2	BMII Male

Table 5.7: continued

	C3	C4+CAM	*Lepus*	Maize	*Ovis*	*Sylvilagus*	max C4+CAM	Population
97.5%	0.158	0.195	0.106	0.803	0.166	0.134	0.2	BMII Male
50%	0.06	0.053	0.026	0.737	0.053	0.041	0.1	BMII Male
2.5%	0.003	0.003	0.001	0.66	0.002	0.002	0.1	BMII Male
97.5%	0.166	0.097	0.107	0.812	0.172	0.136	0.1	BMII Male
50%	0.063	0.024	0.025	0.761	0.055	0.041	0.05	BMII Male
2.5%	0.004	0.002	0.001	0.695	0.002	0.002	0.05	BMII Male
97.5%	0.169	0.049	0.109	0.823	0.172	0.142	0.05	BMII Male
50%	0.078	0.175	0.015	0.636	0.035	0.037	0.3	BMII Female
2.5%	0.004	0.01	0.001	0.516	0.001	0.002	0.3	BMII Female
97.5%	0.18	0.295	0.065	0.792	0.135	0.129	0.3	BMII Female
50%	0.085	0.109	0.015	0.693	0.036	0.037	0.2	BMII Female
2.5%	0.005	0.006	0.001	0.601	0.001	0.002	0.2	BMII Female
97.5%	0.189	0.196	0.065	0.804	0.145	0.133	0.2	BMII Female
50%	0.087	0.052	0.015	0.742	0.038	0.038	0.1	BMII Female
2.5%	0.005	0.003	0	0.666	0.001	0.002	0.1	BMII Female
97.5%	0.2	0.099	0.074	0.819	0.161	0.139	0.1	BMII Female
50%	0.09	0.028	0.015	0.764	0.034	0.04	0.05	BMII Female
2.5%	0.005	0.002	0.001	0.686	0.001	0.001	0.05	BMII Female
97.5%	0.206	0.049	0.071	0.828	0.164	0.148	0.05	BMII Female

Table 5.8: A posteriori aggregation table for five populations modeled: Marsh Pass (Arizona) Basketmaker II, Cedar Mesa Pueblo II-III, Cedar Mesa, Basketmaker II adults, males and females. Aggregated categories are C3 plants, C4+CAM+Maize, and fauna (*Ovis* + *Sylvilagus* + *Lepus*).

	Fauna	C4+CAM+maize	C3	Population
50%	0.17	0.783	0.04	Arizona Adult
2.5%	0.089	0.674	0.001	Arizona Adult
97.5%	0.277	0.848	0.15	Arizona Adult
50%	0.14	0.822	0.032	P II-III Adult
2.5%	0.072	0.704	0.001	P II-III Adult
97.5%	0.243	0.881	0.123	P II-III Adult
50%	0.128	0.822	0.041	BMII Adult
2.5%	0.058	0.749	0.002	BMII Adult
97.5%	0.209	0.886	0.144	BMII Adult
50%	0.136	0.817	0.038	BMII Male
2.5%	0.065	0.739	0.002	BMII Male
97.5%	0.222	0.88	0.14	BMII Male
50%	0.105	0.84	0.047	BMII Female
2.5%	0.04	0.769	0.002	BMII Female
97.5%	0.18	0.901	0.156	BMII Female

Table 5.9: Model resource proportion output summary statistics Pueblo II-III diets with and without turkey

		C3	C4+CAM	*Lepus*	Maize	*Ovis*	*Sylvilagus*	Turkey
Without	Mean	0.04	0.231	0.054	0.584	0.051	0.04	
Turkey	SD	0.038	0.179	0.038	0.173	0.042	0.034	
	2.50%	0.001	0.008	0.003	0.138	0.002	0.001	
	25%	0.013	0.088	0.026	0.489	0.019	0.014	
	50%	0.032	0.192	0.049	0.622	0.041	0.032	
	75%	0.057	0.333	0.074	0.718	0.074	0.057	
	97.50%	0.123	0.681	0.136	0.806	0.151	0.12	
With	Mean	0.039	0.272	0.036	0.5	0.043	0.033	0.079
Turkey	SD	0.034	0.186	0.034	0.184	0.037	0.03	0.061
	2.50%	0.001	0.011	0.001	0.078	0.002	0.001	0.003
	25%	0.013	0.12	0.012	0.38	0.015	0.011	0.032
	50%	0.031	0.244	0.027	0.527	0.033	0.026	0.066
	75%	0.056	0.393	0.05	0.647	0.061	0.047	0.111
	97.50%	0.122	0.698	0.114	0.771	0.132	0.102	0.225

Table 5.10: Linear constraint table for models for Pueblo II-III diets with turkeys.

	C3	C4+CAM	*Lepus*	Maize	*Ovis*	*Sylvilagus*	Turkey	max C4+CAM
50 %	0.038	0.144	0.026	0.623	0.039	0.03	0.058	0.3
2.5 %	0.001	0.007	0.001	0.427	0.002	0.001	0.003	0.3
97.5 %	0.129	0.291	0.109	0.783	0.144	0.109	0.211	0.3
50 %	0.041	0.099	0.025	0.667	0.041	0.032	0.054	0.2
2.5 %	0.001	0.005	0.001	0.5	0.002	0.001	0.003	0.2
97.5 %	0.135	0.194	0.107	0.79	0.147	0.113	0.207	0.2
50 %	0.041	0.049	0.025	0.714	0.044	0.035	0.051	0.1
2.5 %	0.001	0.003	0.001	0.566	0.002	0.002	0.002	0.1
97.5 %	0.139	0.097	0.104	0.804	0.149	0.118	0.216	0.1
50 %	0.042	0.025	0.025	0.738	0.047	0.036	0.05	0.05
2.5 %	0.002	0.002	0.001	0.577	0.003	0.002	0.002	0.05
97.5 %	0.139	0.049	0.114	0.813	0.15	0.122	0.214	0.05

Table 5.11: Aggregation table for models for Pueblo II-III diets with turkeys.

	Fauna	C4+CAM+maize	C3
50%	0.106	0.781	0.031
2.50%	0.036	0.633	0.001
97.50%	0.207	0.857	0.122

CHAPTER 6

PROJECT REVIEW AND CONCLUSIONS

This sixth and final chapter reviews and critiques the results of the isotope ecology sampling and modeling, identifying both shortcomings in the research design and areas for potential future study.

6.1 Methods Review and Critique

The last four chapters have offered the background (Chapter 2), field and laboratory methods (Chapter 3) and statistical analyses (Chapter 4) that are the prerequisites for formal stable isotope mixing models of the diets of the Cedar Mesa Basketmaker II (Chapter 5). Before suggesting the potential for behavioral or archaeological interpretation, it is useful to review the project as a whole, and to consider what portions of the sampling and modeling procedures can be improved in future work.

The study design sampled both modern plant species and archaeofauna. Taxa selection was made to 1) be representative of the resources commonly found in the regional archaeological record, 2) contain species that represent all three photosynthetic pathways, and 3) sample across organ types (leaf, fruit, root, stem, and seed). These three dimensions encompassed the major causes of variation in stable isotope values. Experiments were also conducted on banana yucca to separate and analyze the edible portion of the roasted stem as well as the inedible fiber that correlates to quids in the archaeological record.

Despite elevation banding of species along temperature and moisture gradients, and the known sensitivity of C3 and CAM plants to such gradients on larger spatial scales, elevation effects on $\delta^{13}C$ were not evidenced at the species level on Cedar Mesa. Similarly, although plant $\delta^{15}N$ values suggest nitrogen fixing soil crusts as the dominant nitrogen source in the Cedar Mesa ecosystem, crustal development indices did not correlate with $\delta^{15}N$. Personal observation suggests that local soil moisture variation at any particular elevation may have a far greater effect on plant $\delta^{13}C$ (and perhaps $\delta^{15}N$) values than

elevation or crustal development at the spatial scale of this sampling.

In the roasting experiments, small isotopic offsets between yucca tissues were observed, but the total variation is small relative to the differences between species within either C3 or C4+CAM categories. Thus, the mix of species has a much larger effect on stable isotope values than the variation introduced by local ecology or by the choice of the tissue sampled. Consequently, the project's sampling regime encompasses the environmental variability encountered by a human forager on Cedar Mesa. However, elsewhere in the Southwest, where *Agavae* species dominate the diet, further roasting experiments may be warranted, since, in such cases, the intratissue variation may be larger than the variation among plausible C4+CAM species. In such a case, the homogenization protocols used in this study can be improved.

Although this project's sample of local resources represents an improvement over previous datasets from the region, several issues need further resolution through future research.

1. Among the modern floral samples, *Helianthus* could only be obtained from a roadside context, where the gravels from the roadbed may be affecting carbon and nitrogen isotope ratios.
2. Modern floral isotope values have not been compared with archaeological specimens to verify that modern isotope ratios correspond to those encountered by Basketmaker II individuals.
3. Archaeological maize samples from two sites in the study area returned nonoverlapping $\delta^{15}N$ ranges. One site shows maize values consistent with crustal nitrogen inputs, the other suggests minimal crustal inputs. Further sampling is needed to assess how widespread this variability is and if it signifies differences in agricultural technique (dry farming or spring subirrigation)
4. The *Lepus* sample (n=2) is too small. Further sampling is required using Cedar Mesa datasets to determine whether the ecological patterns identified in other species are also present in *Lepus*.

Despite these methodological issues, there is strong regional patterning when Cedar Mesa taxa are compared with identical taxa from the Great Salt Lake in Northern Utah,

and with samples from Chihuahua, Mexico. Cedar Mesa food-web $\delta^{15}N$ values are consistently depleted by about 3‰ relative to these regions—equivalent to a difference of one trophic level. This is likely due to the effects of nitrogen fixation in Cedar Mesa soil crusts, but makes extension of this sample to areas lacking such crusts potentially suspect—particularly for diets not dominated by maize.

6.2 Isotope Model Review

The results presented in Chapter 5 suggest that, for Cedar Mesa stable isotope diet models, the location of the central peak and the shape of the distribution of model outputs for maize and C4+CAM proportions differ depending both on the population modeled and on the use of local or regional resource datasets. However, the range of solution values is consistent across all populations and resources used—that is, model results are relatively insensitive to small changes in either human or resource isotope values.

Further, while, C4+CAM and maize proportion distributions vary in shape, model results are always highly ($r^2 > 0.90$) correlated. Thus, extrinsic linear constraints on C4+CAM consumption or resource aggregation can substantially reduce the ranges of feasible source proportions. In Chapter 5, such constraints were presented purely mathematically. To utilize such models in making archaeological interpretations, the real world justifications of both constraints must be made clear.

Resource aggregation is useful if the combined resources create a single analytical unit. Thus, aggregation is suitable for fauna, but also is suitable if C4+CAM and maize are treated as a single analytic unit. This can occur if CAM and wild C4 inputs are believed to be trivial relative to maize, or if the question being pursued is one of total C4 and CAM plant contributions to diet (e.g., C4+CAM+maize), rather than the relative proportions of cultigens and wild resources.

Previous studies of Basketmaker II plant macrofossils suggest that maize is by far the dominant element in Basketmaker II diets. Chapter 1 noted that the Western Basketmaker II showed high maize ubiquity in all subregions. Cedar Mesa is no exception. Midden analyses from Cedar Mesa show high maize ubiquities but also a macrobotanical distributions dominated by maize, with maize often exceeding the mass of other species by an order of magnitude (see Figure 3 in Matson and Chisholm (2007)). Similarly, coprolites

from Basketmaker II contexts at Turkey Pen Ruin in Grand Gulch (Aasen 1984; Reinhard 1988) show maize components dominating total mass. Counts of macrobotanicals from Boomerang Shelter (Androy 2003) suggest a similar distribution, if the analysis is corrected for the small size of Cheno-am seeds.

There are several problems in trying to compare these datasets, including postdepositional biases in species represented and the varying timescales of coprolite (one day), collagen (multidecadal) and midden (multicentennial) data. However, all three lines of evidence, representing different depositional timeframes, suggest diets quite high in maize with supplemental Cheno-am contributions. This in turn suggests that the aggregated C4+CAM+maize category is predominantly maize. Consequently, in diet models that aggregate resources, the C4+CAM+maize category may be taken as a proxy for maize alone, among the Western Basketmaker II.

6.3 Model Results and Implications for Further Work

Table 5.8 in Chapter 5 gives the results of resource aggregation for all models. Maize/C4 plant contributions vary between 67% and 90% while total faunal inputs vary between 7 and 28%. Marsh Pass Basketmaker II burials (500 B.C.-1 A.D.) predate the Cedar Mesa Basketmaker II (100-300 A.D.) and Puebloan burials (1100-1200 A.D.). For the earliest Basketmaker II period, the ranges of C4/maize are only reduced by 5% relative to later periods and the faunal ranges are only increased by 1-3% relative to later periods. This suggests that diets were quite high ($>$ 70% by mass) in C4+CAM+maize from the very beginning of the western Basketmaker II occupation. Both pre- and post- A.D. 1 Western Basketmaker II and the Cedar Mesa Pueblo II-III show similar diets dominated by C4+CAM+maize plants. This result is consistent with the interpretation from Chapter 1 of the Western Basketmaker II as inhabiting a region where maize is—of necessity—the dominant element in the diet.

Chapter 1 ended by noting that the relationship of Western and Eastern Basketmaker II ecology to economy and culture could not be fully addressed by this study, due to the small sample of Eastern Basketmaker II burials. This study's results illustrate an additional difficulty and one that precludes the use of Basketmaker III data from the Eastern Basketmaker II region. Figure 6.1 plots Eastern and Western Basketmaker II and III whole diet values against the resource polygon from Cedar Mesa Utah (see Table 2.1 in

Chapter 2). The Basketmaker III population plots outside the resource polygon indicating that Cedar Mesa data cannot be used to reconstruct diets on the La Plata River. While Durango Basketmaker II diets can be modeled, the relatively positive nitrogen values of both populations suggest that differences in isotope ecology may be present. Further resource sampling in the Eastern Basketmaker II region is required.

While Eastern Basketmaker II diets cannot be fully characterized given present data, pre-AD 1 Basketmaker II diets form Marsh Pass, Arizona; post-AD 1 diets from Cedar Mesa; and PII-PIII diets form Cedar Mesa can. What is remarkable in these models is their stability. Over this 1000-year span, the average estimates for C4+CAM+maize differ by less than 5%, the average faunal inputs by 5%, and the C3 plant inputs are unchanged.

Given this stability, a number of concepts currently utilized in the Basketmaker II-III and Pueblo I periods will need to be examined more closely. Several broader scale questions in the current Ancestral Puebloan literature may be clarified by these results:

1. The post Basketmaker II Neolithic demographic transition cannot be explained by increasing maize dependence, as Kohler and colleges began to recognize in the 2014 revision to the 2008 model (Kohler and Reese 2014; Kohler et al. 2008)
2. Changes in ground-stone morphology towards greater efficiency will need to be assessed in terms of time constraints, rather than being attributed to increasing amounts of maize consumption or grinding. This concept is already being recognized in technology models (Crown and Wills 1995; Adams 2014).
3. The use of limestone cooking in post A.D. Basketmaker II and its disappearance in later periods will need to be assessed in terms of small shifts in average maize use as maize consumption appears stable (though high) through time (Matson 2016; Ellwood et al. 2013; Battillo 2017)

Thus, this study, by providing a representative sample of wild resources at Cedar Mesa, has illustrated the challenges of sampling and the scale of variation in isotopic baselines within a region. By examining the correlations in mixing model outputs, this study has shown that greater attention to the "feasible region" can result in more precise descriptions of the combinations of resources consumed. Finally, this study, by providing a quantitative estimate of human diet in the BMII period, may yet provide a common

independent baseline for investigators pursuing broader questions of the relationships between subsistence strategies and ecological, demographic, technological and behavioral change.

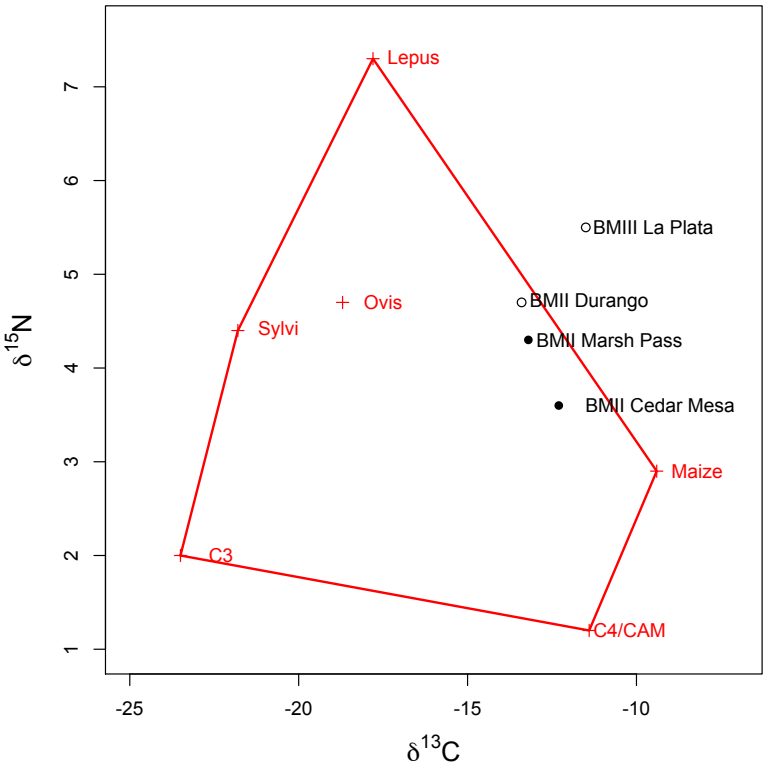

Figure 6.1: Cedar Mesa resource polygon and four Basketmaker II and III populations. While the Durango Basketmaker II could theoretically be modeled using Cedar Mesa data (and such a model would show higher faunal inputs similar to Marsh Pass), the La Plata Basketmaker III sample falls outside the Cedar Mesa polygon, suggesting perhaps regional differences in isotope ecology. Local sampling is needed to test this inference.

APPENDIX

DATA TABLES

Table A.1: Sample stable isotope assay data: Species, Organ Sampled, Photosynthetic pathway, Sample Site (see Table 3.3), Elevation, Crustal development level (original 5 level index (color and bumpiness) reduced to 3 level index for analysis $0 => 0, 1,2 => 2, 3,4 => 3$), Notes, weight of sample, isotope ratios and elemental concentrations

Species	Organ	Photo	ID	Site	Elev.	Crust Level	Notes	Weight	δ^{15}N	δ^{13}C	Wt%N	Wt%C	C:N
YuccB	Seed	CAM	1	THR	5324	1		1.752	-0.2	-14.7	1.9	51.9	27.9
YuccB	Seed	CAM	2	THR	5730	3		1.614	-1.8	-14.4	2.1	54	25.4
YuccB	Seed	CAM	3	THR	5730	3		1.738	-1.8	-16	2.5	52	20.8
YuccB	Seed	CAM	4	THR	5725	3		0.819	1	-14	2.5	56.6	22.9
YuccB	Seed	CAM	6	THR	5728	3		1.668	-0.8	-14.9	2.5	54.1	21.9
YuccB	Seed	CAM	7	THR	5732	3		1.757	-2.8	-14.8	2.2	54.4	24.3
YuccB	Seed	CAM	8	THR	5957	2		0.902	0.2	-15.9	2.2	57.8	26.3
YuccB	Seed	CAM	10	THR	5961	3		1.787	-1	-14.5	2.7	52.5	19.7
YuccB	Seed	CAM	11	THR	5965	3		0.836	-0.7	-14.1	3.3	60	18.1
YuccB	Seed	CAM	12	THR	5893	1		1.122	0.2	-14.5	3	56.3	18.7
YuccB	Seed	CAM	14	THR	5929	2		0.736	1.5	-14.3	3.1	60.1	19.7
YuccB	Seed	CAM	15	THR	5929	2		1.711	0	-14.7	2.7	58	21.4
YuccB	Seed	CAM	16	MCC	5959	4		1.686	1.8	-14.4	2.2	50.2	22.7
YuccB	Seed	CAM	17	SK	7014	4		0.788	1	-13.7	2.8	54.5	19.6
YuccB	Seed	CAM	18	SK	6677	NA		1.673	-2	-14.4	2.5	55.3	22.5
YuccB	Seed	CAM	20	SK	6584	1		1.7	-0.1	-14.2	2.6	54.2	20.6
YuccB	Seed	CAM	21	SK	6489	1		1.639	0.6	-13.5	3.2	59.4	18.5
YuccB	Seed	CAM	22	MCC	6038	3		0.866	1.7	-15.6	2.2	54	24.1
YuccB	Seed	CAM	24	SFR	6276	4		1.629	-0.6	-13.5	3	55.2	18.7
YuccB	Seed	CAM	25	SFR	6182	5		0.832	1.2	-14.7	2.1	44.2	20.9
YuccB	Seed	CAM	26	SFR	6193	3		1.628	-1.5	-13.9	3.5	55.4	16
YuccB	Seed	CAM	29	SFR	6076	1		0.889	0.4	-14.1	2.6	55.8	21.7
YuccB	Seed	CAM	30	CSR	6463	3							NA
YuccB	Seed	CAM	32	CSR	6093	4		0.803	2.9	-14.5	1.7	48.8	29.1
YuccB	Fruit	CAM	1	THR	5324	1		2.242	-0.4	-13.4	0.5	42.4	81.7
YuccB	Fruit	CAM	2	THR	5730	3		2.706	-4.8	-14.6	0.3	41.7	157
YuccB	Fruit	CAM	3	THR	5730	3		2.757	-2.5	-14.4	1.8	43.7	24.4
YuccB	Fruit	CAM	4	THR	5725	3		2.486	-3.2	-13.9	0.9	42.1	45.4
YuccB	Fruit	CAM	6	THR	5728	3		2.342	-4.9	-14.2	0.3	42.5	167.8
YuccB	Fruit	CAM	7	THR	5732	3		2.479	-6.2	-13.3	0.2	42.5	186.4
YuccB	Fruit	CAM	8	THR	5957	2		2.572	-1.3	-14.6	0.6	43.7	74.9
YuccB	Fruit	CAM	10	THR	5961	3		1.842	-0.8	-15.4	1.5	41.6	28.4
YuccB	Fruit	CAM	11	THR	5965	3		1.809	-0.5	-15	0.6	40.2	63.3
YuccB	Fruit	CAM	12	THR	5893	1		1.959	0.5	-14.7	0.9	42.4	47.7
YuccB	Fruit	CAM	14	THR	5929	2		1.699	-1.6	-14	1.4	83.4	58.1
YuccB	Fruit	CAM	15	THR	5929	2		2.3	0.1	-14.6	1.2	43.3	35.1
YuccB	Fruit	CAM	16	MCC	5959	4		2.572	-1.3	-14.6	0.6	43.7	74.9
YuccB	Fruit	CAM	17	SK	7014	4		2.573	-3	-14	0.5	43.8	93.3

Table A.1: continued

Species	Organ	Photo	ID	Site	Elev.	Crust Level	Notes	Weight	δ^{15}N	δ^{13}C	Wt%N	Wt%C	C:N
YuccB	Fruit	CAM	18	SK	6677	NA		1.961	-0.3	-14.8	0.5	42.8	83
YuccB	Fruit	CAM	20	SK	6584	1		1.791	0	-14.4	1.3	42.5	31.5
YuccB	Fruit	CAM	21	SK	6489	1		2.294	-2	-13.6	0.7	43.6	65.9
YuccB	Fruit	CAM	22	MCC	6038	3		2.256	-1.1	-17.5	0.6	43	66.5
YuccB	Fruit	CAM	24	SFR	6276	4		1.744	-0.9	-14.3	1.4	47.1	33.1
YuccB	Fruit	CAM	25	SFR	6182	5		2.435	-3.3	-15.2	0.4	43.1	102.5
YuccB	Fruit	CAM	26	SFR	6193	3		2.462	-5	-14.1	0.4	44.2	112.6
YuccB	Fruit	CAM	29	SFR	6076	1		2.322	-3.4	-15.7	0.4	42.1	116.7
YuccB	Fruit	CAM	30	CSR	6463	3		1.79	1.1	-14.9	1.2	46.6	39.1
YuccB	Fruit	CAM	32	CSR	6093	4		2.431	-2.7	-14.9	0.3	42.3	146.2
YuccB	Heart	CAM	1	THR	5324	1		2.436	-0.4	-14.2	2.6	43.6	16.9
YuccB	Heart	CAM	2	THR	5730	3		2.001	-1.5	-14.3	1.3	44.1	33.6
YuccB	Heart	CAM	3	THR	5730	3		1.71	-0.8	-16.2	1.2	43.6	35
YuccB	Heart	CAM	4	THR	5725	3		2.145	3.7	-14.6	0.4	37.9	89.9
YuccB	Heart	CAM	6	THR	5728	3		2.006	0.1	-15.7	0.6	38.6	61.4
YuccB	Heart	CAM	7	THR	5732	3		1.88	3.1	-14.6	0.4	36.5	100.1
YuccB	Heart	CAM	8	THR	5957	2		1.807	3.9	-16.5	0.4	39.9	93.7
YuccB	Heart	CAM	10	THR	5961	3		1.776	1.7	-14.7	0.8	42.1	53.8
YuccB	Heart	CAM	11	THR	5965	3		1.908	-0.2	-13.7	1	38.8	37.5
YuccB	Heart	CAM	12	THR	5893	1		2.101	-1.2	-14.8	1.1	45.2	41.3
YuccB	Heart	CAM	14	THR	5929	2		2.39	-0.4	-15.3	0.9	45.7	52.9
YuccB	Heart	CAM	15	THR	5929	2		1.748	4.6	-14.2	0.5	42.5	90.4
YuccB	Heart	CAM	16	MCC	5959	4		1.901	2.4	-14.2	1.2	38.8	33.1
YuccB	Heart	CAM	17	SK	7014	4		2.39	3.9	-12.6	0.5	42.1	88.6
YuccB	Heart	CAM	18	SK	6677	NA		1.958	-1.8	-14.9	1.9	43.8	23.3
YuccB	Heart	CAM	20	SK	6584	1		2.014	6.6	-12.9	0.4	41.9	113.5
YuccB	Heart	CAM	21	SK	6489	1		1.873	2.3	-14.6	0.7	43	61.4
YuccB	Heart	CAM	22	MCC	6038	3		2.233	0.6	-15.5	0.9	44.1	47.1
YuccB	Heart	CAM	24	SFR	6276	4		2.062	-0.2	-13.7	1.1	46.1	40.3
YuccB	Heart	CAM	25	SFR	6182	5		1.909	9	-14.4	0.3	41.8	124.1
YuccB	Heart	CAM	26	SFR	6193	3		2.029	0.5	-14	0.6	44	70.7
YuccB	Heart	CAM	29	SFR	6076	1		1.705	3.6	-14.4	0.5	45	96.4
YuccB	Heart	CAM	30	CSR	6463	3		2.284	2.5	-14.6	1.4	44.8	32.7
YuccB	Heart	CAM	32	CSR	6093	4		2.014	11.5	-13.3	0.2	38.9	180.9
OpunSp	Leaves	CAM	1	FMC	4932	5		2.34	1.2	-11.8	1.7	36.1	21.5
OpunSp	Leaves	CAM	2	FMC	4932	5		1.958	6.9	-12	0.7	34.8	53.5
OpunSp	Leaves	CAM	3	FMC	4932	5		2.847	3	-13.3	0.4	33.5	91.8
OpunSp	Leaves	CAM	5	FMC	4932	5		2.589	2	-11.7	0.7	34.3	52
OpunSp	Leaves	CAM	7	FMC	4932	3		2.55	3.9	-12.6	0.4	36	88.6
OpunSp	Leaves	CAM	8	FMC	4932	3		1.569	2.2	-12.7	0.7	37.6	50.6
OpunSp	Leaves	CAM	10	FMC	4932	3		2.702	0.2	-10.8	0.3	28.4	102.8
OpunSp	Leaves	CAM	11	FMC	4932	3		2.026	6.3	-12	1	35.9	35.7
OpunSp	Leaves	CAM	12	FMC	4932	3		2.595	3.7	-13.2	0.5	34.7	69.2
OpunSp	Leaves	CAM	13	FMC	4932	3		1.78	1.4	-14	1	35	36.3
OpunSp	Leaves	CAM	14	FMC	4932	3		1.63	1.5	-12.7	0.8	34.7	45.3
OpunSp	Leaves	CAM	9	FMC	4932	3		2.324	-2.9	-13.4	0.3	34.9	101.8
OpunSp	Leaves	CAM	19	THR	5831	3		1.768	1.6	-13.7	0.9	34.8	38.6
OpunSp	Leaves	CAM	20	THR	5831	3		1.794	2.1	-12.3	0.8	34.3	42.7
OpunSp	Leaves	CAM	21	THR	5831	3		1.896	3.3	-12.9	0.6	35	55.7
OpunSp	Leaves	CAM	22	THR	5831	3		2.741	-2.1	-12.7	0.5	35.5	73.7
OpunSp	Leaves	CAM	23	THR	5831	3		2.6	-1.3	-13	0.5	36.5	71.6
OpunSp	Leaves	CAM	24	THR	5831	3		2.001	2.3	-13.3	0.8	36.8	48.8
OpunSp	Leaves	CAM	25	MCC	6045	4		2.204	0.4	-12.4	0.6	33.4	53.6
OpunSp	Leaves	CAM	26	MCC	6045	4		2.119	1.7	-12.4	0.8	36.2	44.6

Table A.1: continued

Species	Organ	Photo	ID	Site	Elev.	Crust Level	Notes	Weight	δ^{15}N	δ^{13}C	Wt%N	Wt%C	C:N
OpunSp	Leaves	CAM	27	MCC	6045	4		1.883	3.2	-12.8	1	37.4	39.2
OpunSp	Leaves	CAM	28	MCC	6045	4		1.66	2.3	-12.6	1.2	35.4	29.7
OpunSp	Leaves	CAM	29	MCC	6045	4		2.169	5.6	-12.1	0.9	36.3	42.5
OpunSp	Leaves	CAM	30	MCC	6045	4		1.661	5.6	-12.2	0.9	33.1	38.8
OpunSp	Fruit	CAM	1	FMC	4932	5		1.9	3.1	-11.6	0.8	36.9	45.5
OpunSp	Fruit	CAM	2	FMC	4932	5		1.783	9	-11.6	1	35.5	36.1
OpunSp	Fruit	CAM	3	FMC	4932	5		1.973	4.2	-11.1	1.2	36.3	30.8
OpunSp	Fruit	CAM	5	FMC	4932	5		2.223	0.6	-10.7	1.4	33.8	24.4
OpunSp	Fruit	CAM	7	FMC	4932	3		2.082	7.7	-11.4	3	36.7	12.1
OpunSp	Fruit	CAM	8	FMC	4932	3		2.073	-1	-12.4	1.4	32.2	23.3
OpunSp	Fruit	CAM	10	FMC	4932	3		1.799	2	-12.3	0.7	31.8	47.5
OpunSp	Fruit	CAM	11	FMC	4932	3		1.892	4.4	-11.8	0.9	34.4	39.2
OpunSp	Fruit	CAM	12	FMC	4932	3		1.714	6.3	-11.8	0.9	32.8	36.6
OpunSp	Fruit	CAM	13	FMC	4932	3		1.529	0.7	-12.8	1.6	35	21.7
OpunSp	Fruit	CAM	14	FMC	4932	3		2.338	-0.9	-12.7	1.3	35.8	27.1
OpunSp	Fruit	CAM	9	FMC	4932	3		2.196	3.3	-12.3	1.2	37	30.1
OpunSp	Fruit	CAM	19	THR	5831	3		1.974	-1.4	-11.8	1.1	38.1	33.8
OpunSp	Fruit	CAM	20	THR	5831	3		1.949	4	-12.6	0.8	35.1	42.6
OpunSp	Fruit	CAM	21	THR	5831	3		1.775	2.8	-11.9	1	36.1	38
OpunSp	Fruit	CAM	22	THR	5831	3		1.937	2.8	-11.3	0.8	35.2	45.8
OpunSp	Fruit	CAM	23	THR	5831	3		2.381	-1.6	-12.4	1.7	36	21.1
OpunSp	Fruit	CAM	24	THR	5831	3		2.505	-0.7	-12.9	1.1	35.1	33.2
OpunSp	Fruit	CAM	25	MCC	6045	4		2.042	0.9	-12.8	1.1	34.4	30.8
OpunSp	Fruit	CAM	26	MCC	6045	4		1.93	2.4	-13.4	1.2	34.3	28.9
OpunSp	Fruit	CAM	27	MCC	6045	4		1.788	3.4	-11.8	0.8	32.3	40.6
OpunSp	Fruit	CAM	28	MCC	6045	4		1.718	2.5	-12	1	34.2	33.5
OpunSp	Fruit	CAM	29	MCC	6045	4		2.136	4.3	-11.4	1.2	39.5	33.1
OpunSp	Fruit	CAM	30	MCC	6045	4		1.852	4.2	-12.1	1.1	32.9	31.2
AmarR	Seed	C4	1	SMC	5877	0		1.71	-0.4	-12	3.1	47.5	15.2
AmarR	Seed	C4	2	SMC	5877	0		1.78	0.2	-12.9	2.9	46.8	16.2
AmarR	Seed	C4	3	SMC	5877	0		2.036	-2.2	-12.3	2.6	40.6	15.4
AmarR	Seed	C4	4	SMC	5877	0		2.088	-0.5	-12.3	3.2	45	14
AmarR	Seed	C4	5	SMC	5877	0		2.186	-0.4	-12.3	2.9	45.1	15.6
AmarR	Seed	C4	6	SMC	5877	0		1.629	0.5	-12.6	3.1	44.9	14.4
AmarR	Seed	C4	7	SMC	5877	0		1.627	1.1	-13	2.9	46.1	16.1
AmarR	Seed	C4	8	SMC	5877	0		2.205	0.1	-11.6	3.4	45.1	13.3
AmarR	Seed	C4	9	SMC	5877	0		1.882	-0.3	-12.1	2.8	41	14.8
AmarR	Seed	C4	10	SMC	5877	0		1.991	-1	-12.3	3.5	44.9	12.8
AmarR	Seed	C4	11	SMC	5877	0		2.147	-1.5	-12.6	3	45.4	15.2
AmarR	Seed	C4	12	SMC	5877	0		2.394	-0.7	-12	2.8	44.9	15.9
AmarR	Seed	C4	13	SMC	5877	0		2.372	1.2	-12.6	3.1	45.4	14.7
AmarR	Seed	C4	14	SMC	5877	0		2.204	-0.5	-11.8	3.4	46.3	13.5
AmarR	Seed	C4	15	SMC	5877	0		2.572	-1	-11.9	3.4	45.4	13.2
AmarR	Seed	C4	16	FMC	4742	0		1.992	0	-11.7	4	44.5	11.2
AmarR	Seed	C4	17	FMC	4742	0		1.819	0.7	-11.8	3.9	42.4	10.9
AmarR	Seed	C4	18	FMC	4742	0		2.034	1	-13.5	2.8	43.4	15.8
AmarR	Seed	C4	19	FMC	4742	0		0.428	3.4	-12.5	3.8	43.8	11.4
AmarR	Seed	C4	20	FMC	4742	0		1.65	-0.4	-12.8	3	43.3	14.4
AmarR	Seed	C4	21	FMC	4742	0		1.901	4	-11.7	3.6	43	12
AmarR	Seed	C4	22	FMC	4742	0		2.168	5.3	-11.6	4.1	44.6	10.7
AmarR	Seed	C4	23	FMC	4742	0		1.822	1.2	-13.1	3.1	44.6	14.3
AmarR	Seed	C4	24	FMC	4742	0		2.201	4.5	-11.6	3.4	43.4	12.9
AmarR	Seed	C4	25	FMC	4742	0		1.622	1.6	-12.6	4	42	10.5
AmarR	Seed	C4	26	FMC	4742	0		1.978	3.8	-11.7	3.1	42.8	13.7

Table A.1: continued

Species	Organ	Photo	ID	Site	Elev.	Crust Level	Notes	Weight	δ^{15}N	δ^{13}C	Wt%N	Wt%C	C:N
AmarR	Leaves	C4	1	SMC	5877	0		1.657	0.8	-13.4	3.5	31.7	9.2
AmarR	Leaves	C4	2	SMC	5877	0		1.609	0.7	-12.7	3.4	32.4	9.5
AmarR	Leaves	C4	3	SMC	5877	0		1.75	-1	-13.6	4.7	33.4	7.1
AmarR	Leaves	C4	4	SMC	5877	0		1.74	2.1	-13	3.9	31.7	8.1
AmarR	Leaves	C4	5	SMC	5877	0		1.646	0.2	-13.9	3.7	34.3	9.3
AmarR	Leaves	C4	6	SMC	5877	0		1.619	0.2	-12.8	3.1	32.3	10.4
AmarR	Leaves	C4	7	SMC	5877	0		1.601	1.1	-13.8	3.7	35	9.4
AmarR	Leaves	C4	8	SMC	5877	0		1.868	0	-13.6	4.1	34.4	8.5
AmarR	Leaves	C4	9	SMC	5877	0		1.766	-0.1	-13.6	3.6	33.9	9.5
AmarR	Leaves	C4	10	SMC	5877	0		1.696	-0.1	-13.7	4.6	35.7	7.8
AmarR	Leaves	C4	11	SMC	5877	0		1.686	0.3	-13.8	4	33.8	8.4
AmarR	Leaves	C4	12	SMC	5877	0		1.739	0.5	-13.4	3.9	33.4	8.6
AmarR	Leaves	C4	13	SMC	5877	0		1.656	1.9	-13.6	3.8	33.2	8.7
AmarR	Leaves	C4	14	SMC	5877	0		1.68	0.6	-13.3	3.4	33.2	9.7
AmarR	Leaves	C4	15	SMC	5877	0		1.698	0.3	-13.5	4.6	38.4	8.4
AmarR	Leaves	C4	16	FMC	4742	0		1.932	1.1	-13.8	5	35.2	7
AmarR	Leaves	C4	17	FMC	4742	0		1.783	2.7	-13.6	5.2	35.9	6.9
AmarR	Leaves	C4	18	FMC	4742	0		1.583	0.8	-14.7	3.4	35.1	10.3
AmarR	Leaves	C4	19	FMC	4742	0		1.889	0	-14.7	3.4	38.1	11.1
AmarR	Leaves	C4	20	FMC	4742	0		1.676	-1	-14	4.1	34.8	8.5
AmarR	Leaves	C4	21	FMC	4742	0		1.736	2.4	-12.9	4.3	34.4	8
AmarR	Leaves	C4	22	FMC	4742	0		1.853	3.3	-13.5	3.6	31.1	8.7
AmarR	Leaves	C4	23	FMC	4742	0		1.753	1.3	-14.4	3.6	33.4	9.2
AmarR	Leaves	C4	24	FMC	4742	0		1.737	5.7	-13.9	4.9	35.6	7.2
AmarR	Leaves	C4	25	FMC	4742	0		1.722	1	-14.2	4.6	36.2	7.8
AmarR	Leaves	C4	26	FMC	4742	0		1.639	4.1	-12.5	3.8	31.4	8.3
AtriC	Seed	C4	1	CSR	6516	2		1.959	7.9	-12.5	1.5	43	28.5
AtriC	Seed	C4	2	CSR	6516	2		1.85	7.6	-13.7	1.3	40	30.3
AtriC	Seed	C4	3	CSR	6516	2		1.749	6.5	-13.3	1.5	41.2	26.7
AtriC	Seed	C4	4	CSR	6516	2		1.795	8.4	-13	1.1	43.6	39.6
AtriC	Seed	C4	5	CSR	6516	2		2.167	5.4	-13.5	1.1	42.9	37.7
AtriC	Seed	C4	6	CSR	6516	2		1.835	6	-13.5	1.6	43.2	26.4
AtriC	Seed	C4	9	SFR	6512	2		1.871	5.8	-14	2.2	42.6	19.6
AtriC	Seed	C4	10	SFR	6512	2		1.895	5.1	-13.4	2	40.1	19.6
AtriC	Seed	C4	11	SFR	6512	2		1.785	5.8	-13.6	1	42.5	41.4
AtriC	Seed	C4	12	SFR	6512	2		2.356	7.4	-13.5	0.9	43.7	50.5
AtriC	Seed	C4	13	SFR	6512	2		1.778	5.5	-13.7	2.2	42.1	19.1
AtriC	Seed	C4	14	SFR	6512	2		1.858	5.5	-13.1	1.2	40.2	32.3
AtriC	Seed	C4	16	FMC	4742	1		1.819	3.7	-13.3	1.9	41.9	22.6
AtriC	Seed	C4	18	FMC	4742	1		1.776	0.5	-12.6	1.7	41	24.6
AtriC	Seed	C4	20	FMC	4742	1		2.243	0.2	-12.8	1.7	42.3	25.5
AtriC	Seed	C4	22	FMC	4742	1		1.911	2.6	-12.7	0.7	43.6	65.4
AtriC	Seed	C4	24	FMC	4742	1		1.89	1.4	-13.5	2.4	43.3	18.2
AtriC	Seed	C4	26	FMC	4742	1		1.76	8.3	-13.2	1.1	42.5	37.9
AtriC	Seed	C4	31	FCD	4542	1		2.303	6.7	-13.4	0.8	43.5	53.9
AtriC	Seed	C4	32	FCD	4542	1		1.83	7.5	-12.9	1.1	43.9	41.5
AtriC	Seed	C4	33	FCD	4542	1		1.964	8.6	-13.5	0.9	39.7	42.9
AtriC	Seed	C4	34	FCD	4542	1		1.789	8	-14	1.2	42.4	36.1
AtriC	Seed	C4	35	FCD	4542	1		1.782	7.6	-14.1	2	43.8	21.6
AtriC	Seed	C4	37	FCD	4542	1		1.957	7.6	-14.1	1.2	40.3	34.7
HeliA	Seed	C3	2	BL2	5298	0	Brown	1.74	-0.6	-30.3	3.4	52	15.4
HeliA	Seed	C3	3	BL2	5298	0	Black	1.764	-1.3	-30.9	2.3	48.4	21.2
HeliA	Seed	C3	4	BL2	5298	0	Black	1.664	-0.8	-29.1	2.8	51.5	18.6
HeliA	Seed	C3	6	BL1	5456	0	Black	1.765	4.2	-27.3	2.7	47	17.5

Table A.1: continued

Species	Organ	Photo	ID	Site	Elev.	Crust Level	Notes	Weight	δ^{15}N	δ^{13}C	Wt%N	Wt%C	C:N
HeliA	Seed	C3	7	BL1	5456	0	Brown	1.767	0.5	-26.4	3.3	51.1	15.4
HeliA	Seed	C3	8	BL1	5456	0	Black	1.761	-0.8	-26.6	4	46.4	11.7
HeliA	Seed	C3	9	BL1	5456	0	Black	1.68	-0.5	-26	2.9	51.9	18.2
HeliA	Seed	C3	11	BL3	5235	0	Black	1.76	0.5	-28	3.3	48.6	14.6
HeliA	Seed	C3	12	BL3	5235	0	Brown	1.768	0	-27.2	2.6	51.3	19.5
HeliA	Seed	C3	13	BL3	5235	0	Black	1.859	-0.7	-26	2.9	53	18.3
HeliA	Seed	C3	14	BL3	5235	0	Black	1.848	-0.7	-24.8	2.5	48.2	19.3
HeliA	Seed	C3	15	BL3	5235	0	Black	1.871	4.7	-28.6	3.2	45.7	14.4
HeliA	Seed	C3	16	U95	6777	0	Brown	1.734	8.1	-27.1	2.2	54.9	25.5
HeliA	Seed	C3	17	U95	6777	0	Brown	1.807	6.1	-28.6	1.9	53	27.3
HeliA	Seed	C3	18	U95	6777	0	Black	1.746	1.6	-29	2.1	47.3	22.5
HeliA	Seed	C3	19	U95	6777	0	Black	1.65	5	-29.7	2.1	47.4	23
HeliA	Seed	C3	20	U95	6777	0	Brown	1.769	1.7	-30	2	51.9	25.4
HeliA	Seed	C3	21	U95	6777	0	Brown	1.837	6.3	-29.5	2.2	49.3	22.6
HeliA	Seed	C3	22	U95	6777	0	Black	1.737	7.2	-29.1	2.6	47.7	18.2
HeliA	Seed	C3	23	U95	6777	0	Brown	1.849	2.8	-29.8	2.6	51.8	20.1
HeliA	Seed	C3	24	U95	6777	0	Black	1.721	2.6	-30.5	2.1	56	26.2
HeliA	Seed	C3	25	U95	6777	0	Brown	1.615	2.9	-31.1	2	51.5	25.4
HeliA	Seed	C3	26	U95	6777	0	Brown	1.822	1.9	-30.8	2.4	53.6	22.2
HeliA	Seed	C3	27	U95	6777	0	Brown	1.836	1.6	-31.4	2.4	53	22.4
MentM	Seed	C3	2	BWR	4892	2		1.747	-0.1	-23.3	4.1	51.7	12.7
MentM	Seed	C3	3	BWR	4892	2		1.673	2	-22.1	3.9	55.3	14
MentM	Seed	C3	4	BWR	4892	2		1.77	2.2	-22.8	3.9	53.4	13.7
MentM	Seed	C3	5	BWR	4892	2		1.883	-0.3	-27.1	1.6	41.2	25.1
MentM	Seed	C3	6	FCD	4542	1		1.794	-0.6	-23.2	4	53.5	13.5
MentM	Seed	C3	7	FCD	4542	1		1.911	0.5	-21.7	4	54.1	13.6
MentM	Seed	C3	8	FCD	4542	1		1.688	0.3	-21.8	3.6	50.4	14.1
MentM	Seed	C3	9	FCD	4542	1		1.923	0.6	-23.6	3.8	50.5	13.4
MentM	Seed	C3	16	THR	5766	1		1.615	-0.1	-27.2	2.7	53.5	20
MentM	Seed	C3	17	THR	5766	1		2.1	1	-27.4	3.2	53.2	16.5
MentM	Seed	C3	18	THR	5766	1		1.986	-0.5	-24.6	2.9	47.9	16.7
MentM	Seed	C3	19	THR	5766	1		2.154	0.1	-24.4	3.3	53.8	16.1
MentM	Seed	C3	20	THR	5766	1		1.934	-3	-24	2.8	50.9	18
MentM	Seed	C3	21	THR	5766	1		1.588	-3.1	-22.9	3.7	54.7	14.9
MentM	Seed	C3	22	THR	5766	1		2.87	-2.3	-22.8	3.8	56.3	14.7
MentM	Seed	C3	23	THR	5766	1		2.739	-2.3	-22.4	2.9	53.7	18.8
MentM	Seed	C3	24	THR	5766	1		2.532	-0.2	-22.4	3.6	56	15.4
MentM	Seed	C3	25	THR	5766	1		2.385	-0.2	-23	3.3	54	16.3
MentM	Seed	C3	26	CWC	4833	1		2.497	4.1	-27.2	3.4	51.7	15
MentM	Seed	C3	27	CWC	4833	1		2.983	1.4	-27.5	3.5	54.4	15.7
MentM	Seed	C3	28	CWC	4833	1		2.993	0.4	-24.5	3.9	53.5	13.6
MentM	Seed	C3	29	CWC	4833	1		2.849	4	-25.4	3.3	54	16.3
MentM	Seed	C3	30	CWC	4833	1		2.577	3.4	-26.9	3.6	55.3	15.2
MentM	Seed	C3	31	CWC	4833	1		2.92	5.1	-26.7	3.7	53.6	14.4
MentM	Seed	C3	32	CWC	4833	1		2.806	4.6	-24.6	3.5	54.6	15.6
MentM	Seed	C3	33	CWC	4833	1		2.985	5.5	-24.4	3.9	54.4	14.1
CleoS	Seed	C3	1	FCC	4611	1		2.404	3.9	-23.2	3.8	50.1	13.3
CleoS	Seed	C3		FCC	4611	1		2.614	3.6	-23.1	3.7	52.2	14.2
CleoS	Seed	C3	3	FCC	4611	1		0.633	5.6	-23.4	8	40.9	5.1
CleoS	Seed	C3	4	FCC	4611	1		1.81	5.1	-25.7	3.5	52.6	15.1
CleoS	Seed	C3	6	FCC	4611	1		1.732	3.4	-24.5	3.6	53.8	14.9
CleoS	Seed	C3	7	FCC	4611	1		1.824	5	-26.6	3.4	50.3	14.9
CleoS	Seed	C3	8	FCC	4611	1		1.726	0.5	-24.1	3.3	49	14.8
CleoS	Seed	C3	9	FCC	4611	1		1.669	0.5	-24.9	3.3	49.6	15.2

Table A.1: continued

Species	Organ	Photo	ID	Site	Elev.	Crust Level	Notes	Weight	δ^{15}N	δ^{13}C	Wt%N	Wt%C	C:N
CleoS	Seed	C3	10	FCC	4611	1		1.435	1.8	-26.3	3.8	52.7	13.7
CleoS	Seed	C3	11	FCD	4542	1		1.775	5.5	-24	3.6	55.6	15.3
CleoS	Seed	C3	12	FCD	4542	1		1.637	4.7	-23.7	2.9	52.6	18.1
CleoS	Seed	C3	13	FCD	4542	1		1.537	4.8	-23.6	3.9	54.5	13.8
CleoS	Seed	C3	14	FCD	4542	1		1.577	5.1	-24.6	3.6	54.7	15.3
CleoS	Seed	C3	16	SC	5505	3		1.707	2.1	-23.5	3.2	44.1	13.7
CleoS	Seed	C3	23	SC	5505	3		1.618	2.1	-24.2	3.6	51.9	14.5
CleoS	Seed	C3	24	SC	5505	3		1.6	4.7	-24.3	3.8	52.3	13.8
CleoS	Seed	C3	25	SC	5505	3		1.495	2.8	-25.5	3.9	53.7	13.6
CleoS	Seed	C3	26	SC	5505	3		1.654	4.7	-24.5	3.1	49.7	16.2
CleoS	Seed	C3	27	SC	5505	3		1.714	5.2	-23.7	3.8	51.5	13.4
CleoS	Seed	C3	33	SC	5505	3		1.709	3.9	-24.8	3.6	50.5	13.9
CleoS	Seed	C3	34	BC	5466	2		1.651	3.1	-23	3.9	50.9	13.1
CleoS	Seed	C3	35	BC	5466	2		1.677	2.6	-24.6	3.5	51.4	14.6
CleoS	Seed	C3	37	BC	5466	2		1.659	4.5	-23.7	5.5	39.9	7.3
CleoS	Seed	C3	38	BC	5466	2		1.668	3.5	-24	3.7	50.2	13.6
CleoS	Seed	C3	39	BC	5466	2		1.627	3	-24.1	3.4	50.6	14.7
CleoS	Leaves	C3	1	FCC	4611	1		1.956	5.4	-24.9	5.2	41.2	7.8
CleoS	Leaves	C3	3	FCC	4611	1		2.094	8.2	-26.8	5.6	44	7.8
CleoS	Leaves	C3	4	FCC	4611	1		2.103	8.4	-28	5.1	43	8.4
CleoS	Leaves	C3	6	FCC	4611	1		2.017	7	-26.1	5.5	42.7	7.8
CleoS	Leaves	C3	7	FCC	4611	1		2.087	6.7	-26.2	5.5	42.1	7.7
CleoS	Leaves	C3	8	FCC	4611	1		2.167	4.6	-26.1	6	43.1	7.2
CleoS	Leaves	C3	9	FCC	4611	1		2.265	6	-26.9	4.9	41.7	8.4
CleoS	Leaves	C3	10	FCC	4611	1		2.149	8.5	-28.3	5.5	42	7.7
CleoS	Leaves	C3	11	FCD	4542	1		1.978	9	-28.5	5	41.4	8.3
CleoS	Leaves	C3	12	FCD	4542	1		2.055	8.6	-28.1	5.3	41.8	7.9
CleoS	Leaves	C3	13	FCD	4542	1		1.933	7.6	-28.1	4.3	39.9	9.3
CleoS	Leaves	C3	14	FCD	4542	1		1.973	8.9	-27	5.2	40.6	7.7
CleoS	Leaves	C3	16	SC	5505	3		2.021	5.8	-27.3	4.2	39.8	9.5
CleoS	Leaves	C3	23	SC	5505	3		1.935	3.7	-27.1	4.6	41	9
CleoS	Leaves	C3	24	SC	5505	3		1.939	5	-27.4	4.4	41.6	9.4
CleoS	Leaves	C3	25	SC	5505	3		2.046	6.6	-25.7	4.5	40.5	9
CleoS	Leaves	C3	26	SC	5505	3		1.977	7	-27	4.3	41.5	9.6
CleoS	Leaves	C3	27	SC	5505	3		1.994	5.8	-26.1	4.8	41.6	8.6
CleoS	Leaves	C3	33	SC	5505	3		2.097	8	-27.4	5.5	40.7	7.4
CleoS	Leaves	C3	34	BC	5466	2		2.044	7.5	-27.2	5.3	42.3	7.9
CleoS	Leaves	C3	35	BC	5466	2		1.926	6.7	-27.5	4.9	39.7	8.1
CleoS	Leaves	C3	37	BC	5466	2		2.005	8.1	-27.5	6.2	43.3	7
CleoS	Leaves	C3	38	BC	5466	2		1.921	8.1	-27.4	4.8	41.5	8.6
CleoS	Leaves	C3	39	BC	5466	2		1.982	7.3	-27.5	4.7	40.4	8.6
OryzH	Seed	C3	1	BWR	4892	2		1.651	-1.8	-23.8	1.5	40.9	26.7
OryzH	Seed	C3	2	BWR	4892	2		1.572	-1.9	-23.9	1.4	43.2	31.1
OryzH	Seed	C3	3	BWR	4892	2		1.657	-1.1	-23.8	2.2	41.5	19
OryzH	Seed	C3	4	BWR	4892	2		1.601	-0.6	-25	1.4	44.9	32.6
OryzH	Seed	C3	5	BWR	4892	2		1.578	0.1	-23.9	1.8	45.1	25.2
OryzH	Seed	C3	6	BWR	4892	2		1.642	-1	-24.6	1.4	44.6	32.4
OryzH	Seed	C3	12	FCD	4542	1		1.674	3.6	-24.4	1.2	44.6	37.1
OryzH	Seed	C3	13	FCD	4542	1		1.676	4.2	-23.1	1.8	44.2	24.4
OryzH	Seed	C3	14	FCD	4542	1		1.764	4.1	-23.6	2.3	43.2	19
OryzH	Seed	C3	15	FCD	4542	1		1.756	3.1	-22.9	2	42.8	21
OryzH	Seed	C3	16	THR	5638	3		1.577	0	-23.9	1.8	40.5	22.8
OryzH	Seed	C3	17	THR	5638	3		1.696	0.9	-23.5	1.9	43.8	23.2
OryzH	Seed	C3	18	THR	5638	3		1.61	-2.3	-24.7	2.2	41.3	18.7

Table A.1: continued

Species	Organ	Photo	ID	Site	Elev.	Crust Level	Notes	Weight	δ^{15}N	δ^{13}C	Wt%N	Wt%C	C:N
OryzH	Seed	C3	20	THR	5638	3		1.723	-0.6	-24.7	2	42.9	21.4
OryzH	Seed	C3	21	THR	5638	3		1.737	-0.8	-23.8	2.1	43.9	21
OryzH	Seed	C3	22	THR	5638	3		1.759	-2.5	-25	1.5	43.9	29.4
OryzH	Seed	C3	26	SMC	5940	1		1.696	-2.3	-24.4	1.6	43.3	27.9
OryzH	Seed	C3	27	SMC	5940	1		1.507	-3.3	-22.4	0.7	45.2	68.1
OryzH	Seed	C3	32	FCD	4542	2		1.636	4	-23.9	1.3	44.8	33.3
OryzH	Seed	C3	33	FCD	4542	2		1.729	0.9	-24	0.7	44.9	60.8
OryzH	Seed	C3	36	MCC	6045	4		1.736	-0.3	-23.2	2.1	41.9	19.9
OryzH	Seed	C3	37	MCC	6045	4		1.63	0	-22.6	2.2	42.7	19.1
OryzH	Seed	C3	38	MCC	6045	4		1.627	0.2	-23	2.1	42.5	20.3
OryzH	Seed	C3	39	MCC	6045	4		1.684	0	-24.5	2.1	42.5	20.3
Typh	Root	C3	2	AC1	4864	0	Dry	2.322	4.8	-26.4	0.5	43.3	85.7
Typh	Root	C3	3	AC1	4864	0	Dry	1.816	7.2	-27	0.5	41.3	85
Typh	Root	C3	4	AC1	4864	0	Dry	2.236	3.1	-26.6	0.7	39.3	58.3
Typh	Root	C3	5	AC1	4864	0	Dry	2.914	-2.6	-26.3	0.2	41	216.1
Typh	Root	C3	6	AC1	4864	0	Dry	1.985	4.1	-27	0.7	41.3	62.7
Typh	Root	C3	7	AC1	4864	0	Dry	2.293	7.8	-26.6	0.3	41.5	122.7
Typh	Root	C3	8	AC2	4981	0	Wet	2.637	-0.1	-27.7	0.2	39.8	187.5
Typh	Root	C3	9	AC2	4981	0	Wet	2.04	10.6	-26.7	0.4	37.1	105.7
Typh	Root	C3	10	AC2	4981	0	Wet	1.9	5.3	-27.8	0.7	36.5	49.7
Typh	Root	C3	11	AC2	4981	0	Wet	2.386	-0.6	-27.8	0.3	38.5	153
Typh	Root	C3	12	AC2	4981	0	Wet	2.002	10.4	-27.3	0.3	40.2	124.1
Typh	Root	C3	13	AC2	4981	0	Wet	2.499	0.4	-28.3	0.2	41.8	169.9
Typh	Root	C3	17	PS	6611	0	Dry	1.965	2.9	-28	0.6	36.1	63.9
Typh	Root	C3	18	PS	6611	0	Dry	2.091	2	-27.2	3.1	36.2	11.8
Typh	Root	C3	20	PS	6611	0	Dry	1.974	5.7	-28.2	0.5	40.9	87.7
Typh	Root	C3	21	PS	6611	0	Dry	1.979	2.6	-27.4	2.1	33.6	16
Typh	Root	C3	22	PS	6611	0	Dry	1.756	15.1	-27	2.1	37.5	17.5
Typh	Root	C3	23	PS	6611	0	Dry	2.046	5.3	-28.9	0.4	38.1	104.8
Typh	Root	C3	24	PS	6611	0	Wet	1.871	6	-29	0.5	39.9	79.3
Typh	Root	C3	25	PS	6611	0	Wet	1.899	5.5	-28.6	0.4	40.9	102
Typh	Root	C3	26	PS	6611	0	Wet	2.074	1.3	-27.4	0.7	39.2	58.1
Typh	Root	C3	27	PS	6611	0	Wet	2.127	5.6	-29.2	0.4	40.3	106.5
Typh	Root	C3	28	PS	6611	0	Wet	2.019	1.9	-27.7	1	35.8	35
Typh	Root	C3	29	PS	6611	0	Wet	2.052	3.2	-27.4	0.5	39.5	73.1
RhusT	Fruit	C3	1	FMC	4850	1		1.462	-1.3	-27.8	1.4	51.6	37.2
RhusT	Fruit	C3	3	FMC	4850	1		1.839	-0.1	-27.3	1.5	48.1	31.8
RhusT	Fruit	C3	5	FMC	4850	1		1.764	-0.7	-26.2	1.9	51.1	26.2
RhusT	Fruit	C3	7	FMC	4850	1		1.522	-2.5	-25.9	1	51.3	53.7
RhusT	Fruit	C3	9	FMC	4850	1		1.582	-2.8	-26.7	1.2	52.3	42.4
RhusT	Fruit	C3	11	FMC	4850	1		1.611	-3.1	-28.1	1.2	51.2	43.8
RhusT	Fruit	C3	13	CW95	4542	3		1.732	-0.4	-24.5	2	50.1	24.5
RhusT	Fruit	C3	14	CW95	4542	3		1.607	0.3	-25.4	1.9	52.1	26.8
RhusT	Fruit	C3	15	CW95	4542	3		1.833	0.1	-24.3	2	48.2	24.4
RhusT	Fruit	C3	16	SMC	5940	1		1.65	-3.4	-25.8	2.2	51.3	23.8
RhusT	Fruit	C3	17	SMC	5940	1		1.669	-3.6	-25.5	1.8	47.6	25.8
RhusT	Fruit	C3	18	SMC	5940	1		1.802	-3.2	-24.9	2.1	49	23.3
RhusT	Fruit	C3	19	SMC	5940	1		1.658	-1.5	-25.8	1.9	51.2	26.5
RhusT	Fruit	C3	20	SMC	5940	1		1.863	-2.2	-25.1	2.5	48.6	19.6
RhusT	Fruit	C3	21	SMC	5940	1		1.606	-2.2	-25.7	1.8	48.6	27.5
RhusT	Fruit	C3	26	NMC	5933	1		1.686	-4.3	-26	2	48.9	24.4
RhusT	Fruit	C3	27	NMC	5933	1		1.75	-2.6	-24.1	2.1	48.7	23.1
RhusT	Fruit	C3	28	NMC	5933	1		1.54	-4.3	-26.7	1.4	49.6	34.6
RhusT	Fruit	C3	29	NMC	5933	1		1.858	-2.3	-26.9	1.9	49.1	26.4

Table A.1: continued

Species	Organ	Photo	ID	Site	Elev.	Crust Level	Notes	Weight	δ^{15}N	δ^{13}C	Wt%N	Wt%C	C:N
RhusT	Fruit	C3	30	NMC	5933	1		1.681	-1.2	-27.1	2	49.5	24.2
RhusT	Fruit	C3	31	CW95	4542	3		1.608	0.7	-26.1	2.3	48.3	21.4
RhusT	Fruit	C3	32	CW95	4542	3		1.742	0.4	-25.5	1.7	48.7	28.2
RhusT	Fruit	C3	33	CW95	4542	3		1.737	0.9	-26.1	1.7	49.5	28.9
RhusT	Fruit	C3	37	NMC	5933	1		1.685	-3.1	-26.4	1.7	53.9	30.8

Table A.2: Fauna assay data. ID number, taxon, isotope ratios and elemental concentrations

Sample ID	Species	$\delta^{13}C$	$\delta^{15}N$	Wt%N	Wt%C	C:N ratio	Atomic C:N
3223	medium artiodactyl	-16.2	5.1	16.0	43.9	2.7	3.2
3224	medium artiodactyl	-19.1	2.9	15.5	42.6	2.7	3.2
3225	Sylvilagus	-18.7	3.9	15.4	42.8	2.8	3.2
3226	Sylvilagus	-20.3	2.5	15.4	43.2	2.8	3.3
3227	Lepus	-14.4	5.8	15.8	43.4	2.7	3.2
3228	Sylvilagus	-20.2	2.3	15.1	42.5	2.8	3.3
3230	Ovis canadensis	-15.0	5.4	15.1	41.8	2.8	3.2
3231	Canis	-15.5	7.6	15.6	43.2	2.8	3.2
3232	Sylvilagus	-20.6	3.3	14.8	41.7	2.8	3.3
3233	Ovis canadensis	-15.1	5.2	15.5	42.9	2.8	3.2
3234	Meleagris gallopavo	-9.7	5.5	13.4	37.5	2.8	3.3
3235	medium artiodactyl	-17.9	2.9	15.1	41.8	2.8	3.2
3236	Ovis canadensis	-17.8	5.4	14.9	41.5	2.8	3.2
3237	Ovis canadensis	-14.4	5.3	14.8	41.3	2.8	3.3
3238	Ovis canadensis	-17.5	4.2	15.4	42.5	2.8	3.2
3239	Ovis canadensis	-15.1	4.9	15.4	42.6	2.8	3.2
3240	Ovis canadensis	-15.5	5.1	15.5	42.9	2.8	3.2
3241	Ovis canadensis	-16.5	4.0	15.8	43.6	2.7	3.2
3242	Ovis canadensis	-17.5	4.3	15.4	42.7	2.8	3.2
3243	Ovis canadensis	-16.9	3.9	15.4	42.5	2.8	3.2
3244	Ovis canadensis	-15.2	5.1	15.5	42.7	2.8	3.2
3245	Ovis canadensis	-17.4	5.2	15.8	43.6	2.8	3.2
3246	Ovis canadensis	-17.2	4.0	14.5	40.4	2.8	3.2
3247	Sylvilagus	-20.2	3.3	14.8	41.1	2.8	3.2
3248	Sylvilagus	-19.4	3.6	15.7	43.4	2.8	3.2
3249	Sylvilagus	-20.0	3.2	14.4	39.8	2.8	3.2
3250	Sylvilagus	-20.9	4.4	14.1	39.2	2.8	3.2
3251	Sylvilagus	-21.0	2.5	15.0	41.8	2.8	3.3
3252	Sylvilagus	-18.2	3.5	15.1	42.7	2.8	3.3
3253	Lepus	-17.2	6.8	14.9	41.6	2.8	3.3
3254	Sylvilagus	-20.0	3.7	15.2	42.3	2.8	3.2
3255	Sylvilagus	-19.5	3.8	15.3	42.5	2.8	3.2
3256	Sylvilagus	-19.4	3.6	15.0	41.2	2.7	3.2
3257	Sylvilagus	-18.0	3.9	13.8	38.3	2.8	3.2
3258	Cynomys	-18.3	3.6	15.2	41.1	2.7	3.2
3259	Cynomys	-19.2	5.8	14.5	40.4	2.8	3.3
3260	Cynomys	-18.3	3.8	15.0	41.3	2.7	3.2
3261	Ovis canadensis	-19.4	3.6	14.5	40.3	2.8	3.2
3262	Meleagris gallopavo	-7.8	5.6	15.4	42.7	2.8	3.2
3263	Meleagris gallopavo	-8.4	6.7	14.9	41.2	2.8	3.2
3264	Meleagris gallopavo	-7.9	6.5	14.8	40.9	2.8	3.2
3265	Meleagris gallopavo	-7.5	6.2	15.3	42.2	2.8	3.2
3266	Meleagris gallopavo	-7.7	6.3	15.5	42.6	2.8	3.2
3229	Sylvilagus	-20.2	3.8	3.5	11.8	3.4	3.9

Table A.3: Yucca sample stable isotope assay data: Tissue Sampled, Specimen ID, Elevation, Sample Site (see Table 3.3), weight of sample, isotope ratios and elemental concentrations

Tissue	ID	Elev.	Site	Weight	$\delta^{15}N$	$\delta^{13}C$	Wt % N	Wt % C	C:N
Seed	1	5324	THR	1.752	-0.2	-14.7	1.9	51.9	27.9
Seed	2	5730	THR	1.614	-1.8	-14.4	2.1	54	25.4
Seed	3	5730	THR	1.738	-1.8	-16	2.5	52	20.8
Seed	4	5725	THR	0.819	1	-14	2.5	56.6	22.9
Seed	6	5728	THR	1.668	-0.8	-14.9	2.5	54.1	21.9
Seed	7	5732	THR	1.757	-2.8	-14.8	2.2	54.4	24.3
Seed	8	5957	THR	0.902	0.2	-15.9	2.2	57.8	26.3
Seed	10	5961	THR	1.787	-1	-14.5	2.7	52.5	19.7
Seed	11	5965	THR	0.836	-0.7	-14.1	3.3	60	18.1
Seed	12	5893	THR	1.122	0.2	-14.5	3	56.3	18.7
Seed	14	5929	THR	0.736	1.5	-14.3	3.1	60.1	19.7
Seed	15	5929	THR	1.711	0	-14.7	2.7	58	21.4
Seed	16	5959	SK	1.686	1.8	-14.4	2.2	50.2	22.7
Seed	17	7014	SK	0.788	1	-13.7	2.8	54.5	19.6
Seed	18	6677	SK	1.673	-2	-14.4	2.5	55.3	22.5
Seed	20	6584	SK	1.7	-0.1	-14.2	2.6	54.2	20.6
Seed	21	6489	SK	1.639	0.6	-13.5	3.2	59.4	18.5
Seed	22	6038	SK	0.866	1.7	-15.6	2.2	54	24.1
Seed	24	6276	SFR	1.629	-0.6	-13.5	3	55.2	18.7
Seed	25	6182	SFR	0.832	1.2	-14.7	2.1	44.2	20.9
Seed	26	6193	SFR	1.628	-1.5	-13.9	3.5	55.4	16
Seed	29	6076	SFR	0.889	0.4	-14.1	2.6	55.8	21.7
Seed	30	6463	CSR						
Seed	32	6093	CSR	0.803	2.9	-14.5	1.7	48.8	29.1
Fruit	1	5324	THR	2.242	-0.4	-13.4	0.5	42.4	81.7
Fruit	2	5730	THR	2.706	-4.8	-14.6	0.3	41.7	157
Fruit	3	5730	THR	2.757	-2.5	-14.4	1.8	43.7	24.4
Fruit	4	5725	THR	2.486	-3.2	-13.9	0.9	42.1	45.4
Fruit	6	5728	THR	2.342	-4.9	-14.2	0.3	42.5	167.8
Fruit	7	5732	THR	2.479	-6.2	-13.3	0.2	42.5	186.4
Fruit	8	5957	THR	2.572	-1.3	-14.6	0.6	43.7	74.9
Fruit	10	5961	THR	1.842	-0.8	-15.4	1.5	41.6	28.4
Fruit	11	5965	THR	1.809	-0.5	-15	0.6	40.2	63.3
Fruit	12	5893	THR	1.959	0.5	-14.7	0.9	42.4	47.7
Fruit	14	5929	THR	1.699	-1.6	-14	1.4	83.4	58.1
Fruit	15	5929	THR	2.3	0.1	-14.6	1.2	43.3	35.1
Fruit	16	5959	SK	2.572	-1.3	-14.6	0.6	43.7	74.9
Fruit	17	7014	SK	2.573	-3	-14	0.5	43.8	93.3
Fruit	18	6677	SK	1.961	-0.3	-14.8	0.5	42.8	83
Fruit	20	6584	SK	1.791	0	-14.4	1.3	42.5	31.5
Fruit	21	6489	SK	2.294	-2	-13.6	0.7	43.6	65.9
Fruit	22	6038	SK	2.256	-1.1	-17.5	0.6	43	66.5
Fruit	24	6276	SFR	1.744	-0.9	-14.3	1.4	47.1	33.1
Fruit	25	6182	SFR	2.435	-3.3	-15.2	0.4	43.1	102.5
Fruit	26	6193	SFR	2.462	-5	-14.1	0.4	44.2	112.6
Fruit	29	6076	SFR	2.322	-3.4	-15.7	0.4	42.1	116.7
Fruit	30	6463	CSR	1.79	1.1	-14.9	1.2	46.6	39.1
Fruit	32	6093	CSR	2.431	-2.7	-14.9	0.3	42.3	146.2
Raw Stem	1	5324	THR	2.436	-0.4	-14.2	2.6	43.6	16.9
Raw Stem	2	5730	THR	2.001	-1.5	-14.3	1.3	44.1	33.6
Raw Stem	3	5730	THR	1.71	-0.8	-16.2	1.2	43.6	35
Raw Stem	4	5725	THR	2.145	3.7	-14.6	0.4	37.9	89.9
Raw Stem	6	5728	THR	2.006	0.1	-15.7	0.6	38.6	61.4

Table A.3: continued

Tissue	ID	Elev.	Site	Weight	δ^{15}N	δ^{13}C	Wt % N	Wt % C	C:N
Raw Stem	7	5732	THR	1.88	3.1	-14.6	0.4	36.5	100.1
Raw Stem	8	5957	THR	1.807	3.9	-16.5	0.4	39.9	93.7
Raw Stem	10	5961	THR	1.776	1.7	-14.7	0.8	42.1	53.8
Raw Stem	11	5965	THR	1.908	-0.2	-13.7	1	38.8	37.5
Raw Stem	12	5893	THR	2.101	-1.2	-14.8	1.1	45.2	41.3
Raw Stem	14	5929	THR	2.39	-0.4	-15.3	0.9	45.7	52.9
Raw Stem	15	5929	THR	1.748	4.6	-14.2	0.5	42.5	90.4
Raw Stem	16	5959	SK	1.901	2.4	-14.2	1.2	38.8	33.1
Raw Stem	17	7014	SK	2.39	3.9	-12.6	0.5	42.1	88.6
Raw Stem	18	6677	SK	1.958	-1.8	-14.9	1.9	43.8	23.3
Raw Stem	20	6584	SK	2.014	6.6	-12.9	0.4	41.9	113.5
Raw Stem	21	6489	SK	1.873	2.3	-14.6	0.7	43	61.4
Raw Stem	22	6038	SK	2.233	0.6	-15.5	0.9	44.1	47.1
Raw Stem	24	6276	SFR	2.062	-0.2	-13.7	1.1	46.1	40.3
Raw Stem	25	6182	SFR	1.909	9	-14.4	0.3	41.8	124.1
Raw Stem	26	6193	SFR	2.029	0.5	-14	0.6	44	70.7
Raw Stem	29	6076	SFR	1.705	3.6	-14.4	0.5	45	96.4
Raw Stem	30	6463	CSR	2.284	2.5	-14.6	1.4	44.8	32.7
Raw Stem	32	6093	CSR	2.014	11.5	-13.3	0.2	38.9	180.9
Roasted Stem	1	5324	THR	2.475	-0.2	-14	1.5	43.4	28
Roasted Stem	2	5730	THR	2.075	-3.1	-14.1	1.4	42.9	31.4
Roasted Stem	3	5730	THR	2.346	-1.6	-15.3	0.9	44.5	49.8
Roasted Stem	4	5725	THR	2.331	-1.1	-13.8	1	42.8	44.7
Roasted Stem	6	5728	THR	2.342	-2.9	-14.8	1.2	44.2	38.1
Roasted Stem	7	5732	THR	2.211	-5.2	-14.3	0.6	40.8	66.5
Roasted Stem	8	5957	THR	2.529	-4.4	-15.6	0.4	38.3	101
Roasted Stem	10	5961	THR	1.953	-1	-14.1	1.2	42.1	35.9
Roasted Stem	11	5965	THR	2.1	-1.5	-14.2	1.2	40.3	33.8
Roasted Stem	12	5893	THR	2.427	-4.8	-14.5	0.5	43.6	87.6
Roasted Stem	14	5929	THR	2.654	-2.6	-14.9	0.6	45.7	80.5
Roasted Stem	15	5929	THR	2.54	-1.1	-14.3	0.7	43.9	66.2
Roasted Stem	16	5959	SK	1.753	1.9	-13.7	1.7	42	24.2
Roasted Stem	17	7014	SK	2.167	-0.7	-13.1	1	47.3	45.1
Roasted Stem	18	6677	SK	2.672	-3	-14.9	1.7	44.5	26.9
Roasted Stem	20	6584	SK	2.591	-1.6	-13.2	0.8	40.1	50
Roasted Stem	21	6489	SK	1.825	1.3	-13.6	0.8	42.6	55.8
Roasted Stem	22	6038	SK	1.944	-0.2	-15	1	40.8	42.1
Roasted Stem	24	6276	SFR	2.444	-0.6	-12.7	1.2	42.4	35
Roasted Stem	25	6182	SFR	2.303	-3.4	-14.9	0.5	39.5	87.3
Roasted Stem	26	6193	SFR	1.827	-1.4	-13.5	0.8	41.8	50.4
Roasted Stem	29	6076	SFR	2.446	-4.6	-14.5	0.5	43.5	83.4
Roasted Stem	30	6463	CSR	1.847	1.5	-14.2	1.4	41.4	29
Roasted Stem	32	6093	CSR	2.431	-1.3	-14	0.4	42.9	113.2
Fiber	1	5324	THR	1.648	-1.3	-14.1	1.4	41.6	30.1
Fiber	2	5730	THR	1.792	-3.7	-14	1.5	43.2	28.8
Fiber	3	5730	THR	1.602	-2.9	-14	1	39.5	38.4
Fiber	4	5725	THR	1.589	-2.7	-12.9	1.4	39.2	27.5
Fiber	6	5728	THR	1.774	-3.4	-14.6	0.8	41.5	53
Fiber	7	5732	THR	1.724	-5.7	-13.9	0.6	36.9	61.4
Fiber	8	5957	THR	1.716	-2.1	-15.9	0.5	39.4	74.6
Fiber	10	5961	THR	1.734	-3	-13.6	1.3	38.2	29.7
Fiber	11	5965	THR	1.799	-3.1	-14.4	1.2	40	33.2
Fiber	12	5893	THR	1.648	-3.1	-13.9	0.7	39.7	56.3
Fiber	14	5929	THR	1.714	-2.4	-14.7	0.9	43.9	50.5
Fiber	15	5929	THR	1.628	-3.5	-14.5	0.9	41.9	48.4

Table A.3: continued

Tissue	ID	Elev.	Site	Weight	δ^{15}N	δ^{13}C	Wt % N	Wt % C	C:N
Fiber	16	5959	SK	1.701	-0.2	-13.9	1.2	40	32.3
Fiber	17	7014	SK	1.707	-1.7	-13.5	0.8	42.1	53.7
Fiber	18	6677	SK	1.692	-3.4	-14.8	1.3	43.8	34.4
Fiber	20	6584	SK	1.656	-1.4	-13.3	1	40.9	43
Fiber	21	6489	SK	1.712	-2.1	-13.7	0.9	41	45.9
Fiber	22	6038	SK	1.773	-1.8	-14.9	1.1	41.6	37.5
Fiber	24	6276	SFR	1.755	-2.5	-13.6	1.3	43.9	33.9
Fiber	25	6182	SFR	1.725	-2.6	-15	0.8	40.5	52.4
Fiber	26	6193	SFR	1.758	-3.7	-13.9	1	41.7	43.7
Fiber	29	6076	SFR	1.651	-3.6	-14.6	0.8	43.1	51.4
Fiber	30	6463	CSR	1.751	-0.5	-13.7	1	39.6	41
Fiber	32	6093	CSR	1.699	-2.9	-14.2	0.6	41.4	64.8
Non-Fiber	1	5324	THR	1.942	0.2	-14.5	1.8	42.1	23.4
Non-Fiber	2	5730	THR	1.888	-1.7	-14.1	1.2	44.2	37
Non-Fiber	3	5730	THR	1.775	1.1	-13.3	1.1	42.6	37.1
Non-Fiber	4	5725	THR	2.224	0.1	-14.1	1.4	40.7	30
Non-Fiber	6	5728	THR	2.024	-0.6	-14.7	1	43.2	43.8
Non-Fiber	7	5732	THR	2.418	-0.7	-13.9	0.6	41.5	71.9
Non-Fiber	8	5957	THR	1.806	5.3	-15.3	0.3	41.6	123
Non-Fiber	10	5961	THR	2.06	-0.3	-13.6	1.1	41.7	38.1
Non-Fiber	11	5965	THR	1.756	66.3	-13.8	1.5	39.3	26.1
Non-Fiber	12	5893	THR	2.369	0.9	-14	0.4	43.6	104.6
Non-Fiber	14	5929	THR	2.001	15.7	-15	0.6	46.7	82.9
Non-Fiber	15	5929	THR	2.112	0.9	-14.6	0.6	43.1	67.3
Non-Fiber	16	5959	SK	2.048	2.1	-14.1	1.9	39.7	20.9
Non-Fiber	17	7014	SK	2.073	2.4	-13.2	0.5	41.4	76.6
Non-Fiber	18	6677	SK	1.894	-2.2	-14.7	1.9	44.9	24.2
Non-Fiber	20	6584	SK	2.023	2.2	-13.1	0.8	39.9	50.8
Non-Fiber	21	6489	SK	1.897	2.6	-13.4	0.8	40.5	52.6
Non-Fiber	22	6038	SK	1.933	-1.8	-14.1	0.9	42.5	44.9
Non-Fiber	24	6276	SFR	2.06	0.2	-12.4	1.5	41.7	28.1
Non-Fiber	25	6182	SFR	1.878	5.5	-15.2	0.5	42.7	90.8
Non-Fiber	26	6193	SFR	2.139	0.1	-13.2	0.8	44.8	56.1
Non-Fiber	29	6076	SFR	2.041	1.2	-14.7	0.5	43.8	91.6
Non-Fiber	30	6463	CSR	2.094	1.8	-14.6	2	43.8	22.1
Non-Fiber	32	6093	CSR	1.957	8.7	-13	0.3	43.4	155.2

Table A.4: Location data for all sample sites. Note that Yucca samples are individually located.

Site ID	Elev	mE	mN	Site	Species
AC-1	4864	617572	4156815	Arch Canyon 1	Typh
AC-2	4981	616882	4156456	Arch canyon	Typh
BC	5466	586914	4143505	Bullet Canyon	CleoS
BWR	4892	621180	4150670	Butler Wash Road	MentM OryzH
CWC	4880	618695	4151631	Comb Camp	MentM
CW-95	4542	616165	4138718	Comb Wash U95	RhusT
FCC	4611	616165	4138718	Fish Canyon Canyon	CleoS
FCD	4542	616165	4138718	Fish Canyon Dunes	CleoS OryzH MentM
FMC-1	4742	620900	4143158	Fish Mouth Canyon	AmarR AtriC
FMC-2	4850	620717	4143180	Butler Wash Fish Mouth Cyn	RhusT
FMC-3	4932	620717	4143180	Butler Wash Fish Mouth Cyn 2	OpunSp
MCC	6045	612118	4155467	Mule Canyon Corral	OpunSp OryzH
NMC	5933	612011	4156292	Mule Canyon North Mule	RhusT
PS	6611	605676	4156847	Pine Springs	Typh
SC	5505	586509	4145515	Sheiks Canyon	CleoS
CSR-1	6516	593485	4139307	Cigarette Springs Road	AtriC
SFR-1	6512	595304	4144353	Snow Flat Road	AtriC
SFR-2	6276	602306	4143722	Snow Flat Road	YuccB-24
SFR-2	6182	602956	4143583	Snow Flat Road	YuccB-25
SFR-2	6193	602909	4143597	Snow Flat Road	YuccB-26
SFR-2	6193	602909	4143597	Snow Flat Road	YuccB-27
SFR-2	6076	603883	4142898	Snow Flat Road	YuccB-28
SFR-2	6076	603883	4142898	Snow Flat Road	YuccB-29
CSR-2	6463	598788	4158465	Cigarette Springs Road	YuccB-30
CSR-2	6463	598788	4158465	Cigarette Springs Road	YuccB-31
CSR-2	6093	602399	4137870	Cigarette Springs Road	YuccB-32
CSR-2	6093	602399	4137870	Cigarette Springs Road	YuccB-33
SK	5959	612165	4155267	Salvation Knoll	YuccB-16
SK	7014	604783	4155771	Salvation Knoll	YuccB-17
SK	6677	605352	4156261	Salvation Knoll	YuccB-18
SK	6677	605352	4156261	Salvation Knoll	YuccB-19
SK	6584	606542	4156372	Salvation Knoll	YuccB-20
SK	6489	607839	4156182	Salvation Knoll	YuccB-21
SK	6038	612282	4155272	Salvation Knoll	YuccB-22
SK	6036	612282	4155297	Salvation Knoll	YuccB-23
SMC-1	5877	611969	4155284	South Mule Canyon	AmarR
SMC-2	5940	610838	4155997	Mule Canyon House on Fire	OryzH RhusT
TOH-1	5766	620472	4159949	Tower House Road	MentM
THO-2	5638	621343	4159634	Comb Ridge Road to Ridge	OryzH
TOH-3	5831	618688	4158395	Comb Ridge Tower House	OpunSp
TOH-3	5324	622118	4159688	Tower House Road	YuccB-1
TOH-3	5730	620955	4159402	Tower House Road	YuccB-2

Table A.4: continued

Site ID	Elev	mE	mN	Site	Species
TOH-3	5730	620963	4159369	Tower House Road	YuccB-3
TOH-3	5725	621002	4159334	Tower House Road	YuccB-4
TOH-3	5727	620969	4159330	Tower House Road	YuccB-5
TOH-3	5728	620957	4159314	Tower House Road	YuccB-6
TOH-3	5732	620918	4159332	Tower House Road	YuccB-7
TOH-3	5957	618451	4159917	Tower House Road	YuccB-8
TOH-3	5957	618451	4159917	Tower House Road	YuccB-9
TOH-3	5961	618480	4159899	Tower House Road	YuccB-10
TOH-3	5965	618488	4159880	Tower House Road	YuccB-11
TOH-3	5893	618669	4158392	Tower House Road	YuccB-12
TOH-3	5893	618669	4158392	Tower House Road	YuccB-13
TOH-3	5929	618795	4159161	Tower House Road	YuccB-14
TOH-3	5929	618795	4159161	Tower House Road	YuccB-15
US-95	6777	607345	4157278	Helianthus U-95	HeliA
US-B	5298	625092	4158258	Blanding U-95	HeliA
US-B	5456	627280	4158404	Blanding U-95	HeliA
US-B	5235	626457	4157697	Blanding U-95	HeliA

REFERENCES

Aasen, D. K. 1984. "Pollen, Macrofossil, and Charcoal Analyses of Basketmaker Coprolites from Turkey Pen Ruin, Cedar Mesa, Utah." PhD thesis, Washington State University.

Adams, J. L. 1999. "Refocusing the Role of Food-grinding Tools as Correlates for Subsistence Strategies in the US Southwest." *American Antiquity* 64 (3): 475–498.

— . 2014. *Ground Stone Analysis: A Technological Approach*. Salt Lake City: University of Utah Press.

Adams, K. R., and S. S. Murray. 2008. "Animas-La Plata Project: Environmental Studies." Chap. Archaeobotanical Results, ed. by J. M. Potter, vol. 10. X. Phoenix: SWCA Environmental Consultants.

Adams, K. R., and K. L. Petersen. 1999. "Colorado Prehistory: A Context for the Southern Colorado River Basin." Chap. 2: Enviroment, ed. by W. D. Lipe, M. D. Varien, and R. H. Wilshusen, 14–50. Denver: Colorado Council of Professional Archaeologists.

Altschul, J. H., and E. K. Huber. 2000. "Foundations of Anasazi Culture: The Basketmaker-Pueblo Transition." Chap. Economics, Site Structure, and Social Organization During the Basketmaker III Period, ed. by P. Reed, 145–160. Salt Lake City: University of Utah Press.

Ambrose, S. H., and L. Norr. 1993. "Prehistoric Human Bone." Chap. Experimental Evidence for the Relationship of the Carbon Isotope Ratios of Whole Diet and Dietary Protein to those of Bone Collagen and Carbonate, 1–37. Berlin: Springer.

Amundson, R., A. T. Austin, E. A. Schuur, K. Yoo, V. Matzek, C. Kendall, A. Uebersax, D Brenner, and W. T. Baisden. 2003. "Global Patterns of the Isotopic Composition of Soil and Plant Nitrogen." *Global Biogeochemical Cycles* 17 (1).

Androy, J. 2003. "Agriculture and Mobility in the Basketmaker II Period: The Coprolite Evidence." MA thesis, Northern Arizona University.

Arneson, L. S., and S. E. MacAvoy. 2005. "Carbon, Nitrogen, and Sulfur Diet-Tissue Discrimination in Mouse Tissues." *Canadian Journal of Zoology* 83 (7): 989–995.

Atkins, V. M., and L. McClanahan, eds. 1990. *Anasazi Basketmaker: Papers from the 1990 Wetherill-Grand Gulch Symposium*. Salt Lake City: Cultural Resource Series No. 24, Bureau of Land Management.

Badenhorst, S., and J. C. Driver. 2009. "Faunal Changes in Farming Communities from Basketmaker II to Pueblo III (AD 1–1300) in the San Juan Basin of the American Southwest." *Journal of Archaeological Science* 36 (9): 1832–1841.

Battillo, J. M. 2017. "Supplementing Maize Agriculture in Basketmaker II Subsistence: Dietary Analysis of Human Paleofeces from Turkey Pen Ruin (42SA3714)." PhD thesis, Southern Methodist University.

Bell, W. H., and E. F. Castetter. 1941. *The Utilization of Yucca, Sotol, and Beargrass by the Aborigines in the American Southwest: Ethnobotanical Studies in the American Southwest VII*. Vol. 5. New Mexico University Biological Series Bulletin 5. Albuquerque: The University of New Mexico.

Bellorado, B. A. 2009. "Animas La Plata Project: Special Studies." Chap. A Reconstruction of Prehistoric Subsistence Agriculture in Ridges Basin, 215–234. SWCA Environmental Consultants.

— . 2011. "Pushing the Limits and Tormenting Corn Seeds: Cultural Adaptations and Climatic Change in the Upper San Juan During the Basketmaker II Period and Beyond." *Southwestern Lore* 77:33–47.

Bellorado, B. A., and K. C. Anderson. 2013. "Early Pueblo Responses to Climate Variability: Farming Traditions, Land Tenure, and Social Power in the Eastern Mesa Verde Region." *Kiva* 78 (4): 377–416.

Bellwood, P. S., and M. Oxenham. 2011. "The Neolithic Demographic Transition and its Consequences." Chap. The Expansions of Farming Societies and the Role of the Neolithic Demographic Transition, ed. by J.-P. Bocquet-Appel and O. Bar-Yosef. Dordrecht: Springer.

Bellwood, P. S., and C. Renfrew, eds. 2002. *Examining the Farming / Language Dispersal Hypothesis*. Oxbow Books Oxford: McDonald Institute for Archaeological Research.

Belnap, J. 2002. "Nitrogen Fixation in Biological Soil Crusts from Southeast Utah, USA." *Biology and Fertility of Soils* 35 (2): 128–135.

Belnap, J., R. Prasse, and K. Harper. 2001. "Biological Soil Crusts: Structure, Function, and Management." Chap. Influence of Biological Soil Crusts on Soil Environments and Vascular Plants, 281–300. Berlin, Heidelberg: Springer.

Belnap, J., J. Williams, and J. Kaltenecker. 1999. "Structure and Function of Biological Soil Crusts." *UNITED STATES DEPARTMENT OF AGRICULTURE FOREST SERVICE GENERAL TECHNICAL REPORT PNW*: 161–178.

Benson, L. V. 2011. "Factors Controlling Pre-Columbian and Early Historic Maize Productivity in the American Southwest, Part 1: The Southern Colorado Plateau and Rio Grande Regions." *Journal of Archaeological Method and Theory* 18 (1): 1–60.

Benson, L. V., and M. S. Berry. 2009. "Climate Change and Cultural Response in the Prehistoric American Southwest." *Kiva* 75 (1): 87–117.

Benson, L. V., D. Ramsey, D. W. Stahle, and K. L. Petersen. 2013. "Some Thoughts on the Factors that Controlled Prehistoric Maize Production in the American Southwest with Application to Southwestern Colorado." *Journal of Archaeological Science* 40 (7): 2869–2880.

Bernstein, E. J., C. M. Albano, T. D. Sisk, T. E. Crews, and S. Rosenstock. 2014. "Establishing Cool-Season Grasses on a Degraded Arid Rangeland of the Colorado Plateau." *Restoration Ecology* 22 (1): 57–64.

Berry, C. F., and M. S. Berry. 1986. "Anthropology of the Desert West: Essays in Honor of Jesse D Jennings." Chap. Chronological and Conceptual Models of the Southwestern Archaic, ed. by C. J. Condie and D. D. Fowler. Antrhopological Papers no 110. Salt Lake City: University Of Utah Press.

Berry, M. S. 1982. *Time, Space, and Transition in Anasazi Prehistory*. Salt Lake City: University of Utah Press.

Betancourt, J. L. 1984. "Late Quaternary Plant Zonation and Climate in Southeastern Utah." *The Great Basin Naturalist*: 1–35.

Binford, L. R. 1980. "Willow Smoke and Dog's Tails: Hunter-gatherer Settlement Systems and Archaeological Site Formation." *American Antiquity* 45 (1): 4–20.

Blackburn, F. M., and R. A. Williamson. 1997. *Cowboys and Cave Dwellers: Basketmaker Archaeology in Utah's Grand Gulch*. Santa Fe: School of American Research Press.

Blaxter, K. L., and J. A. F. Rook. 1953. "The Heat of Combustion of the Tissues of Cattle in Relation to their Chemical Composition." *Brit. J. Nutrition* 7:83–91.

Bocinsky, R. K., B. S. Chisholm, and B. M. Kemp. 2011. "Basketmaker III Turkey Use: Multiple Lines of Evidence." In *76th Annual Meeting of the Society for American Archaeology*. Paper presented at. Sacramento, CA.

Bocinsky, R. K. 2011. "Is a Bird in Hand Really Worth Two in the Bush?: Models of Turkey Domestication on the Colorado Plateau." PhD thesis, Washington State University.

Bocquet-Appel, J.-P. 2002. "Paleoanthropological Traces of a Neolithic Demographic Transition." *Current Anthropology* 43 (4): 637–650.

Bowling, D. R., D. E. Pataki, and J. T. Randerson. 2008. "Carbon Isotopes in Terrestrial Ecosystem Pools and CO2 fluxes." *New Phytologist* 178 (1): 24–40.

Brand, M. 1994. "Prehistoric Anasazi Diet: A Synthesis of Archaeological Evidence." PhD thesis, University of British Columbia.

Brandt, C. 2002. "Archaeological Investigations in the Fruitland Project Area: Late Archaic, Basketmaker, Pueblo I, and Navajo Sites in Northwestern New Mexico." Chap. Macrobotanical Remains. Dolores: La Plata Archaeological Consultants.

Brenner, C. J., S. Boomgarden, and M. D. Lewis. 2014. *The Isotope Chemistry of Range Creek Maize – Experimental Gardening and Maize 13C and 15N'*. Paper presented at the 34th Great Basin Anthropological Conference, Boise 2014.

Brown, S. 2013. "How big a sample do I need?" `http://www.tc3.edu/instruct/sbrown/stat/sampsiz.htm` accessed June 1, 2013.

Burrillo, R. 2015. "Beans, Baskets, and Basketmakers Testing the Assumption that Ceramics were Necessary for the Adoption of Bean Cultivation on the Prehistoric Colorado Plateau." *Journal of Anthropology and Archaeology* 3 (1): 1–22.

Burrillo, R., J. B. Coltrain, and M. D. Lewis. 2015. *$\delta^{18}O$ Variability in Water Sources on the Colorado Plateau: Preliminaries to Stable Isotope Models of Prehistoric Irrigation*. Poster presented at the Global Change and Sustainability Center Research Symposium. Salt Lake City, UT.

Carlson, B. A., and J. D. Kingston. 2014. "Chimpanzee Isotopic Ecology: A Closed Canopy C3 Template for Hominin Dietary Reconstruction." *Journal of Human Evolution* 76:107–115.

Castetter, E. 1935. *Uncultivated Native Plants Used as Foods-Ethnobotanical Studies in the American Southwest*. Vol. 4. New Mexico University Biological Series Bulletin 1. Albuquerque.

Caut, S., E. Angulo, and F. Courchamp. 2009. "Variation in Discrimination Factors ($\Delta^{15}N$ and $\Delta^{13}C$): The Effect of Diet Isotopic Values and Applications for Diet Reconstruction." *Journal of Applied Ecology* 46 (2): 443–453.

Charles, M. C., and S. J. Cole. 2006. "Chronology and Cultural Variation in Basketmaker II." *Kiva* 72 (2): 167–216.

Charles, M. C., L. M. Sesler, and T. D. Hovezak. 2006. "Understanding Eastern Basketmaker II Chronology and Migrations." *Kiva* 72 (2): 217–238.

Chisholm, B., and R. G. Matson. 1994. "Carbon and Nitrogen Isotopic Evidence on Basketmaker II Diet at Cedar Mesa, Utah." *Kiva* 60 (2): 239–255.

Cleland, T. P., K. Voegele, and M. H. Schweitzer. 2012. "Empirical Evaluation of Bone Extraction Protocols." *PLoS One* 7 (2): e31443.

Cole, S. J. 1994. "Roots of Anasazi and Pueblo Imagery in Basketmaker II Rock Art and Material Culture." *Kiva* 60 (2): 289–311.

Cole, S. J., and J. Moe. 2001. "Final Report of the BLM-Earthwatch Utah Canyons Rock Art Project and the Mill Creek Archaeological Project 1993–1999." Draft on file at the Bureau of Land Utah State Offices Salt Lake City.

Colton, H. S. 1939. "Prehistoric Culture Units and their Relationships in Northern Arizona." *Northern Arizona Society of Science and Art* 17.

Coltrain, J. B. 1996. "The Steinaker Gap Burials and their Implications for Farming Along the Basin/Plateau Rim: A Stable Carbon and Radio-Isotope Study." *Steinaker Gap: An Early Fremont Agriculture Farmstead. Museum of Peoples and Cultures Technical Series* 94:18.

Coltrain, J. B., and J. C. Janetski. 2013. "The Stable- and Radio-isotope Chemistry of Southeastern Utah Basketmaker II Burials: Dietary Analysis Using the Linear Mixing Model SISUS, Age and Sex Patterning, Geolocation and Temporal Patterning." *Journal of Archaeological Science* 40 (12): 4711–4730.

Coltrain, J. B., J. C. Janetski, and S. W. Carlyle. 2006. "The Stable- and Radio-isotope Chemistry of Eastern Basketmaker and Pueblo Groups in the Four Corners Region of the American Southwest: Implications for Anasazi Diets, Origins, and Abandonments in Southwestern Colorado." *Histories of Maize: Multidisciplinary Approaches to the Prehistory, Linguistics, Biogeography, Domestication, and Evolution of Maize*: 275–287.

— . 2007. "The Stable- and Radio-isotope Chemistry of Western Basketmaker Burials: Implications for Early Puebloan Diets and Origins." *American Antiquity* 72 (2): 301–321.

Coltrain, J. B., J. C. Janetski, and M. D. Lewis. 2012. "A Reassessment of Basketmaker II Cave 7: Massacre Site or Cemetery Context." *Journal of Archaeological Science* 39 (7): 2220–2230.

Coltrain, J. B., and S. W. Leavitt. 2002. "Climate and Diet in Fremont Prehistory: Economic Variability and Abandonment of Maize Agriculture in the Great Salt Lake Basin." *American Antiquity* 67 (3): 453–485.

Coltrain, J. B., and T. W. Stafford Jr. 1999. "Prehistoric Lifeways in the Great Basin Wetlands." Chap. Stable Carbon Isotopes and Salt Lake Wetlands Diet: Towards an Understanding of the Great Basin Formative, ed. by B. E. Hemphill and C. S. Larsen, 55–83. Salt Lake City: University Of Utah Press.

Comstock, J. P., and J. R. Ehleringer. 1992. "Plant Adaptation in the Great Basin and Colorado Plateau." *The Great Basin Naturalist*: 195–215.

Cooper, C., K. Lupo, R. Matson, W. Lipe, C. Smith, and M. Richards. 2016. "Short-term Variability of Human Diet at Basketmaker II Turkey Pen Ruins, Utah: Insights from Bulk and Single Amino Acid Isotope Analysis of Hair." *Journal of Archaeological Science: Reports* 5:10–18.

Criss, R. E. 1999. *Principles of Stable Isotope Distribution*. Oxford: Oxford University Press.

Crown, P. L., ed. 2000. *Women and Men in the Prehispanic Southwest*. Santa Fe: School of American Research Press.

Crown, P. L., and W. H. Wills. 1995. "The Origins of Southwestern Ceramic Containers: Women's Time Allocation and Economic Intensification." *Journal of Anthropological Research* 51 (2): 173–186.

Dalerum, F., and A. Angerbjörn. 2005. "Resolving Temporal Variation in Vertebrate Diets Using Naturally Occurring Stable Isotopes." *Oecologia* 144 (4): 647–658.

Dalley, G. F. 1973. *Highway U-95 Archeology: Comb Wash to Grand Flat Volume I. Technical Report*. Salt Lake City: University of Utah Department of Anthropology.

Danielson, D., and K. Reinhard. 1998. "Human Dental Microwear Caused by Calcium Oxalate Phytoliths in Prehistoric Diet of the Lower Pecos Region, Texas." *Karl Reinhard Papers/Publications. 24. American Journal of Physical Anthropology* 107:297–304.

Dawson, T. E., S. Mambelli, A. H. Plamboeck, P. H. Templer, and K. P. Tu. 2002. "Stable Isotopes in Plant Ecology." *Annual Review of Ecology and Systematics* 33 (1): 507–559.

Decker, K. W., and L. L. Tieszen. 1989. "Isotopic Reconstruction of Mesa Verde Diet from Basketmaker III to Pueblo III." *Kiva* 55 (1): 33–47.

DeNiro, M. J., and S. Epstein. 1978. "Influence of Diet on the Distribution of Carbon Isotopes in Animals." *Geochimica et Cosmochimica Acta* 42 (5): 495–506.

Doleman, W. 2005. "The Late Archaic Across the Borderlands: From Foraging to Farming." Chap. Environmental Constraints on Forager Mobility and the Use of Cultigens in Southeastern Arizona and Southern New Mexico, ed. by B. Vierra, 113–140. Austin: University of Texas Press.

Eddy, F. W. 1966. *Prehistory in the Navajo Reservoir District*. Vol. Museum of New Mexico Papers in Anthropology (no. 15). Santa Fe: Museum of New Mexico Press.

— . 1972. "Culture Ecology and the Prehistory of the Navajo Reservoir District." *Southwestern Lore* 38 (1): 1–75.

Ehleringer, J. R. 1995. "Ecophysiology of Photosynthesis." Chap. Variation in Gas Exchange Characteristics Among Desert Plants, 361–392. Berlin, Heidelberg: Springer.

Ehleringer, J. R., and T. E. Cerling. 2002. "C3 and C4 Photosynthesis." *Encyclopedia of Global Environmental Change* 2:186–190.

Ehleringer, J. R., and T. A. Cooper. 1988. "Correlations Between Carbon Isotope Ratio and Microhabitat in Desert Plants." *Oecologia* 76 (4): 562–566.

Ehleringer, J. R., and R. K. Monson. 1993. "Evolutionary and Ecological Aspects of Photosynthetic Pathway Variation." *Annual Review of Ecology and Systematics* 24 (1): 411–439.

Eickmeier, W. G., and M. M. Bender. 1976. "Carbon Isotope Ratios of Crassulacean Acid Metabolism Species in Relation to Climate and Phytosociology." *Oecologia* 25 (4): 341–347.

Ellwood, E. C., M. P. Scott, W. D. Lipe, R. Matson, and J. G. Jones. 2013. "Stone-boiling Maize with Limestone: Experimental Results and Implications for Nutrition Among SE Utah Pre-ceramic Groups." *Journal of Archaeological Science* 40 (1): 35–44.

Elyea, J., and P. Hogan. 1983. "Economy and Interaction Along the Lower Chaco River." Chap. Regional Interaction: The Archaic Adaptation, ed. by P. Hogan and J. C. Winter, 393–402. Albuquerque: Office of Contract Archeology / the Maxwell Museum of Anthropology, University of New Mexico.

Erhardt, E., B. Wolf, M. Ben-David, and E. Bedrick. 2014. "(2014) Stable Isotope Sourcing Using Sampling." *Open Journal of Ecology, 4, 289-298. doi: 10.4236/oje.2014.46027*.

Evans, D. R., and J. Belnap. 1999. "Long-term Consequences of Disturbance on Nitrogen Dynamics in an Arid Ecosystem." *Ecology* 80 (1): 150–160.

Fahrni, G. 2011. "Basketmaker Chronology Near Moab." *Southwestern Lore* 77:73–80.

Farquhar, G. D., J. R. Ehleringer, and K. T. Hubick. 1989. "Carbon Isotope Discrimination and Photosynthesis." *Annual Review of Plant Biology* 40 (1): 503–537.

Feinman, G. M., K. G. Lightfoot, and S. Upham. 2000. "Political Hierarchies and Organizational Strategies in the Puebloan Southwest." *American Antiquity*: 449–470.

Flanagan, L. B., C. S. Cook, and J. R. Ehleringer. 1997. "Unusually Low Varbon Isotope Ratios in Plants from Hanging Gardens in Southern Utah." *Oecologia* 111 (4): 481–489.

Foresman, P. S. 2018. "Maize Image (Released to Public Domain)." `HTTPS://COMMONS.WIKIMEDIA.ORG/WIKI/FILE:EAR\protect\_398\protect\_(PSF).PNG` accessed Jan 15, 2018.

Fowler, C. S. 1986. "Handbook of North American Indians: 11 Great Basin." Chap. Subsistence, ed. by W. L. D'Azevedo, 64–97. Washington, D.C.: Smithsonian Institution.

Froehle, A. W., C. M. Kellner, and M. J. Schoeninger. 2010. "FOCUS: Effect of Diet and Protein Source on Carbon Stable Isotope Ratios in Collagen." *Journal of Archaeological Science* 37 (10): 2662–2670.

Fry, B. 2013a. "Alternative Approaches for Solving Underdetermined Isotope Mixing Problems." *Marine Ecology Progress Series* 472:1–13.

— . 2013b. "Minmax Solutions for Underdetermined Isotope Mixing Problems: Reply to Semmens et al.(2013)." *Marine Ecology Progress Series* 490:291–294.

Gannes, L. Z., C. M. Del Rio, and P. Koch. 1998. "Natural Abundance Variations in Stable Isotopes and their Potential Uses in Animal Physiological Ecology." *Comparative Biochemistry and Physiology Part A: Molecular & Integrative Physiology* 119 (3): 725–737.

Geib, P. R. 1996. *Glen Canyon Revisited*. Salt Lake City: University of Utah Press.

Geib, P. R. 2011. *Foragers and Farmers of the Northern Kayenta Region*. Salt Lake City: University of Utah Press.

Geib, P. R., and W. B. Hurst. 2013. "Should Dates Trump Context? Evaluation of the Cave 7 Skeletal Assemblage Radiocarbon Dates." *Journal of Archaeological Science* 40 (6): 2754–2770.

Geib, P. R., and K. Spurr. 2000. "Foundations of Anasazi Culture: The Basketmaker-Pueblo Transition." Chap. The Basketmaker Transition on the Rainbow Plateau. Ed. by P. F. Reed. Salt Lake City: University of Utah Press.

Germain, L. R., P. L. Koch, J. Harvey, and M. D. McCarthy. 2013. "Nitrogen Isotope Fractionation in Amino Acids from Harbor Seals: Implications for Compound-specific Trophic Position Calculations." *Marine Ecology Progress Series* 482:265–277.

Gilpin, D. 1994. "Lukachukai and Salina Springs: Late Archaic/Early Basketmaker Habitation Sites in the Chinle Valley, Northeastern Arizona." *Kiva* 60 (2): 203–218.

Glen Rice, G., and S. A. LeBlanc, eds. 2001. *Deadly Landscapes: Case Studies in Prehistoric Southwestern Warfare*. Salt Lake City: University of Utah Press.

Guernsey, S. J. 1931. *Explorations in Northeastern Arizona: Report on the Archaeological Fieldwork of 1920-1923*. New Haven: Peabody Museum.

Guernsey, S. J., and A. V. Kidder. 1921. *Basket-maker Caves of Northeastern Arizona: Report on the Explorations, 1916-17*. New Haven: The Museum. The Museum. Peabody Museum.

Haas Jr, W. R. 2001. "The Basketmaker II Fiber Industry of Boomerang Shelter, Southeastern Utah: a Synthesis of Cordage Morphology Analysis and Experimentation." *Kiva* 67 (2): 167–185.

Hansen, D. T., and R. H. Fish. 1993. *Soil Survey of San Juan County, Utah, Central Part*. USDA Soil Conservation Service.

Hard, R. J., R. P. Mauldin, and G. R. Raymond. 1996. "Mano Size, Stable Carbon Isotope Ratios, and Macrobotanical Remains as Multiple Lines of Evidence of Maize Dependence in the American Southwest." *Journal of Archaeological Method and Theory* 3 (3): 253–318.

Hasse, W. R. 1983. "Pueblo II and Pueblo III Settlement Patterns on Cedar Mesa, Southeastern Utah." MA thesis, Washington State University.

Hays-Gilpin, K. A. 1996. "Interpreting Southwestern Diversity: Underlying Principles and Overarching Patterns, Anthropological Research Paper, (48)." Chap. Anasazi Iconography: Medium and Motif, 55–67. Tucson: Arizona State University Press.

— . 2000. "Women and Men in the Prehispanic Southwest." Chap. 3: Gender, Ideology and Ritual Activities, ed. by P. L. Crown, 91–136. Santa Fe: School of American Research Press.

Heath, T. A. 2018. "Wolf Image (Public domain Dedication 1.0)." `HTTP://PHYLOPIC.ORG/IMAGE/E4E306CD-73B6-4CA3-A08C-753A856F7F12/` accessed Jan 15, 2018.

Heaton, T. H. E. 1986. "Isotopic Studies of Nitrogen Pollution in the Hydrosphere and Atmosphere: A Review." *Chemical Geology: Isotope Geoscience Section* 59:87–102.

Hobbie, E. A., and R. A. Werner. 2004. "Intramolecular, Compound-specific, and Bulk Carbon Isotope Patterns in C3 and C4 Plants: A Review and Synthesis." *New Phytologist* 161 (2): 371–385.

Hobson, K. A., D. M. Schell, D. Renouf, and E. Noseworthy. 1996. "Stable Carbon and Nitrogen Isotopic Fractionation Between Diet and Tissues of Captive Seals: Implications for Dietary Reconstructions Involving Marine Mammals." *Canadian Journal of Fisheries and Aquatic Sciences* 53 (3): 528–533.

Hoen, D. K., S. L. Kim, N. E. Hussey, N. J. Wallsgrove, J. C. Drazen, and B. N. Popp. 2014. "Amino Acid 15 N Trophic Enrichment Factors of Four Large Carnivorous Fishes." *Journal of Experimental Marine Biology and Ecology* 453:76–83.

Holmes, C. 2017. "Markov Chain Monte Carlo and Applied Bayesian Statistics: a Short Course." `http://www.stats.ox.ac.uk/\protect\nobreakspace{}cholmes/Courses/BDA/bda\protect\_mcmc.pdf` accessed April 15 2017.

Holstad, E. C. 2010. "Basketmaker II Stone-boiling Technology at Cedar Mesa, Utah: An Experimental Study." MA thesis, Department of Anthropology, Washington State University.

Homburg, J. A., J. A. Sandor, and J. B. Norton. 2005. "Anthropogenic Influences on Zuni Agricultural Soils." *Geoarchaeology* 20 (7): 661–693.

Hovezak, T. D., and L. M. Sesler. 2006. "New Data on Northwest New Mexico's Los Pinos Phase: A Classic Basketmakers II Occupation?" *Kiva* 7 (2): 239–257.

Hovezak, T. D., L. M. Sesler, and S. L. Fuller. 2002. *Archaeological Investigations in the Fruitland Project Area: Late Archaic, Basketmaker, Pueblo I, and Navajo Sites in Northwestern New Mexico*. Dolores: La Plata Archaeological Consultants.

Huckell, B. B. 1996. "The Archaic Prehistory of the North American Southwest." *Journal of World Prehistory* 10 (3): 305–373.

Hurst, W., F. E. Smiley, and M. R. Robins. 2011. "Early Farmers at the Earth's Backbone: Basketmaker II in the Comb Ridge Area." *Southwestern Lore* 77:89–101.

Irwin-Williams, C., and C. V. Haynes. 1970. "Climatic Change and Early Population Dynamics in the Southwestern United States." *Quaternary Research* 1 (1): 59–71.

Jennings, J. D. 1966. *Glen Canyon: A Summary*. Salt Lake City: University of Utah Press.

Karamanos, R., and D. Rennie. 1981. "The Isotope Composition of Residual Fertilizer Nitrogen in Soil Columns." *Soil Science Society of America Journal* 45 (2): 316–321.

Kearns, T. M., J. L. McVickar, and L. S. Reed. 2000. "Foundations of Anasazi Culture: The Basketmaker-Pueblo Transition." Chap. The Early to Late Basketmaker III Transition in Tohatchi Flats, New Mexico, ed. by P. S. Reed, 115–142. University of Utah Press.

Keeley, L. H. 1996. *War Before Civilization*. Oxford: Oxford University Press.

Kellner, C. M., and M. J. Schoeninger. 2007. "A Simple Carbon Isotope Model for Reconstructing Prehistoric Human Diet." *American Journal of Physical Anthropology* 133 (4): 1112–1127.

Kemp, B. M., W. D. Lipe, and R. Matson. 2011. "New Insights from Old Collections: Cedar Mesa, Utah, Revisited." *Southwestern Lore* 77 (2): 103–113.

Kemp, B. M., C. Monroe, P. R. Geib, W. D. Lipe, and R. Matson. 2010. "Genetic Analysis of Human Coprolites from Southeastern Utah." Laboratory of Archaeology University

of British Columbia Vancouver. Available as pdf files at: https://research.wsulibs.wsu.edu:8443/xmlui/handle/2376/2668.

Kidder, A. V. 1924. "An Introduction to the Study of Southwestern Archaeology, with a Preliminary Account of the Excavations at Pecos. Papers of the Southwestern Expedition, No. 1." *New Haven: Phillips Academy*.

Kidder, A. V. 1927. "Southwestern Archeological Conference." *Science* 66:489–491.

Kidder, A. V., and S. J. Guernsey. 1919. *Archeological Explorations in Northeastern Arizona*. Vol. 65. US Government Printing Office.

Kintigh, K., J. Altschul, M. Beaudry, R. Drennan, A. Kinzig, T. Kohler, W. Limp, H. Maschner, W. Michener, T. Pauketat, P. Peregrine, J. Sabloff, T. Wilkinson, H. Wright, and M. Zeder. 2014. "Grand Challenges for Archaeology." *American Antiquity* 79 (1): 5–24.

Kohler, T. A. 2013. "How the Pueblos Got Their Sprachbund." *Journal of Archaeological Method and Theory* 20 (2): 212–234.

Kohler, T. A., and K. M. Reese. 2014. "Long and Spatially Variable Neolithic Demographic Transition in the North American Southwest." *Proceedings of the National Academy of Sciences* 111 (28): 10101–10106.

Kohler, T. A., and M. D. Varien, eds. 2012. *Emergence and Collapse of Early Villages: Models of Central Mesa Verde Archaeology*. Berkeley: University of California Press.

Kohler, T. A., M. P. Glaude, J.-P. Bocquet-Appel, and M. K. Brian. 2008. "The Neolithic Demographic Transition in the US Southwest." *American Antiquity* 73 (4): 645–669.

Kohler, T. A., R. K. Bocinsky, D. Cockburn, S. A. Crabtree, M. D. Varien, K. E. Kolm, S. Smith, S. G. Ortman, and Z. Kobti. 2012a. "Modelling Prehispanic Pueblo Societies in Their Ecosystems." *Ecological Modelling* 241:30–41.

Kohler, T. A., D. Cockburn, P. L. Hooper, R. K. Bocinsky, and Z. Kobti. 2012b. "The Coevolution of Group Size and Leadership: An Agent-based Public Goods Model for Prehispanic Pueblo Societies." *Advances in Complex Systems* 15 (1).

Kohler, T. A., S. G. Ortman, K. E. Grundtisch, C. M. Fitzpatrick, and S. M. Cole. 2014. "The Better Angels of Their Nature: Declining Violence Through Time Among Prehispanic Farmers of the Pueblo Southwest." *American Antiquity* 79 (3): 444–464.

Leach, J. D., and K. D. Sobolik. 2010. "High Dietary Intake of Prebiotic Inulin-type Fructans in the Prehistoric Chihuahuan Desert." *British Journal of Nutrition* 103 (11): 1558–1561.

LeBlanc, S. A. 1999. *Prehistoric Warfare in the American Southwest*. Salt Lake City: University of Utah Press.

LeBlanc, S. A., L. S. Kreisman, B. M. Kemp, F. E. Smiley, S. W. Carlyle, A. N. Dhody, and T. Benjamin. 2007. "Quids and Aprons: Ancient DNA from Artifacts from the American Southwest." *Journal of Field Archaeology* 32 (2): 161–175.

Lee-Thorp, J. A. 2008. "On Isotopes and Old Bones." *Archaeometry* 50 (6): 925–950.

Lekson, S. H. 2002. "War in the Southwest, War in the World." *American Antiquity* 67 (4): 607–624.

— . 2008. *A History of the Ancient Southwest*. Santa Fe: School of American Research Press.

Lewis, M. D., and J. B. Coltrain. 2014. *Intra-species Isotopic Variability in Edible Native Plants from the Colorado Plateau*. Paper presented at the 34th Great Basin Anthropological Conference: Boise.

Lewis, M. D., J. B. Coltrain, and R. Burrillo. 2017. *Regional Variability in Stable Isotope Food-Web Baselines and Sex-Based Differences in Diet: An Example from Early Agriculturists in Southeastern Utah*. Paper presented at the 82th Annual Society for American Archaeology Meetings: Vancouver BC.

Lipe, W., and B. Pitblado. 1999. "Colorado Prehistory: A Context for the Southern Colorado River Basin." Chap. 4: Paleoindian and Archaic Periods, ed. by W. D. Lipe, M. D. Varien, and R. H. Wilshusen, 95–131. Colorado Council of Professional Archaeologists.

Lipe, W. D. 1970. "Reconstructing Prehistoric Pueblo Societies." Chap. 4: Anasazi Communities on the Red Rock Plataeu, Southeastern Utah, ed. by W. A. Longacre, 84–139. Santa Fe: School of American Research Press.

— . 2007. "Bibliography of Reports and Publications Related to the Cedar Mesa Project." `http://hdl.handle.net/2376/737` accessed August 7th, 2017.

Lipe, W. D., R. K. Bocinsky, B. S. Chisholm, R. Lyle, D. M. Dove, R. Matson, E. Jarvis, K. Judd, and B. M. Kemp. 2016. "Cultural and Genetic Contexts for Early Turkey Domestication in the Northern Southwest." *American Antiquity* 81 (1): 97–113.

Lipe, W. D. D., L. Ellyson, K. Bocinsky, R. Lyle, and R. Matson. 2017. *Costly Gobbling: Raising Turkeys in the Central Mesa Verde Area*. paper presented at the 82th Annual Society for American Archaeology meetings: Vancouver BC. Vancouver BC.

Logan, J. M., T. D. Jardine, T. J. Miller, S. E. Bunn, R. A. Cunjak, and M. E. Lutcavage. 2008. "Lipid Corrections in Carbon and Nitrogen Stable Isotope Analyses: Comparison of Chemical Extraction and Modeling Methods." *Journal of Animal Ecology* 77 (4): 838–846.

Louderback, L. A., B. M. Pavlik, and A. M. Spurling. 2013. "Ethnographic and Archaeological Evidence Corroborating Yucca as a Food Source, Mojave Desert, USA." *Journal of Ethnobiology* 33 (2): 281–297.

Mabry, J. 2005. "The Late Archaic Across the Borderlands: From Foraging to Farming." Chap. 3 Changing Knowledge and Ideas About the First Farmers in Southeastern Arizona, ed. by B. J. Vierra, 41–83. Austin: University of Texas Press.

Maclean, W., J. Harnly, J. Chen, S. Chevassus-Agnes, G Gilani, G. Livesey, and P Warwick. 2003. "Food and Agriculture Organization of the United Nations Technical Workshop Report." Chap. Food Energy–Methods of Analysis and Conversion Factors, vol. 77. Rome: FAO.

Marino, B. D., and M. B. McElroy. 1991. "Isotopic Composition of Atmospheric CO2 Inferred from Carbon in C4 Plant Cellulose." *Nature* 349 (6305): 127–131.

Martin, D. L. 1991. *Black Mesa Anasazi Health: Reconstructing Life from Patterns of Death and Disease*. Carbondale: Southern Illinois University Press.

Martin, S. L. 1999. "Virgin Anasazi Diet as Demonstrated Through the Analysis of Stable Carbon and Nitrogen Isotopes." *Kiva* 64 (4): 495–514.

Matson, R. G. 1991. *The Origins of Southwestern Agriculture*. Tucson: University of Arizona Press.

— . 1994. "Anomalous Basketmaker II Sites on Cedar Mesa: Not so Anomalous After All." *Kiva* 60 (2): 219–237.

— . 2006. "What is Basketmaker II?" *Kiva* 72 (2): 149–165.

— . 2016. "The Nutritional Context of the Pueblo III Depopulation of the Northern San Juan: Too Much Maize?" *Journal of Archaeological Science: Reports* 5:622–631.

Matson, R. G., and B. Chisholm. 1991. "Basketmaker II Subsistence: Carbon Isotopes and Other Dietary Indicators from Cedar Mesa, Utah." *American Antiquity* 56 (3): 444–459.

Matson, R., and B. Chisholm. 2007. "Basketmaker II Subsistence." In *Poster presented at 72nd Annual Meeting of the Society for American Archaeology*. Austin Texas.

Matson, R., W. D. Lipe, and W. R. Haase. 1988. "Adaptational Continuities and Occupational Discontinuities: the Cedar Mesa Anasazi." *Journal of Field Archaeology* 15 (3): 245–263.

— . 1990. *Human Adaptation on Cedar Mesa, Southeastern Utah. (1990 updated 2014)*. `https://circle.ubc.ca/handle/2429/19586`.

McBride, P. 1994. "Across the Colorado Plateau: Anthropological Studies for the Transwestern Pipeline Expansion Project." Chap. Description of Anasazi Archaeobotanical remains, ed. by J. Winter, 443–457. Office of Contract Archaeology / Maxwell Museum of Anthropology, University of New Mexico.

McCaffery, H., R. H. Tykot, K. D. Gore, and B. R. DeBoer. 2014. "Stable Isotope Analysis of Turkey (*Meleagris gallopavo*) Diet from Pueblo II and Pueblo III Sites, Middle San Juan Region, Northwest New Mexico." *American Antiquity* 79 (2): 337–352.

McNitt, F. 1966. *Richard Wetherill, Anasazi: Pioneer Explorer of Southwestern Ruins*. Albuquerque: University of New Mexico Press.

Minnis, P. E. 2000. *Ethnobotany: A Reader*. Norman: University of Oklahoma Press.

Moore, J. W., and B. X. Semmens. 2008. "Incorporating Uncertainty and Prior Information into Stable Isotope Mixing Models." *Ecology Letters* 11 (5): 470–480.

Morris, D. H. 1990. "Changes in Groundstone Following the Introduction of Maize into the American Southwest." *Journal of Anthropological Research* 46 (2): 177–194.

Morris, E. H., and R. F. Burgh. 1954. *Basket Maker II Sites near Durango Colorado*. Washington D.C: Carnegie Institution of Washington.

Mowrer, K. 2006. "Basketmaker II Mortuary Practices: Social Differentiation and Regional Variation." *Kiva* 72 (2): 259–281.

Munson, S. M., J. Belnap, C. D. Schelz, M. Moran, and T. W. Carolin. 2011. "On the Brink of Change: Plant Responses to Climate on the Colorado Plateau." *Ecosphere* 2 (6): 1–15.

Nardoto, G. B., P. d. Godoy, E. S. d. Ferraz, J. P.H. B. Ometto, and L. A. Martinelli. 2006. "Stable Carbon and Nitrogen Isotopic Fractionation Between Diet and Swine Tissues." *Scientia Agricola* 63 (6): 579–582.

Newsome, S. D., D. L. Phillips, B. J. Culleton, T. P. Guilderson, and P. L. Koch. 2004. "Dietary Reconstruction of an Early to Middle Holocene Human Population from the Central California Coast: Insights from Advanced Stable Isotope Mixing Models." *Journal of Archaeological Science* 31 (8): 1101–1115.

Nordenskiöld, G. 1893. *The Cliff Dwellers of the Mesa Verde, Southwestern Colorado: Their Pottery and Implements*. Norstedt (reprint 1990 Mesa Verde Museum Association).

Olive, P. J., J. K. Pinnegar, N. V. Polunin, G. Richards, and R. Welch. 2003. "Isotope Trophic-step Fractionation: a Dynamic Equilibrium Model." *Journal of Animal Ecology* 72 (4): 608–617.

Ortiz, A. 1979. *Handbook of North American Indians: Volume 9, Southwest*. Washington, D.C.: Smithsonian.

Ortman, S. G., S. Diederichs, K. Schleher, J. Fetterman, M. Espinosa, and C. Sommer. 2016. "Demographic and Social Dimensions of the Neolithic Revolution in Southwest Colorado." *Kiva* 82 (3): 232–258.

Parry, W., F. E. Smiley, and G. Burgett. 1994. "The Archaic Occupation of Black Mesa, Arizona." *Archaic Hunter-Gatherer Archaeology in the American Southwest. Eastern New Mexico University Contributions in Anthropology* 13 (1): 185–230.

Pataki, D., S. Bush, P Gardner, D. Solomon, and J. Ehleringer. 2005. "Ecohydrology in a Colorado River Riparian Forest: Implications for the Decline of *Populus fremontii*." *Ecological Applications* 15 (3): 1009–1018.

Phillips, D. L., and J. W. Gregg. 2003. "Source Partitioning Using Stable Isotopes: Coping with Too Many Sources." *Oecologia* 136 (2): 261–269.

Phillips, D. L., S. D. Newsome, and J. W. Gregg. 2005. "Combining Sources in Stable Isotope Mixing Models: Alternative Methods." *Oecologia* 144 (4): 520–527.

Phillips, D. L., R. Inger, S. Bearhop, A. L. Jackson, J. W. Moore, A. C. Parnell, B. X. Semmens, and E. J. Ward. 2014. "Best Practices for Use of Stable Isotope Mixing Models in Food-web Studies." *Canadian Journal of Zoology* 92 (10): 823–835.

Plog, S. 2008. *Ancient Peoples of the American Southwest*. London: Thames / Hudson.

Pollock, K. H. 2001. "Pits Without Pots: Basketmaker II Houses and Lithics of Southeastern Utah." MA thesis, Washington State University.

Potter, J. M., ed. 2008. *Animas-La Plata Project: Environmental Studies. SWCA Anthropological Research Papers no. 10, vol. X.* Phoenix: SWCA Environmental Consultants.

Potter, J. M. 2011. "Durango Basketmaker II Redux: New Data from the Animas-La Plata Project." *Kiva* 76 (4): 431–452.

Powell, S., and F. E. Smiley, eds. 2002. *Prehistoric Culture Change on the Colorado Plateau: Ten Thousand Years on Black Mesa*. Tucson: University of Arizona Press.

Rawlings, T. A., and J. C. Driver. 2010. "Paleodiet of Domestic Turkey, Shields Pueblo (5MT3807), Colorado: Isotopic Analysis and its Implications for Care of a Household Domesticate." *Journal of Archaeological Science* 37 (10): 2433–2441.

Reed., A. D., and M. D. Metcalf. 1999. *Colorado Prehistory: A Context for the Northern Colorado River Basin*. Ed. by W. D. Lipe, M. D. Varien, and R. H. Wilshusen. Denver: Colorado Council of Professional Archaeologists.

Reed, P. F. 2002. *Foundations of Anasazi Culture: The Basketmaker-Pueblo Transition*. Salt Lake City: University of Utah Press.

Reinhard, K. J. 1988. "Diet, Parasitism, and Anemia in the Prehistoric Southwest." PhD thesis, Texas A&M University.

Reinhard, K. J., and D. R. Danielson. 2005. "Pervasiveness of Phytoliths in Prehistoric Southwestern Diet and Implications for Regional and Temporal Trends for Dental Microwear." *Journal of Archaeological Science* 32 (7): 981–988.

Reinhard, K. J., K. L. Johnson, S. LeRoy-Toren, K. Wieseman, I. Teixeira-Santos, and M. Vieira. 2012. "Understanding the Pathoecological Relationship Between Ancient Diet and Modern Diabetes through Coprolite Analysis: A Case Example from Antelope Cave, Mojave County, Arizona." *Current Anthropology* 53 (4): 506–512.

Reynolds, C. R. 2012. "Meat at the Origins of Agriculture: Faunal Use and Resource Pressure at the Origins of Agriculture in the Northern U.S. Southwest." PhD thesis, University of Iowa.

Roth, J. D., and K. A. Hobson. 2000. "Stable Carbon and Nitrogen Isotopic Fractionation Between Diet and Tissue of Captive Red Fox: Implications for Dietary Reconstruction." *Canadian Journal of zoology* 78 (5): 848–852.

Sandor, J. A., J. B. Norton, J. A. Homburg, D. A. Muenchrath, C. S. White, S. E. Williams, C. I. Havener, and P. D. Stahl. 2007. "Biogeochemical Studies of a Native American Runoff Agroecosystem." *Geoarchaeology* 22 (3): 359–386.

Sanisidro, O. 2018. "Deer Image (Public Domain Dedication 1.0)." `http://phylopic.org/image/bb553480-e37f-4236-8c69-ce9fa8116b39/` accessed Jan 15, 2018.

Schoeller, D. A. 1999. "Isotope Fractionation: Why Aren't We What We Eat?" *Journal of Archaeological Science* 26 (6): 667–673.

Schoeninger, M. J. 1999. "Prehistoric Lifeways in the Great Basin Wetlands: Bioarchaeological Reconstruction and Interpretation." Chap. Prehistoric Subsistence Strategies in the Stillwater Marsh Region of the Carson Desert, 151–166. University of Utah Press, Salt Lake City.

Schoeninger, M. J., and M. J. DeNiro. 1984. "Nitrogen and Carbon Isotopic Composition of Bone Collagen from Marine and Terrestrial Animals." *Geochimica et Cosmochimica Acta* 48 (4): 625–639.

Schwarcz, H. P., T. L. Dupras, and S. I. Fairgrieve. 1999. "15 N Enrichment in the Sahara: In Search of a Global Relationship." *Journal of Archaeological Science* 26 (6): 629–636.

Schwarcz, H. P., and M. J. Schoeninger. 1991. "Stable Isotope Analyses in Human Nutritional Ecology." *Yearbook of Physical Anthropology* 34 (S13): 283–321.

Schwarcz, H. P., and M. J. Schoeninger. 2012. "Handbook of Environmental Isotope Geochemistry." Chap. Stable Isotopes of Carbon and Nitrogen as Tracers for Paleo-diet Reconstruction, 725–742. Springer.

Schwinning, S., J. Belnap, D. R. Bowling, and J. R. Ehleringer. 2008. "Sensitivity of the Colorado Plateau to Change: Climate, Ecosystems, and Society." *Ecology and Society* 13 (2).

Sealy, J., M. Johnson, M. Richards, and O. Nehlich. 2014. "Comparison of Two Methods of Extracting Bone Collagen for Stable Carbon and Nitrogen Isotope Analysis: Com-

paring Whole Bone Demineralization with Gelatinization and Ultrafiltration." *Journal of Archaeological Science* 47:64–69.

Semmens, B. X., E. J. Ward, A. C. Parnell, D. L. Phillips, S. Bearhop, R. Inger, A. Jackson, and J. W. Moore. 2013. "Statistical Basis and Outputs of Stable Isotope Mixing Models: Comment on Fry (2013)." *Marine Ecology Progress Series* 490:285–289.

Sesler, L. M., and T. D. Hovezak. 2011. "Farming at the Edge of Paradise: Basketmaker II Emergence in New Mexico's San Juan Basin." *Southwestern Lore* 77:9–19.

Simmons, A. H. 1989. "Human Adaptations and Cultural Change in the Greater Southwest: Research Series No. 32." Chap. The Unknown Archeology of the Southwest: The Archaic, ed. by A. H. Simmons, A. L. W. Stodder, D. D. Dykeman, and P. A. Hicks, 39–74. Fayetteville: Arkansas Archeological Survey.

Simms, S. R. 2008. *Ancient Peoples of the Great Basin and Colorado Plateau*. Walnut Creek: Left Coast Press.

Smeal, D., M. O'Neill, and R. Arnold. 2005. "Forage Production of Cool Season Pasture Grasses as Related to Irrigation." *Agricultural Water Management* 76 (3): 224–236.

Smiley, F. E. 1998. "Archaeological Chronometry: Radiocarbon and Tree-Ring Models and Applications from Black Mesa, Arizona." Chap. Applying Radiocarbon Models: Lolomai Phase Chronometry on Black Mesa, ed. by F. E. Smiley and R. V. Ahlstrom, 99–134. 16. Center for Archaeological Investigations (Occasional Papers).

Spangler, J. D., A. T. Yentsch, and R. Green. 2010. *Farming and Foraging on the Southwestern Frontier: An Overview of Previous Research of the Archaeological and Historical Resources of the Greater Cedar Mesa Area: Antiquities Section Selected Papers Volume IX, No. 18*. Salt Lake City: Utah Division of State History.

Sperry, L. J., J. Belnap, and R. D. Evans. 2006. "*Bromus tectorum* Invasion Alters Nitrogen Dynamics in an Undisturbed Arid Grassland Ecosystem." *Ecology* 87 (3): 603–615.

Spielmann, K. A., M. J. Schoeninger, and K. Moore. 1990. "Plains-pueblo Interdependence and Human Diet at Pecos Pueblo, New Mexico." *American Antiquity* 55 (4): 745–765.

Stock, B. C., and B. X. Semmens. 2013. "MixSIAR GUI User Manual. Version 3.1." `https://rdrr.io/github/brianstock/MixSIAR/` accessed Jan 15, 2017.

Szarek, S. R., and J. H. Troughton. 1976. "Carbon Isotope Ratios in Crassulacean Acid Metabolism Plants Seasonal Patterns from Plants in Natural Stands." *Plant Physiology* 58 (3): 367–370.

Szpak, P., C. D. White, F. J. Longstaffe, J.-F. Millaire, and V. F. V. Sánchez. 2013. "Carbon and Nitrogen Isotopic Survey of Northern Peruvian Plants: Baselines for Paleodietary and Paleoecological Studies." *PLoS One* 8 (1): e53763.

Tieszen, L. L., T. W. Boutton, K. G. Tesdahl, and N. A. Slade. 1983. "Fractionation and Turnover of Stable Carbon Isotopes in Animal Tissues: Implications for δ 13 C Analysis of Diet." *Oecologia* 57 (1): 32–37.

Trepte, A., and T. M. Keesey. 2018. "Grass Image (Share Alike License 3.0)." `http://phylopic.org/image/5b0c9499-e8ca-4b2e-a561-a7096710b509/` accessed Jan 15, 2018.

Ugan, A., and J. Coltrain. 2011. "Variation in Collagen Stable Nitrogen Values in Black-tailed Jackrabbits (*Lepus californicus*) in Relation to Small-scale Differences in Climate, Soil, and Topography." *Journal of Archaeological Science* 38 (7): 1417–1429.

— . 2012. "Stable Isotopes, Diet, and Taphonomy: A Look at Using Isotope-based Dietary Reconstructions to Infer Differential Survivorship in Zooarchaeological Assemblages." *Journal of Archaeological Science* 39 (5): 1401–1411.

unattributed. 2018. "Grass Image (Public Domain Mark 1.0)." `http://phylopic.org/image/6aafb42e-ffba-49ba-b21e-11c85da85830/` accessed Jan 15, 2018.

van de Water, P. K., S. W. Leavitt, and J. L. Betancourt. 2002. "Leaf δ^{13}C Variability with Elevation, Slope Aspect, and Precipitation in the Southwest United States." *Oecologia* 132 (3): 332–343.

van Groenigen, J.-W., and C. van Kessel. 2002. "Salinity-induced Patterns of Natural Abundance Carbon-13 and Nitrogen-15 in Plant and Soil." *Soil Science Society of America Journal* 66 (2): 489–498.

Varien, M. D. 1999. "The Sand Canyon Archaeological Project: Site Testing." *Electronic document, `http://www.crowcanyon.org/ResearchReports/SiteTesting/start.asp` last accessed Jan 2018* 1.

Vierra, B. J. 2008. "Archaeology Without Borders: Contact, Commerce, and Change in the US Southwest and Northwestern Mexico." Chap. 5: Early Agriculture on the Southeastern Periphery of the Colorado Plateau, ed. by L. D. Webster and M. E. McBrinn, 71–88. Boulder: University Press of Colorado.

Vierra, B. J., and W. H. Doleman. 1994. "Archaic Hunter-Gatherer Archaeology in the American Southwest." Chap. The Organization of Archaic Settlement-subsistence Systems in the Northern Southwest, ed. by B. J. Vierra, 1:76–102. 13. Eastern New Mexico University Contributions in Anthropology.

Vogler, L. E., K. Langenfeld, and D. Gilpin. 1993. *DAA' AK' EH NITSAA: An Overview of the Cultural Resources of the Navajo Indian Irrigation Project, Northwestern New Mexico: Navajo Nation Papers in Anthropology No. 29*. Window Rock AZ: Navajo Nation Archaeology Department.

Wandsnider, L. 1997. "The Roasted and the Boiled: Food Composition and Heat Treatment with Special Emphasis on Pit-hearth Cooking." *Journal of Anthropological Archaeology* 16 (1): 1–48.

Warinner, C., N. R. Garcia, and N. Tuross. 2013. "Maize, Beans and the Floral Isotopic Diversity of Highland Oaxaca, Mexico." *Journal of Archaeological Science* 40 (2): 868–873.

Warinner, C., and N. Tuross. 2009. "Alkaline Cooking and Stable Isotope Tissue-diet Spacing in Swine: Archaeological Implications." *Journal of Archaeological Science* 36 (8): 1690–1697.

Webster, M. 2001. *Prehistoric Diet and Human Adaptation in West Central Chihuahua, Mexico*. University of Calgary.

Welsh, S. L., N. Atwood, S. Goodrich, and L. Higgins, eds. 1987. *A Utah Flora (Great Basin Naturalist Memoirs Number 9)*. Provo: Brigham Young University Press.

Werning, S. 2018. "Rabbit Image (Creative Commons Attribution 3.0 Unported)." `http://phylopic.org/image/dea688b6-9168-4e79-a106-366888148eb1/` accessed Jan 15, 2018.

White, W. M. 2013. *Geochemistry*. Wiley Online Library.

Wilcox, D. R., and J. Haas. 1994. "Themes in Southwest Prehistory." Chap. 10: The Scream of the Butterfly: Competition and Conflict in the Prehistoric Southwest, ed. by G. J. Gumerman, 211–238. Santa Fe: School of American Research Press.

Wilshusen, R. H., and E. M. Perry. 2008. "The Neolithic Demographic Transition and its Consequences." Chap. Evaluating the Emergence of Early Villages in the North American Southwest in Light of the Proposed Neolithic Demographic Transition, ed. by J. Bocquet-Appel and O. Bar-Yosef, 417–438. Berlin, Heidelberg: Springer.

Wilshusen, R. H., G. Schachner, and J. R. Allison, eds. 2012. *Crucible of Pueblos: The Early Pueblo Period in the Northern Southwest*. 71. Los Angeles: Cotsen Institute of Archaeology Press, University of California.

Wilson, C. J. 1974. *Highway U-95 Archeology: Comb Wash to Grand Flat Volume II. Technical Report.* Salt Lake City: University of Utah Department of Anthropology.

Wolf, N., S. A. Carleton, and C. Martínez del Rio. 2009. "Ten Years of Experimental Animal Isotopic Ecology." *Functional Ecology* 23 (1): 17–26.

Yoneyama, T., Y. Ohta, and T. Ohtani. 1983. "Variations of Natural 13C and 15N Abundances in the Rat Tissues and Their Correlation." *Radioisotopes* 32 (7): 330.

Zigmond, M. L. 1981. *Kawaiisu Ethnobotany*. Salt Lake City: University of Utah Press.